

SISSA

Scuola
Internazionale
Superiore di
Studi Avanzati

Physics Area - PhD course in
Theoretical Particle Physics

Exploring low-dimensional QFT using Perturbation Theory and beyond

Candidate:
Giacomo Sberveglieri

Advisor:
Marco Serone

Academic Year 2021-22



Abstract

In quantum field theory (QFT) perturbation theory, despite giving rise to asymptotic series, is a powerful tool that provides a lot of useful information. However, the asymptotic nature of perturbative series demands that they be treated with due care to exploit them to the fullest. To do so, we have to resort to Borel resummation, trans-series, and the theory of resurgence. In this thesis, we focus on QFTs in $d < 4$ dimensions and study them starting from their perturbative series. When these series are Borel summable, there is no need to invoke trans-series since Borel resumming the perturbative series alone is enough to reproduce full results.

This is the case of Euclidean $O(N)$ symmetric ϕ^4 vector models in $d = 3$ and $N = 1$ ϕ^4 theory in $d = 2$. We investigate the critical regime and phase diagrams of these theories paying attention to the renormalization scheme dependence. In particular, we find non-perturbative, finite changes of scheme for a one-parameter family of renormalization schemes. This allows us to determine the exact analytic renormalization dependence of the critical couplings and to investigate in three dimensions a strong-weak duality relation closely linked to the one found by Chang and Magruder long ago. Interestingly, for some schemes, the weak fixed point and the strong one move into the complex plane in complex conjugate pairs, making the phase transition no longer visible from the classically unbroken phase. We verify all our considerations by Borel resumming several perturbative series in the classically unbroken phase. In $d = 3$ we computed them up to order eight.

We also investigate integrable field theories with renormalons where the perturbative series are not Borel summable. Here, focusing on the free energy in the presence of a chemical potential coupled to a conserved charge, we study in detail the interplay between the resurgent structure and the $1/N$ expansion. Our findings turn out to be different in the three models we analyzed. For some models, we find terms in $1/N$ expansion that can be fully decoded in terms of a resurgent trans-series with one or more IR renormalon corrections, the non-linear sigma model and principal chiral field, respectively. In the Gross-Neveu model, instead, each term in the $1/N$ expansion includes non-perturbative corrections, which can not be predicted by a resurgent analysis of the corresponding perturbative series.

Preface

This PhD thesis is based on the following papers:

- G. Sberveglieri, M. Serone, and G. Spada, *Renormalization scheme dependence, RG flow, and Borel summability in ϕ^4 Theories in $d < 4$* , *Phys. Rev. D* **100** (2019), no. 4 045008, [[arXiv:1905.02122](#)],
- G. Sberveglieri, M. Serone, and G. Spada, *Self-Dualities and Renormalization Dependence of the Phase Diagram in 3d $O(N)$ Vector Models*, *JHEP* **02** (2021) 098, [[arXiv:2010.09737](#)],
- L. Di Pietro, M. Mariño, G. Sberveglieri, and M. Serone, *Resurgence and $1/N$ Expansion in Integrable Field Theories*, *JHEP* **10** (2021) 166, [[arXiv:2108.02647](#)],
- G. Sberveglieri and G. Spada, *in preparation*.

Contents

| | | |
|----------|---|-----------|
| 1 | Introduction | 9 |
| 2 | Borel resummation and Resurgence | 15 |
| 2.1 | Asymptotic Series | 16 |
| 2.2 | Borel Resummation | 18 |
| 2.2.1 | Lateral Borel Resummation and NP contributions | 19 |
| 2.3 | Large-order behavior and NP effects | 20 |
| 2.4 | Theory of Resurgence | 22 |
| 2.5 | Numerical approaches for Borel transforms | 25 |
| 2.5.1 | Padé-Borel method | 26 |
| 2.5.2 | Conformal mapping method | 27 |
| 3 | Borel Summability: To the IR fixed points in super-renormalizable ϕ^4 theories | 29 |
| 3.1 | RG and RS Dependence | 31 |
| 3.2 | Different classes of RSs in ϕ^4 Theories in $d < 4$ | 33 |
| 3.2.1 | Use of RG Flows: the RS $\tilde{\mathcal{S}}$ | 33 |
| 3.2.2 | No Use of RG Flows: the RS \mathcal{S} | 35 |
| 3.3 | Borel Summability and RS Dependence | 38 |
| 3.4 | RS Dependence in Minimal Schemes and Self-Dualities | 43 |
| 3.5 | Connection with Chang and Magruder Dualities | 48 |
| 3.6 | Fixed Points Annihilation and Analyticity Domain | 50 |
| 3.6.1 | Large N Non-Perturbative Mass Gap in $d = 2$ | 52 |
| 3.7 | Numerical Results in the $d = 2$ ϕ^4 Theory | 54 |
| 3.7.1 | Large-Order Behavior | 55 |
| 3.7.2 | Mass and Critical Exponent ν | 56 |
| 3.8 | Numerical Results in $d = 3$ $O(N)$ Models | 58 |
| 3.8.1 | Perturbative Coefficients up to g^8 | 59 |
| 3.8.2 | Self-Duality | 62 |
| 3.8.3 | Scheme Dependence of Critical Couplings | 64 |

| | | |
|----------|---|------------|
| 3.9 | Improved Numerical Results in $d = 3$ $O(N)$ Models | 66 |
| 3.9.1 | Numerical Strategies | 67 |
| 3.9.2 | Critical regime in the RS $\tilde{\mathcal{S}}$ | 75 |
| 4 | Non-Borel Summability: Renormalons in integrable field theories | 77 |
| 4.1 | Ordinary integrals at large N | 79 |
| 4.2 | Free energy and integrability | 82 |
| 4.3 | The non-linear sigma model | 86 |
| 4.3.1 | General aspects | 86 |
| 4.3.2 | The $1/N$ expansion from QFT | 87 |
| 4.3.3 | The $1/N$ expansion from the Bethe ansatz | 96 |
| 4.3.4 | Trans-series expansion and comparison with perturbation theory | 98 |
| 4.4 | The principal chiral field model | 101 |
| 4.4.1 | General aspects | 101 |
| 4.4.2 | Exact solution at large N | 102 |
| 4.4.3 | Trans-series expansion | 105 |
| 4.5 | The Gross–Neveu model | 111 |
| 4.5.1 | General aspects | 112 |
| 4.5.2 | Trans-series expansion | 113 |
| 4.5.3 | Higher orders in the $1/N$ expansion | 115 |
| 5 | Conclusions | 123 |
| A | The Lambert W Function | 129 |
| B | Large N for $O(N)$ Models in $d < 4$ | 131 |
| C | Vacuum Energy Renormalization in $d = 3$ $O(N)$ Models | 137 |
| D | Series Coefficients in $d = 3$ $O(N)$ Models | 141 |
| D.1 | Series Coefficients in the RS \mathcal{S} | 141 |
| D.2 | Series Coefficients in the RS $\tilde{\mathcal{S}}$ | 143 |
| E | $d = 0$ reduction of quartic vector models | 147 |
| F | Existence, uniqueness and analyticity in $1/N$ of the TBA equations | 151 |
| F.1 | Non-Linear sigma model | 152 |
| F.2 | Principal Chiral Field | 155 |
| F.3 | Gross-Neveu model | 156 |

Chapter 1

Introduction

Quantum field theory (QFT) is a powerful framework that allows to describe many different physical phenomena, ranging from physics at very high energies to condensed matter physics. It has produced over the last decades many high precision results. However, at the same time, we are very far from having a complete understanding of it, and we can't solve exactly most physical systems we study in QFT. Even when working in simple models, it is difficult to compute observables. An important tool that can often come to our help and stands out for its wide scope of application, is perturbation theory. We are able to address the study of many problems by starting at a point of the parameter space in which they are solvable exactly, typically the free theory, adding a small perturbation parametrized by a coupling $g \ll 1$ and Taylor expanding the equations in power series in g . Clearly, the resulting series provides information in the limit $g \rightarrow 0$. It is natural to ask what else is computable from them and when the series breaks down, namely how far we may go in the strong coupling region. We can rephrase these questions in the following one: what are the convergence properties of the perturbative series? It turns out that, generically speaking, the perturbative series are asymptotic, i.e. they have zero radius of convergence. Why it has to be the case was presented first by Dyson starting from a very simple observation [5]: typically negative values of the coupling, no matter how small, completely alter the properties of the theory, making it unstable or ill-defined, hence the value $g = 0$, around which we are expanding, is non-analytic and our perturbative series asymptotic. Clearly, this is an important piece of information that we should take in consideration every time we are using perturbation theory. Furthermore, the fact that the perturbative series are divergent power series is the starting point to improve perturbation theory, making it an even more relevant tool to investigate quantum physics. The asymptotic character concretely manifests itself in the fact that the coefficients of the series have a leading factorial growth. Just computing more and more terms is not enough to reproduce the exact result we are expanding since, eventually, our series will start to diverge. A systematic way to do this is Borel resummation. This procedure consists in defining a convergent series (Borel transform) starting from the original one after dividing

its terms by a factorially growing coefficient, resumming it, and taking the inverse Laplace transform. In this way we are able to find a suitable analytic continuation of our asymptotic series. However, this is not the end of the story: different functions can have the same asymptotic expansion and the Borel transforms are not entire functions. The asymptotic character of the perturbative series is, in fact, an indication of the presence of non-perturbative (NP) effects, contributions of the type $e^{-1/g}$ that are “invisible” to perturbation theory. Thus the natural objects to consider should include these contributions together with the perturbative series. They are formal linear combinations of power series with exponential prefactors, i.e. of the following form

$$\sum_n a_n g^n + \sum_\ell e^{-\frac{A_\ell}{g}} \sum_n a_n^{(\ell)} g^n.$$

They are called trans-series and go beyond traditional asymptotic expansions since they include explicit exponentially small corrections. It actually turns out that already in the large-order behavior of the coefficients of the perturbative series there is much information on the NP effects, and looking at the singularity structure of the Borel transforms we can reconstruct the trans-series. The general framework to study these relations is the theory of resurgence [6].

A series is said to be Borel summable if no singularity hinders the integration to be performed for the resummation. Furthermore, if we can prove that we are reconstructing the exact function, namely the asymptotic series is Borel summable to exact result, the trans-series will contain only the perturbative part. In these cases we do not have to worry about any additional NP correction. The only obstacle left between us and the exact result is the computation of as many coefficients as possible. The longer perturbative series we manage to calculate, the more accurate will be our evaluation of the final result we are interested in. When instead singularities are in the domain of integration, the perturbative series is said to be non-Borel summable. Properly deforming the contour of integration we can anyhow perform the resummation, at the cost, however, of introducing a NP ambiguity dictated by our choice in the deformation of the contour. This ambiguity will eventually be compensated by the contributions coming from other sectors $\ell > 0$ of the trans-series. This time reproducing the exact result will be considerably more complicated. We have to write down the trans-series and to combine the result of the (lateral) Borel resummation of its series. In order to write down the trans-series, we can exploit resurgence relations to reconstruct the coefficients $a_n^{(\ell)}$, but this requires a detailed knowledge of the asymptotic form of the perturbative coefficients a_n .

In this thesis we are going to investigate QFT in $d < 4$ space-time dimensions via perturbation theory and Borel resummation techniques. We will do so both in the case of Borel summable perturbative series and non-Borel summable ones. In the former, we focus on $O(N)$ models, where Borel summability has been established [7–9], we investigate the critical regime and phase diagrams paying particular attention to the renormalization scheme dependence. In the latter, instead, we choose some notable examples of integrable field theories that at the same

time have a rich physical phenomenology and renormalons and for which we can extract long perturbative series. We study their resurgent properties. Renormalons lead to singularities of the Borel transform and to NP contributions in the trans-series, but differently from instantons, whose semiclassical interpretation is clear, our knowledge regarding them is still very limited.

Below, we highlight the main new results of this thesis and present its structure.

Chapter 2. We introduce the reader to some basic concepts that will be fundamental throughout the rest of the thesis: Borel resummation and theory of resurgence. Starting from the asymptotic character of the perturbative series, we quickly examine tools and procedures to go beyond standard perturbation theory. The discourse remains quite general, although we associate physical meaning with the objects we encounter along the way. The review takes place with the help of a simple example presented multiple times from different points of view.

Chapter 3. We study N -component ϕ^4 theories in $2 \leq d < 4$ dimensions, using Borel resummation techniques of the perturbative series at fixed integer dimensions. We will consider in particular $d = 2$, $N = 1$ ϕ^4 theory and $O(N)$ models in $d = 3$. At fixed dimension we can not study directly the critical theory due to the presence of IR divergences. Nevertheless, in a physical renormalization scheme, the gapless phase can be reached starting from the unbroken phase by Borel resumming the perturbative series [10]. The usage of perturbative Renormalization group (RG) techniques has been at the base of several works for the extraction of critical exponents using resummation techniques. Since the coupling constant is relevant in $d < 4$ dimensions, the RG is entirely governed by renormalization scheme-dependent terms. Thus, we introduce a different class of renormalization schemes (RSs), that we call “minimal”. In these schemes divergences are removed without the need of possibly inverting infinite perturbative series and counterterms contain a finite number of terms in perturbation theory. Moreover, in these schemes, that we indicate by \mathcal{S} , the critical phase is defined when the physical mass gap M^2 vanishes, while in the non-minimal RS used in ref. [10], that we indicate by $\tilde{\mathcal{S}}$, it is reached looking for zeroes of the β -function. The minimal schemes have several advantages. We show that only in such schemes the known proofs of Borel summability apply.¹ Moreover, working in minimal schemes, we are able to find non-perturbative, finite changes of scheme. Exploiting them, we investigate the phase diagram of 3d $O(N)$ models (and 2d $N = 1$ ϕ^4 theory), we find that they admit two descriptions connected by a strong-weak duality relation (within the same phase of the theory), closely related to the one found by Chang and Magruder long ago [11, 12].

We determine the exact analytic renormalization dependence of the critical couplings in the weak and strong branches as a function of the renormalization scheme (parametrized by κ) and for any N . It is shown that for $\kappa = \kappa_*$ the two fixed points merge and then, for $\kappa < \kappa_*$, they

¹It should be stressed that we are not claiming here that the theory is not Borel resumable in RSs such as the one in ref. [10], but that this does not automatically follow from proofs performed in other schemes [7–9].

move into the complex plane, making the phase transition no longer visible from the classically unbroken phase. Similar considerations apply in 2d for the $N = 1$ ϕ^4 theory, where the role of classically broken and unbroken phases is inverted. We verify all these considerations Borel resumming the perturbative series. In $d = 2$ looking at the scheme dependence of the critical coupling and at the effectiveness of the Borel resummation in the determination of the critical exponent ν . If in 2d we mapped an already computed series in different RSs, for the 3d $O(N)$ models we computed from scratch the perturbative series for the vacuum energy and for the mass gap up to order eight. We provide numerical evidence for the self-duality and verify that in renormalization schemes where the critical couplings are complex the theory is gapped. However, the study of the critical regimes is hindered by large uncertainty. We improved our numerical techniques and computed also the series for the 1PI functions $\Gamma^{(2)'}$ and $\Gamma^{(4)}$ at zero external momentum up to order eight. Interestingly enough, studying the critical regime in RS \tilde{S} in $d = 3$ grants more accurate results. As a byproduct of our study, we are about to share in [4] a complete package containing the values of all the Feynman diagrams in $d = 3$ up to order eight and many other useful tools.

Chapter 4. We study in detail the interplay between resurgent properties and the $1/N$ expansion in various integrable field theories with renormalons. In theories with renormalons the perturbative series is factorially divergent even after restricting to a given order in $1/N$, making the $1/N$ expansion a natural testing ground for the theory of resurgence. We look at three asymptotically free theories in two dimensions which are integrable: the $O(N)$ non-linear sigma model (NLSM), the $SU(N)$ principal chiral field (PCF), and the $O(N)$ Gross–Neveu (GN) model. They have renormalons and at the same time can be studied in detail, both in perturbation theory and in the $1/N$ expansion. We focus on the free energy in the presence of a chemical potential coupled to a conserved charge, which has a non-trivial structure and can be computed exactly with the thermodynamic Bethe ansatz (TBA). The TBA equations can be exploited to generate several terms in the $1/N$ expansion, and thanks to a powerful method developed in [13, 14] it is possible to extract the perturbative series for the free energy at very high orders. Our investigations in the three models lead to very different findings. In some examples, like the first $1/N$ correction to the free energy in the NLSM, the terms in the $1/N$ expansion can be fully decoded in terms of a resurgent trans-series in the coupling constant. In the PCF we find a new, explicit solution for the large N free energy which can be written as the median resummation of a trans-series with infinitely many, analytically computable IR renormalon corrections. However, in the GN model, each term in the $1/N$ expansion includes non-perturbative corrections which can not be predicted by a resurgent analysis of the corresponding perturbative series. Moreover, in this chapter we try to answer the question regarding the nature of the $1/N$ expansion itself. While for the NLSM and PCF model longer series would be needed for conclusive results, in the GN model, where this is convergent, we analytically continue the

series beyond its radius of convergence and show how the continuation matches with known dualities with sine-Gordon theories.

Chapter 2

Borel resummation and Resurgence

Interacting theories in quantum field theory (QFT) that are exactly solvable are the exception rather than the rule. Luckily, in a broad range of different systems, we can resort to perturbation theory, one of the few universal analytical tools we have in quantum physics. However, the perturbative series typically are divergent asymptotic series. Dyson first in the context of Quantum Electro Dynamics presented a simple argument on why this has to be the case [5]. Dyson's argument can be rephrased in a more general form such that it concerns most of QFTs and quantum mechanical systems. Let's consider a generic observable in the path integral formulation in quantum mechanics (QM) or QFT:

$$\mathcal{E}(g) = \int \mathcal{D}\phi G[\phi] e^{-\frac{S[\phi]}{g}}, \quad (2.1)$$

where $S[\phi]$ is the Euclidean action and ϕ denotes collectively all the fields. We see that the point $g = 0$, around which we are expanding, has to be a singular point since as soon as we move to negative values, the physics changes completely, and $\mathcal{E}(g)$ blows up being the exponent unbounded from below. We conclude that perturbative expansions generically have null radius of convergence and are divergent. The asymptotic character of these series brings with itself a plethora of interesting mathematical and physical consequences that are worth studying. The most important ones are: optimal truncation, the Borel resummation, the presence of non-perturbative effects, their link with the large-order behavior of the series coefficients, the need to upgrade the perturbative series to a trans-series, and the whole general framework of the theory of resurgence.

In this chapter, we will briefly review these aspects together with some of the key introductory ingredients for the vast framework of the theory of resurgence.

2.1 Asymptotic Series

A formal power series

$$\varphi(x) = \sum_{n=0}^{\infty} a_n x^n \quad (2.2)$$

is asymptotic to the function $f(x)$ if, for every N , the remainder after $N + 1$ terms of the series is smaller than the last retained term as $x \rightarrow 0$, i.e.

$$f(x) - \sum_{n=0}^N a_n x^n = \mathcal{O}(x^{N+1}), \quad \text{as } x \rightarrow 0. \quad (2.3)$$

Notice that the truncated series, $\varphi_N(x) = \sum_{n=0}^N a_n x^n$, does not approach $f(x)$ in the limit of $N \rightarrow \infty$ for any fixed x , in contrast to what happens in convergent series. This leads to two new remarkable features when compared to series with non-vanishing radius of convergence. Different functions can have the same asymptotic expansion: all the functions of the form

$$\tilde{f}(x) = f(x) + h(x) e^{-\alpha/x} \quad (2.4)$$

have indeed the same expansion around $x = 0$ for any α and any $h(x)$ sufficiently regular function. Adding more and more terms in the partial sum, i.e. increasing N , we will first approach the true value of $f(x)$, but after a while, inevitably, we will restart to get away from it and eventually, our truncated series will diverge. It is natural to ask which is the partial sum that gives the best possible estimate of $f(x)$, in other words, which is $N = N_{\text{Best}}$ that truncates the series in the optimal way, so that the remainder $\Delta_N = f(x) - \varphi_N(x)$ is minimized. This procedure is called *optimal truncation*. The maximal “resolution” we can achieve with this method depends on the behavior of the coefficients a_n of our series at large n . Let us assume that for $n \gg 1$

$$a_n \approx \Gamma(n + b) A^{-n}, \quad (2.5)$$

with the parameter b real positive, we will get to see that this is the typical form in most of the interesting cases.¹ Minimizing an estimate of the reminder we obtain:

$$N_{\text{Best}} \approx \left\lfloor \frac{|A|}{x} \right\rfloor \quad \text{and} \quad \Delta_{N_{\text{Best}}} = \epsilon(x) \approx e^{-|A/x|}. \quad (2.6)$$

A couple of aspects are worth emphasizing. Notice that the more we go at strong coupling, the fewer and fewer terms we should keep till we reach a point for which optimal truncation makes the whole series useless. Moreover, notice that the optimal resolution $\epsilon(x)$ of an asymptotic

¹The series of this kind are Gevrey-1 series, we could generalize the analysis that follows by taking instead Gevrey- p formal series whose large-order behavior is of the kind $a_n \approx \Gamma(pn + b)$.

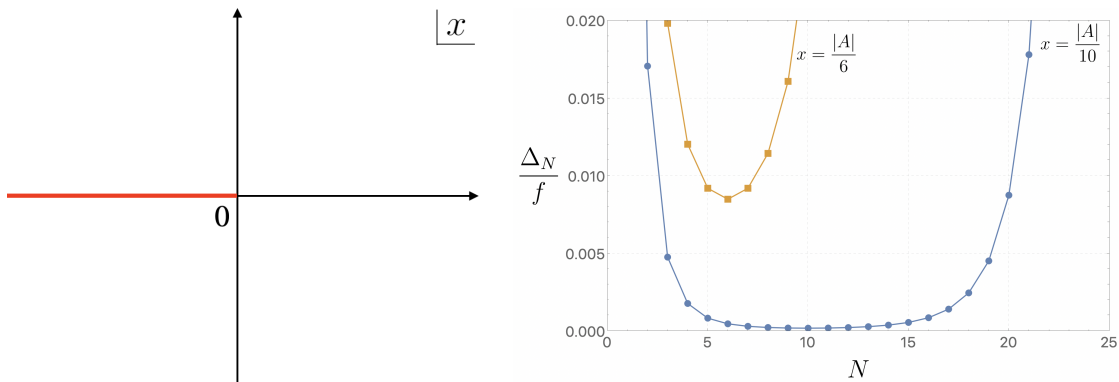


Figure 2.1: (Left) The complex plane x with in red the branch-cut $[-\infty, 0]$ of the function $f(x)$ defined in (2.7). (Right) The ratio $\Delta_N(x)/f(x)$ as a function of N at which we are truncating the asymptotic series, for $f(x)$ defined in (2.7).

series is consistent with the intrinsic ambiguity of (2.4), this is sometimes called *non-perturbative ambiguity*. Its strength is given by the absolute value of A , namely the factor that determines the growth behavior at next-to-leading order after the factorial. Finally, it is interesting to comment on the effectiveness of a divergent series when we find ourselves in the case at very weak coupling, $x \ll |A|$, if we have access to a fairly few coefficients of our series $N < N_{\text{Best}}$, as it happens in several physical cases, we are allowed to neglect the divergence of the series altogether.

Example Let us consider the function

$$f(x) \equiv \int_0^\infty dt \frac{e^{-t}}{1 - xt/A} \quad \text{with} \quad A < 0. \quad (2.7)$$

Despite being very simple, it has all the typical features of our divergent series. The function $f(x)$ is not analytic in $x = 0$, and it has a branch-cut all along the real negative axis, see the left panel in fig. 2.1. When we expand $f(x)$ at the origin we find the divergent series $\varphi(x) = \sum_0^\infty A^{-n} n! x^n$. In the right panel of fig. 2.1 we show the ratio between the reminder $\Delta_N(x)$ and the $f(x)$ for $x = |A|/10$ and $x = |A|/6$ as a function of N at which we are truncating the series. Notice that the values of N_{Best} are, as expected, 10 and 6, respectively.

We have seen how optimal truncation allows keeping somehow under control the divergence of our asymptotic series, but it is far from being satisfactory, especially at stronger coupling. We will see how we can do much better taking into account all the information of the terms of the series and possibly also incorporating the small exponential effects that started to show up.

2.2 Borel Resummation

The Borel resummation is a standard tool to make sense of asymptotic expansions and try to construct functions from their expansions. Given a divergent series $\varphi(x)$ like the one in (2.2), with the typical large-order behavior of (2.5), we define its *Borel transform* $\mathcal{B}\varphi(z)$ as the function obtained by removing the factorial growth of its coefficients

$$\varphi(x) = \sum_{n=0}^{\infty} a_n x^n \quad \Longrightarrow \quad \mathcal{B}\varphi(t) = \sum_{n=0}^{\infty} \frac{a_n}{n!} t^n. \quad (2.8)$$

Now the Borel transform is analytic in a neighborhood of the origin $t = 0$ and its coefficients grow exponentially. It has a non-zero radius of convergence, determined by the nearest singularity at $t = A$, pole or branch-cut. However, typically $\mathcal{B}\varphi(t)$ can be continued to a wider region in the complex plane. If the positive real axis is free of singularities, we can inverse Laplace transform it to compute what is called the *Borel resummation* $s(\varphi)(x)$ of the original series $\varphi(x)$,

$$s(\varphi)(x) = \int_0^{\infty} dt e^{-t} \mathcal{B}\varphi(xt). \quad (2.9)$$

In this case we say that $\varphi(x)$ is *Borel summable*. The Borel resummation $s(\varphi)(x)$ and the function $f(x)$, the original function we expanded, are both asymptotically equivalent to the same divergent series. We will indicate “asymptotically equivalent to” with the symbol \sim . However, since different functions can admit the same asymptotic series, only after assuming some analyticity properties of $f(x)$ near the origin we can prove that $s(\varphi)(x) = f(x)$.² On the other hand, in certain cases we might be able to rewrite $f(x)$ in the form (2.9) and so the $s(\varphi)(x) = f(x)$ is proven directly.³ Summarizing, $s(\varphi)(x)$ finally associates a finite value to the divergent sum (2.2), for each x . Moreover, when $s(\varphi)(x) = f(x)$ we reconstructed the exact (non-perturbative) result from the asymptotic series, the asymptotic series is Borel summable to the exact result.

Example Let us continue with the same function of the first example and construct the Borel transform associated to the series $\varphi(x)$. It is going to be

$$\mathcal{B}\varphi(t) = \sum_{n=0}^{\infty} A^{-n} t^n = \frac{1}{1 - t/A}. \quad (2.10)$$

²These assumption have been given by Watson (see e.g. theorem 136 in chap.VIII of ref. [15]). An improved version was found by Nevanlinna and rediscovered in ref. [16]. In section 3.3, we will encounter them when briefly reviewing the early proofs of the Borel summability of Schwinger functions in the $d = 2$ [7] and $d = 3$ [8] $N = 1$ ϕ^4 theory.

³See the recent works [17, 9].

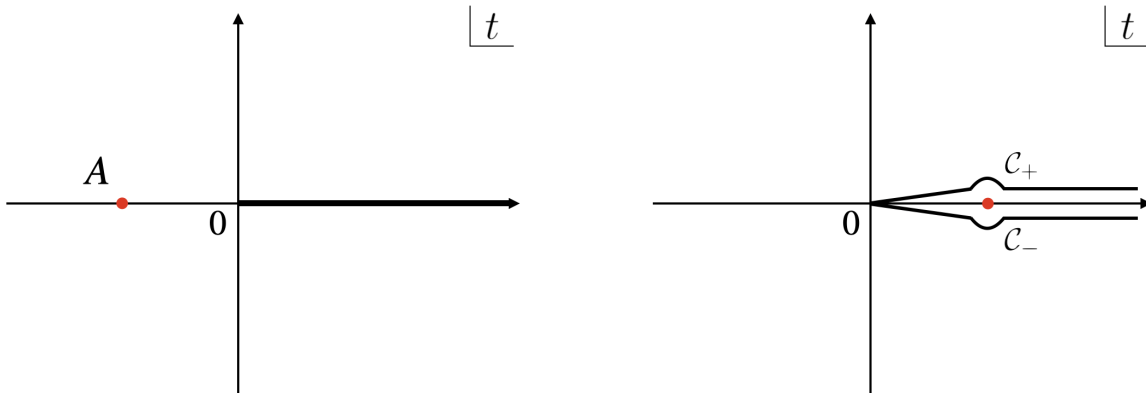


Figure 2.2: (Left) The complex plane of t , Borel plane, for the function defined in (2.10), with singularity at $t = A$ with $A < 0$, the path of integration for the inverse Laplace transform is along the positive real axis. (Right) In the case of $A > 0$, a singularity forces us to deform the integration contour to avoid it from above or below, \mathcal{C}_+ and \mathcal{C}_- respectively.

Now since $A < 0$ we know that we can Borel resum $\varphi(x)$ and that since we get the original definition of the function in (2.7) $s(\varphi)(x) = f(x)$. This example is one of those cases where the uniqueness comes for free from the form of the starting function. In the left panel fig. 2.2 we plot on the plane of complex t , the Borel plane, with the singularity of $\mathcal{B}\varphi(t)$ and the path of integration for the inverse Laplace transform.

In physical interesting cases, even in the case of asymptotic series is Borel summable to the exact result, the story is not that simple: typically we do not know all $\varphi(x)$ but a truncated version of it. Therefore, we have to find ways to approximate $\mathcal{B}\varphi(t)$ and analytically continue it on the whole positive real axis. Section 2.5 will be dedicated to this topic. We are now going to investigate what happens when singularities hinder the integration (2.9) and what can be done.

2.2.1 Lateral Borel Resummation and NP contributions

In case of one or more singularities located on the positive real axis, the integration in (2.9) is ill-defined. This should not stop us from proceeding. In fact, we will show that going on will bring us to far-reaching conclusions.

We can deform the contour of integration slightly above or below the positive real axis. The function obtained in this way are

$$s_{\pm}(\varphi)(x) = \frac{1}{x} \int_{\mathcal{C}_{\pm}} dt e^{-t/x} \mathcal{B}\varphi(t), \quad (2.11)$$

where \mathcal{C}_{\pm} are the contours avoiding the singularities, as in the right panel of fig. 2.2. The functions $s_{\pm}(\varphi)(x)$ are called *lateral Borel resummations* of $\varphi(x)$. Since we deformed our integration

along paths in the complex plane, even if all coefficients of our series are real, the lateral Borel resummations will be, in general, complex-valued functions. Notice that the choice of the path gives rise to an ambiguity and the order of this ambiguity, supposing the usual large-order behavior (2.5), is $e^{-|A/x|}$. Once again, we see the appearance of an exponentially small extra contribution that could not be captured by our original series $\varphi(x)$, but at the same time is encoded in its coefficients, or better, in their growth.

Example This time let us consider our usual series $\varphi(x) = \sum_0^\infty A^{-n} n! x^n$ but with $A > 0$. We can construct the Borel transform of (2.10), but this time the singularity is on the integration path for the inverse transform, so we perform a lateral Borel resummation, see the right panel of fig. 2.2. It is interesting to evaluate the (non-perturbative) ambiguity

$$\epsilon(x) = s_+(\varphi)(x) - s_-(\varphi)(x) = \frac{1}{x} \int_{\mathcal{C}_+ - \mathcal{C}_-} dt e^{-t/x} \mathcal{B}\varphi(t) = \frac{1}{x} \oint_{C_A} dt \frac{e^{-t/x}}{1 - t/A} = \frac{2\pi i}{x} A e^{-A/x}, \quad (2.12)$$

where C_A is the circle surrounding the pole.

The interesting cases are certainly more complicated than this. In most cases, not all the coefficients are known. Nevertheless, one can try to look at the large-order behavior. It will be of the kind (2.5). The fact that the series is alternating in sign, has some other type of periodicity, or is non-alternating can give us an important clue on the location of the dominating singularity and hence on the summability of the series.

2.3 Large-order behavior and NP effects

The large-order behavior of the divergent series is controlled by the singularities of its Borel transform. The typical large-order behavior in (2.5), as we have seen, gives rise to a singularity at $t = A$, while b instead characterizes the brunch-cut structure of $\mathcal{B}\varphi(t)$ at $t = A$ (in the presented example we took $b = 1$ and so we had just a pole singularity). At the same time the singularity structure of the Borel transform determines the way in which the Borel resummation “jumps” when we adopt different prescriptions to avoid the singularities. We have

$$a_n \approx \Gamma(n + b) A^{-n}, \quad \mathcal{B}\varphi(t) \propto \left(1 - \frac{t}{A}\right)^{-b} + \dots, \quad \text{and} \quad \epsilon(x) \approx x^{-b} e^{-A/x}. \quad (2.13)$$

These are respectively properties of the divergent series, its Borel transform, and the Borel resummation, and they are in direct relation with each other (as we have shown in the case with this exact growth with $b = 1$).

Before inserting these elements into a proper framework and looking at a generalization, let us dedicate the rest of this section to giving a better, more physical, interpretation to A . We

start with the simplest zero-dimensional prototype for the general path integral of (2.1)

$$Z(x) = \frac{1}{\sqrt{x}} \int_{\mathcal{C}_0} dz e^{-V(z)/x}, \quad (2.14)$$

where $V(z)$ is in general a complex function and, for simplicity, an entire function and \mathcal{C}_0 is the real axis. The perturbative expansion of $Z(x)$ around $x = 0$ corresponds to the saddle-point expansion of the integral (2.14). We expect this expansion to be asymptotic. Due to the fact that the function $V(z)$ in general has multiple saddle points and each one with its own perturbative expansion, we have to combine them properly deforming the integration contour, effectively splitting it into a sum of several disjoint contours. These are going to be the steepest descent trajectories associated to each saddle point. This procedure and the way of combining them is called Lefschetz-thimble decomposition.⁴ No matter if the saddle points contribute to the integral (2.14), they govern the large order behavior of the series expansion of adjacent saddles. Let $z_c^{(i)}$ the i saddle-point of $V(z)$ and let be $c_n^{(i)}$ the coefficients of the series associated to it, the large order behavior of expansion around $z_c^{(0)}$ is given by [19]

$$c_n^{(0)} \approx \Gamma(n) \left(V(z_c^{(1)}) - V(z_c^{(0)}) \right)^{-n}, \quad (2.15)$$

where $z_c^{(1)}$ is the leading adjacent saddle to $z_c^{(0)}$. Thus the difference between the values of $V(z)$ at the saddle determines the factor A in the large-order behavior and so the position of the leading singularity on the Borel plane.

Now moving to QM and QFT, the non-trivial saddle points are the instanton configurations and the singularities on the Borel plane are the complex instantonic actions. The connection between the large-order behavior of perturbation theory and non-perturbative effects was first noticed at the quantitative level in QM by Bender and Wu considering the quartic anharmonic oscillator in [20] and after extended to QFT by Lipatov [21] and other authors [22–24].

The quartic anharmonic oscillator is indeed nowadays one of the most straightforward models to study. It is possible to extract the perturbative series for the ground state energy E as a function of the coupling g and see how the growing number of Feynman diagrams, order by order, is at the origin of the factorial divergence of this series. Moreover, it can be shown how the next-to-leading exponential growth is determined by a one-instanton configuration at negative values of the coupling. The perturbative series actually turns out to be alternating in sign and Borel resummable, since the singularity of its Borel transform is on the negative real axis. The presence of this instanton determines a discontinuity for E at negative values of the coupling, this makes $g = 0$ a non-analytic point. Finally, this discontinuity appears as the difference between the lateral Borel resummations when performed over and under the negative real axis.

Likewise, in QFT an instanton configuration ϕ_* with finite action $S[\phi_*]$ gives rise to a singu-

⁴For an introduction on this topic, see e.g. section 3 of [18].

larity at $S[\phi_*]$ in the Borel transform of any correlation function. Out of the infinite integration variables of the path integral we can single out the one corresponding to the value of the action and rewrite the generic path integral (2.1) as [25]

$$\mathcal{E}(g) = \int \mathcal{D}\phi G[\phi] e^{-\frac{S[\phi]}{g}} = \int_0^\infty dt e^{-t} \int \mathcal{D}\phi G[\phi] \delta\left(t - \frac{S[\phi]}{g}\right) = \int_0^\infty dt e^{-t} B(gt). \quad (2.16)$$

The function $B(gt)$ is now the path integral restricted to the section of phase space with fixed action and plays essentially the role of Borel transform of $\mathcal{E}(g)$. If we have finite action instantons ϕ_* then $B(gt)$ is singular at $S[\phi_*]$. In fact, the manipulation in (2.16) is actually not legitimate when there are finite action critical points for real field configurations, apart from the trivial one. This argument is indeed quite heuristic if not treated with proper care as done in ref. [9], where it is used together with Derrick's theorem and steepest descent methods to establish Borel summabilities of a large class of scalar field theories in $d < 4$.

In QFT there is another type of source of factorial divergence in perturbation theory. They are the so-called *renormalons*. Like instantons they give origin to singularities on the Borel plane, but they are of completely different nature. They were first discovered in renormalizable QFT [26], but we still lack their complete understanding. Renormalons will play an important role in chapter 4.

2.4 Theory of Resurgence

In this section we arrange the elements already presented in the context of the theory of resurgence [6], this will allow us to generalize several concepts and introduce some new important elements.⁵ First of all, we need a single object that gathers both the perturbative series and non-perturbative contributions. Let us introduce

$$\Phi(x, C) = \varphi^{(0)}(x) + \sum_{\ell=1}^{\infty} C^\ell e^{-\frac{\ell A}{x}} \varphi^{(\ell)}(x) \quad \text{with} \quad \varphi^{(\ell)}(x) \equiv \sum_{n=0}^{\infty} a_n^{(\ell)} x^n. \quad (2.17)$$

and call it a *trans-series*. Notice that it upgrades the power series by the inclusion of non-analytic terms. In fact, we can view it as a double series in two parameters: a perturbative one x and a NP one $e^{-A/x}$. The series $\varphi^{(0)}(x) = \varphi(x)$ is the usual perturbative series. There are more general versions of trans-series, depending on the quantity and model that we are studying. For example, there could be several instanton actions (or renormalon singularities) A_i , in this case the sum will be on several ℓ_i with different prefactors C_i .⁶ Moreover, in general the series $\varphi^{(\ell)}(x)$

⁵The framework of the theory of resurgence is very vast and this section, despite the title, is far from being an introduction to the topic, for that see e.g. [27], an introduction that includes an extensive list of references. Suggested pedagogical review are also [28, 29].

⁶The most general form of trans-series has a quite richer structure, e.g they can contain also terms like $\log(x)$.

can have a prefactor x^{-b_ℓ} where b_ℓ is a characteristic exponent. It is important to remark that the series $\varphi^{(\ell)}(x)$ are generically asymptotic series, thus $\Phi(x, C)$ generically diverges for every non-vanishing values of x . The parameter C is called the *trans-series parameter*. It weights the NP contributions and, as we will see, it cannot be determined a priori, its value does not enter directly in the resurgent relations, but it plays a very important role. Many important trans-series can be interpreted as solutions to ordinary differential equations (ODEs) with irregular singular points.

Example Let us continue with our usual example from a new point of view. The ODE

$$x^2 \frac{df}{dx} + (x - A)f(x) + A = 0 \quad (2.18)$$

is a variation of Euler's equation, that has an irregular singular point at $x = 0$. It is easy to see that the asymptotic power series $\varphi^{(0)}(x) = \sum_{n=0}^{\infty} a_n x^n$ with $a_n = A^{-n} n!$ is solution of (2.18). In addition, we can construct a one-parameter family of formal solutions to the ODE

$$\Phi(x, C) = \varphi^{(0)}(x) + C x^{-1} e^{-\frac{A}{x}}. \quad (2.19)$$

We found the trans-series associated to our usual divergent series. Moreover, we start to appreciate the role of the trans-series parameter C : it parametrizes different choices of boundary conditions for our problem.

In the example just presented, the series in ℓ is truncated since we were dealing with a linear ODE. When passing to nonlinear ones, we find a structure like the one in (2.17) or more complicated.

Let us now look the trans-series in the context of the Borel resummation. We construct the Borel transform $\mathcal{B}\varphi^{(0)}(t)$ of the perturbative series. In the case of the trans-series (2.17), we expect $\mathcal{B}\varphi^{(0)}(t)$ to have singularities at the values $t = \ell A$ for $\ell \in \mathbb{N}$ and $\ell > 0$. It can be shown that the expansions around these singularities are in direct contact with the Borel transforms of the series of the other NP sectors, if we consider logarithmic branch-cuts,

$$\mathcal{B}\varphi^{(0)}(t) \Big|_{t=\ell A} = -\frac{S^\ell}{2\pi i} \log(t) \mathcal{B}\varphi^{(\ell)}(t). \quad (2.20)$$

Already inside the perturbative series we have information regarding all the non-perturbative sectors, or better all the information regarding all other sectors. The constant S is called *Stokes constant*. Since the singularities of the Borel transforms dictated the large-order behavior of

their associated asymptotic series we can rewrite relation (2.20) in terms of the coefficients $a_n^{(\ell)}$,

$$a_n^{(0)} \approx \Gamma(n) A^{-n} \sum_{\ell=1}^{\infty} \frac{S^\ell}{2\pi i} \ell^{-n} \sum_{k=0}^{\infty} (\ell A)^k \frac{\Gamma(n-k)}{\Gamma(n)} a_k^{(\ell)}, \quad (2.21)$$

valid at large order.

When Borel resumming the series we already know that particular care has to be taken when we would like to integrate along a ray that crosses singularities. Let us introduce the generalized version of the Borel resummation along an arbitrary direction with angle θ on the complex plane, s_θ . Its integration path is $(0, e^{i\theta} \infty)$ and trivially $s_0(\varphi) = s(\varphi)$. The respective generalization for lateral Borel resummations are $s_{\theta\pm}$, in which we avoid the singularities on the direction with angle θ above or below. The directions along which our Borel transform has singularities are called *Stokes lines*. We know already that there will be an ambiguity concerning how these singularities should be avoided by deforming the integration contour and that this ambiguity encloses information concerning other (NP) sectors. Now since trans-series incorporate all of them, we should look at the whole Borel resummed trans-series,

$$s_\theta(\Phi)(x; C) = s_\theta(\varphi^{(0)})(x) + \sum_{\ell=1}^{\infty} C^\ell e^{-\frac{\ell A}{x}} s_\theta(\varphi^{(\ell)})(x). \quad (2.22)$$

Focusing on our example with just one type of instanton contribution A , we have that at $\theta = \arg(A)$ there will be a Stokes line, and, thanks to the resurgent relations of the kind of eq. (2.20), the following equation will be true,

$$s_{\theta+}(\Phi)(x; C) = s_{\theta-}(\Phi)(x; C + S). \quad (2.23)$$

The trans-series parameter jumps when crossing the Stokes line.

Example In the simple case that we are examining, for the trans-series (2.19) we choose the normalization $\varphi^{(1)} = A$, so that recalling (2.12) we have

$$s_{\theta+}(\varphi^{(0)})(x) - s_{\theta-}(\varphi^{(0)})(x) = S x^{-1} e^{-\frac{\ell A}{x}} \varphi^{(1)}(x), \quad \text{with} \quad S = 2\pi i \quad (2.24)$$

and it is direct to see that (2.23) is valid.

When one has a richer structure the relation (2.24) becomes rapidly more complicated, in the case of (2.17)

$$s_{\theta+}(\varphi^{(\ell)})(x) - s_{\theta-}(\varphi^{(\ell)})(x) = \sum_{k \geq 1} \binom{\ell+k}{\ell} S^k e^{-\frac{kA}{x}} s_{\theta-}(\varphi^{(\ell+k)})(x), \quad \ell \geq 0. \quad (2.25)$$

In this and even richer cases, all the relations between the different sectors ℓ become more clear when introducing other operators such as the Stokes automorphism and the alien derivatives. However, they go beyond the scope of this work, we suggest again [27] for a pedagogical introduction.

Let us look back at the relation (2.23) and at the role of the trans-series parameters. We have seen that their values do not enter in the resurgence relations, namely they are not encoded in the behavior of the coefficients of any of the series. At the level of trans-series they remain generic parameters. Their values are fixed together with the prescriptions on how to Borel resum the trans-series, namely on how to choose the integration path, and thanks to additional NP information, such as the reality of the exact function. For example, given $f(x) \sim \Phi(x, C)$ for which the real axis is a Stokes line, there will be C_+ and $C_- = C_+ + S$, such that one can reconstruct $f(x) = s_+(\Phi)(x; C_+) = s_-(\Phi)(x; C_-)$.

The idea that different sectors “talk” to each other sounds very reasonable if we go back to our zero-dimensional path integral of eq. (2.14), we have already seen in (2.15) that saddle points determine each other expansions.⁷ The same is valid for path integrals in QM and QFT, the sectors in the trans-series are nothing but the perturbative expansion for $\ell = 0$ and for $\ell > 0$ the ℓ -instanton sectors with the power series $\varphi^{(\ell)}$ being the result of perturbation theory computed around the instanton backgrounds. However, there are also NP effects for which we still lack a very clear semiclassical interpretation that are at the origin of singularities on the Borel plane, that enter in the trans-series, and for which resurgence seems to work anyway. These are the renormalons.

As we have already mentioned, in a typical QFT we do not have the luxury of knowing all the perturbative series. That is why a systematic implementation of resurgence is very difficult. Scenarios in which the theory of resurgence apply to the fullest are quite rare in QFT. Just in the recent years we are seeing a growing number of physical setups in which resurgence plays an important role. In chapter 4, we will present a model with a physical observable with a trans-series as in (2.17), yet analytically tractable. We will get the chance to test numerically relationship like those in (2.25).

2.5 Numerical approaches for Borel transforms

In physical interesting problems the exact form of the Borel transform $\mathcal{B}\varphi(t)$ is usually not available. For most QM and QFT observables, we can only obtain a finite number of terms in the perturbative series. That is why prior to inverse Laplace transform we need to find a way to approximate $\mathcal{B}\varphi(t)$. We can not simply truncate the series (2.8) up to some order N and exchange the order of sum and integration. This will give us back our original truncated

⁷Moreover, saddle-point analysis and Lefschetz-thimble decomposition lies at the center of the origin of the Stokes phenomena and of the Stokes lines.

asymptotic expansion. In exchanging the sum and integration we would end up committing a similar misstep as the original one when we generated the perturbative series. The function $\mathcal{B}\varphi(t)$ has a finite radius of convergence dictated by the first singularity, $\rho = |A|$, but at the same time the integration we need to perform is over the whole positive real axis

$$s(\varphi)(x) = \int_0^\infty dt e^{-t} \sum_{n=0}^{\infty} \frac{a_n}{n!} (xt)^n \neq \sum_{n=0}^{\infty} \frac{a_n}{n!} x^n \int_0^\infty dt e^{-t} t^n = \sum_{n=0}^{\infty} a_n x^n = \varphi(x). \quad (2.26)$$

For a finite truncation of the series of the Borel transform sum and integration commute but we would end up with the truncate perturbative series we started from.

In order to proceed, we can adopt two possible strategies. We can use the known coefficients to find a proper ansatz for $\mathcal{B}\varphi(t)$, namely whose expansion matches our coefficients. An effective way of doing so is to use Padé approximants. On the other hand, we can enlarge the radius of convergence over the whole domain of integration by manipulating the series. We can achieve this via a conformal map. Both methods provide an approximation of the exact result that improves with the number of the known coefficients. It is obvious that since they are approximations, one has to provide an estimate of the uncertainty together with the result. We will devote the following two subsections to presenting the main aspects of these methods.⁸

2.5.1 Padé-Borel method

Given a series expansion of a function $h(x) = \sum_{k=0}^{\infty} h_k x^k$, its Padé approximant of order $[m/n]$ consist of the rational function

$$h^{[m/n]}(x) = \frac{\sum_{i=0}^m p_i x^i}{1 + \sum_{j=1}^n q_j x^j}, \quad (2.27)$$

where the $m + n + 1$ coefficients p_i and q_j are fixed by expanding (2.27) around $x = 0$ and matching them with h_n up to the highest possible order, i.e. $h(x) - h^{[m/n]}(x) = \mathcal{O}(x^{m+n+1})$. The usage of Padé approximants is a very efficient technique to analytically continue a function when just some coefficient of the Taylor expansion are known. Since they are manifestly analytic at the origin, they work at best when they have to approximate a function with this same property. This is why in the context of perturbative series and asymptotic expansion, it is more convenient to use them to approximate the Borel transform, hence the name Padé-Borel method.⁹ Moreover, it is known that for convergent series, parametrically diagonal Padé approximants, i.e. with

⁸There are further details that are not treated here. First of all, the generalization of the Borel transforms to the Borel-Le Roy transforms with the introduction of the parameter b . Moreover, when doing conformal mapping, another summation variable can be introduced, s . For the techniques used in this work on how to find the best values of b and s and how to give reasonable estimates to the uncertainty of the resummation with both Padé-Borel method and conformal mapping method, see [9].

⁹There are many other cases in which Padé approximants are of use. For example, in chapter 4 we will encounter a series in $1/N$ with a finite radius of convergence and consider its Padé approximants.

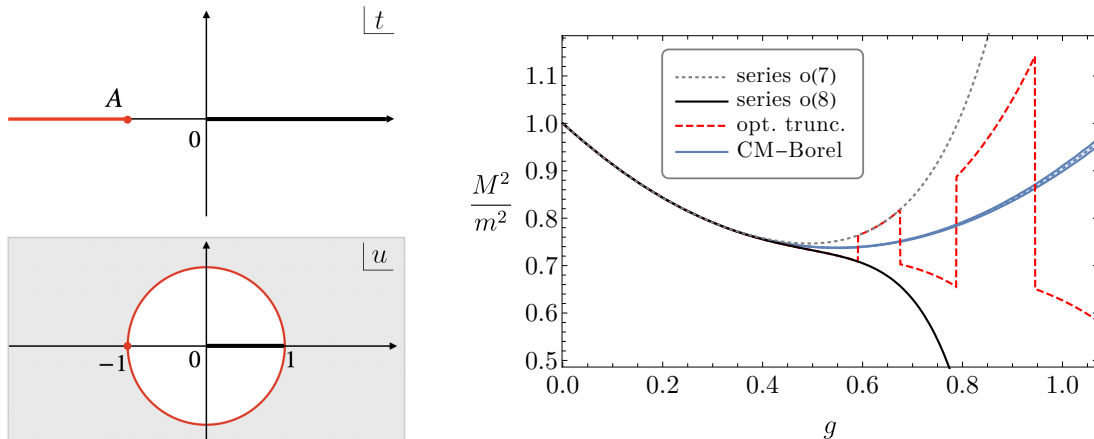


Figure 2.3: (Left up) The complex t plane for a Borel transform whose singularity is at $t = A$ on the negative real axis. The integration path as usual being on the positive real one. (Left down) The complex u plane after having performed the change of variable in (2.28). The real positive axis $t \in [0, \infty]$ got mapped into $u \in [0, 1]$ and the branch-cut $t \in [-\infty, -|A|]$ into the boundary of the disk. (Right) The mass gap M^2 for the $d = 3$ ϕ^4 theory, in the $\overline{\text{MS}}$ scheme, as a function of the coupling constant g obtained by ordinary perturbation theory up to g^7 and g^8 (dotted grey and black lines), optimal truncation (red dotted line) and Borel resummation via conformal mapping method (blue line)

$m = n$, converge (in capacity) to the exact function and the location of their poles and zeros define an appropriate locus of branch-cuts connecting branch-point singularities [30] (see e.g. app. D of [31] for a brief overview and [32] for a comprehensive introduction). Thus Padé-Borel method, when knowing a large number of coefficients, allows to accurately reproduce the Borel transform and, consequently, the Borel resummation. In addition, doing so gives the possibility of reconstructing the singularity structure of $\mathcal{B}\varphi(t)$ and gaining information on the large-order behavior of the perturbative series and on possible NP effects. On the other hand, when we have at our disposal just few coefficients, the approximant can show spurious unphysical poles that might give rise to numerical instabilities in the integration. This is why when studying the ϕ^4 models in $d = 2$ and $d = 3$ in chapter 3, this method turns out to be somewhat less effective than conformal mapping.

2.5.2 Conformal mapping method

We have seen that NP effects determine the position of the singularities of the Borel transform. We can exploit this information to manipulate our coefficients and, with a conformal map, enlarge the radius of convergence on the whole domain of integration [33]. Let us present an example in the case of the leading singularity being on the negative real axis, $A < 0$. We can use the change of variable $t \rightarrow u$ of the form

$$t(u) = 4|A| \frac{u}{(1-u)^2}, \quad (2.28)$$

so that it maps the whole plane into the disk of unit radius $|u| = 1$. Notably, the singularity at $t = -|A|$ is mapped at $u = -1$, the point at infinity in t at $u = 1$, and the branch-cut singularity $t \in [-\infty, -|A|]$ to the boundary of the disk. The integral in t from 0 to ∞ becomes an integral in $u \in [0, 1]$. Assuming any other singularity on the negative real axis the series expansion $\widetilde{\mathcal{B}}\varphi(u) \equiv \mathcal{B}\varphi(t(u))$ has radius of convergence $\rho = 1$, i.e. on the whole domain of integration, see the left panel of fig. 2.3. Thus, it is possible to commute sum and integration. When we have additional NP information about one or more singularities of the Borel transform, the conformal mapping method at low orders turns out to be more reliable than the Padé-Borel one due to the usage of this information. This will be the case of chapter 3 where we know the values of the action at the leading complex instanton configuration. In chapter 4, on the contrary, we will have (longer) non-Borel summable series, so we will not be able to use conformal mapping method and we will extensively use Padé approximants to reconstruct the Borel transform to lateral Borel resum them.

We report in the right panel of fig. 2.3 a plot that will appear later in this work (fig. 3.8). At this stage, we can neglect its physical interpretation, its purpose is just to show a comparison between some of the methods to tackle asymptotic expansions we talked about in this chapter. We are starting from a divergent truncated series in g , knowing the coefficients up to g^8 . Moreover, we know that it is Borel summable to exact result. Going towards strong coupling, we can see how at around $g = 0.5$ our perturbative series starts to break down and to diverge, black line in the plot. What we can do is to begin to keep less and less terms doing optimal truncation, the dashed line in red. This keeps under control the divergence but does provide a very inaccurate result at this stage. If instead we Borel resum our series using conformal mapping method we can confidently reproduce, the error bands are almost invisible, our exact quantity way further in the strongly coupled region. When we know relatively few coefficients of a perturbative series and we know that is Borel summable to exact result, notice how we are able to study regimes that otherwise would be totally out of reach, thanks to Borel resummation and sensible numerical approximations. This is what we will do in the next chapter.

Chapter 3

Borel Summability: To the IR fixed points in super-renormalizable ϕ^4 theories

The main aim of this chapter is to study the three-dimensional $O(N)$ symmetric ϕ^4 models and the two-dimensional $N = 1$ ϕ^4 theory using Borel resummation techniques of the perturbative series in the unbroken phase. These theories are some of the most studied examples of non-integrable theories with interesting RG flows. As well-known, by tuning the mass parameter these theories flow in the IR to a notable class of interacting conformal field theories. Perturbative RG techniques have been extensively used in the analysis of critical phenomena of these theories (see ref. [34] for a review that includes an extensive list of references). The two main approaches developed in the past use RG methods either starting from $d = 4 - \epsilon$ dimensions, the so-called ϵ -expansion [35], or by keeping the space dimension fixed at $d = 2, 3$, respectively [10]. In the ϵ -expansion we can establish in a renormalization scheme-independent and analytic way the existence of weakly coupled fixed points for $\epsilon \ll 1$. Moreover, we can directly study the critical theory because of the absence of IR divergences. The gapless phase can also be accessed, for $2 < d < 4$, using large N techniques. Both large N and ϵ -expansion techniques are however not enough if one wants to analyze the theory at finite N within a non-perturbative definition of the theory, that requires to work with fixed integer dimensions. At fixed dimension, IR divergences force us to work away from criticality with $m^2 \neq 0$. One instead considers the massive theory and establishes the presence of IR fixed points by looking for zeroes of a properly defined β -function. These are necessarily strongly coupled and require a Borel resummation of the perturbative series to be established.¹

¹Borel resummation is needed also in the ϵ -expansion if one wants to reach physical dimensions at $\epsilon = 1$ or at $\epsilon = 2$, given the asymptotic nature of the associated series. However, the Borel summability of the ϵ -expansion in the ϕ^4 theory remains to be proven. The main difficulty here is to find a non-perturbative definition of the theory

The Borel summability of the fixed dimension perturbative series in the ϕ^4 theory at parametrically small coupling and in the unbroken phase $m^2 > 0$ has been established long ago [7, 8] (see also ref. [37]) and recently extended for finite values of the coupling and to a more general class of scalar field theories, including for instance $d = 3$ N -component ϕ^4 theories with both $m^2 > 0$ and $m^2 < 0$, using steepest descent arguments [9, 38]. However, we will show that these arguments directly apply just to some classes of renormalization schemes. Not to those where the physical renormalization is only reached working order by order in perturbation, like the one used in [10], but to minimal renormalization schemes. In these schemes we can study the theory in a framework that can be compared with purely non-perturbative methods. In $d = 2$ several papers have indeed shown that the gapless phase can be reached in this way using lattice [39–42], Hamiltonian truncation [43–45]² and Borel resummation [9, 38] methods.

Moreover, we will show how working in this class of schemes, exploiting the super renormalizability of our theories, non-perturbative changes of schemes can be studied and used to investigate the phase diagram of the theories and its RS dependence. Nonetheless, it turns out that studying the critical regime of 3d the $O(N)$ models in the non-minimal RS introduced in [10] grants greater accuracy.

The chapter is structured as follows.

Content

We start in section 3.1 by reviewing known facts about RS-dependence of relevant (and irrelevant) couplings. We continue in section 3.2, where first we review the approach proposed in ref. [10], based on a properly defined β -function and then recall how the critical regime can be analyzed in minimal RSs with no need of RG techniques. In section 3.3 we briefly review the proofs of Borel summability of scalar field theories of refs. [7, 8] and ref. [9], emphasizing their renormalization scheme dependence. We show that they straightforwardly apply just to minimal RSs, where only one mass counterterm is introduced, that can be determined in closed form in perturbation theory, having only a finite number of terms. We define a specific class of minimal RSs in section 3.4, parametrized by the variable κ . We will work with them in all remaining sections apart from the last. We show that 3d $O(N)$ models (in fact, we will consider at the same time both $d = 2$ and $d = 3$) admit two descriptions, equivalent to all orders in perturbation theory, related by a strong-weak duality relation (within the same phase of the theory), closely linked to a duality found by Chang and Magruder [11, 12]. In section 3.5 we describe this connection and the corresponding expected phase diagram for $N = 1$. We carry on

in d -dimensions for non-integer d . So far the Borel summability is assumed based on the large-order behavior of the series [22] and the successful results of numerical resummations at finite order, see e.g. ref. [36] for a recent six-loop study.

²Hamiltonian truncations based on light-cone quantization have also been used [46, 47] but they require a non-trivial transformation to get mapped to the minimal covariant schemes we will discuss [48, 49].

in section 3.6 analyzing the exact analytic dependence of the critical couplings in the weak and strong branches as a function of the RS parameter κ , for any N .

From section 3.7 we report our numerical results based on Borel resummations. We start in the $d = 2$ ($N = 1$) ϕ^4 theory. Resumming the series for the mass gap M , defined as the pole of the propagator, for different values of κ , we determine how the critical coupling moves as the RS is varied, confirming the theoretical expectations. We study the effectiveness of the Borel resummation as the RS is varied by computing the accuracy in the determination of a physical observable, the critical exponent ν . In section 3.8 the numerical study is performed for the 3d $O(N)$ models. We focus our attention on the 0 and 2-point functions. We discuss how we obtained the perturbative coefficients up to order eight of the vacuum energy density Λ and of the mass gap M^2 and how they are related in different RSs. We show the absence of a gapless phase for certain values of $\kappa < \kappa_*$, and provide evidence for the self-duality of the $O(N)$ models by comparing the values obtained for Λ and M^2 in the weak branch and (part of) the strong branch close to the self-dual point. Finally, we determine how the critical coupling in the weak branch moves as the RS is varied, confirming the theoretical expectations, and we compare the values of the critical coupling with those obtained in the literature using lattice methods. The results are in fair agreement, but with large uncertainties, due to the low accuracy of our resummations. The section 3.9 is instead devoted to presenting the numerical strategies that we used to compute the perturbative series in $d = 3$ for the 1PI 0, 2, and 4-point functions up to order eight. We use these series to study the critical regime of the $O(N)$ models in the scheme proposed in [10].

3.1 RG and RS Dependence

It is well-known that RG techniques allow us to improve the perturbative expansion by resumming certain logarithmic (leading, next to leading, etc) contributions [50]. Before discussing the RS dependences of RG flows and possibly of the Borel summability, it is useful to review basic known facts about the RS dependence of β -functions and the uses of RG in ϕ^4 theories in $d < 4$. There are no new results in this section, so the expert reader might skip it and pass directly to section 3.

By definition, the β -function coefficients in mass-independent RSs (such as minimal subtraction when using dimensional regularization) depends only on the coupling constants and not on ratios of the sliding scale μ with mass parameters. In particular, in presence of p marginal couplings g_i ($i = 1, \dots, p$), we have

$$\beta_i = \mu \frac{dg_i}{d\mu} = \beta_0^{ijk} g_j g_k + \mathcal{O}(g^3), \quad (3.1)$$

where β_0^{ijk} are constants. Among mass-independent RSs, the leading β -function coefficients β_0^{ijk}

are RS-independent (for $p = 1$ the next to leading term is also RS-independent). More in general, in presence of dimensionful couplings, the β -function coefficients can be RS-dependent, even when mass effects are neglected. Indeed, if we denote by g_i and \tilde{g}_i the couplings in two different RSs, we have by dimensional analysis

$$\tilde{g}_i = g_i + \mu^{\Delta_i - \Delta_j - \Delta_k} c_{ijk} g_j g_k + \mathcal{O}(g^3), \quad (3.2)$$

where Δ_i denote the classical scaling dimensions of the couplings g_i and c_{ijk} are constant coefficients. Dimensional analysis fixes also the form of the perturbative expansion of the β -functions. In terms of the dimensionless rescaled couplings $h_i = \mu^{-\Delta_i} g_i$'s, we have

$$\beta_i = \mu \frac{dh_i}{d\mu} = -\Delta_i h_i + b_0^{ijk} h_j h_k + \mathcal{O}(h^3), \quad (3.3)$$

where b_0^{ijk} are constant coefficients. It is immediate to get the relation between the two leading β -function coefficients in the two RSs:

$$\tilde{b}_0^{ijk} = b_0^{ijk} + c_{ijk}(\Delta_i - \Delta_j - \Delta_k). \quad (3.4)$$

Universal coefficients arise when $\Delta_i - \Delta_j - \Delta_k = 0$. Renormalization schemes where classical dimensional analysis is preserved at the quantum level, like minimal subtraction when using dimensional regularization, give automatically $b_0^{ijk} = 0$ when $\Delta_i - \Delta_j - \Delta_k \neq 0$, and only keep the RS-independent coefficients.³ Such dimensional arguments have important simple implications, not always fully appreciated in the literature. For instance, in an effective field theory with irrelevant couplings and no relevant or marginal couplings, in the limit where mass effects are negligible, the dimensionless counterpart λ of the irrelevant coupling with the smallest dimension Δ has a trivial β -function to *all orders in perturbation theory*:

$$\beta_\lambda = -\Delta\lambda, \quad (\lambda \text{ smallest irrelevant coupling}). \quad (3.5)$$

This is the case, for instance, for the gauge coupling in Yang-Mills or for the quartic coupling of a ϕ^4 effective theory in $d \geq 5$. In these cases there is no analogue of the log resummation needed in treating marginal couplings and hence no need to improve the perturbative expansion. On the other hand, in mass-dependent RSs, such as momentum subtraction, dimensional arguments do not apply and in general β_λ is non-trivial. The corresponding RG flow that one obtains amounts

³This property is a consequence of dimensional regularization of setting to zero power-like divergences and keeping only the logarithmic ones. Logarithmic divergences are the only ones not saturated by UV physics and sample uniformly all energy scales. Since the IR physics should be insensitive to the details of the different RSs, we conclude that the associated β -function coefficients should be RS-independent. In presence of dimensionful couplings dimensional regularization is no longer a mass-independent RS, since by dimensional analysis β -functions can depend on masses.

to resum RS-dependent threshold effects.

3.2 Different classes of RSs in ϕ^4 Theories in $d < 4$

The bare euclidean action (or equivalently the bare Landau-Ginzburg Hamiltonian) for $O(N)$ -invariant ϕ^4 vector models reads

$$S_B = \int d^d x \left[\frac{1}{2} (\partial_\mu \phi)^2 + \frac{1}{2} m_B^2 \phi^2 + \lambda_B (\phi^2)^2 \right], \quad (3.6)$$

where $\phi = (\phi_1, \dots, \phi_N)$ is an N -component scalar. In $d = 2$ and $d = 3$, scalar theories with up to quartic couplings are super-renormalizable. Aside from the ground state energy, which will be neglected for now, only the mass term requires renormalization, the coupling constant λ_B and the elementary field (wave function renormalization) being finite. Finiteness of the coupling immediately implies that in a mass-independent RS (e.g. minimal subtraction) we have a trivial β -function to all orders in perturbation theory. There are no logs to be resummed and, like in the $d = 5$ case mentioned below (3.5), no RS-independent terms appear in β , besides the classical contribution. Yet, one can define a non-minimal RS where β is non-trivial and study the associated RG flow [10].

3.2.1 Use of RG Flows: the RS $\tilde{\mathcal{S}}$

Although the wave function renormalization Z and the coupling constant counterterm $Z_{\tilde{g}}$ are not necessary, yet we can define renormalized parameters using a momentum subtraction RS like we would do in $d = 4$ as follows:

$$\phi = \sqrt{Z} \phi_R, \quad Z m_B^2 = \tilde{M}^2 + \delta \tilde{M}^2, \quad \lambda_B = \tilde{M}^{4-d} \tilde{g} \frac{Z_{\tilde{g}}}{Z^2}, \quad (3.7)$$

and fix the counterterms by the following three conditions at zero momentum:

$$\begin{aligned} \Gamma_{ij}^{(2)}(p=0) &= \delta_{ij} \tilde{M}^2, & \frac{d\Gamma_{ij}^{(2)}(p=0)}{dp^2} &= \delta_{ij}, \\ \Gamma_{ijkl}^{(4)}(p_1 = p_2 = p_3 = 0) &= 8\tilde{g} \tilde{M}^{4-d} (\delta_{ij} \delta_{kl} + \delta_{ik} \delta_{jl} + \delta_{il} \delta_{jk}), \end{aligned} \quad (3.8)$$

where i, j, k, l are $O(N)$ indices and as usual $\Gamma^{(n)}$ are related to the bare 1PI Schwinger functions $\Gamma_B^{(n)}$ as $\Gamma^{(n)} = \Gamma_B^{(n)} Z^{n/2}$. We will denote the RS defined by (3.8) as $\tilde{\mathcal{S}}$. Correspondingly all parameters in the RS $\tilde{\mathcal{S}}$ will be labeled with a tilde. No sliding scale μ needs to be introduced, yet a β -function can be defined in the spirit of the original Callan and Symanzik derivation [51, 52]. Since λ_B does not depend on the physical mass \tilde{M} , we have $\tilde{M} d\lambda_B/d\tilde{M} = 0$, that gives rise to

the following equation

$$\tilde{\beta}(\tilde{g}) \equiv \tilde{M} \frac{d\tilde{g}}{d\tilde{M}} \Big|_{\lambda_B} = (d-4) \left(\frac{d \log(\tilde{g} Z_{\tilde{g}} / Z^2)}{d\tilde{g}} \right)^{-1}. \quad (3.9)$$

In contrast to the more familiar form of the Callan Symanzik equations for which one has $\mu d\Gamma_B^{(n)} / d\mu = 0$ and thus homogeneous equations in $\Gamma^{(n)}$, we now have (omitting $O(N)$ indices)

$$\left[\tilde{M} \frac{\partial}{\partial \tilde{M}} + \tilde{\beta}(\tilde{g}) \frac{\partial}{\partial \tilde{g}} - \frac{n}{2} \tilde{\eta}(\tilde{g}) \right] \Gamma^{(n)} = \tilde{M}^2 \tilde{\sigma} \Gamma^{(n,1)}, \quad (3.10)$$

where $\Gamma^{(n,1)}$ are the 1PI n -point functions with one insertion of the renormalized composite operator $\phi_R^2 = \phi^2 Z_{\phi^2}$ at zero momentum, while the parameters $\tilde{\eta}$ and $\tilde{\sigma}$ are defined as follows:

$$\tilde{\eta}(\tilde{g}) = \tilde{M} \frac{d \log Z}{d\tilde{M}} \Big|_{\lambda_B} = \tilde{\beta}(\tilde{g}) \frac{d \log Z}{d\tilde{g}}, \quad (3.11)$$

$$\tilde{\sigma} = \frac{1}{Z_{\phi^2}} \frac{1}{\tilde{M}^2} \tilde{M} \frac{d m_B^2}{d\tilde{M}} \Big|_{\lambda_B}. \quad (3.12)$$

The counterterm Z_{ϕ^2} can be fixed by demanding

$$\Gamma_{ij}^{(2,1)}(p_1 = p_2 = 0) = \delta_{ij}. \quad (3.13)$$

From Z_{ϕ^2} and Z we can determine the anomalous dimension of ϕ^2 as

$$\tilde{\eta}_{\phi^2} = -\tilde{M} \frac{d \log(Z_{\phi^2} / Z)}{d\tilde{M}} \Big|_{\lambda_B} = -\tilde{\beta}(\tilde{g}) \frac{d \log(Z_{\phi^2} / Z)}{d\tilde{g}}. \quad (3.14)$$

Consistency between (3.8) and the CS equation (3.10) with $n = 2$ gives

$$\tilde{\sigma} = 2 - \tilde{\eta}. \quad (3.15)$$

In $d = 2$, $N = 1$ and $d = 3$ for any N , starting from the unbroken phase ($m^2 > 0$), we expect there should exist a critical value of the coupling \tilde{g} where the theory becomes gapless and a CFT arises.^{4,5} This non-trivial IR fixed point should be visible as a non-trivial zero of $\tilde{\beta}$. The expansion of $\tilde{\beta}$ in perturbation theory reads

$$\tilde{\beta} = (d-4)\tilde{g} + \mathcal{O}(\tilde{g}^2). \quad (3.16)$$

⁴Non-unitary CFTs can arise for other values of N , such as $N = 0$, which describes self-avoiding random walks.

⁵The possibility that the critical theory is scale-, but not conformal, invariant has been recently excluded for the $d = 3$ ϕ^4 theory [53].

When $d = 3$ or $d = 2$, a non-trivial zero is necessarily strongly coupled. The presence of a non-trivial fixed point cannot be established perturbatively, but it can at the non-perturbative level, namely upon Borel resumming the perturbative expansion. Several resummation of the β -function $\tilde{\beta}(\tilde{g})$ over the years have shown indeed the presence of a zero for some non-perturbative value of the coupling in $d = 2$ and $d = 3$ [33, 54–57, 9]. In the RS $\tilde{\mathcal{S}}$ this zero defines the critical coupling \tilde{g}_c :

$$\tilde{\beta}(\tilde{g}_c) = 0. \quad (3.17)$$

When we approach the critical regime the correlation length diverges, $\tilde{M} \rightarrow 0$, the right-hand side in (3.10) can be neglected and the Schwinger 1PI functions $\Gamma^{(n)}$ satisfy the scaling relations valid for a conformal invariant theory. Once \tilde{g}_c is determined, one can Borel resum the perturbative series in \tilde{g} for $\tilde{\eta}$ and $\tilde{\eta}_{\phi^2}$ and identify the (RS independent) critical exponents η and ν as

$$\eta \equiv \tilde{\eta}(\tilde{g}_c), \quad \eta_{\phi^2} \equiv \tilde{\eta}_{\phi^2}(\tilde{g}_c), \quad \nu = \frac{1}{2 - \eta_{\phi^2} + \eta}. \quad (3.18)$$

Other critical exponents can be obtained using scaling relations.

3.2.2 No Use of RG Flows: the RS \mathcal{S}

Let us call *minimal RSs*, the classes of schemes in which the renormalization procedure has minimum impact on the action and counterterms are introduced only when necessary to cancel divergences in the actual dimensionality one is considering. In a super-renormalizable theory, such counterterms contain a finite number of terms in perturbation theory.⁶

As we have discussed, for $d < 4$ in the action (3.6) only the mass term requires renormalization, the quartic coupling and the field ϕ being finite. Thus, in the minimal RSs we only introduce a mass counterterm δm^2 .

We present here two notable examples of minimal RSs: $\overline{\text{MS}}$ scheme and what we call intermediate scheme. For the former, we consider dimensional regularization and define the renormalized mass and coupling in $d = 2$ or $d = 3$ as

$$m_B^2 = m^2 + \delta m^2, \quad \lambda_B = \mu^\epsilon \lambda, \quad d = n - \epsilon, \quad n = 2, 3. \quad (3.19)$$

Note that λ has mass dimension 2 and 1 in $d = 2$ and $d = 3$, respectively. We follow the natural choice and simply set $\mu = m$ in (3.45). However, we will see starting from section 3.4 that redefining μ is equivalent to change the counterterms and gives rise to a simple one-parameter

⁶It is important to emphasize here that the minimal schemes alluded here are different from the so-called “minimal subtraction without ϵ -expansion” introduced in refs. [58, 59] and sometimes used in the statistical physics community. The minimal RSs, that we are referring to, are not necessarily related to dimensional regularization. In contrast to our schemes, in the “minimal subtraction without ϵ -expansion” of refs. [58, 59], counterterms are computed using minimal subtraction with dimensional regularization in $d = 4$, and as such contain an infinite number of terms in perturbation theory.

class of renormalization schemes. Within dimensional regularization, the tadpole and the sunset diagrams are the only divergent diagrams respectively in two and three dimensions. On the other hand, the intermediate scheme is defined by $m_B^2 = m_I^2 + \delta m_I^2$ and $\lambda_B = \lambda$ and imposing the following conditions for the mass counterterm δm_I^2 :

$$\begin{aligned} \delta m_I^2 &= - \text{tadpole} & (d=2), \\ \delta m_I^2 &= - \left(\text{tadpole} + \text{circle}(p=0) \right) & (d=3). \end{aligned} \tag{3.20}$$

In $d=2$ $\overline{\text{MS}}$ scheme with $\mu = m$ and the intermediate are the same and they are equivalent, in an operatorial formalism, to normal order the operators with respect to the mass m . In $d=3$, even if they differ, there is an explicit mapping between the two schemes, see (3.100).⁷

Let us denote \mathcal{S} a generic minimal RS in ϕ^4 theories in $d < 4$. In the RS \mathcal{S} we have that to all orders in perturbation theory

$$\frac{\delta m^2}{m^2} = a_1^{(d)} g + \delta_{d,3} a_2^{(d)} g^2, \tag{3.21}$$

where $a_i^{(d)}$ are divergent coefficients⁸ and g is the effective dimensionless coupling constant defined as

$$g = \frac{\lambda}{m^{4-d}}. \tag{3.22}$$

Callan-Symanzik equations like (3.10) can be considered also in the RS \mathcal{S} . In this case one simply gets

$$\left[m \frac{\partial}{\partial m} + \beta(g) \frac{\partial}{\partial g} - \frac{n}{2} \eta(g) \right] \Gamma_B^{(n)} = m^2 \sigma \Gamma_B^{(n,1)}, \tag{3.23}$$

where

$$\beta(g) \equiv m \frac{dg}{dm} \Big|_{\lambda_B} = (d-4)g, \quad \eta = 0, \quad \sigma = 2 \begin{cases} 1 + \frac{N+2}{\pi} g, & d=2, \\ 1 + \sigma_1^{(3)} g - 2 \frac{(N+2)}{\pi^2} g^2, & d=3. \end{cases} \tag{3.24}$$

where $\sigma_1^{(3)}$ is a dependent scheme quantity. Note that the mass m entering (3.23) is the renormalized mass m and *not* the pole mass M as defined in (3.25) below. As a consequence, in the critical regime $M \rightarrow 0$ the term proportional to $\Gamma_B^{(2,1)}$ does not vanish, in contrast to what hap-

⁷The name intermediate comes from the fact that, being suitable for numerical computations, in this work, in $d=3$, it is an intermediate step towards other schemes. In subsection 3.8.1 it will be mapped to a one-parameter family of minimal RSs and in section 3.9 to the RS $\tilde{\mathcal{S}}$, likewise done in ref. [60] where $\tilde{\mathcal{S}}$ is dubbed M .

⁸This is the general form, actually for the RSs where we use dimensional regularization we have that $a_2^{(3)} = 0$.

pens in (3.10) in the RS $\widetilde{\mathcal{S}}$ when $\widetilde{M} \rightarrow 0$. Hence demanding $\beta = 0$ in (3.23) does not correspond to a (non-trivial) critical regime and no interesting RG flow is expected from β in (3.24).

Renormalization group methods are not essential and we can access the critical regime by a direct computation of observables. One can define the pole mass M as the zero of $\Gamma_B^{(2)}$ for complex values of the Euclidean momentum or define the mass gap as the $\Gamma_B^{(2)}$ at zero momentum. We will use the first definition for our studies of the scheme dependence in $d = 2$ following ref. [9] while the latter for $d = 3$, since it is more convenient.

$$\Gamma_{B,ij}^{(2)}(p^2 = -M^2) \equiv 0 \quad (d = 2), \quad (3.25)$$

$$M^2 \equiv \Gamma_{B,ij}^{(2)}(p = 0) \quad (d = 3). \quad (3.26)$$

The critical coupling can be determined directly as the value of g where the theory is gapless:

$$M(g_c) = 0. \quad (3.27)$$

The critical exponent ν , defined as

$$M(g) \propto |g_c - g|^\nu, \quad g \rightarrow g_c, \quad (3.28)$$

can be computed by resumming a properly defined function of M^2 . For instance, if

$$L(g) \equiv \frac{2g^2}{g\partial_g \log M^2}, \quad (3.29)$$

ν can be extracted as [9]

$$\nu = \left. \frac{g_c}{\partial_g L} \right|_{g=g_c}. \quad (3.30)$$

The exponent η can be determined directly from its definition as the power-like decay of the two-point function at the critical point:

$$\langle \phi_i(x)\phi_j(0) \rangle_{g=g_c} \approx \frac{\delta_{i,j} c_\phi}{|x|^{d-2+\eta}}, \quad i, j = 1, \dots, N, \quad (3.31)$$

where c_ϕ is a constant. This is the approach that has been taken in ref. [9] to determine g_c , ν and η in the $d = 2$ ϕ^4 theory. Alternatively, ν could be determined more directly by means of (3.18), where η_{ϕ^2} is extracted as

$$\langle \phi^2(x)\phi^2(0) \rangle_{g=g_c} \approx \frac{c_{\phi^2}}{|x|^{2(d-2+\eta_{\phi^2})}}, \quad (3.32)$$

where again c_{ϕ^2} is a constant. It is worth emphasizing that the value of η found using the above

procedure in the RS \mathcal{S} is in good agreement with the exact result $\eta = 1/4$, while a long standing mismatch is found when using (3.18) in the RS $\tilde{\mathcal{S}}$. A similar long standing mismatch occurs in the evaluation of $\omega \equiv \tilde{\beta}'(\tilde{g}_c)$ in the RS $\tilde{\mathcal{S}}$, which significantly differs from the exact value $\omega = 2$. We have verified that no improvement is achieved by resumming ω from the expression of $\tilde{\beta}$ derived in ref. [9], which includes two more orders in the known perturbative expansion. These problems seem to be related to possible non-analyticities in $\tilde{\beta}(\tilde{g})$ that give rise to a poor convergence of the numerical Borel resummation to the exact result [61, 62], though they might also be a signal of absence of Borel summability in the RS $\tilde{\mathcal{S}}$ for such observables. It would be interesting to check if the mismatch for ω disappears (like for η) if the RS \mathcal{S} is used and ω extracted directly from a two-point function, such as $\langle \phi^4(x)\phi^4(0) \rangle_{g=g_c}$.⁹

In $d = 3$ for the $O(N)$ models, instead, we will see that studying the critical regime in the RS \mathcal{S} is pretty challenging, at fixed same number of loop l the RS $\tilde{\mathcal{S}}$ allows the computation of more accurate values for g_c and ν . We are still in the process of fully understanding the causes why RS \mathcal{S} under-performs in $d = 3$, we suspect that this might be due to the particular analytic structure for the observables. We will discuss it in section 3.6.

A direct approach to the critical regime without the use of RG techniques allows to bypass the need of evaluating the 4-pt function $\Gamma^{(4)}$. The number of diagrams with l loops in a $2n$ -pt function $\Gamma^{(2n)}$ is expected to scale as the number of loop diagrams in the vacuum energy with $l + n$ loops. This is seen by noting that if we connect the $2n$ external lines in pairs, we get a vacuum energy graph with n more loops. Large order estimates confirm this expectation. At fixed number of loops l , then, evaluating the 4-pt function is computationally more challenging than evaluating the 2-pt function, due to the larger number of Feynman diagrams. Moreover, in $d = 2$, as we already mentioned, the normal ordering with respect to the mass m , in an operatorial formalism, is in direct relation to the RS \mathcal{S} and this scheme has been used in the literature as a reference RS to compare various non-perturbative computations of the critical coupling [39–45, 63].

Note that the definition of g_c given by (3.27) could be adopted also in the RS $\tilde{\mathcal{S}}$, bypassing the evaluation of the beta-function $\tilde{\beta}$. Similarly one could compute η and η_{ϕ^2} directly from eqs. (3.31) and (3.32).

3.3 Borel Summability and RS Dependence

In this section we review previous results on the Borel summability of Schwinger functions in the $\lambda\phi^4$ theory, contained in both the early [7, 8] and the more recent papers [9, 17], and show how they depend on the RS.

We first briefly review the early proofs of the Borel summability of Schwinger functions in the $d = 2$ [7] and $d = 3$ [8] $N = 1$ ϕ^4 theory. These papers are in the context of constructive

⁹We thank A. Pelissetto for drawing our attention to the critical exponent ω .

quantum field theory, an area of research particularly active in the late 60s and in the 70s, that tries to give a rigorous mathematical foundation to quantum field theories, see e.g. ref. [64] for an overview. We do not enter into details, but only mention the key steps and the logic followed in these papers, focusing on the RS chosen. As starting point the bare action (3.6) is renormalized by adding mass counterterms (we neglect vacuum energy counterterms) as in (3.21). In particular, bare and renormalized fields and couplings are identified. In $d = 2$ the RS chosen in ref. [7] is identical to normal ordering with respect to the mass m^2 and hence coincides with the RS \mathcal{S} . The renormalization conditions in $d = 3$ are not given in an explicit form in ref. [8], but they are essentially equivalent to the RS \mathcal{S} . In particular, only $\mathcal{O}(\lambda)$ and $O(\lambda^2)$ mass counterterms are present,¹⁰ as in the condition (3.21) defining the RS \mathcal{S} . In both $d = 2$ and $d = 3$, the local operators $\phi(x_i)$ are smeared with sufficiently regular functions f_i with compact support around a region surrounding x_i to define a field $\phi_{f_i} = \int d^2x_i f(x_i)\phi(x_i)$. Finally, it is shown that for $|\lambda| < \epsilon$, $\text{Re } \lambda > 0$ and large enough $m^2 > 0$ (i.e. at parametrically weak coupling $g \ll 1$ in our notation), the $2n$ -point smeared Schwinger functions

$$G_{2n}^{\text{sm}}(\lambda) = \frac{\int \mathcal{D}\phi \phi_{f_1} \dots \phi_{f_{2n}} e^{-S_B[\phi]}}{\int \mathcal{D}\phi e^{-S_B[\phi]}} \quad (3.33)$$

are analytic in λ with bounded derivatives:

$$\left| \frac{d^k}{d\lambda^k} G_{2n}^{\text{sm}}(\lambda) \right| \leq C_1 C_2^k k!^2, \quad (3.34)$$

with C_1 and C_2 two constants.¹¹ Under suitable conditions on the smearing functions f_i , the analyticity domain of $G_{2n}^{\text{sm}}(\lambda)$ can be extended to a region including points where $\text{Re } \lambda < 0$. The asymptotic series of the smeared Schwinger functions $G_{2n}^{\text{sm}}(\lambda)$ satisfy then the sufficient criterion for Borel summability as given by Watson (see e.g. theorem 136 in chap.VIII of ref. [15]). Soon after, it was pointed out that the analytic continuation to a region including points where $\text{Re } \lambda < 0$ is unnecessary. One can instead use a necessary and sufficient criterion of Borel summability, found long ago by Nevanlinna and rediscovered in ref. [16], that requires a domain of analyticity only in a region with $\text{Re } \lambda > 0$, see fig. 3.1. In the $d = 2$ case [7] the analyticity of the Schwinger functions is extended for more general functions involving normal-ordered composite operators of the form ϕ^q , with q a positive integer, and for generic bounded polynomial potentials with degree P . In this case, the factor $k!^2$ in (3.34) is replaced by $k!^{P/2}$.¹²

¹⁰In eq.(2.1.1) of ref. [8] only the $O(\lambda^2)$ term appears, the $O(\lambda)$ one being hidden in the normal ordering operation.

¹¹The bound (3.34) found in ref. [8] is actually proportional to $k!^{2+\xi}$, with $\xi > 0$, and one has to generalize Watson criterion to show Borel summability. We thank J. Magnen for discussions on this issue and for pointing out that the limit $\xi \rightarrow 0$ might be taken by using the so called multiscale expansion [65].

¹²Note that the ordinary Watson criterion for Borel summability requires $P = 4$. Presumably this is the reason why the authors [7] did not discuss Borel summability of theories with higher order interaction terms. On the

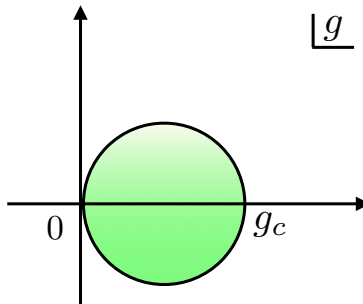


Figure 3.1: The green disk shows the minimum region of analyticity for a Borel resummable function [16] (the origin is excluded).

We now review and expand a bit some of the considerations made in ref. [9] about the Borel summability of scalar field theories in $d < 4$. For concreteness we focus on $O(N)$ vector models, though most considerations apply more in general. Consider a $2n$ -point Schwinger function

$$G_{2n}^B(x_1, \dots, x_n) = \mathcal{N} \int \mathcal{D}\phi \phi(x_1) \dots \phi(x_{2n}) e^{-S_B[\phi]}, \quad (3.35)$$

where \mathcal{N} is an irrelevant constant factor, we omitted $O(N)$ indices, and S_B is the bare action (3.44). We renormalize the theory in the RS \mathcal{S} using (3.21). It is useful to rescale fields and coordinates as follows:

$$\phi(x) = \frac{m}{\sqrt{\lambda}} \Phi(y), \quad y = mx, \quad (3.36)$$

and rewrite (3.35), omitting also the space dependences, as

$$G_{2n} = G_{2n}^0 = \mathcal{N}' g^{-n} m^{(d-2)n} \int \mathcal{D}\Phi \Phi(y_1) \dots \Phi(y_{2n}) e^{-\delta S[\Phi]} e^{-S[\Phi]/g}, \quad g = \frac{\lambda}{m^{4-d}}, \quad (3.37)$$

with

$$S[\Phi] = \int d^d y \left[\frac{1}{2} (\partial \Phi)^2 + \frac{1}{2} \Phi^2 + (\Phi^2)^2 \right], \quad (3.38)$$

$$\delta S[\Phi] = \left(a_1^{(d)} + \delta_{d,3} a_2^{(d)} g \right) \int d^d y \left[\frac{1}{2} \Phi^2 \right]. \quad (3.39)$$

The counterterm action δS , in both $d = 2$ and $d = 3$, is subleading to S in a saddle point expansion in g and does not change the saddle point structure of $S[\Phi]$ if the convergence of the path integral at large field values is dictated by S . This is the case in the RS \mathcal{S} , since

other hand, the arguments made in ref. [9] and reviewed in what follows allow us to conclude that these theories are Borel resummable in the proper loopwise expansion. For instance, for a ϕ^{2p} potential the loopwise parameter is $g_{2p} = (\lambda/m^2)^{1/(p-1)}$ and Schwinger functions are Borel summable in g_{2p} , though they are not in λ/m^2 .

δS is quadratic in the field, while S is quartic. A simple scaling argument, equivalent to an euclidean version of Derrick's theorem [66, 23], allows us to show that the action S does not have any non-trivial critical points with finite energy, aside from the trivial one $\Phi = 0$, for real field configurations. The combination of reality and boundedness of the action and the presence of a unique critical point makes the domain of integration of the path integral (3.35) a single Lefschetz thimble, guaranteeing the Borel summability of the Schwinger functions $G^{(2n)}$ [17].¹³ A similar argument is expected to apply for Schwinger functions involving composite operators constructed out of ϕ and their derivatives.

It might be useful to compare the results of refs. [7, 8] with those of ref. [9]. While the proof of refs. [7, 8] requires a detailed study of the analytic properties of the exact Schwinger functions in the coupling constant λ , the argument based on Lefschetz thimbles in ref. [9] makes it possible to avoid such study and to reach the same conclusion in a simpler way. Borel summability holds for all real values of the coupling where the Schwinger functions are well-defined. On physical grounds, we expect this to hold until the theory undergoes a phase transition, in which case Schwinger functions or their derivatives can diverge. We can in turn use the necessary and sufficient criterion of Borel summability of ref. [16] to establish that Schwinger functions should be analytic in the region in fig. 3.1. We expect this region to extend until the critical coupling g_c where a second order phase transition (or of any other kind, for more general theories) occurs.¹⁴ Moreover, the simplicity of the arguments in ref. [9] immediately allows us to establish Borel summability for more general theories beyond the ϕ^4 with positive squared mass term, the subject of study in refs. [7, 8].¹⁵ Of course, the more heuristic derivation of ref. [9] does not match the standard of mathematical rigor typically requested in constructive quantum field theory. In particular, as physicists we do *assume* that the Schwinger functions (and the theory itself) exist. In contrast, in constructive field theory the existence of a non-perturbative definition of the theory is generally the first important point to be established, Borel summability (if any) being a by-product. Interestingly enough, despite the approaches and the methodologies substantially differ among refs. [7, 8] and [9], in both cases Borel summability is only established in RSs equal or equivalent to the minimal one we denoted by \mathcal{S} .

It is not difficult to show which additional complications can occur in our construction to prove the Borel summability in other non-minimal RSs. For instance, by repeating the steps

¹³More precisely, we mean that for any choice of non-coincident points x_i the resulting series in g is Borel summable. Alternatively, as in refs. [7, 8], we could smear the local operators $\phi(x_i)$ by means of some functions f_i and consider their smeared version ϕ_{f_i} . The asymptotic series of the smeared Schwinger functions G_{2n}^{sm} would then be Borel summable for any sensible choice of smearing functions f_i .

¹⁴Schwinger functions analytically continued past a phase transition might still be physically sensible. See refs. [9, 38] for more details and for some numerical evidence in the $d = 2$ ϕ^4 case.

¹⁵See ref. [67] for a very recent paper where Borel summability in certain low dimensional theories is established in the context of constructive quantum field theory.

from (3.36) to (3.39) in the RS $\tilde{\mathcal{S}}$, we would define

$$\phi_{\mathbb{R}}(x) = \frac{\tilde{M}^{(d-2)/2}}{\sqrt{\tilde{g}}} \Phi_{\mathbb{R}}(y), \quad y = \tilde{M}x, \quad (3.40)$$

and write

$$G_{2n} = Z^n G_{2n}^B = \mathcal{N}' Z^n \tilde{g}^{-n} \tilde{M}^{(d-2)n} \int \mathcal{D}\Phi_{\mathbb{R}} \Phi_{\mathbb{R}}(y_1) \dots \Phi_{\mathbb{R}}(y_{2n}) e^{-\delta S[\Phi_{\mathbb{R}}]} e^{-S[\Phi_{\mathbb{R}}]/\tilde{g}}, \quad (3.41)$$

with $S[\Phi_{\mathbb{R}}]$ as in (3.38) and

$$\delta\tilde{S}[\Phi_{\mathbb{R}}] = \int d^d x \left[\frac{1}{2} \frac{Z-1}{\tilde{g}} (\partial\Phi_{\mathbb{R}})^2 + \frac{1}{2} \frac{\delta\tilde{M}^2}{\tilde{g}} \Phi_{\mathbb{R}}^2 + \frac{Z_{\tilde{g}}-1}{\tilde{g}} (\Phi_{\mathbb{R}}^2)^2 \right]. \quad (3.42)$$

The counterterm $\delta\tilde{S}$ is still subleading to S in a saddle point expansion in \tilde{g} , but now two subtleties arise. First, the counterterms Z , $Z_{\tilde{g}}$ and $\delta\tilde{M}^2$ entering $\delta\tilde{S}$ are not expressions that can be computed in closed form. They can only be determined order by order in perturbation theory but the resulting series are in general asymptotic and would require to be resummed. In other words, the RS $\tilde{\mathcal{S}}$ is intrinsically perturbative in nature and hence is not suitable to be used to establish a property of a theory that goes beyond perturbation theory, like its Borel summability. Second, in contrast to δS , $\delta\tilde{S}$ contains terms quartic in the field $\Phi_{\mathbb{R}}$, which could in principle change the convergence properties of the path integral at large field values as dictated by S , and possibly invalidate the statement that a resummation of the saddle point expansion around solutions of S reconstructs the full result. In light of that, the Borel summability of the expansion in \tilde{g} cannot be assessed. We are not aware of any paper in the constructive quantum field theory literature where the Borel summability of $d = 2$ or $d = 3$ field theories is established or even attempted in non-minimal RSs such as $\tilde{\mathcal{S}}$.

A non-perturbative change of RS of the form $g = g(\tilde{g})$ would not affect Borel summability if this mapping preserves the necessary and sufficient conditions for Borel summability, namely a region of analyticity as in fig. 3.1 in the \tilde{g} complex plane and a bound on the growth of the coefficients of its asymptotic expansion. Unfortunately, we typically do not have access to such non-perturbative mapping, and only know it in perturbation theory. In this case we will have

$$g \sim \tilde{g} + \sum_{k=2}^{\infty} a_k \tilde{g}^k. \quad (3.43)$$

In general the above series is asymptotic (that's why the \sim sign instead of an equality), as it happens for instance when relating the coupling g in the RS \mathcal{S} with the coupling \tilde{g} in the RS $\tilde{\mathcal{S}}$. We should then first of all face the problem of proving the Borel summability of the series (3.43), in general a non-trivial task. Even if we can somehow prove that the series (3.43) is Borel

resummable to its exact form $g(\tilde{g})$, we will still not be able to prove that Borel summability of Schwinger functions in one RS implies that in the other RS. Indeed, given an observable $F(g)$ which is Borel reconstructed from its asymptotic series $\sum_{k=0}^{\infty} F_k g^k$ in the RS with coupling g , naively plugging (3.43) in the series for $F(g)$ will not in general give rise to a Borel resummable series in \tilde{g} . Borel summability of the composed series expansion of $F(g(\tilde{g}))$ would follow if $\sum_{k=0}^{\infty} F_k g^k$ were convergent (see e.g. proposition 2.11 of ref. [68] or section 4.4c of ref. [69]) or if both $F(g)$ and $g(\tilde{g})$ satisfy certain analyticity properties close to the origin which are stronger than the ones required for Borel summability [70, 71]. Hence, without further assumptions, we would be unable to prove the Borel summability of the observable F in the RS with coupling \tilde{g} .

3.4 RS Dependence in Minimal Schemes and Self-Dualities

Let us look back at (3.43). In renormalizable theories it is generally hard to go beyond it because the process of renormalization occurs to all orders in perturbation theory. On the other hand, super-renormalizable theories require a finite number of subtractions and therefore provide a playground for theories where we can hope to do better than (3.43). This is the case when working on change of schemes inside the minimal RSs. If g and g' denote the renormalized couplings in two minimal renormalization schemes we can expect to find the exact form of the finite change of scheme $g' = g'(g)$. We will do that in what follows for quartic $O(N)$ -invariant scalar theories in $d = 2$ and $d = 3$ dimensions for a one-parameter family of renormalization schemes within the same family (like MS vs $\overline{\text{MS}}$). Let us rewrite once again the euclidean action of the theories,

$$S = \int d^d x \left[\frac{1}{2} (\partial_\mu \phi_i)^2 + \frac{1}{2} m_B^2 \phi_i^2 + \lambda_B (\phi_i^2)^2 + \rho_B \right], \quad i = 1, \dots, N. \quad (3.44)$$

As we have seen, for $d < 4$ only the mass term and the vacuum energy term require renormalization, the quartic coupling and the field ϕ being finite. We consider dimensional regularization and define the renormalized mass and coupling in $d = 2$ or $d = 3$ as

$$m_B^2 = m^2 + \delta m^2, \quad \lambda_B = \mu^\epsilon \lambda, \quad \rho_B = \mu^{-\epsilon} (\rho + \delta \rho), \quad d = n - \epsilon, \quad n = 2, 3. \quad (3.45)$$

Note that λ has mass dimension 2 and 1 in $d = 2$ and $d = 3$, respectively. The introduction of an RG scale μ might confuse the reader. In fact, there are no large log's to be resummed in perturbation theory and consequently no need to introduce a further mass scale μ in the problem. The natural choice would be to simply set $\mu = m$ in (3.45). However, changing $\mu \rightarrow \mu e^{-\kappa/2}$, where κ is an arbitrary real parameter, is equivalent to change the counterterms δm^2 and $\delta \rho$ in (3.45) and hence is a convenient way to introduce a simple one-parameter class of

renormalization schemes.¹⁶ That said, all the considerations below could be derived using e.g. cut-off regularization at fixed dimension, but at the price of having more complicated expressions in $d = 3$.

Let us assume that $m^2 > 0$, so that we are in the classically unbroken phase of the theory. To all orders in perturbation theory the β functions are easily determined since there are no contributions to β_λ and only one to β_{m^2} in both $d = 2$ and $d = 3$, given respectively by the first and second diagrams in fig. C.1 of appendix C. One has¹⁷

$$\beta_\lambda = 0, \quad \beta_{m^2} = 2b_{d-1}\lambda^{d-1}, \quad d = 2, 3, \quad (3.46)$$

where

$$b_1 = -\frac{N+2}{\pi}, \quad b_2 = \frac{N+2}{\pi^2}. \quad (3.47)$$

If we denote by m^2 the squared mass parameter in the original scheme, in the scheme where $\mu \rightarrow \mu e^{-\kappa/2}$ we get a squared mass parameter m'^2 equal to

$$m'^2(\mu) = m^2(\mu) + \lambda^{d-1}b_{d-1}\kappa. \quad (3.48)$$

Using the running of the mass term, this can be written more explicitly as

$$m^2 + \lambda^{d-1}b_{d-1} \log \frac{\mu^2}{m^2} = m'^2 + \lambda^{d-1}b_{d-1} \log \frac{\mu^2}{m'^2} - \lambda^{d-1}b_{d-1}\kappa, \quad (3.49)$$

where $m^2(\mu^2 = m^2) \equiv m^2$, $m'^2(\mu^2 = m'^2) \equiv m'^2$. The relation (3.49) can be further rewritten as

$$f_d(x) = f_d(x') + \kappa, \quad (3.50)$$

where

$$f_d(x) \equiv \log x + (-1)^d x, \quad x \equiv \frac{1}{N+2} \left(\frac{\pi}{g} \right)^{d-1}, \quad g \equiv \frac{\lambda}{m^{4-d}}. \quad (3.51)$$

Note that g is the dimensionless loopwise expansion parameter while the variable x (in units of λ) is proportional to the squared mass term in both $d = 2$ and $d = 3$ dimensions. We can use (3.50) to find an exact change of scheme $x' = x'(x)$.

Consider first the $d = 2$ case. Solving for x' we get for any κ the unique solution

$$x' = W_0 \left(x e^{x-\kappa} \right), \quad (3.52)$$

where W_0 is the principal branch of the Lambert function W . This function will repeatedly

¹⁶In $4d$ a relation of this kind with $\kappa = \log(4\pi) - \gamma_E$ links the MS and $\overline{\text{MS}}$ schemes.

¹⁷We do not report here the β function for the vacuum energy, which for $d = 3$ can be found in (C.3), since it does not play any role in the analysis that follows. The vacuum energy will be neglected until section 3.8.

appear in our considerations, so we refer the reader to appendix A for its definition and a brief summary of some of its properties. This solution agrees with the one obtained in perturbation theory by expanding g' for small g :

$$g' = g + \frac{(N+2)\kappa}{\pi}g^2 + \frac{(N+2)^2\kappa(\kappa-1)}{\pi^2}g^3 + \dots \quad (3.53)$$

Instead of expanding W for large values of its argument, that involves iterative logs, one can alternatively expand for small κ , by noting that at order n in perturbation theory the change of scheme involves a polynomial of degree $n-1$ in κ . Defining $y = x - \kappa$, we are left with the expansion of $W(ye^y + \kappa e^y)$ for small κ . The Taylor expansion around $\kappa = 0$ can be performed using (A.6) and the fact that by definition $W(ye^y) = y$. We get

$$x' = x - \kappa + \sum_{n=1}^{\infty} \frac{\kappa^n}{n!} \frac{p_n(x - \kappa)}{(1 + x - \kappa)^{2n-1}}. \quad (3.54)$$

Expanding this relation for large values of x finally reproduces, to all orders in perturbation theory, the perturbative change of scheme given in (3.53). This expansion for large x is of the form

$$x' = x - \kappa + \kappa \sum_{n=1}^{\infty} \frac{q_n(\kappa)}{x^n}, \quad (3.55)$$

where q_n are polynomials of degree $n-1$ in κ . The coefficients of the monomials entering q_n alternate in sign and indicate that the convergence properties of the series are better when $\kappa > 0$. We have not determined the exact radius of convergence $R(\kappa)$ of the series (3.55) but we have checked that $R(\kappa) \sim 1/|\kappa|$.

It is well-known that the $N = 1$ ϕ^4 theory has a second-order phase transition at a critical value of the (inverse) coupling x_c in the same universality class of the $d = 2$ Ising model.¹⁸ Given $x_c(\kappa = 0) \equiv x_c$, the exact relation (3.52) allows us to find the analytic form of the dependence of the critical coupling on the renormalization scheme:

$$x_c(\kappa) = W_0(x_c e^{x_c - \kappa}). \quad (3.56)$$

For $\kappa \rightarrow -\infty$, we have

$$x_c(\kappa) \approx |\kappa| + x_c, \quad (3.57)$$

and the fixed point coupling approaches the Gaussian one, while in the opposite limit $\kappa \rightarrow \infty$,

$$x_c(\kappa) \approx x_c e^{x_c} e^{-\kappa} \quad (3.58)$$

¹⁸For $N = 2$ vortices appear and the theory has a Berezinskii-Kosterlitz-Thouless transition [72–74]. For $N \geq 3$ the theories are gapped and no transition occurs. See [75] for a recent analysis of 2d $O(N)$ models for continuous values of N between -2 and 2 .

the coupling goes to infinity exponentially in κ . As the renormalization scheme is varied, we always find a fixed point and hence the phase transition is “visible” from the (classically) unbroken phase in $d = 2$ for any choice of κ .

Let us now consider the more interesting case of $d = 3$, where the apparently innocuous sign difference between $d = 2$ and $d = 3$ in (3.51) completely changes the picture. Solving for x' , for any κ we now get two solutions

$$x'_w = -W_{-1}\left(-xe^{-x-\kappa}\right), \quad x'_s = -W_0\left(-xe^{-x-\kappa}\right), \quad (3.59)$$

where $x'_w > 1$ and $x'_s < 1$, associated to the two different branches W_{-1} and W_0 of the Lambert function, see appendix A. We label the two branches as weak (w) and strong (s) branches. The solution that agrees with the one obtained in perturbation theory is obtained by expanding W_{-1} for $x \rightarrow +\infty$, which corresponds to $xe^{-x} \rightarrow 0^+$. Using (A.5), we get

$$x'_w \approx x + \kappa + \dots \quad (3.60)$$

The perturbative change of scheme is obtained by proceeding as before and can be written in the form of (3.54), with the obvious replacement $x \rightarrow -x$. The other non-perturbative solution is obtained by expanding W_0 for $x \rightarrow +\infty$ and gives

$$x'_s \approx xe^{-x-\kappa}. \quad (3.61)$$

Two solutions occur also for $\kappa = 0$ and indicate that $O(N)$ vector models in $d = 3$ admit two “dual” descriptions in the classically unbroken phase. They are related as follows:

$$x_s = -W_0(-x_w e^{-x_w}), \quad \text{or} \quad x_w = -W_{-1}(-x_s e^{-x_s}), \quad (3.62)$$

for $x_w > 1$ and $x_s < 1$. In terms of mass scales the first relation in (3.62) gives

$$\lim_{m \rightarrow \infty} m_s^2 \approx m^2 e^{-\frac{\pi^2 m^2}{(N+2)\lambda^2}}, \quad (3.63)$$

where $m_w^2 \equiv m^2$. Interestingly enough, (3.63) can be interpreted as the “dynamically generated” RG invariant scale

$$\Lambda_{\text{RG}}^2 = \mu^2 e^{-\frac{\pi^2}{(N+2)g^2(\mu)}}, \quad (3.64)$$

that arises from the β -function for g^2 :

$$\beta_{g^2} = -\frac{2(N+2)}{\pi^2}(g^2)^2. \quad (3.65)$$

By taking $\mu = m$, $g(m) = \lambda/m$, we see that Λ_{RG} coincides with the weak coupling limit (3.63)

of m_s . The strong and weak branch fuse at the self-dual point

$$x_{\text{SD}} = 1 \quad \Rightarrow \quad g_{\text{SD}} = \frac{\pi}{\sqrt{N+2}}, \quad (d=3). \quad (3.66)$$

In the large N limit with $\lambda \rightarrow 0$, $N \rightarrow \infty$, and $\lambda N = \text{fixed}$, the two-loop term in (3.49) drops out and correspondingly the function $f(x)$ trivializes. No self-duality survives in this large- N limit.

A similar analysis can be done for $m^2 < 0$, namely in the classically broken phase, but now the value of N matters. For $N > 1$ in $d = 2$ the Coleman-Mermin-Wagner theorem [76,77] forbids the appearance of Goldstone bosons, so the theory is always non-perturbatively gapped and we cannot expect to be able to deduce strongly coupled effects by merely looking at perturbative counterterms. This is in agreement with the fact that for $N > 1$ in $d = 2$ Borel summability is not guaranteed [9]. For $N > 1$ in $d = 3$ a continuous symmetry is spontaneously broken and massless Goldstone bosons appear. The relation (3.49), based on the presence in the theory of a single $O(N)$ -invariant mass scale, no longer holds and a more refined analysis is required (see also footnote 20). For simplicity, in what follows we focus on the case $N = 1$, for which we expect that the analysis made above for $m^2 > 0$ also holds for $m^2 < 0$.¹⁹ We denote the parameters in the broken phase with a hat and continue to keep generic N in the formulas, with the understanding that $N = 1$. The β -functions (3.46) still apply, but we now have

$$\widehat{m}^2(\mu^2 = \widehat{m}^2) = -\frac{1}{2}\widehat{m}^2, \quad (3.67)$$

where $-\widehat{m}^2/4$ is the renormalized mass term in the action, such that the particle excitation has squared mass $\widehat{m}^2 > 0$. In the broken phase (3.50) reads

$$\widehat{f}_d(\widehat{x}) = \widehat{f}_d(\widehat{x}') + \widehat{\kappa}, \quad (3.68)$$

where

$$\widehat{f}_d(\widehat{x}) \equiv \log \widehat{x} - (-1)^d \widehat{x}, \quad \widehat{x} \equiv \frac{1}{2(N+2)} \left(\frac{\pi}{\widehat{g}} \right)^{d-1}, \quad \widehat{g} \equiv \frac{\lambda}{\widehat{m}^{4-d}}. \quad (3.69)$$

We see that, as far as the scheme dependence is concerned, the $d = 2$ and $d = 3$ theories in the broken phase behave respectively like the $d = 3$ and $d = 2$ theories in the unbroken phase! The whole analysis made before applies with this replacement. In particular, we conclude that the $d = 2$ $N = 1$ theory admits a self-duality in the broken phase. The strong and weak branch fuse

¹⁹However, the situation simplifies at large N , where we can see the non-perturbatively generated mass gap from an analytic continuation in the coupling space, see subsection 3.6.1.

at the self-dual point

$$\widehat{x}_{\text{SD}} = 1 \quad \Rightarrow \quad \widehat{g}_{\text{SD}} = \frac{\pi}{2(N+2)}, \quad (d=2). \quad (3.70)$$

3.5 Connection with Chang and Magruder Dualities

We have seen in section 3.4 how to perform an exact change of renormalization schemes within the same phase of the theory. However, classically unbroken and broken phases are simply characterized by the sign of the squared mass term and since the latter is in fact divergent, we should be able to push further our change of schemes (for $N = 1$) and to relate one phase to another, passing through infinite coupling ($m^2 = 0$). The relation (3.48) still applies and, in light of (3.67), reads now

$$\log(x/2) + (-1)^d x = \log \widehat{x} - (-1)^d \widehat{x} + \kappa, \quad (3.71)$$

in terms of the variables defined in (3.51) and (3.69). The relation (3.71) states that a theory in the broken phase with negative squared mass term $-\widehat{m}^2/2$ is equivalent to a theory in the unbroken phase with squared mass term m^2 (with the same λ) provided the two mass scales are related as in (3.71). The theories are “dual” because they can be seen as the same theory where the mass term is renormalized differently. For $\kappa = 0$ in $d = 2$, the relation (3.71) coincides with Chang duality [11], originally derived using a normal ordering prescription. In $d = 3$ relation (3.71) gives rise to a duality first discussed by Magruder [12].²⁰ The original derivation of [12] made use of cut-off regularization and a different renormalization scheme (without the need of introducing a RG scale μ), where an extra term proportional to \sqrt{x} appeared on both sides of (3.71) due to a divergence induced by the one-loop tadpole-like diagram. The presence of such term hinders an analytic solution of the duality relation and it obscures the close analogy between the $d = 2$ and the $d = 3$ cases. This divergence depends on the renormalization scheme and is set to zero in minimal subtraction schemes based on dimensional regularization. Note that no duality occurs for non-integer d , since the log terms in (3.71) can only appear for integer dimensions.

²⁰Magruder actually wrote down a duality for arbitrary N by adding $O(N)$ group theoretical factors to the $N = 1$ case, as if the symmetry would be linearly realized, see (3.17) of [12]. For instance, the term proportional to $\Lambda - \mu$ on the right hand side of the counterterm (3.16) in [12] would naturally arise if all particles in the one-loop tadpole-like diagram responsible for the linear divergence had mass μ^2 . Massless particles would induce IR divergences in the sunset diagram contribution, proportional to $\log(\mu/\Lambda)$ in (3.16). Due to the derivative interactions of Goldstone bosons, we expect that IR divergences cancel, but in a non-trivial way in a linear parametrization in terms of the field-components of ϕ_i . A duality might still hold for $N > 1$ but establishing it requires to understand how to map operators in a theory from a phase to another, where a global symmetry is linearly or non-linearly realized, respectively.

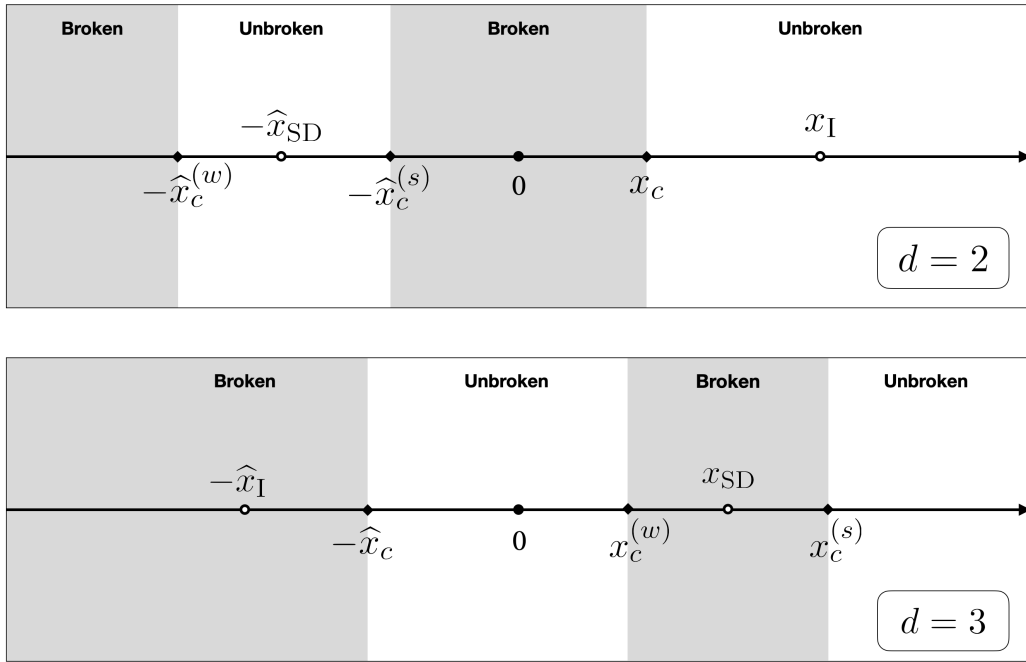


Figure 3.2: Phase structure of the $N = 1$ ϕ^4 theory according to the Chang-Magrunder dualities in $d = 2$ and $d = 3$, in schemes where respectively $x_c < x_I$ and $\hat{x}_c < \hat{x}_I$, as a function of the parameter x (proportional to the squared mass).

For $\kappa = 0$ and at fixed x (\hat{x}), the solutions in \hat{x} (x) of (3.71) are

$$\hat{x}_w = -W_{-1}(-\omega x e^x), \quad \hat{x}_s = -W_0(-\omega x e^x), \quad x = W_0\left(\frac{\hat{x}}{\omega} e^{-\hat{x}}\right) \quad (d = 2), \quad (3.72)$$

$$\hat{x} = W_0(x \omega e^{-x}), \quad x_s = -W_0\left(-\frac{\hat{x}}{\omega} e^{\hat{x}}\right), \quad x_w = -W_{-1}\left(-\frac{\hat{x}}{\omega} e^{\hat{x}}\right) \quad (d = 3), \quad (3.73)$$

with $\omega = 1/2$. Note that (3.72) and (3.73) are related by the map

$$x \leftrightarrow \hat{x}, \quad \omega \leftrightarrow \frac{1}{\omega}, \quad (3.74)$$

which is again a manifestation of the interplay between unbroken and broken phases in $d = 2$ and $d = 3$. In $d = 2$, at fixed x , the two solutions in (3.72) are real for $x e^x / 2 < 1/e$, i.e. for (setting $N = 1$)

$$g \geq g_I \equiv \frac{\pi}{3W_0(2/e)} \approx 2.26, \quad (d = 2). \quad (3.75)$$

In $d = 3$, at fixed \tilde{x} , the two solutions in (3.73) are real for $2\hat{x}e^{\hat{x}} < 1/e$, i.e. for (setting $N = 1$)

$$\hat{g} \geq \hat{g}_I \equiv \left(\frac{\pi^2}{6W_0(1/(2e))}\right)^{1/2} \approx 3.23, \quad (d = 3). \quad (3.76)$$

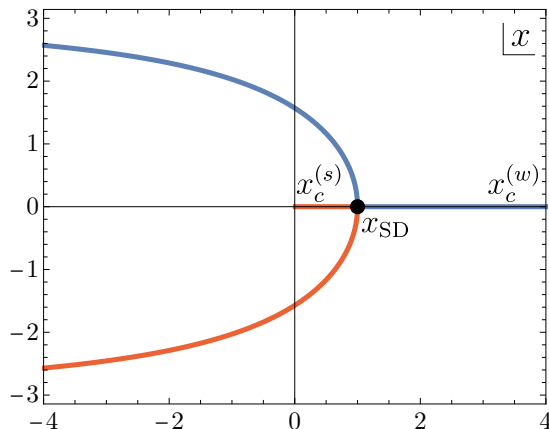


Figure 3.3: Positions in the complex x plane of the critical values of the weak ($x_c^{(w)}$ blue line) and strong ($x_c^{(s)}$ red line) branches as the renormalization scheme κ is varied. The black dot corresponds to the self-dual point $x_{\text{SD}} = 1$ where the critical points merge.

Depending on the value of the coupling, the theories admit one or three equivalent descriptions. We summarize the phase structure in fig. 3.2. In $d = 2$ the theory admits only one description in the classically unbroken phase for $x > x_I$, where x_I is the map of the self-dual point \hat{x}_{SD} by means of (3.71). The region $0 < x < x_I$ can instead be mapped to $0 < \hat{x} < \hat{x}_{\text{SD}}$ and $\hat{x} > \hat{x}_{\text{SD}}$, so three descriptions are possible, one in the classically unbroken and two in the classically broken phases. Within our class of schemes the position of the self-dual coupling is invariant while the positions of the critical couplings, denoted by x_c , $\hat{x}_c^{(w)}$ and $\hat{x}_c^{(s)}$ with obvious notation, depend on the renormalization schemes and are related, as discussed in the next section. In the schemes where $x_c > x_I$ in $d = 2$, the unbroken region around \hat{x}_{SD} disappears and the phase transition is accessible only from the unbroken phase. In $d = 3$ the structure is the same after the substitutions $x \leftrightarrow \hat{x}$ and inverting the role of broken and unbroken phases.

3.6 Fixed Points Annihilation and Analyticity Domain

It is well-known that $d = 3$ $O(N)$ quartic models undergo a second-order phase transition for any value of N . So, how could one trust the existence of a strong-weak duality in these theories based on perturbative treatments around the (classically) unbroken phase? In particular, where is the broken phase? We will now address these questions.

Suppose that in a given renormalization scheme the $d = 3$ $O(N)$ models have a phase transition for $o(1)$ real values of $x_c^{(w)}$ and $x_c^{(s)}$ in the weak and strong branches, respectively. The existence of such schemes will be proved in section 3.8. Using (3.59) we can determine how the

fixed points move when we change renormalization scheme:

$$\begin{aligned} x_c^{(w)}(\kappa) &= -W_{-1}\left(-x_c^{(w)}e^{-x_c^{(w)}-\kappa}\right), \\ x_c^{(s)}(\kappa) &= -W_0\left(-x_c^{(s)}e^{-x_c^{(s)}-\kappa}\right), \end{aligned} \quad (3.77)$$

where $x_c^{(w)} \equiv x_c^{(w)}(\kappa = 0)$, $x_c^{(s)} \equiv x_c^{(s)}(\kappa = 0)$.²¹ For $\kappa > 0$, as κ increases, $x_c^{(w)}(\kappa)$ and $x_c^{(s)}(\kappa)$ respectively increases and decreases, moving far apart. On the other hand, for $\kappa < 0$, as $|\kappa|$ increases $x_c^{(w)}(\kappa)$ and $x_c^{(s)}(\kappa)$ respectively decreases and increases, approaching each other, until they merge when the argument of the two branches of the Lambert function equal $-1/e$, namely at the self-dual point

$$x_c^{(w)}(\kappa_*) = x_c^{(s)}(\kappa_*) = x_{\text{SD}} = 1, \quad \kappa_* = 1 + \log(x_c e^{-x_c}). \quad (3.78)$$

For κ slightly smaller than κ_* , $x_c^{(w)}$ and $x_c^{(s)}$ move in the imaginary axis in a complex conjugate pair. As κ decreases they move backwards in an approximate parabolic trajectory and then they move towards $|x| \rightarrow \infty$ in parallel along the negative real axis with $\text{Im } x_c^{(w)} \rightarrow \pi$, $\text{Im } x_c^{(s)} \rightarrow -\pi$, see fig. 3.3. More precisely, for $\kappa \rightarrow -\infty$, we have

$$x_c^{(w)}(\kappa) \approx -|\kappa| + i\pi, \quad x_c^{(s)}(\kappa) \approx -|\kappa| - i\pi, \quad (3.79)$$

and both critical couplings approach the free theory, while for $\kappa \rightarrow \infty$ we have

$$x_c^{(w)}(\kappa) \approx \kappa + x_c^{(w)}, \quad x_c^{(s)}(\kappa) \approx x_c^{(s)} e^{-x_c^{(s)}} e^{-\kappa}. \quad (3.80)$$

This implies that for $\kappa < \kappa_*$ the phase transition cannot be seen in $d = 3$ $O(N)$ theories when starting from the classically unbroken phase, with real values of the coupling. In these schemes we can then hope to have access to the strong-weak duality starting from perturbative considerations, without encountering non-analyticities associated with phase transitions. Note that this is independent of the Magruder duality and hence apply for any N .

A few studies of the 2d and 3d ϕ^4 theories have been performed away from criticality, and there was no consensus on the appearance of first/second-order phase transitions when $m^2 > 0$. Studies using the Gaussian effective potential were either inconclusive on the appearance of a phase transition [78] or found a phase transition that could be first or second-order [79]. Ref. [80] studied the ϕ^4 theory at finite volume using Monte Carlo and finite states truncations, and found no phase transition for $m^2 > 0$. We see that this problem was in fact a red herring, since the appearance of the phase transition (more precisely a gapless phase for real values of the coupling) for $m^2 > 0$ is a renormalization scheme-dependent question.

²¹Note that the parameter κ in (3.77) is shifted by a constant with respect to the κ defined in section 3.8.

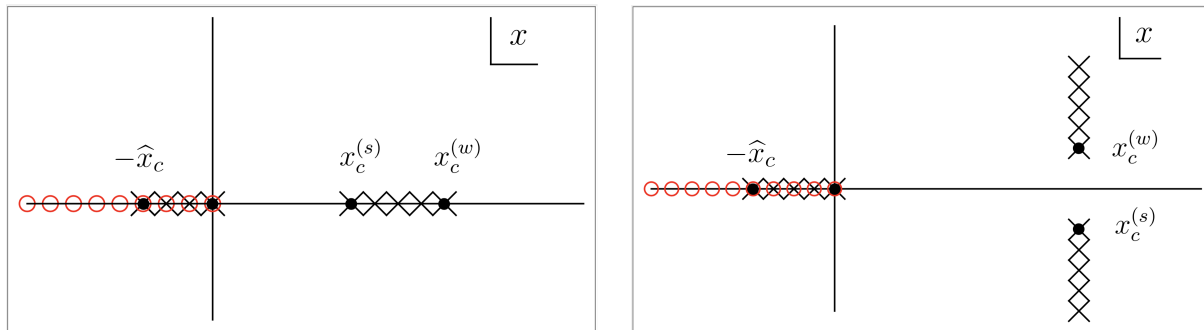


Figure 3.4: Conjectured minimal singularity structure of observables as analytic functions of the coupling x (proportional to m^2) for $O(N)$ vector theories in $d = 3$ for $\kappa > \kappa_*$ (left) and $\kappa < \kappa_*$ (right).

We can speculate about the analyticity properties of generic observables $F(x)$ as analytic functions of x , see fig. 3.4.²² We expect that $F(x)$ should have a branch-cut singularity at infinity, which corresponds to the usual branch-cut associated to perturbative asymptotic expansions around free theories. Self-duality implies that the origin should also be a singular branch-point. In the assumption of maximal analyticity, the branch-cut at infinity and the one at the origin are continuously connected. This branch-cut is depicted by red circles in fig. 3.4. In addition to that, we expect further branch-cut singularities in correspondence of the critical values $x_c^{(w)}$ and $x_c^{(s)}$, either on the real line or in the complex plane, depending on the choice of renormalization scheme. For $N > 1$ we do not really know the analytic structure in the classically broken phase ($\text{Re } x < 0$). Assuming again maximal analyticity, we might have a single critical value on the real line at $-\widehat{x}_c$ for any κ , as expected in the $N = 1$ case. The further branch-cuts associated to $x_c^{(w)}$, $x_c^{(s)}$ and $-\widehat{x}_c$ are depicted by black crossed lines in fig. 3.4. These are the minimal singularities that we expect in the complex x plane, but of course others could be present. It would be extremely interesting to understand if the analyticity properties of observables, together with perturbative data and the self-duality condition $F(x_w) = F(x_s)$ might allow for an exact solution for the $O(N)$ models.

3.6.1 Large N Non-Perturbative Mass Gap in $d = 2$

It is well-known that the appearance of a non-perturbative mass gap can be derived at leading order in a $1/N$ large N expansion in $d = 2$ $O(N)$ vector models [81]. We will see here how such a mass gap can be interpreted to arise from an analytic continuation of the squared mass from positive to negative values. By introducing a Hubbard-Stratonovich (HS) field $\sigma(x)$ we can rewrite S as in (B.5). Neglecting the vacuum energy and the counterterm $\check{\delta}m^2$, sub-leading in

²²A relevant class of observables are Schwinger n -point functions smeared with Schwarzian test functions.

$o(N^{-1})$, we have

$$\check{S} = \int d^d x \left[\frac{1}{2} (\partial_\mu \phi_i)^2 + \frac{1}{2} m^2 \phi_i^2 - \frac{1}{2} \sigma^2 + \frac{1}{2} \check{v} \sigma \phi_i^2 + \sigma \delta_T \right]. \quad (3.81)$$

Note that m^2 in (3.81) can be positive or negative. If we integrate out the scalar fields ϕ_i we get an effective potential for σ . Its extremum is given in the $\overline{\text{MS}}$ scheme by

$$\sigma = -\frac{m^2}{\check{v}} + \frac{N\check{v}}{8\pi} W(M^2), \quad (3.82)$$

where

$$M^2 = \frac{\pi \mu^2}{\check{\lambda}} e^{\frac{\pi m^2(\mu)}{\check{\lambda}}} \quad (3.83)$$

and $\check{\lambda}$ is fixed in the large N limit, see (B.2). Note that M is an RG-invariant scale with respect to the large N limit of the β -function in (3.46). In particular, we can set $\mu^2 = |m|^2$. The value of $m^2(\mu^2 = |m|^2)$ corresponds by definition to the classical mass term in the action. In the classically unbroken case, we have $m^2 > 0$ and (3.82) boils down to $\sigma = 0$, since $W(xe^x) = x$ by definition and the two terms in (3.82) cancels each other ($8\check{\lambda} = N\check{v}^2$). As expected, the HS field gets no VEV in the unbroken case and the gap in the theory is determined by the classical mass term m . On the other hand, in the classically broken phase $m^2 < 0$ and the Lambert function does not “trivialize”. Correspondingly the HS field gets a VEV, the classical m^2 term in (3.81) is cancelled by the first term in (3.82) and we are left with a positive non-perturbative mass term equal to

$$m_{\text{np}}^2 = \frac{\check{\lambda}}{\pi} W(M^2). \quad (3.84)$$

In the parametric weakly coupled limit $\check{\lambda}/|m^2| \rightarrow 0$, we have

$$m_{\text{np}}^2 \approx |m^2| e^{-\frac{\pi|m^2|}{\check{\lambda}}}. \quad (3.85)$$

Both the perturbative and non-perturbative mass gaps arise from (3.82). We can then also interpret the NP mass gap as the analytic continuation of the perturbative one from $m^2 > 0$ to $m^2 < 0$, passing through infinite coupling.²³ Interestingly enough, the non-perturbative scale (3.85) can also be deduced from IR renormalons that would appear in a perturbative expansion around the “naive” vacuum $\sigma = 0$ [83].

²³A mass gap seen as analytic continuation past infinity in the large N limit of non-linear $O(N)$ sigma models has been suggested in [82].

3.7 Numerical Results in the $d = 2$ ϕ^4 Theory

In this section we determine the critical coupling and the critical exponent ν for the $d = 2$, $N = 1$, ϕ^4 theory for different values of κ , introduced in section 3.4, in order to study the RS-dependence and the effectiveness of the Borel resummation. We numerically confirm the theoretical expectation on how the value critical coupling g_c varies in the one-parameter family of RSs. On the other hand ν , being a direct physical observable, should be RS-independent, so its evaluation in different RSs provides also a consistency check of the results.

Let us consider the perturbative expression for the mass gap defined in (3.25). Its expression up to order g^8 has been found in ref. [9] in the RS where the normal ordering is performed with respect to a the mass m . This corresponds to having a counterterm δm with value exactly opposite to the tadpole diagrams. We identify this scheme with $\kappa = 0$. Starting from this, we compute the perturbative series in a generic scheme parametrized by κ by using the expansion of (3.52). We get:

$$\begin{aligned}
\frac{M^2}{m^2} = & 1 + \frac{3}{\pi}\kappa g - \left(\frac{3}{2} + \frac{9}{\pi^2}\kappa\right)g^2 + \left(\frac{9}{\pi} + \frac{63\zeta(3)}{2\pi^3} + \left(\frac{27}{\pi^3} + \frac{9}{2\pi}\right)\kappa + \frac{27}{2\pi^3}\kappa^2\right)g^3 \\
& - \left(14.655869(22) + \frac{27}{2\pi^4}(6 + 5\pi^2 + 14\zeta(3))\kappa + \frac{27}{2\pi^4}(9 + \pi^2)\kappa^2 + \frac{27}{\pi^4}\kappa^3\right)g^4 \\
& + \left(65.97308(43) + 51.538171(63)\kappa + \frac{81}{4\pi^5}(36 + 17\pi^2 + 42\zeta(3))\kappa^2 + \frac{81}{2\pi^5}(11 + \pi^2)\kappa^3 + \frac{243}{4\pi^5}\kappa^4\right)g^5 \\
& - (347.8881(28) + 301.2139(16)\kappa + 114.49791(12)\kappa^2 + \\
& \frac{81}{2\pi^6}(105 + 37\pi^2 + 84\zeta(3))\kappa^3 + \frac{243}{4\pi^6}(25 + 2\pi^2)\kappa^4 + \frac{729}{5\pi^6}\kappa^5)g^6 \\
& + \left(2077.703(36) + 1948.682(14)\kappa + 828.4327(39)\kappa^2 + 205.20516(19)\kappa^3 + \right. \\
& \left. \frac{243}{8\pi^7}(675 + 197\pi^2 + 420\zeta(3))\kappa^4 + \frac{729}{20\pi^7}(137 + 10\pi^2)\kappa^5 + \frac{729}{2\pi^7}\kappa^6\right)g^7 \\
& - \left(13771.04(54) + 13765.22(21)\kappa + 6373.657(40)\kappa^2 + 1778.1465(75)\kappa^3 + 323.93839(27)\kappa^4 + \right. \\
& \left. \frac{2187}{20\pi^8}(812 + 207\pi^2 + 420\zeta(3))\kappa^5 + \frac{2187}{20\pi^8}(147 + 10\pi^2)\kappa^6 + \frac{6561}{7\pi^8}\kappa^7\right)g^8. \tag{3.86}
\end{aligned}$$

This is the same series one obtains by doing computations the RS where the normal ordering is performed with respect to a generic scale $\mu = me^{\kappa/2}$, so that for $\kappa \neq 0$ the one-loop tadpole diagram no longer vanishes:

$$\text{---}\bigcirc\text{---} + \text{---}\blacksquare\text{---} = \frac{3}{\pi}\kappa\lambda, \tag{3.87}$$

and hence all loop diagrams involving tadpoles cannot be neglected. The expansion of (3.52)

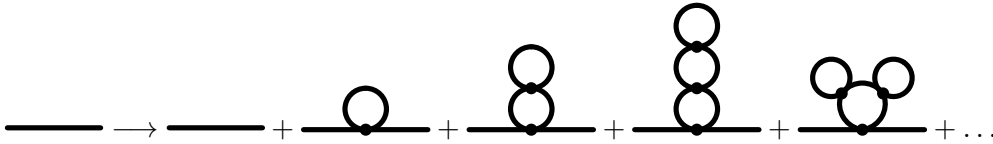


Figure 3.5: Starting from the the 1PI propagator $p^2 + m^2$ and expanding (3.52) in for small λ we have the series which accounts for the bubble diagrams. Each term is regularized as in (3.87).

applied to the tree-level term m^2 produces all higher-loop bubble diagrams, see fig. 3.5 for their form up to three-loop level.

3.7.1 Large-Order Behavior

The large-order behavior of the perturbative expansion of n -point Schwinger functions G_n in N -component ϕ^4 theories in $2 \leq d < 4$ dimensions has been worked out in ref. [84] by looking at the semi-classical complex instanton configurations. Following the notation of ref. [9],²⁴ the large-order behavior of the coefficients $G_n^{(k)}$ of the Schwinger functions G_n is given by

$$G_n^{(k)} = c_n (-a)^k \Gamma(k + b_n + 1) \left(1 + \mathcal{O}(k^{-1})\right). \quad (3.88)$$

The knowledge of the coefficients entering (3.88) is valuable when using numerical Borel resummation techniques (in particular the coefficient a is crucial to use the conformal mapping method), but they will not be needed in the discussion that follows. It is enough for our purposes to know that the coefficients a and b_n are both expected to be RS-independent while c_n is not [84]. It is straightforward to verify this expectation when the c_n 's do not depend on m^2 using the expansion of (3.52). For large k we find

$$G_n^{(k)}(\kappa) = c_n(\kappa) (-a)^k \Gamma(k + b_n + 1) \left(1 + \mathcal{O}(k^{-1})\right), \quad (3.89)$$

where

$$c_n(\kappa) = e^{\kappa/a} c_n. \quad (3.90)$$

While the choice of RS affects only the overall factor in the large-order estimate, the approach to the asymptotic behavior might and indeed does significantly change as the RS is varied. This is relevant in practice, since we always deal with truncated series. Let us consider the perturbative expression for the mass gap defined in (3.86). We can see that the coefficient multiplying the g^n term is a polynomial of degree $n - 1$ in κ for $n > 1$. The $\mathcal{O}(\kappa^{n-1})$ term is determined by the change of scheme and is equal to $\kappa^{n-1} (-3/\pi)^n \times 1/(1 - n)$. Thus more and more low orders terms are dominated by the $\mathcal{O}(\kappa^{n-1})$ contribution as $|\kappa|$ gets larger and larger. As a consequence,

²⁴Note a typo in eq. (3.14) of ref. [9]. The correct formula should be $b_n = n/2$.

| κ | Loop Order | | | | | |
|----------|------------|---------|---------|--------|--------|--------|
| | 3 | 4 | 5 | 6 | 7 | 8 |
| -4 | -3.1927 | -5.0170 | -1.6675 | 4.1456 | 0.6531 | 1.2648 |
| -3 | -3.0862 | 5.3535 | 0.6678 | 1.1928 | 1.0617 | 1.0789 |
| -2 | -0.7251 | 1.4431 | 1.0521 | 1.0513 | 1.0331 | 1.0309 |
| -1 | 0.7251 | 1.0847 | 0.9993 | 0.9825 | 0.9791 | 0.9829 |
| 0 | 1.0040 | 0.9531 | 0.9113 | 0.9076 | 0.9158 | 0.9284 |
| 1 | 0.9665 | 0.8468 | 0.8232 | 0.8311 | 0.8489 | 0.8695 |
| 2 | 0.8712 | 0.7535 | 0.7423 | 0.7585 | 0.7830 | 0.8097 |
| 3 | 0.7767 | 0.6736 | 0.6711 | 0.6925 | 0.7214 | 0.7521 |
| 4 | 0.6947 | 0.6064 | 0.6095 | 0.6341 | 0.6653 | 0.6983 |

Table 3.1: The ratio of ratios $R_M^{(k)}(\kappa)$ as given by (3.91) for different values of κ and of the loop order k .

when $\kappa < 0$ many perturbative terms at low order will have the same sign and differ from the asymptotic estimate (3.89). We compare the ratios of the series of M^2 in (3.86) with the ratio of the corresponding asymptotic series for the two-point function G_2 :

$$R_M^{(k)}(\kappa) = \frac{r_{2,\text{asym}}^{(k)}}{r_{M,\kappa}^{(k)}}, \quad r_{n,\text{asym}}^{(k)} = \frac{G_n^{(k)}}{G_n^{(k-1)}}, \quad r_{M,\kappa}^{(k)} = \frac{M^{2(k)}(\kappa)}{M^{2(k-1)}(\kappa)}, \quad (3.91)$$

and report $R_M^{(k)}(\kappa)$ for different loop orders k and values of κ in table 3.1. The behavior described above is evident. At about $\kappa = -5$ all the terms in (3.86) are positive (apart from the linear term evidently negative). For $\kappa > 0$, we see that the alternation of signs is preserved but the deviation from the asymptotic behavior increases with κ .

3.7.2 Mass and Critical Exponent ν

We report here the results for the mass gap M and the critical exponent ν obtained by a numerical Borel resummation, starting from the truncated expansion (3.86). We do not report the details of our numerical implementation. A short introduction to the resummation methods used can be found in chapter 2, while a more detailed description can be found in ref. [9], together with the procedures to estimate the uncertainties.

We show in the left panel of fig. 3.6 the mass gap M as a function of the coupling g , for different values of κ . All the plots are obtained using the conformal mapping method at order g^8 . We have checked that similar, but less accurate, results are obtained using Padé-Borel approximants. We verified that these values are in agreement with equation (3.56), see in the right panel of fig. 3.6. The numerical findings on how x_c depends on κ confirm the theoretical

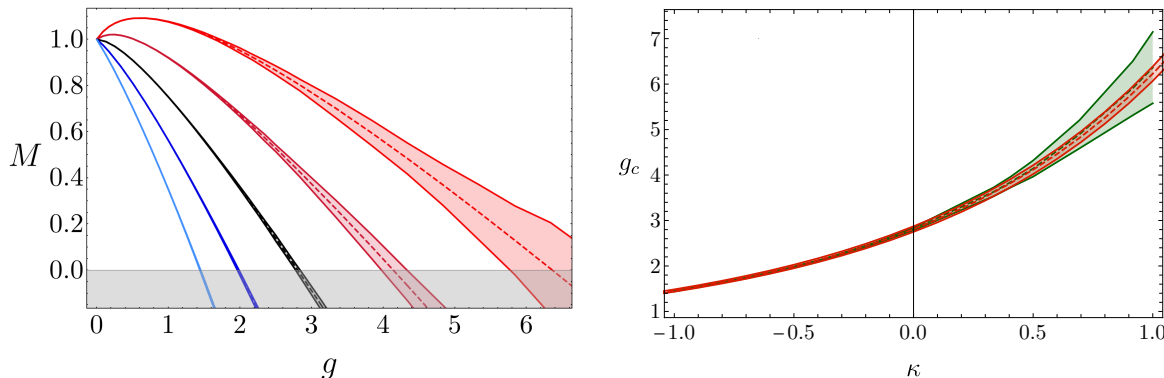


Figure 3.6: (Left panel) The pole mass M as a function of the coupling constant g using conformal mapping for different values of κ , in order (from left) $-1, -\frac{1}{2}, 0$ (in black), $\frac{1}{2}, 1$. (Right panel) In green critical coupling g_c , determined as $M(g_c) = 0$ using conformal mapping, reported as a function of κ , in red the analytic curve for $g_c(\kappa)$ from (3.56) given as value of reference $g_c(\kappa = 0)$.

expectation of section 3.4. As expected, the phase transition is visible from the (classically) unbroken phase in $d = 2$ for any choice of κ . The larger negative values κ takes, the smaller g_c becomes, until the critical regime becomes almost accessible in perturbation theory. Naively one might believe that using a RS with $\kappa \ll -1$ should allow us to get better determinations of the critical regime. This is however not the case, because for large values of κ the tadpole correction (3.87) becomes large and perturbation theory unreliable. Large values of κ , that in this case effectively plays the role of a large log, completely modify the asymptotic behavior of (3.86), thus spoiling the resummation. The breakdown of perturbation theory is most clear if we take the limit

$$\kappa \rightarrow -\infty, \quad g \rightarrow 0, \quad \text{with } g\kappa \equiv y = \text{fixed}. \quad (3.92)$$

In this limit the mass gap (3.86) reduces to

$$M^2 = m^2 \left(1 + \frac{3}{\pi} y \right). \quad (3.93)$$

The critical coupling is predicted to be at $y_c = -\pi/3$ and correspondingly we would analytically get $\nu = 1/2$, which corresponds to the mean field theory value, far from the actual result $\nu = 1$. In the limit (3.92) we should instead keep in the scalar propagator the one-loop tadpole term, effectively replacing m^2 with M^2 . In the critical regime where $M \rightarrow 0$ we will then have to face IR divergences that make the perturbative expansion in g (and its resummation) ill-defined.

We now turn to the determination of ν . For $\kappa \neq 0$, where M^2 includes a linear term in g , it is useful to resum

$$L_\kappa(g) \equiv \frac{2g}{g\partial_g \log M^2}, \quad (3.94)$$

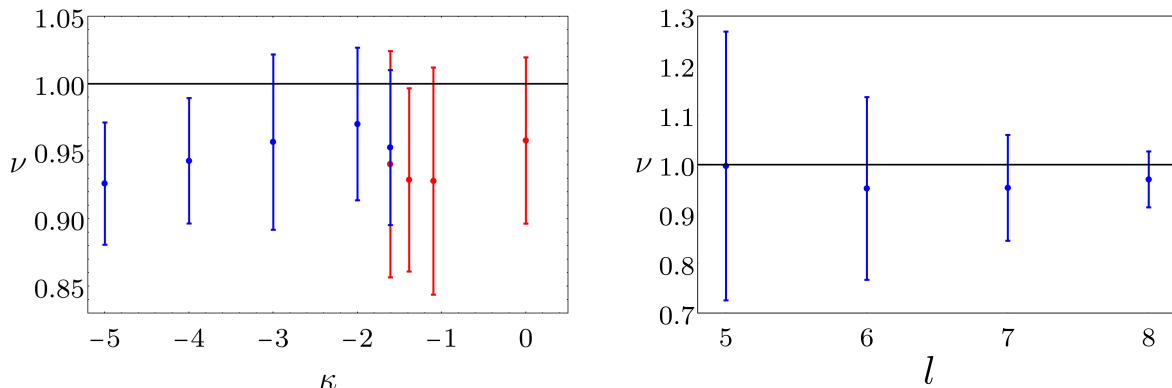


Figure 3.7: (Left panel) The critical exponent ν for different values of κ . The blue points are computed with conformal mapping, the red ones with Padé-Borel approximants. (Right panel) The critical exponent ν is computed with conformal mapping resummation technique for $\kappa = -2$ as function of the number of loops l kept.

instead of using (3.29), as in the $\kappa = 0$ case [9], and extract ν as

$$\nu = \frac{1}{\partial_g L_\kappa} \Big|_{g=g_c}. \quad (3.95)$$

We show in the left panel of fig. 3.7 the values of ν so determined, as a function of κ , in the range $\kappa \in [-5, 0]$. The resummation using Padé-Borel approximants are not affected by spurious poles only in the range of $\kappa \in [-2, -1]$ and for the value corresponding to the normal ordering RS $\kappa = 0$. The conformal mapping shows an increasingly worse convergence for values of $\kappa > -\frac{3}{2}$, presumably because $L_\kappa(g)$ has a series that differs more and more from the asymptotic one. As can be seen, for the more negative values of κ the computed value for ν starts to depart from its correct value $\nu = 1$, drifting towards $\nu = 1/2$, as expected from the previous discussion. We have numerically verified that $\nu \rightarrow 1/2$ as $\kappa \rightarrow -\infty$ if we erroneously continue to resum the perturbative expansion. The accuracy in the determination of ν does not significantly change as κ is varied in the range where the use of perturbative expansion is justified. For illustration, we show in the right panel of fig. 3.7 the value of ν as a function of the coefficient terms kept in the resummation for the value $\kappa = -2$. The improvement as l , number of loops kept in the series, increases is manifest.

3.8 Numerical Results in $d = 3$ $O(N)$ Models

We report in this section the results obtained by resumming the perturbative series for the vacuum energy and the mass gap defined as

$$\Lambda \equiv \Gamma^{(0)}, \quad M^2 \equiv \Gamma^{(2)}(p = 0), \quad (3.96)$$

as a function of the coupling g in 3d $O(N)$ vector models. We confirm the theoretical expectations made in the previous sections. In particular, we provide evidence for the self-duality of these models and determine how the critical coupling g_c depends on the renormalization scheme. We used as usual two independent methods for the resummation: conformal mapping and reconstruction of the Borel function via Padé approximants (in the following denoted for short conformal-Borel and Padé-Borel respectively). We do not report the details of the numerical implementation, which can be found in [9].²⁵ The parameters needed to perform the conformal mapping in 3d $O(N)$ models are well-known and can be found e.g. in [84]. In all our results we find agreement between conformal-Borel and Padé-Borel methods, typically with slightly smaller uncertainties in the first one, and a consistent convergence of the results as the number of loops used in the resummation is increased. For this reason, in order to avoid clutter in the figures, we have decided to only plot quantities computed using conformal-Borel to the maximum available order.

3.8.1 Perturbative Coefficients up to g^8

We have computed the perturbative expansion of the zero-point function and the two-point function at zero external momentum up to order g^8 . The computation has been performed numerically in momentum space using various simplifications introduced in [85, 86, 60]. In the following we summarize the principal aspects of the computation.

Choice of the scheme. Since we compute loop integrals numerically, a direct use of dimensional regularization is unfeasible. It is instead convenient to regularize divergences without introducing a regulator, subtracting to integrands of Feynman diagrams their values at a given fixed momentum, as proposed long ago by Zimmermann [87]. In this intermediate scheme (labeled with the subscript I) the mass counterterm δm_I^2 not only removes the divergence coming from the sunset-diagram (here chosen in such a way that the sunset diagram is regularized to be exactly zero at $p = 0$) but it cancels also the one-loop tadpole-like diagram:

$$\delta m_I^2 = - \left(\text{Sunset} + \text{Tadpole}_{p=0} \right). \quad (3.97)$$

Renormalization of higher order diagrams is then trivially implemented by substituting every tadpole and sunset subdiagram by its regularized counterpart:

$$\text{Tadpole}_{\text{reg}} = 0, \quad (3.98)$$

²⁵Padé approximants with poles on the positive real axis of the Borel variable were excluded in [9]. These are now included taking the Cauchy principal value and adding to the error estimate the residue at the pole.

$$\text{---} \circlearrowleft \text{---} \underset{\text{reg}}{p} = -\lambda^2 \frac{N+2}{\pi^2} \left[2 - \log \left(1 + \frac{p^2}{9m_I^2} \right) - \frac{6m_I}{|p|} \arctan \left(\frac{|p|}{3m_I} \right) \right]. \quad (3.99)$$

All the diagrams involving tadpoles are set to zero, greatly reducing the number of integrals to compute. The vacuum energy counterterm in this scheme is chosen such that all contributions up to $o(g_I^3)$ vanish.

Simplification of the integrands and numerical computation. In order to improve the efficiency of the numerical integration we performed some analytical simplifications [85,86] on the integrands that allowed us to greatly reduce the cost of the integrals for every diagram.²⁶ We have then numerically integrated each diagram using the Monte Carlo VEGAS algorithm [88] from the python module `vegas` and later combined all the results with their corresponding $O(N)$ symmetry factors. As a sanity check, we compared the large N limit of the perturbative expressions for Λ and M^2 so obtained with those directly computed using large N techniques and found total agreement within the accuracy of the numerical evaluation of Feynman diagrams. We report in appendix B the computation of Λ and M^2 at the first non-trivial order in the large N limit. As a further check, we have computed the series of $d\Gamma^{(2)}/dp^2(p=0)$ and $\Gamma^{(4)}(p=0)$ up to order g_I^8 . In this way, as explained in section 6.1 of [9], we can determine the series expansion of the β -function and of the critical exponent η in the physical scheme of [10] and have verified that they match with those appearing in the literature, known up to order \tilde{g}^7 and \tilde{g}^6 respectively [89].

Mapping to the $\overline{\text{MS}}$ scheme. As a last step we have switched to the $\overline{\text{MS}}$ scheme by perturbatively reexpanding $m_I^2(m^2)$ in powers of λ . The matching of the schemes is obtained by imposing the relation

$$m_I^2 + \delta m_I^2 = m^2 + \delta m^2, \quad (3.100)$$

with m^2 and δm^2 in the $\overline{\text{MS}}$ scheme and we write $\delta m_I^2 = -\Sigma_1 - \Sigma_{2a}(0)$. The explicit expressions for Σ_1 , Σ_{2a} and δm^2 can be found in the appendix C. We get

$$m_I^2 = m^2 - \lambda m_I \frac{N+2}{\pi} + \lambda^2 \frac{N+2}{\pi^2} \left(\log \frac{9m_I^2}{m^2} - 1 \right). \quad (3.101)$$

By iteratively substituting m_I in the right-hand side we then find the sought expansion. The first three orders are

$$m_I^2 = m^2 \left[1 - g \frac{N+2}{\pi} + g^2 \frac{(N+2)(N+4 \log 3)}{2\pi^2} - g^3 \frac{(N+2)^2(N+6+8 \log 3)}{8\pi^3} + o(g^4) \right]. \quad (3.102)$$

²⁶Let us here skip further details, since in section 3.9.1 we are going to present the numerical strategies more systematically and with some aspects upgraded.

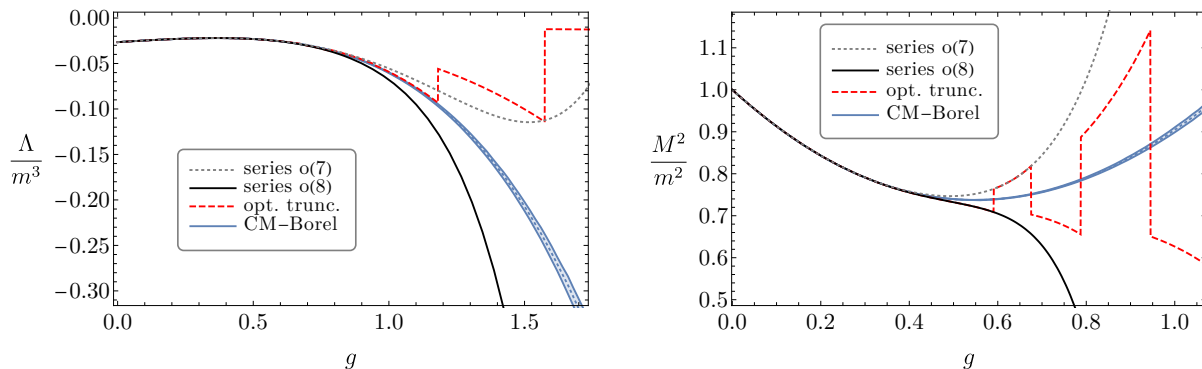


Figure 3.8: The vacuum energy Λ and the mass gap M^2 as a function of the coupling constant g obtained by ordinary perturbation theory up to g^7 and g^8 (dotted grey and black lines), optimal truncation (red dotted line) and conformal-Borel resummation (blue line).

The vacuum energy is divergent up to order g^3 and needs to be regularized by a vacuum energy counterterm $\delta\rho$. The computation of diagrams up to $o(g^3)$ in the $\overline{\text{MS}}$ scheme is presented in appendix C. The final Taylor expansion up to order g^8 of both Λ and M^2 in the $\overline{\text{MS}}$ scheme is reported in appendix D. We can now derive the series for Λ and M^2 for the whole one-parameter class of renormalization schemes presented in section 3.4. We identify $\kappa = 0$ with the $\overline{\text{MS}}$ scheme above. Starting from this, it is straightforward to compute the perturbative series in a generic scheme parametrized by κ by using the expansion of (3.59). We refrain to write the whole lengthy series for Λ and M^2 as a function of N and κ . For illustration, we just report below the terms up to $o(g^2)$ in both series:

$$\begin{aligned} \frac{M^2}{m^2} &= 1 - g \frac{N+2}{\pi} + g^2 \frac{(N+2)(N+4 \log 3 - 2\kappa)}{2\pi^2} + \dots, \\ \frac{\Lambda - \rho}{m^3} &= -\frac{N}{12\pi} + g \frac{N(N+2)}{16\pi^2} - g^2 \frac{N(N+2)}{8\pi^3} \left(\frac{N+2}{4} - 3 + 4 \log 2 - \kappa \right) + \dots \end{aligned} \quad (3.103)$$

For simplicity of notation the dependence on κ of the parameters m^2 , g and ρ has been left implicit in (3.103). Note that the series above could equivalently be interpreted as the series in the $\overline{\text{MS}}$ scheme with $\kappa = 0$, but with parameters m^2 and ρ evaluated at the scale $\kappa = \log(\mu^2/m^2)$. In this way, a sanity check of the validity of the change of scheme is obtained by demanding that both M^2 and Λ satisfy the Callan-Symanzik equations

$$\begin{aligned} (\mu\partial_\mu + \beta_{m^2}\partial_{m^2})M^2 &= 0, \\ (\mu\partial_\mu + \beta_{m^2}\partial_{m^2} + \beta_\rho\partial_\rho)\Lambda &= 0, \end{aligned} \quad (3.104)$$

with β_{m^2} and β_ρ given by (3.46) and (C.3), respectively. We always normalize the vacuum energy as $\rho(\kappa = 0) = \rho(m) = 0$. This implies that in computing Λ in a scheme with $\kappa \neq 0$ the parameter

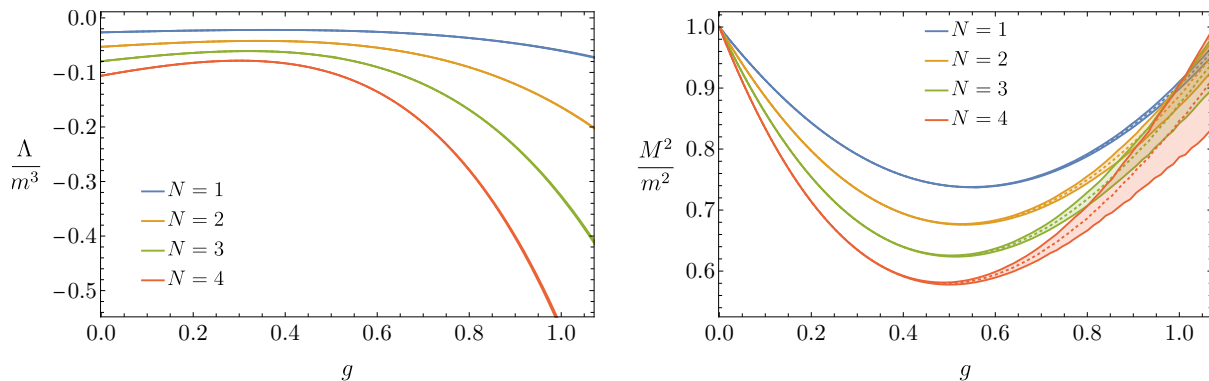


Figure 3.9: The vacuum energy Λ and the mass gap M^2 as a function of the coupling constant g for different values of N in the scheme $\kappa = 0$. The results shown correspond to conformal-Borel resummation.

$\rho(\kappa)$ is non-vanishing and should be taken into account.

3.8.2 Self-Duality

We report here the results obtained by numerical Borel resummation of the perturbative series for Λ and M^2 for different values of N and provide evidence for the self-duality of 3d $O(N)$ vector models. We start by showing the need of resumming the perturbative series in the region of couplings of interest. To this purpose, we compare in fig. 3.8 Λ and M^2 as a function of the coupling g computed using the perturbative seven and eight loop results, optimal truncation, and Borel resummations. We take $N = 1$ and choose the renormalization scheme $\kappa = 0$, where M^2 does not vanish for real values of g . A similar analysis applies for other values of N . In both figures it is clear that perturbation theory breaks down before $g_{\text{SD}} = \pi/\sqrt{3}$ at a value of $g \approx 1$ for Λ and $g \approx 0.6$ for M^2 , and we observe that these values slightly decrease while increasing N . Therefore resummation techniques are required in order to study the self-duality.

As discussed in the previous sections, for $\kappa < \kappa_*$ the phase transition is expected to be not visible from the unbroken phase. We show in fig. 3.9 Λ and M^2 as a function of the coupling g at $\kappa = 0$ computed for different values of N and using conformal-Borel resummation. The right panel in fig. 3.9 clearly shows that $M^2(g)$ is always positive, with the curve $M^2(g)$ developing a minimum around $g = 0.6$ and then continuing to increase for larger values of g , as shown in fig. 3.11 for $N = 1$; this confirms the absence of a gapless phase. We can determine $\kappa_*(N)$ by computing the critical coupling for a value of κ where the transition occurs and then use the map to determine the values of $\kappa_*(N)$ where the two critical points merge. Taking as reference value $\kappa = 5$, we get for the first values of N $\kappa_*(1) = 3.5(2)$, $\kappa_*(2) = 3.3(2)$, $\kappa_*(3) = 3.2(2)$ and $\kappa_*(4) = 3.1(3)$.

Let us now focus on the region $\kappa < \kappa_*$, where M^2 vanishes for complex values of the coupling, and discuss the self-duality. First of all let us explain why we can probe self-duality using

resummations of the perturbative series. The complex points where M^2 vanish are generally expected to be non-analytic points for Schwinger functions. Given a quantity $F(g)$ admitting a Borel resumable asymptotic expansion around $g = 0$, the region in the complex g plane where the Borel reconstruction of the function is guaranteed to reproduce the original function is given by a disk [16] with a radius which is determined by the first singularities of $F(g)$ in the positive half-plane. In our case the complex critical points are further away from the origin than the self-dual point. This implies that the disk of minimal analyticity extends beyond the latter and allows us to explore (part of) the strong branch when $\kappa < \kappa_*$.

If self-duality is *assumed*, we can extract useful information on the asymptotic behavior of an observable $F(g)$ at strong coupling $g \rightarrow \infty$. Let $F(g)$ be an observable with mass dimension n . After an appropriate rescaling we can write its Taylor expansion in the weak branch as

$$F(g) \sim m^n g^{k_0} f(g), \quad f(g) = 1 + \sum_{k=1}^{\infty} c_k g^k, \quad g = \frac{\lambda}{m^{4-d}}, \quad (3.105)$$

where $k_0 \geq 0$ is the first non-vanishing order in perturbation theory. The \sim is used because the series is only formal (asymptotic). We consider both the $d = 2$ and $d = 3$ cases together, and for simplicity drop the hats in $d = 2$ on the couplings. Self-duality implies

$$F(g_w) = F(g_s) \quad \Rightarrow \quad g_w^{k_0 - \frac{n}{4-d}} f(g_w) = g_s^{k_0 - \frac{n}{4-d}} f(g_s). \quad (3.106)$$

In the limit $g_w \rightarrow 0$, we obtain the scaling at strong coupling from (3.63) as

$$g_w^{-1} \sim (\log g_s)^{\frac{1}{d-1}}, \quad (3.107)$$

which plugged into (3.106) gives

$$\lim_{g \rightarrow \infty} f(g) \sim g^{-k_0 + \frac{n}{4-d}} (\log g)^\alpha, \quad \alpha = \frac{1}{d-1} \left(\frac{n}{4-d} - k_0 \right). \quad (3.108)$$

Therefore the scaling of the observable $F(g)$ as $g \rightarrow \infty$ is

$$F(g) \sim m^n g^s (\log g)^\alpha, \quad s = \frac{n}{4-d}. \quad (3.109)$$

Note that in general observables do not admit an analytic strongly coupled asymptotic Taylor expansion around infinity, due to the appearance of the logs.²⁷

We want to test the self-duality, so the scaling (3.109) will *not* be assumed. As a first indirect test of the duality, we find that the parameter s , which is fixed by the optimization procedure

²⁷Non-analytic expansions involving logarithms of the coupling have been invoked to cure IR divergences that appear with massless particles in 2d and 3d [90]. Interestingly enough, we see here how these log's automatically arise from the duality.

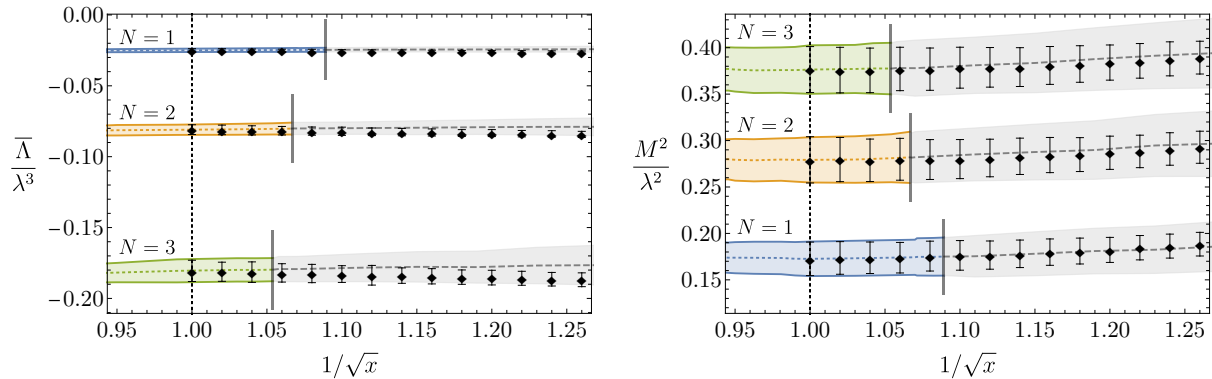


Figure 3.10: The shifted vacuum energy $\bar{\Lambda} = \Lambda - \rho(\lambda)$ (with ρ defined as in (C.3)) and the mass gap M^2 as a function of $\frac{1}{\sqrt{x}} = \frac{\sqrt{N+2}}{\pi}g$, for $N = 1, 2, 3$. The error bands and the central values (dashed lines) are obtained using conformal-Borel resummation. For any N the self-dual point is at $x = 1$. The points correspond to values obtained in the weak branch and mapped in the strong branch using the duality map (3.62). The vertical segment drawn on each band denotes the theoretical disk of analyticity: beyond that value the curves have been drawn in gray. To avoid overlapping of the curves we have applied an offset of $\Delta(M^2/\lambda^2) = (N - 1)/10$ to the data in the right panel. In both panels $\kappa = 5/2$.

in our conformal-Borel resummations [9], is always close to the theoretical prediction (3.109) for both Λ and M^2 . Analogously, with the Padé-Borel resummations we find that the best approximants $[p, q]$ satisfy the relation $p - q = s$.

We show in fig. 3.10 the vacuum energy Λ and the mass gap M^2 as a function of $1/\sqrt{x}$ for different values of N at $\kappa = 5/2$. In order to take into account the vacuum energy shift, necessary to map it from the weak to the strong branch, we report the quantity $\bar{\Lambda} = \Lambda - \rho(\lambda)$, where ρ is defined in (C.3). In this way, $\bar{\Lambda}$ should have an extremum at the self-dual point which, in the variable x , is at $x = 1$ for any value of N . The black points in the figure correspond to values obtained in the weak branch and mapped in the strong branch using (3.62). The vertical segment drawn on each band denotes the disk of analyticity beyond which Borel resummation is not guaranteed to work. Beyond that value, the curves have been drawn in gray. Fig. 3.10 gives us good evidence for the self-duality. Note in particular how $x = 1$ is to a very good accuracy an extremum of both $\bar{\Lambda}$ and M^2 , as expected. Interestingly enough, the agreement persists well beyond the disk of analyticity for both $\bar{\Lambda}$ and M^2 .

3.8.3 Scheme Dependence of Critical Couplings

In this subsection we determine how the critical coupling g_c depends on the renormalization scheme. We show in the left panel of fig. 3.11 M^2 as a function of g for $N = 1$ and different values of κ . As expected, the phase transition is not always visible and by increasing the value of κ two zeros appear. While the value of the first is in principle reliable and should be identified with the weak critical coupling $g_c^{(w)}$, the same cannot be said for the second, since it is reached after the

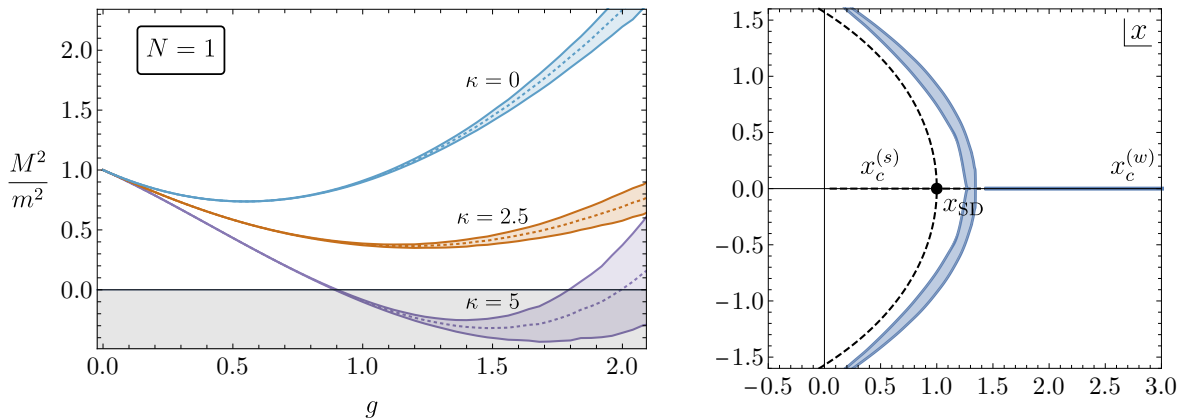


Figure 3.11: (Left) The mass gap M^2/m^2 for $N = 1$ at three different values of κ . (Right) The position of the critical coupling $x_c(\kappa)$ in the complex x plane as κ is varied for $N = 1$. The blue bands are computed with conformal-Borel, the dashed black line is the analytic expectation from (3.77).

theory has passed a phase transition. Being $g = g_c^{(w)}$ a non-analytic point, Borel resummation is not guaranteed for $g > g_c^{(w)}$. For this reason we can only focus on the region where $g \leq g_c^{(w)}$.²⁸ The accuracy of the numerical resummations depends on κ and only a limited range of optimal values of κ (when the phase transition occurs) is expected. Indeed, as κ decreases, the two critical couplings approach each other, and a general instability in the resummation procedure is expected and in fact does occur. On the other hand, if κ increases, although the value of $g_c^{(w)}$ decreases, we are effectively in presence of large logs that spoil the validity of the perturbative expansion, as already noted in $d = 2$. We choose as optimal reference scheme $\kappa = 5$ for any N .²⁹

In the right panel of fig. 3.11 we plot the position of g_c in the complex g -plane as κ is varied and compare it with the analytic prediction given by (3.77). The movement of g_c as κ varies is in fair agreement with the theoretical prediction, but it shows a small disagreement. This discrepancy reflects a systematic slow convergence and low accuracy in the resummations for $\kappa > \kappa_*$. In order to quantify it, we can compare the values of g_c defined as the zero of M^2 and equivalently as the zero of the function $L(g) = (\partial_g \log M^2)^{-1}$. The function L is useful because it can be used to extract the critical exponent ν . For example at $\kappa = 5$, $N = 1$, we find $g_c^{(M^2)}(\kappa = 5) = 0.898(5)$ and $g_c^{(L)}(\kappa = 5) = 0.944(16)$. The two values are not in agreement and indicate the presence of a systematic error which is not captured by our error estimate. Similarly the accuracy in the determination of ν is significantly lower than that found in the literature (see e.g. [57]) in the scheme of [10]. This lack of accuracy might be due to the presence of the self-duality and an analytic structure for observables more difficult to reconstruct numerically.

²⁸It is however interesting to see that the analytic continuation of the Borel resummed mass gap M^2 for $g > g_c^{(w)}$ has a further zero, as expected from the self-duality of the theory (see the purple band in the left panel of fig. 3.11). The numerical accuracy of the resummation does not in any case allow us to determine the second zero accurately enough to possibly test if it is equal to $g_c^{(s)}$.

²⁹The range of optimal values of κ has a mild dependence on N , which can be neglected for low values of N .

| Method | $N = 1$ | $N = 2$ | $N = 4$ |
|------------|-----------------|----------------|-----------------|
| Lattice MC | 1.0670(17) [91] | 0.9509(5) [92] | 0.8238(26) [91] |
| This work | 1.08(3) | 0.94(2) | 0.80(2) |

Table 3.2: Comparison of the (weak) critical coupling g_c^{MC} with the results of Lattice Monte Carlo computations, for 3d $O(N)$ models with $N = 1, 2, 4$.

The value of g_c in $O(N)$ vector models has been computed in the past for $N = 2$ and $N = 1, 4$ in [92, 93] and [91] respectively, using Lattice Monte Carlo methods. Very recently Hamiltonian truncation methods have been developed to study the $N = 1$ theory [94, 95]. A comparison with our results is however still not available, because in [94] the extrapolation to infinite volume has not been taken and in [95] the use of light-cone quantization requires to work out the non-trivial map to pass to a covariant quantization. For this reason we restrict our comparison with the earlier results [91–93]. These works report the value of g_c in $\overline{\text{MS}}$ at the scale $\mu = 8\lambda$, which we denote by g_c^{MC} . A direct computation at that scale is not possible, since our perturbative series will involve logarithms of g . However, we can access this value by using the exact one-loop running of $g_c(\kappa)$. We get

$$(g_c^{\text{MC}})^{-2} = g_c^{-2}(\kappa) - \frac{N+2}{\pi^2} \log\left(\frac{e^\kappa}{64g_c^2(\kappa)}\right). \quad (3.110)$$

The right hand side of (3.110) should be independent of κ , but numerically a dependence on κ remains. We have computed $g_c^{(M^2)}$ and $g_c^{(L)}$ for a set of values of $\kappa \in [5, 6]$, mapped them with (3.110) and then taken an average value as our final estimate. In table 3.2 we compare these values of g_c^{MC} with those given by [91–93]. The values are in agreement, but with large errors on our side.

3.9 Improved Numerical Results in $d = 3$ $O(N)$ Models

Since the uncertainties of the resummations in the minimal scheme turned out to be very large for the critical theory of the $O(N)$ models in $d = 3$, we decided to study those models at criticality via the use of RG flow in the scheme $\tilde{\mathcal{S}}$. In order to do so, we had to improve the numerical precision of our perturbative series for the 1PI functions $\Gamma^{(2)}$, $\Gamma^{(2)'}$ and $\Gamma^{(4)}$ at zero external momentum. Especially the latter two, that in our previous analysis were used just for a check of the first series $\Gamma^{(2)}(p=0)$ with the literature. Now instead, as we have seen in section 3.2.1, all three are needed to compute the series for $\tilde{\beta}(\tilde{g})$, $\tilde{\eta}(\tilde{g})$, and $\tilde{\nu}(\tilde{g})$.

We use this as an opportunity to upgrade the way in which we performed the numerical computations and structure them. Thanks to this, we will provide a package that will appear together with our upcoming paper [4]. The package `Phi4tool` will consist of a simple interface for

displaying Feynman diagrams, their label, symmetry factor, their integrand together with their numerical result. This will fill a gap in the literature. As every diagram is treated independently, it will be useful for studies in ϕ^4 theories with other tensorial structures. The package that we are going to share will work as a repository and thus might come in handy as a source of data for other studies and for performing checks at any order in perturbation theory up to the eight. On the other hand, it is structured so that it will be a good starting point to push forward the computations at the next order (the nine-order for which we already provide diagrams and integrands) and to further improve their efficiency.

In the following subsection, we are going to describe the strategies used in the computation of the perturbative series, using the occasion to list some of the content that will be present in the `Phi4tool` package. Once again, the computations are performed in what we called the intermediate scheme. The subsection after that will be dedicated to presenting our results for the critical phase in the $O(N)$ symmetric field theory computed Borel resumming the perturbative series in the scheme $\tilde{\mathcal{S}}$.

3.9.1 Numerical Strategies

The evaluation of Feynman diagrams in super-renormalizable QFTs poses some technical challenges that must be addressed in order to push the computation to high orders. In fact, the difficulties quickly increase with the perturbative order due, on the one hand, to the growing number of diagram topologies that need to be generated together with their symmetry factors and, on the other hand, to the increased dimensionality of each integral. The latter issue represents the main obstacle to the precise computation of the perturbative series since it is still challenging to obtain high precision results from high-dimensional numerical integrals. In order to tackle this issue, one can reduce the dimension of the integration space by performing part of the integration analytically [86]. An effective way of doing it is to work in momentum space, identify simple subdiagrams in our Feynman diagrams, and substitute them with their analytical value [60]. This is the central operation that we used to compute the perturbative series up to eighth order. However, there are several other measures that turned out to greatly reduce the computational cost and improve the accuracy of our results. In the following, we summarize the main steps of our computation.

Drawing and labeling the Feynman diagrams

The first step to compute the perturbative series consists in the generation of all the Feynman diagrams at each given order, together with their symmetry factors. We leveraged the already available `feynngen` program [96] to generate all the diagrams for the zero, two, and four point function with up to nine quartic vertices. The choice of a renormalization scheme in which the

regularized tadpole is zero greatly reduces the number of Feynman diagrams that one has to compute, since all the diagrams involving tadpoles vanish. We have also generated the diagrams for the theory with both quartic and cubic interactions with up to eight total vertices. We obtained the diagrams for the mixed case with a simple program that, starting from the diagrams with only quartic vertices, repeatedly removed propagators accounting for the proper correction to symmetry factor and collected the resulting diagrams based on their topology.

To organize and order the diagrams, we employed the commonly used *Nickel index* to label them [97, 98]. We will quickly review here how the labeling algorithm works, namely how to assign an index to a given graph and how to read it. Consider an arbitrary undirected connected graph with n internal vertices, already labeled from 0 to $n - 1$, and with some external vertices all labeled “e”. The Nickel Index for this labeled graph \mathcal{G}_L is the sequence constructed in the following way

$$\mathfrak{N}(\mathcal{G}_L) = c(0)|c(1)|\dots|c(n-1)|, \quad (3.111)$$

where $c(i)$ is the sequence of all the vertices connected to the vertex i whose label is $j \geq i$, repeated in case of multiple edges, and ordered in ascending order with the convention that “e” goes first in the order, i.e. $e < 0 < 1 < \dots < n - 1$. In this way, the sequence (3.111) corresponds exactly to one graph, which can be directly reconstructed from the sequence. However, the opposite is not yet true since the string (3.111) depends on the way we enumerated the vertices. In order to overcome this ambiguity, we first establish a way to order different sequences: the strings obtained as above are converted to a numeric field, interpreting each sequence as a number with radix $n + 2$ with the following order to its digits $e < “|” < 0 < 1 < \dots < n - 1$. The correct labeling of the vertices is then identified as the one that corresponds to the sequence with the smallest number, the minimal graph descriptor. For example, in fig. 3.12 we show three possible labelings of the same diagram. The central label is the minimal one, hence the correct Nickel index associated with the diagram.

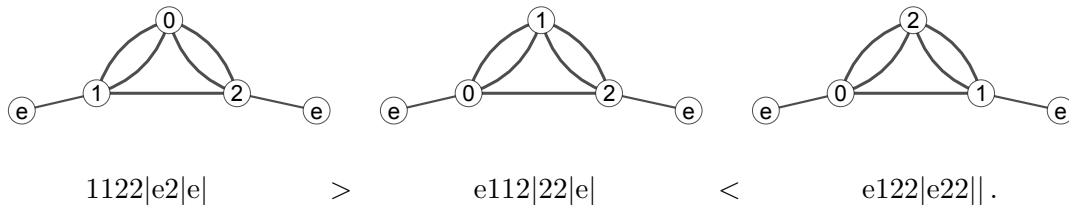


Figure 3.12: Different enumerations and their corresponding sequences. The first one is the biggest of the three since its first digit is 1 and $1 > e$ and the central is smaller than the last since $e11 < e12$. The central one is hence the smallest one, the minimal graph descriptor.

With a simple program, we assigned the Nickel indices to the Feynman diagrams at each order and ordered them according to their graph descriptor. Together with our forthcoming

paper [4] we will provide the text files containing the list of the Feynman diagrams at each order, consisting in their Nickel index, adjacency list (where the name of the vertices is already the one used by the Nickel index), and symmetry factor. The `Phi4tool` package will allow easy access to the data, providing a convenient interface for the visualization of the graphs and their Nickel indices.

Multiplicities: $O(N)$ models and cubic anisotropy

Once the topologies of the Feynman diagrams are known, it is not difficult to compute their respective multiplicities, given a tensorial structure for the quartic vertex. With a simple program, that assigns tensor factors to the vertices and performs contractions, we computed the symmetry factors for the $O(N)$ -symmetric theory and for the N -component cubic-symmetric theory for the zero, two, and four point function up to order eight. We are going to share those lists in text files together with the `Phi4tool` package to quickly navigate through them.

Substitutions of the effective vertices

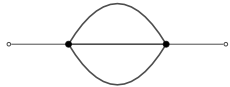

The number of loops of a diagram is given by $l = v_4 + v_3/2 - e/2 + 1$, where v_4 and v_3 are the number of quartic and cubic vertices respectively and e is the number of external lines. Using the spherical coordinates and their symmetries, the dimension of the integration space in 3 dimensions is $D = 1$ for $l = 1$ and $D = 3l - 3$ for $l > 1$. Proceeding directly to write the integrands in momentum space and performing the integrations would result in very demanding computations: to give the reader a feeling of the task, let us make the example of the two-point function with eight quartic vertices, where each of the 1622 non-zero 1PI diagrams would require a 21-dimensional numerical integration. However, it is possible to significantly reduce the complexity of the integration by substituting analytically known subdiagrams, as done long ago by Baker, Nickel, Green and Meiron [85, 54]. They used the analytically known expressions for the 1-loop subdiagrams [99] to compute the 6-loop β -function.

It is possible to perform these substitutions directly at the diagrammatic level before writing the explicit form of the integrands. One just needs to find the known cycles in the graphs and replace the propagators composing the cycle with a complex vertex connected to the vertices of the cycle by new edges. Differently from the propagators, these new edges will not contribute to the integrand. After the substitution, we get a simplified graph, corresponding to an *effective diagram* with a reduced number of loops ℓ . By applying the same procedure to the sunset subdiagrams, we renormalize its divergent contribution, making all the diagrams finite³⁰ (the diagrams with tadpoles are already set to zero). We summarize below the substitutions that we have defined, showing the symbols used to denote the effective vertices and the name of the

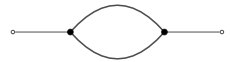

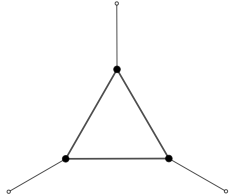
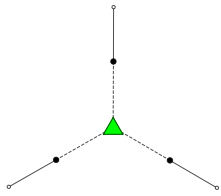
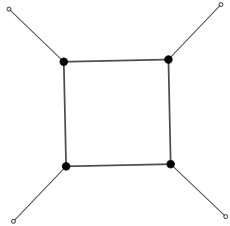
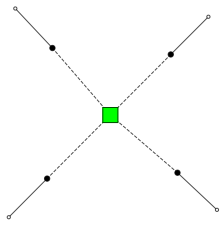
³⁰The zero-point diagrams up to order three are divergent as well, as mentioned in section 3.8.1, we set them to zero.

functions to which they correspond.

Renormalization of sunset subdiagrams. We identified *sunset* subdiagrams and substituted them with analytical effective vertices.

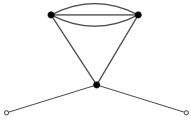

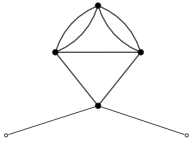

| Subdiagram | Effective vertex | Renormalized function |
|---|---|-----------------------|
|  |  | $\text{sunset}(p)$ |

One loop subdiagrams: bubbles, triangles and squares. We identified three one loop insertions, corresponding to cycles of length 2, 3, and 4, called respectively *bubble*, *triangle*, and *square*, and substituted them with effective vertices that correspond to the analytic functions of the external momenta.



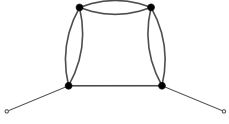

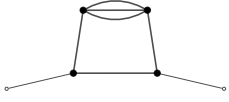



| Subdiagram | Effective vertex | Analytic function |
|---|---|---|
|  |  | $\text{bubble}(p)$ |
|  |  | $\text{triangle}(p_1, p_2, p_3)$ |
|  |  | $\text{square}(p_1, p_2, p_3, p_4, \vec{p}_1 + \vec{p}_2 , \vec{p}_2 + \vec{p}_3)$ |

Carrying on more with this same philosophy, we have identified other specific structures in the diagrams that are amenable for substitutions. These are momentum-independent subdiagrams, for which we know the analytic value, and subdiagrams depending on a single external momentum p , that are substituted either with an analytic function or with a numeric approximation constructed from a tabulation of its values as a function of p .

Momentum independent subdiagrams. We identified two tadpole-like insertions that can be integrated analytically and we added new *effective tadpoles* for them.

| Subdiagram | Effective vertex | Analytic factor |
|---|---|-----------------|
|  |  | tadSunset |
|  |  | tadTrianBub |

Numerical two-point subdiagrams. We identified some multi-loop subdiagrams that depend just on one external momentum p and substituted them with new effective vertices. We have constructed numeric functions for them, tabulating their value as a function of p .

| Subdiagram | Effective vertex | Numeric function |
|---|---|-------------------|
|  |  | triangle2b(p) |
|  |  | square3b(p) |
|  |  | square1s(p) |
|  |  | square1s1b(p) |

Three and four point subdiagrams with zero momentum flow through some legs. We identified other two multi-loop subdiagrams that would in principle depend on more than one external momenta, but we focused on the combination where all except one are equal to zero. These substitutions will affect the portions of the diagrams adjacent to the external legs. We found analytical expressions for some of the combinations, while we resorted

again to numerical tabulations for the others. We report these substitutions below, where we marked with a dotted line the external legs with zero momentum flow. The first substitution is analytical, the other two are numerical.

| Subdiagram | Effective vertex | Function |
|------------|------------------|-------------------------|
| | | $\text{triangle1bA}(p)$ |
| | | $\text{triangle1bN}(p)$ |
| | | $\text{kite}(p)$ |

Clearly, for complex enough diagrams, there might be more than one possible set of substitutions that could translate into different numerical performances. In our implementation we chose to minimize the residual number of loops ℓ and, in case of parity, we prefer the effective diagrams with more analytic substitutions. Still, it happens quite often that there are equivalent effective diagrams, therefore we implemented an algorithm that allowed us to favor some substitutions with respect to the others via a set of weights. We chose the weights based on our empirical experience, noticing that on the one side, squares and triangles seem to produce better results since they reduce the number of propagators left in the integrand, but on the other side, they have a more complicated analytical form that depends on many scalar products that tend to produce more cumbersome integrands which are slower to evaluate. In any case, the best combination of substitutions is diagram dependent and, for the few integrals in which the automatic choice of effective diagram did not produce precise enough results, we tested the other equivalent parametrizations to find the one with the best performance.

Let us present an example of how much these substitutions help in reducing the computation cost at a given order. If we focus on $\Gamma^{(4)}$ with five quartic vertices ($v_4 = 5$), we have 27 diagrams at four loops (corresponding to $D = 9$ integrals) before the substitutions. After the substitutions we get 5 diagrams with zero residual loops (no integration left), 18 diagrams with one residual loop, and 4 diagrams with two residual loops. Therefore we just have to perform 18 one-dimensional integrals and 4 three-dimensional integrals. In Table 3.3 we show two examples

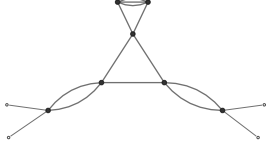
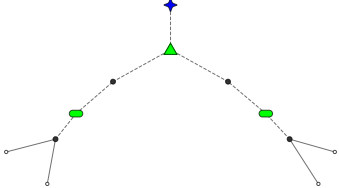
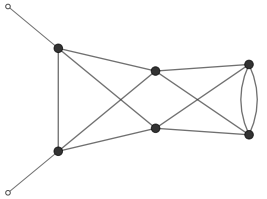
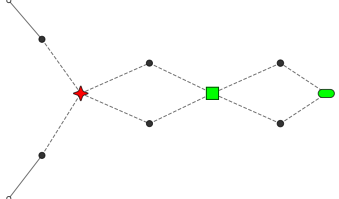
| Feynman diagram | Effective diagram | Effective integrand |
|---|---|--|
|  |  | bubble(0) ² tadSunset triangle(0, 0, 0) |
|  |  | kite(q_1)bubble(q_2) square($q_1, q_2, q_1, q_2, \vec{q}_1 - \vec{q}_2 , \vec{q}_1 + \vec{q}_2 $) |

Table 3.3: Examples of substitutions for two Feynman diagrams. In the first row, we show a four-point diagram at order seven that results in a zero-loop effective diagram after the analytical substitutions of two bubbles, one triangle, and one complex tadpole. In the second row, we show a two-point diagram at order six that results in a two-loop effective diagram after the substitution of a bubble, a square, and a numerical two-point subdiagram.

of six-loop diagrams that, after the substitution of analytic and numeric effective vertices, result in a zero-loop effective diagram and a two-loop effective diagram.

With the `Phi4tool` package it will be possible to draw the Feynman diagrams before and after the insertion of the first three classes of effective vertices.

Momentum assignation: writing the integrands

We are now ready to write the integrands associated to the effective diagrams that we built in the last sections. It is quite straightforward to automatically implement the momentum assignation at every internal edge and then impose the conservation of total momenta at each (effective) vertex. A generic diagram with ℓ effective loops then corresponds to an integral over the ℓ internal momenta of a function of the form $f(\vec{q}_1, \dots, \vec{q}_\ell)$. Additionally, one can make use of the spherical symmetry to reduce the number of integrations by placing the vector q_1 along the axis z and q_2 along the plane $x - z$ so that $q_{1,\theta} = q_{1,\phi} = q_{2,\phi} = 0$. There are however many possible parametrizations depending on the choice of the momenta, some of which may allow further simplifications and be numerically more stable than the others. In particular, we noticed that the scalar products of the momenta, appearing in the propagators and as arguments of the effective vertices, have a sizable impact on the evaluation speed and final precision of the computation, with the best results obtained for the integrands with fewer scalar products due to

the simpler structure which limits accidental cancellations. Moreover, for the remaining scalar products it is better to prefer those expressed in terms of \vec{q}_1 and \vec{q}_2 since, with our choice of coordinates, they depend on fewer angles. Furthermore, it is important to select what functions have the scalar products as arguments, preferring the bubbles and triangles to the propagators. Our implementation, available in the `Phi4tool` package, takes into account all these considerations, scanning different linear combinations of the internal momenta, and picking the best one.

In the case of $\Gamma^{(2)'}(p=0)$ there is an additional step to write the integrand of a diagram, because we need to take the derivative with respect to the external momentum \vec{p} before setting it to zero. We proceed as above by assigning all the momenta, but this time also taking into account \vec{p} and making sure it appears on the least amount of effective vertices and propagators. We then evaluate the derivative of the resulting function $\tilde{f}(\vec{p}, \vec{q}_1, \dots, \vec{q}_\ell)$ with respect to p^2 using the relation

$$\frac{\partial}{\partial p^2} \left(\int \prod_{i=1 \dots \ell} d^d \vec{q}_i \tilde{f}(\vec{p}, \vec{q}_1, \dots, \vec{q}_\ell) \right) \Big|_{p=0} = \int \prod_{i=1 \dots \ell} d^d \vec{q}_i \left(\frac{1}{2d} \frac{\partial}{\partial \vec{p}} \cdot \frac{\partial}{\partial \vec{p}} \tilde{f}(\vec{p}, \vec{q}_1, \dots, \vec{q}_\ell) \Big|_{p=0} \right). \quad (3.112)$$

At this point one can write the integral in spherical coordinates as explained above.

In [4] we are going to provide the text files containing the list of integrands corresponding to the Feynman diagrams with up to eight quartic vertices. For each one of them, there is the Nickel index of the diagram, the value of ℓ , and the function f . With the `Phi4tool` package it will be possible to access the data, as well as to write down the integrands in the form $f(\vec{q}_1, \dots, \vec{q}_\ell)$ for any of the other Feynman diagrams. Moreover, it will allow one to explicitly print the integrand multiplied by the spherical measure in $d=3$ as a function of the radial and angular components of the momenta.

Performing the integration

As the last step, we have to actually perform the numerical integrations for the diagrams of the ϕ^4 theory. Different numbers of effective loops correspond to different dimensions of integration, we found that it is better to differentiate the programs used. The integrals with $\ell=0$ are already analytic expressions with no need of integrating anything, for $\ell=1$ we have 1-dimensional integrals that can be performed with arbitrary precision by Mathematica (a limitation although is present, if there are some numerical functions in the integrand) in a matter of fractions of seconds, for $\ell=2$ we have 3-dimensional integrals that Mathematica can still manage, this time to achieve a precision of at least 10 significative digits we need some hours, so we run those integrals on the SISSA cluster Ulysses. For $\ell \geq 3$, so integrals with $D \geq 6$, we used the Monte

| N | $N = 0$ | $N = 1$ | $N = 2$ | $N = 3$ |
|---------------|------------|------------|------------|------------|
| \tilde{g}_c | 1.415(5) | 1.4137(35) | 1.4048(18) | 1.3912(10) |
| ν | 0.5880(6) | 0.6299(9) | 0.6695(10) | 0.7054(12) |
| η | 0.0277(10) | 0.0324(11) | 0.0344(9) | 0.0342(10) |

Table 3.4: Estimate of critical coupling and critical exponents in the 3d $O(N)$ models with $N = 0, 1, 2, 3$.

Carlo VEGAS algorithm [88] from the python module `vegas`. We run those integrals in part on the SISSA cluster Ulysses and in part on CINECA cluster Marconi, each one of them for one or two days.

We are going to attach to the upcoming work text files for each order containing the values of the Feynman diagrams. For each one of them, there is the Nickel index of the diagram and its value with uncertainty. With the `Phi4tool` package it is possible to quickly have the values of any of the diagrams of the ϕ^4 theory.

3.9.2 Critical regime in the RS $\tilde{\mathcal{S}}$

In the last subsection we described how we computed independently the values of the Feynman diagrams up to order eight for the perturbative series for $\Gamma^{(2)}$, $\Gamma^{(2)'}$ and $\Gamma^{(4)}$ at zero external momentum. Combining them with the symmetry factors we have computed, we are going to use them in [4] to study the three-dimensional $O(N)$ symmetric models and the N -component models with cubic-symmetric quartic interaction in $d = 3$. Here we summarize the results at almost conclusive stage for the $O(N)$ models.

Following the procedure described in section 3.2.1 we passed from the intermediate scheme to the renormalization scheme $\tilde{\mathcal{S}}$. We wrote down in this way the perturbative expansion for the RG functions $\tilde{\beta}(\tilde{g})$, $\tilde{\eta}(\tilde{g})$, $\tilde{\eta}_{\phi^2}(\tilde{g})$, and $\tilde{\nu}(\tilde{g})$. For all of them we compute the series up to the eight order, one more respect to what appears in the literature. After rescaling the coefficients to adopt the normalization used by Nickel in [98] $\tilde{g} = \tilde{g}(N + 8)/(48\pi)$ we checked them with the literature. We compared the coefficients of the series of $\tilde{\eta}$ and $\tilde{\eta}_{\phi^2}$ up to order \tilde{g}^7 for $N = 0, 1, 2$, and 3 with those computed by Murray and Nickel appearing in the appendix of [57]. We compare also the coefficients of $\tilde{\beta}$ with those in [54]. We found complete agreement in all cases. Our series for $\tilde{\beta}(\tilde{g})$, $\tilde{\eta}(\tilde{g})$, and $\tilde{\nu}(\tilde{g})$ at generic N up to the order eight are reported in appendix D.2.

We Borel resummed these series, as usual, using both methods: Padé-Borel and conformal mapping.³¹ We found agreement between the two, typically with slightly smaller uncertainties in the latter one, and consistent convergence of the results as the number of loops used in the resummation is increased. In table 3.4 we report our results. They are in agreement with those

³¹For a quick introduction see chapter 2, instead the details of the numerical implementation can be found in [9].

appearing in ref. [57] and [100]. Our uncertainties are a bit smaller.³² We checked that this improvement is due to the presence of a longer perturbative series since with one order less, our resummation procedures reproduce errors comparable to theirs. A more detailed analysis, together with the study of the model with cubic anisotropy at the fixed points, will appear in [4].

³²For $N = 0$, there are discrepancies of approximately two error bars between the values for \tilde{g}_c and η computed with fixed dimension resummation in field theory in the scheme \tilde{S} and those computed with Monte Carlo studies [101, 102]. These discrepancies persist and increase slightly for our values at $N = 0$.

Chapter 4

Non-Borel Summability: Renormalons in integrable field theories

The aim of this chapter is to investigate on the interplay between the resurgent structure of perturbation theory and the $1/N$ expansion in theories with renormalons.

Since its discovery [103, 104], the $1/N$ expansion has played an important role as a tool to study non-perturbative aspects of quantum field theory. The reason that is often given for these successes is that the $1/N$ expansion “resums” the perturbative series, and therefore it goes beyond what is available in perturbation theory. Let us be more specific about what we mean by resummation. It is known since the earlier work [105, 106] that the factorial growth of diagrams in perturbation theory is tamed to just an exponential growth at the planar level in large N matrix model QFTs. A similar phenomenon applies to higher order in $1/N$ and QFTs based on vector models. The reduced number of diagrams at fixed order in $1/N$ leads in many theories to expressions that are analytic functions at the origin of the fixed large N coupling constant, order by order in $1/N$.¹ Theories of this kind include zero-dimensional matrix models, $\mathcal{N} = 4$ super Yang–Mills theory in 4d, Chern–Simons–matter theories, or three-dimensional $O(N)$ models that we studied in chapter 3, see also appendix B.

However, there are many theories in which the growth of the coefficients in the perturbative series is not dominated by the proliferation of diagrams, but by integration over momenta of some specific diagrams. This is the phenomenon of renormalons (see e.g. [108] for a review) that we mentioned in chapter 2. The $1/N$ expansion can tame the first kind of growth, but

¹By “expressions” we refer here to physical, and hence RS independent, quantities. At each order in $1/N$, the analyticity properties in the coupling of unphysical quantities, such as beta-functions, depend on the scheme. For instance, in the limit of large number of flavours n_f , the first orders in $1/n_f$ of 4d QED β -functions are analytic in the $\overline{\text{MS}}$ scheme, while they are non-analytic in other schemes [107].

not the second one. For this reason, in these theories, even after restricting to a given order in $1/N$, we will find asymptotic series, and the way the $1/N$ expansion resums them has to be more complex and worth studying. The following questions arise naturally. As each order in the $1/N$ series is a non-perturbative function which resums perturbation theory, can we decode each of these functions in terms of the conventional perturbative series and non-perturbative (renormalon) contributions? Can we in principle recover each of these non-perturbative functions from the perturbative series? These questions fall directly in the framework of the theory of resurgence, that we briefly introduced in chapter 2, specifically see section 2.4. We can extend, in this way, perturbative series to trans-series including the exponentially small contributions originating from the renormalons and ask if the resurgent relations are valid in these setups. Furthermore, the resurgent structure of fully-fledged quantum field theories is quite intricate. We know however that quantum field theories tend to become simpler and more tractable in the $1/N$ expansion. One can then hope that, by looking at the large N limit, one will find somewhat simpler resurgent structures which can be studied analytically. Another more difficult question, due, among other reasons, to the struggle of going to large order in the $1/N$ expansion in QFT, concerns the nature of the $1/N$ expansion itself.

In this chapter in order to answer in detail the questions raised above, we will conduct a study on three different two-dimensional models: the $O(N)$ NLSM, the $SU(N)$ PCF, and the $O(N)$ GN model. They are all integrable, i.e. their S-matrices are known exactly, asymptotically free theories with renormalons.² It was noted long ago by Polyakov and Wiegmann that a Thermodynamic Bethe Ansatz can be used to compute exactly the free energy of these theories in the presence of an external field coupled to a conserved current [113]. In addition, when the external field is large, one can use asymptotic freedom to calculate this observable in perturbation theory, and this was exploited in [114–121] to obtain the relation between the mass gap and the dynamically generated scale (see [122] for a review). In addition, a powerful method developed in [13, 14] makes it possible to extract the perturbative series for the free energy at very high orders. This has led to many quantitative studies of renormalon physics and resurgence in relativistic [123–125] and non-relativistic [126–129] integrable quantum field theories. These quantum integrable models have been also studied in the $1/N$ expansion [118, 130–134].

The chapter is structured as follows.

Content

We start in section 4.1 by considering the $0d$ reduction of certain large N vector models. We show explicitly that each order in $1/N$ is analytic in the 't Hooft coupling, the large N expansion is factorially divergent, while the reduction to $0d$ of the free energy $\mathcal{F}(h)$ defined in (4.16) turns

²As a matter of fact, the existence of renormalon singularities has been analytically established only in integrable models at large N . They were found in the GN model in [109] and studied in some detail in the NLSM, see e.g. [110–112].

out to be analytic at $N = \infty$. In section 4.2 we come back to field theory and introduce the key observable we will consider in this chapter, the free energy $\mathcal{F}(h)$ as a function of a chemical potential h . We review how this can be computed by using the TBA in 2d integrable QFTs. Then we move to the main results, reported in sections 4.3, 4.4, and 4.5.

In section 4.3 we consider the NLSM. We compute $\mathcal{F}(h)$ at the leading and next-to-leading order in the $1/N$ expansion, which resums an infinite number of renormalon diagrams appearing in ordinary perturbation theory, described in detail in [134]. We extract the exact answer both from a direct QFT calculation and from the TBA equations. At this order in $1/N$ there is a single IR renormalon singularity and the exact answer is obtained by the so-called median Borel resummation of the perturbative series. We have also studied the properties of the $1/N$ expansion of $\mathcal{F}(h)$ by exploiting the TBA to generate several terms. Our explicit results do not show factorial growth and are inconclusive. Either the asymptotic regime has not been reached yet or the $1/N$ series is actually convergent. A similar analysis has also been made in the PCF model, with the same inconclusive result.

In section 4.4 we consider the PCF model. We find a new, explicit solution for $\mathcal{F}(h)$ at leading order in $1/N$ from TBA, and for the choice of charges used in [116]. The exact answer can be understood as the median resummation of a non-trivial trans-series which can be obtained analytically and has an infinite number of IR renormalon singularities (in contrast to the solution of [130, 131], which has a single IR renormalon singularity, and similar to the numerical results obtained in [124, 125] for the $O(4)$ NLSM). Therefore, in this case the large N limit provides an explicit, analytic, yet non-trivial example of resurgence and median resummation in a model with infinitely many IR renormalon corrections.

In section 4.5 we consider the GN model. In this case, a new phenomenon appears: at each order in the $1/N$ expansion, the exact answer includes an infinite number of non-perturbative corrections. While ambiguities in imaginary terms nicely cancel between one series and the next in the trans-series, as expected from resurgence, real non-perturbative corrections can *not* be obtained from the resurgent properties of the perturbative series. Therefore, in this case there is a tension between resurgence and the $1/N$ expansion. The $1/N$ series of $\mathcal{F}(h)$ in the GN model turns out to be convergent, with a finite radius of convergence. Using the TBA, we generate many terms in the $1/N$ series. The latter can be analytically continued beyond its radius of convergence. Interestingly, the analytic continuation of this series gives reliable results for small N , such as $N = 4$ and $N = 2$, which are in agreement with the well-known dualities between these models and sine-Gordon theories.

4.1 Ordinary integrals at large N

Before analyzing the 2d QFT models it is useful to consider ordinary integrals, where we can get complete analytic results and show the generic divergent nature of the $1/N$ perturbative series.

A notable example is given by the 0d reduction of the large N quartic vector models, given by

$$I(m, g) = \frac{1}{(2\pi)^{N/2}} \int_{-\infty}^{+\infty} d^N \mathbf{x} e^{-f(\mathbf{x}, m, g)}. \quad (4.1)$$

Here $\mathbf{x} = (x_1, \dots, x_N)$ is a set of N real variables,

$$f(\mathbf{x}, m, g) = \frac{m}{2} \mathbf{x} \cdot \mathbf{x} + \frac{g}{N} (\mathbf{x} \cdot \mathbf{x})^2, \quad (4.2)$$

with $m \in \mathbb{R}$ and $g > 0$. We can trivially rescale m , so we get three different cases: $m = 1$, $m = -1$, and $m = 0$. The integral in (4.1) can be computed analytically, but we won't need its exact expression. The large order behavior of the $1/N$ expansion can be obtained by using steepest descent methods, see appendix E for details. We have

$$I(m, g) \sim 2^{-N/2} e^{-NK(z_c)} |K''(z_c)|^{-1/2} \left(1 + \sum_{p=1}^{\infty} \frac{c_p}{N^p} \right), \quad (4.3)$$

where the symbol \sim in (4.3) reminds us that the right-hand side is a divergent asymptotic series, and $K(z)$ is the function defined in (E.3). For $p \gg 1$ the coefficients c_p in (4.3) read

$$c_p \approx \frac{\hat{I}_c}{\pi} \Gamma(p) \rho^{-p} \sin(p\theta), \quad (4.4)$$

where \hat{I}_c , ρ and θ are explicit functions of g and m reported in (E.8) and (E.9). As discussed in the appendix E, the $1/N$ expansion of (4.1) is divergent asymptotic and Borel resummable for any real value of m and $g > 0$. This result should be contrasted with what we would get by expanding in g at *fixed* N . In this case, taking N to be odd, we can use radial coordinates with radial variable r , so that in a g expansion the relevant saddle points of the integral (4.1) are those of the function

$$f(r) = \frac{m}{2} r^2 + \frac{1}{4} r^4. \quad (4.5)$$

The qualitative and quantitative behaviors of such series are well known. In particular, for $m = 1$ we get one real critical point at $r = 0$ and a Borel resummable expression, for $m = -1$ three real critical points and Borel summability is lost, while for $m = 0$ the three critical points are degenerate and no expansion is possible.

Given the relations (E.8) and (E.9), we can easily get the analyticity properties of the coefficient term c_p as a function of the coupling g . In particular, we see that $c_p = c_p(g)$ are *analytic* at $g = 0$ for any p and go like

$$\lim_{g \rightarrow 0} c_p(g) \approx g^{p+1} + \mathcal{O}(g^{p+2}). \quad (4.6)$$

Other useful examples are given by the 0d reductions of two of the three models considered in this chapter, namely the NLSM and the GN models.

The 0d reduction of the non-linear sigma model is essentially the S^{N-1} sphere. We can define

$$e^{-F_{\text{NLSM}}(0)} \equiv \int_{-\infty}^{+\infty} d^N \mathbf{x} \delta(\mathbf{x} \cdot \mathbf{x} - N) = \frac{1}{2} \Omega_N N^{\frac{N-2}{2}}, \quad (4.7)$$

with $\Omega_N = 2\pi^{N/2}/\Gamma(N/2)$ the volume of the S^{N-1} sphere. The large N expansion reduces essentially to the Stirling approximation of the Gamma function, which is well-known to be divergent asymptotic. In presence of a chemical potential h , the vacuum energy becomes

$$\begin{aligned} e^{-F_{\text{NLSM}}(h)} &\equiv \int_{-\infty}^{+\infty} d^N \mathbf{x} \delta(\mathbf{x} \cdot \mathbf{x} - N) e^{\frac{h^2}{2}(x_1^2 + x_2^2)} \\ &= \left(-\frac{h^2}{2}\right)^{\frac{2-N}{2}} \frac{\pi^{\frac{N}{2}}}{\Gamma(\frac{N-2}{2})} e^{-\frac{h^2 N}{2}} \gamma\left(\frac{N-2}{2}, -\frac{h^2 N}{2}\right), \end{aligned} \quad (4.8)$$

where $\gamma(a, z) = \Gamma(a) - \Gamma(a, z)$ is the incomplete Gamma function. The behavior of the $1/N$ expansion is now determined by the expansion of $\gamma(a, z)$ for large a and z , at fixed ratio z/a . This can be found e.g. in [135], see eq.(8.11.6). After simple algebraic manipulations, we have

$$e^{-(F_{\text{NLSM}}(h) - F_{\text{NLSM}}(0))} = \sum_{k=0}^{\infty} \frac{Q_k(h^2)}{(1+h^2)^{2k+1}} \frac{1}{N^k}, \quad (4.9)$$

where $Q_k(h^2)$ are polynomials of degree k in h^2 for $k > 0$ and $Q_0 = 1$. It can be shown that the above series is absolutely convergent for any real h for $N > 3$. Interestingly enough, while $F_{\text{NLSM}}(h)$ and $F_{\text{NLSM}}(0)$ are separately non-analytic at $N = \infty$, their difference $F_{\text{NLSM}}(h) - F_{\text{NLSM}}(0)$ is a well-defined and analytic function.

The 0d reduction of the Gross-Neveu model is given by the following Grassmann integral:

$$e^{-F_{\text{GN}}(0)} \equiv \sqrt{\frac{N}{2\pi}} \int d^N \boldsymbol{\chi} d^N \bar{\boldsymbol{\chi}} e^{\frac{1}{2N}(\bar{\boldsymbol{\chi}} \cdot \boldsymbol{\chi})^2}, \quad (4.10)$$

where $\boldsymbol{\chi} = (\chi_1, \chi_2, \dots, \chi_{2N})$ is a set of $2N$ complex Grassmannian variables. Introducing an Hubbard-Stratonovich like parameter as in (E.1) we get

$$e^{-F_{\text{GN}}(0)} = 2^{N-\frac{1}{2}} \frac{\Gamma(N + \frac{1}{2})}{N^{N+\frac{1}{2}}}. \quad (4.11)$$

The large N expansion of this result is again manifestly divergent asymptotic. In presence of a

chemical potential h , the vacuum energy becomes

$$e^{-F_{\text{GN}}(h)} \equiv \sqrt{\frac{N}{2\pi}} \int d^N \boldsymbol{\chi} d^N \bar{\boldsymbol{\chi}} e^{\frac{1}{2N}(\bar{\boldsymbol{\chi}} \cdot \boldsymbol{\chi})^2 + h \sum_{i=1,2} \bar{\chi}_i \chi_i} = \left(\frac{2}{N}\right)^N \frac{(2+h)^2 N - 1}{\sqrt{2N}} \Gamma\left(N - \frac{1}{2}\right), \quad (4.12)$$

where the last line is readily computed again introducing an Hubbard-Stratonovich like parameter. We finally have

$$e^{-(F_{\text{GN}}(h) - F_{\text{GN}}(0))} = 1 + \frac{N}{2N-1} h^2. \quad (4.13)$$

Like in the NLSM case, $F_{\text{GN}}(h)$ and $F_{\text{GN}}(0)$ are separately non-analytic at $N = \infty$, but their difference $F_{\text{GN}}(h) - F_{\text{GN}}(0)$ is a well-defined, simple and analytic function.

Summarizing, we have found that the $1/N$ expansion in 0d reductions of large N vector models is asymptotic, and each coefficient in the $1/N$ expansion is analytic in the t' Hooft coupling. In agreement with what was anticipated in the introduction, the factorial growth of diagrams in perturbation theory is reduced to exponential growth, order by order in $1/N$. In contrast, the coefficients in the $1/N$ expansion we will compute in the 2d models will generally be non-analytic in the t' Hooft coupling because (and only because) of the presence of renormalon singularities. We have also shown that the $1/N$ expansion of the relative free energy $F(h) - F(0)$ is better behaved than $F(0)$ and is convergent in the 0d reduction of both the NLSM and the GN models. This suggests that the relative free energy can have better convergent properties in $1/N$ also in the 2d models. It will be explicitly verified that the $1/N$ expansion of this quantity is indeed convergent in the 2d GN model, while we will not be able to draw firm conclusions on its nature in the NLSM and PCF models.

4.2 Free energy and integrability

We summarize in this section the general formulation which applies to the three integrable and asymptotically free models considered in the chapter. More details for each model will be spelled out in subsequent sections.

The key observable we will study in this chapter is the free energy $F(h)$ as a function of an external field h coupled to a conserved charge. Let H be the Hamiltonian of the theory and Q the charge associated to a global conserved current. The external field h can be regarded as a chemical potential, and we can consider the ensemble defined by the operator

$$H - hQ. \quad (4.14)$$

The corresponding free energy per unit volume is defined by

$$F(h) = - \lim_{V, \beta \rightarrow \infty} \frac{1}{V\beta} \log \text{Tr} e^{-\beta(H-hQ)}, \quad (4.15)$$

where V is the volume of space and β is the total length of Euclidean time. More precisely, the observable of interest will be the relative free energy

$$\mathcal{F}(h) \equiv F(h) - F(0). \quad (4.16)$$

From now on, for simplicity, we will refer to $\mathcal{F}(h)$ just as the free energy.

It was pointed out in [113] that in integrable quantum field theories one can calculate $\mathcal{F}(h)$ by using the exact S -matrix and the TBA ansatz, in terms of a linear integral equation. The basic physical intuition behind is the following. Let m be the mass gap of the integrable theory. If the lightest particles in the theory are charged under Q , for $h > m$ the ground state of the theory will no longer be the vacuum, but a state with non-vanishing number density ρ . The latter can be determined in terms of Bethe roots $\chi(\theta)$ by the TBA equation

$$\chi(\theta) - \int_{-B}^B d\theta' K(\theta - \theta') \chi(\theta') = m \cosh \theta, \quad (4.17)$$

where θ is the particle rapidity and $\chi(\theta)$ is supported on the interval (to be determined) $[-B, B]$.

The integral kernel appearing in the Bethe ansatz equation is given by

$$K(\theta) = \frac{1}{2\pi i} \frac{d}{d\theta} \log S(\theta), \quad (4.18)$$

where $S(\theta)$ is the S -matrix element of the particles populating the ground state. In all the cases considered in this chapter only one species of particles with definite charges are present, so S is a scalar quantity. The energy per unit length e and the density ρ are given by

$$e = \frac{m}{2\pi} \int_{-B}^B d\theta \chi(\theta) \cosh \theta, \quad \rho = \frac{1}{2\pi} \int_{-B}^B d\theta \chi(\theta). \quad (4.19)$$

The value of B is fixed by the density ρ and one can eventually obtain an equation of state relating e to ρ . The free energy $\mathcal{F}(h)$ is finally obtained by a Legendre transform of $e(\rho)$:

$$\begin{aligned} h &\equiv \partial_\rho e(\rho), & \mathcal{F}(h) &\equiv e(\rho) - \rho h, \\ \rho &= -\partial_h \mathcal{F}(h), & e(\rho) &= \mathcal{F}(h) + \rho h. \end{aligned} \quad (4.20)$$

In an alternative formulation of the TBA equations, the basic quantity is a function $\epsilon(\theta)$, with support on an interval $[-B, B]$, which describes physically the excitation of holes. This function satisfies the integral equation

$$\epsilon(\theta) - \int_{-B}^B d\theta' K(\theta - \theta') \epsilon(\theta') = h - m \cosh \theta, \quad (4.21)$$

where now the value of B is determined by the condition

$$\epsilon(\pm B) = 0, \quad (4.22)$$

and depends on the external field h . The free energy is then given by

$$\mathcal{F}(h) = -\frac{m}{2\pi} \int_{-B}^B d\theta \cosh \theta \epsilon(\theta). \quad (4.23)$$

We refer the reader to appendix F for the explicit form of the kernel $K(\theta)$ in the three models, for a detailed discussion of the existence and uniqueness of the solutions of (4.17) and (4.21), as well as for the analyticity properties in $1/N$ of $K(\theta)$ in each case.

Given the free energy $\mathcal{F}(h)$, we denote by $\mathcal{F}_k(h)$ its coefficients in a $1/N$ expansion (see (4.30)-(4.32) below for the precise definition for each model). The coefficients $\mathcal{F}_k(h)$ are non-perturbative functions of the external field h and the mass gap m in each model. In order to recast the results in terms of asymptotic expansions of ordinary perturbation theory, we have to define a running coupling constant of some kind. Let us denote by g the coupling constant (before the large N limit) appearing in the Lagrangian description of our models, with beta function given by

$$\beta(g) = \mu \frac{dg}{d\mu} = -\beta_0 g^3 - \beta_1 g^5 + \mathcal{O}(g^7), \quad (4.24)$$

with $\beta_0 > 0$. Since in all the three models considered $\beta_0 \propto N$ we can conveniently define a 't Hooft-like coupling as

$$\alpha \equiv 2\beta_0 g^2, \quad (4.25)$$

so that the β -function up to two loops reads

$$\beta(\alpha) = -\alpha^2 - \xi \alpha^3 + \mathcal{O}(\alpha^4), \quad (4.26)$$

where

$$\xi = \frac{\beta_1}{2\beta_0^2}. \quad (4.27)$$

As it is well-known, the first two terms are renormalization scheme-independent, while all the others are not. A useful definition of running coupling is³

$$\frac{1}{\alpha(\mu)} + \xi \log \alpha(\mu) \equiv \log \left(\frac{\mu}{m} \right). \quad (4.28)$$

³Note that the definition (4.28) slightly differs from the one originally defined in [136] and used in subsequent works where, inside the log, m is replaced by the dynamically generated mass scale Λ . The two definitions are equivalent, but for our purposes (4.28) is more convenient.

Applying $\mu\partial_\mu$ to (4.28) gives

$$\beta_\alpha^{\text{TBA}} = \mu \frac{d\alpha}{d\mu} = -\frac{\alpha^2}{1-\xi\alpha} = -\alpha^2 - \xi\alpha^3 + \dots \quad (4.29)$$

So we see that α is a plausible coupling of the integrable model, in a renormalization scheme where the β -function has exactly the form (4.29). We will refer to this renormalization scheme as the TBA scheme in the following. In the three models we expand the free energy as

$$\mathcal{F}_{\text{NLSM}}(h) = \sum_{k \geq 0} \mathcal{F}_k(h) \Delta^{k-1} \sim -\frac{h^2}{4\pi} \sum_{k \geq 0} \Phi_k(\alpha, C_\pm) \Delta^{k-1}, \quad (4.30)$$

$$\mathcal{F}_{\text{PCF}}(h) = \sum_{k \geq 0} \mathcal{F}_k(h) \bar{\Delta}^{k-1} \sim -\frac{h^2}{8\pi} \sum_{k \geq 0} \Phi_k(\alpha, C_\pm) \bar{\Delta}^{k-1}, \quad (4.31)$$

$$\mathcal{F}_{\text{GN}}(h) = \sum_{k \geq 0} \mathcal{F}_k(h) \Delta^k \sim -\frac{h^2}{2\pi} \sum_{k \geq 0} \Phi_k(\alpha, C_\pm) \Delta^k. \quad (4.32)$$

Several clarifications are in order. In (4.30)-(4.32)

$$\Delta \equiv \frac{1}{N-2}, \quad \bar{\Delta} \equiv \frac{1}{N}, \quad (4.33)$$

the numerical factors have been chosen for convenience and α is the coupling (4.28) evaluated at a convenient scale $\mu \sim h$ that will be spelled out in detail for each model in the next sections. In order to clearly distinguish exact quantities from their asymptotic expansions, we have denoted by $\mathcal{F}_k(h)$ and $\Phi_k(\alpha, C_\pm)$ the exact and the asymptotic expansion in α of the $1/N$ coefficients of $\mathcal{F}(h)$. The factors Φ_k are trans-series of the form

$$\Phi_k(\alpha, C_\pm) = \varphi_k^{(0)}(\alpha) + \sum_{\ell=1}^{\infty} e^{-\frac{2\ell}{\alpha}} \varphi_k^{(\ell)}(\alpha, C_\pm), \quad (4.34)$$

where $\varphi_k^{(\ell)}$ are in general asymptotic divergent series. $\varphi_k^{(0)}$ coincides with the perturbative series, while $\varphi_k^{(\ell)}$ with $\ell > 0$ are the non-perturbative contributions associated with the trans-series. The latter can present a two-fold ambiguity, encoded in the trans-series parameters C_\pm . This ambiguity is balanced by the one due to the non-Borel summability (because of the IR renormalons) of the asymptotic series $\varphi_k^{(\ell)}$ in a way that will be detailed for each model in the next sections. The symbol \sim stands for ‘‘asymptotically equivalent to’’.⁴ Note finally that in the NLSM and in the GN models the Φ_k ’s do not precisely correspond to the expansions of the \mathcal{F}_k ’s because the relation between $\alpha(\mu \sim h)$ and h given by (4.28) depends on Δ by means of the factor ξ .

⁴For simplicity, and with an abuse of notation, we have used the equality sign in the first relations of (4.30)-(4.32), though the convergence of the $1/N$ expansion of \mathcal{F} is established only for the GN model.

4.3 The non-linear sigma model

In this section we present our results for the NLSM. After reviewing general aspects of the theory, we will present two approaches to obtain the exact $\mathcal{F}(h)$ up to next-to-leading order, one based on the diagrammatic calculation in the $1/N$ expansion, and another one based on the expansion of the integral equation from the Bethe ansatz. We will then compare this non-perturbative result with the resummation of the perturbative calculation.

4.3.1 General aspects

The NLSM is described by the Lagrangian density

$$\mathcal{L} = \frac{1}{2} \partial_\mu \phi \cdot \partial^\mu \phi , \quad (4.35)$$

where $\phi = (\phi^1, \dots, \phi^N)$ is an N -uple of real scalar fields satisfying the constraint

$$\phi \cdot \phi = \frac{N}{g^2} . \quad (4.36)$$

In our conventions (4.24) we have

$$\beta_0 = \frac{1}{4\pi\Delta} , \quad \xi = \Delta . \quad (4.37)$$

The NLSM has a global $O(N)$ symmetry. The conserved currents are given by

$$J_\mu^{IJ} = \phi^I \partial_\mu \phi^J - \phi^J \partial_\mu \phi^I , \quad (4.38)$$

where $I, J = 1, \dots, N$, and we denote by Q^{IJ} the corresponding charges. As in [114, 115], we can add a chemical potential h associated to the charge Q^{12} . In the NLSM it is convenient to define the 't Hooft coupling

$$\alpha \equiv \alpha(\mu = h) , \quad (4.39)$$

where $\alpha(\mu)$ is the TBA coupling defined in (4.28).

The free energy $\mathcal{F}(h)$ was computed in perturbation theory in the coupling constant up to two-loops in [114, 115, 136]. In terms of the asymptotic expansions defined in (4.30) and (4.34), we have at leading order in $1/N$ ($k = 0$)

$$\varphi_0^{(0)}(\alpha) = \frac{1}{\alpha} - \frac{1}{2} . \quad (4.40)$$

At next-to-leading order ($k = 1$) the series $\varphi_1^{(0)}(\alpha)$ has been calculated explicitly and at all orders in [134]. It is obtained by selecting Feynman diagrams with the appropriate power of

N , which turn out to be ring diagrams. The resulting series has the factorial growth typical of renormalon behavior, due to integration over momenta, and one finds⁵

$$\varphi_1^{(0)}(\alpha) = 3 \log(2) + \gamma_E - 1 + \frac{\alpha}{2} + \left(\frac{1}{4} - \frac{21\zeta(3)}{32} \right) \alpha^2 + \left(\frac{1}{4} + \frac{35\zeta(3)}{32} \right) \alpha^3 + \mathcal{O}(\alpha^4). \quad (4.41)$$

We can then ask the question of how the $1/N$ expansion resums this series. We will now present two different ways of computing $\mathcal{F}_0(h)$ and $\mathcal{F}_1(h)$ as exact functions of h .

4.3.2 The $1/N$ expansion from QFT

The standard way to perform the $1/N$ expansion is to introduce an auxiliary field σ which implements the constraint (4.36) (see e.g. [137, 138]). Once this is done, we obtain the action

$$\begin{aligned} S &= \int d^2x \left[\frac{1}{2} \partial_\mu \phi_B \cdot \partial^\mu \phi_B + \frac{\sigma_B}{\sqrt{N}} \left(\phi_B \cdot \phi_B - \frac{N}{g_B^2} \right) \right] \\ &= \int d^2x \left[\frac{Z_\phi}{2} \partial_\mu \phi \cdot \partial^\mu \phi + \sqrt{Z_\sigma} Z_\phi \frac{\sigma}{\sqrt{N}} \phi \cdot \phi - Z_g \frac{\sqrt{N}}{g^2} \sigma + \frac{\mu^2}{2} \phi \cdot \phi + C \right]. \end{aligned} \quad (4.42)$$

The subscript B denotes bare quantities and the second line is a rewriting in terms of renormalized fields and counterterms. The additional couplings for $h \neq 0$ are

$$\begin{aligned} S_h &= \int d^2x \left[ih(\phi_B^1 \partial_\tau \phi_B^2 - \phi_B^2 \partial_\tau \phi_B^1) - \frac{h^2}{2} ((\phi_B^1)^2 + (\phi_B^2)^2) \right] \\ &= \int d^2x \left[ihZ_\phi(\phi^1 \partial_\tau \phi^2 - \phi^2 \partial_\tau \phi^1) - Z_\phi \frac{h^2}{2} ((\phi^1)^2 + (\phi^2)^2) + C_h \right]. \end{aligned} \quad (4.43)$$

We do not need a vertex renormalization for h because it couples to a conserved current. Moreover turning on h does not introduce any new UV divergence, so all the counterterms in (4.42) can be taken independent of h . Fixing also the finite part of the counterterms to be h -independent means that we choose the same scheme for $h = 0$ and $h \neq 0$. The only exception is the counterterm C , for which we find that a finite h -dependent shift C_h is needed in order to satisfy a certain “renormalization condition” on the observable that we explain below.

In order to compute the vacuum energy up to NLO, we need to plug in the action the VEVs including their $1/N$ corrections

$$\sigma = \sqrt{N}(\Sigma + \frac{1}{N}\delta\Sigma) + \hat{\sigma}, \quad \phi = \sqrt{N}(\Phi + \frac{1}{N}\delta\Phi) + \hat{\phi}, \quad (4.44)$$

where capital letters denote the VEVs and hatted fields denote the fluctuations. Similarly we

⁵Notice that the constant factor is due to the different definition for α , i.e. (4.28), with respect to the one used in [134].

plug the expansion of the renormalization constants, out of which only Z_g and C are non-trivial already at leading order

$$\begin{aligned} Z_g &= Z_g^{(0)} + \frac{1}{N} \delta Z_g, \quad C = NC^{(0)} + \delta C, \quad C_h = \delta C_h, \\ Z_\phi &= 1 + \frac{1}{N} \delta Z_\phi, \quad Z_\sigma = 1 + \frac{1}{N} \delta Z_\sigma, \quad \mu^2 = \frac{1}{N} \delta \mu^2. \end{aligned} \quad (4.45)$$

It will be convenient to collect some combinations of counterterms

$$\begin{aligned} \delta m^2 &\equiv \delta \mu^2 + 2\Sigma \delta Z_3, \\ \delta Z_3 &\equiv \delta Z_\phi + \frac{1}{2} \delta Z_\sigma. \end{aligned} \quad (4.46)$$

δm^2 is the total counterterm for the mass-squared coupling, and δZ_3 the counterterm for the cubic coupling. As we will show, $h \neq 0$ induces a non-zero VEV for Φ in the 12 plane, which in turn induces a quadratic mixing between $\hat{\sigma}$, $\hat{\phi}^1$ and $\hat{\phi}^2$. In the following we will draw diagrams with the following conventions

$\hat{\phi}$ propagator: $- - - -$;

$\hat{\sigma}$ propagator for $h = 0$: $\equiv \equiv \equiv$; $\hat{\sigma}$ - $\hat{\phi}^1$ - $\hat{\phi}^2$ mixed propagator for $h \neq 0$: $\equiv \equiv \equiv$;

$\hat{\sigma}$ tadpole vertex: \parallel ; VEV insertion: \circ ; Counterterm: \otimes .

Leading order

The LO (leading order) vacuum energy density for $h = 0$ is given by the following diagrams

$$NF_0 = \text{circle} + \frac{\Sigma}{\frac{Z_g^{(0)}}{g^2}} + \otimes_{C^{(0)}}, \quad (4.47)$$

subject to the vanishing tadpole condition (this is equivalent to minimizing the effective potential)

$$\text{circle with tadpole} + \frac{\hat{\sigma}}{\frac{Z_g^{(0)}}{g^2}} = 0. \quad (4.48)$$

We did not write explicitly the tadpole condition for $\hat{\phi}^I$ but it is easily checked that it is solved by $\Phi = 0$. Evaluating the diagrams in the tadpole condition we find

$$-\int \frac{d^2p}{(2\pi)^2} \frac{1}{p^2 + 2\Sigma} + \frac{Z_g^{(0)}}{g^2} = 0 . \quad (4.49)$$

The solution to this equation gives us the physical mass-squared of the scalars at leading order, that we denote as m_0^2 , i.e. $\Sigma = \frac{m_0^2}{2}$. Plugging in the diagrams for the vacuum energy we obtain

$$\begin{aligned} F_0 &= \left[\frac{1}{2} \int \frac{d^2p}{(2\pi)^2} \log[p^2 + 2\Sigma] - \frac{Z_g^{(0)}}{g^2} \Sigma + C^{(0)} \right]_{\Sigma = \frac{m_0^2}{2}} \\ &= \frac{1}{2} \int \frac{d^2p}{(2\pi)^2} \log[p^2 + m_0^2] - \frac{m_0^2}{2} \int \frac{d^2p}{(2\pi)^2} \frac{1}{p^2 + m_0^2} + C^{(0)} . \end{aligned} \quad (4.50)$$

The LO vacuum energy density for $h \neq 0$ is given by

$$NF_0(h) = \text{[diagram: bubble]} + \text{[diagram: tadpole with } h^2 \text{]} + \text{[diagram: tadpole with } \Sigma \text{]} + \text{[diagram: tadpole with } \Sigma \text{]} + \text{[diagram: } C^{(0)} \text{]} , \quad (4.51)$$

subject to the tadpole conditions (now we cannot avoid considering also the tadpole for $\hat{\phi}$, without loss of generality we assume the VEV to be in the direction 1)

$$\text{[diagram: tadpole with } \hat{\sigma} \text{]} + \text{[diagram: tadpole with } \hat{\sigma} \text{]} + \text{[diagram: tadpole with } \hat{\sigma} \text{]} = 0 , \quad (4.52)$$

$$\text{[diagram: tadpole with } h^2 \text{]} + \text{[diagram: tadpole with } \Sigma \text{]} = 0 . \quad (4.53)$$

Assuming $\Phi^1 \neq 0$ the tadpole condition for $\hat{\phi}$ has a unique solution for Σ , namely $\Sigma = \frac{h^2}{2}$. Plugging this in the tadpole condition for $\hat{\sigma}$ we obtain

$$-\int \frac{d^2p}{(2\pi)^2} \frac{1}{p^2 + 2\Sigma} \Big|_{\Sigma = \frac{h^2}{2}} - (\Phi^1)^2 + \frac{Z_g^{(0)}}{g^2} = 0 . \quad (4.54)$$

Using the determination of $\frac{Z_g^{(0)}}{g^2}$ in terms of the mass-squared for the theory with $h = 0$ in (4.49), we get

$$(\Phi^1)^2 = \int \frac{d^2p}{(2\pi)^2} \left(\frac{1}{p^2 + m_0^2} - \frac{1}{p^2 + h^2} \right) = \frac{1}{4\pi} \log \frac{h^2}{m_0^2}. \quad (4.55)$$

Plugging everything back to the vacuum energy density we obtain

$$\begin{aligned} F_0(h) &= \left[\frac{1}{2} \int \frac{d^2p}{(2\pi)^2} \log[p^2 + 2\Sigma] + \left(\Sigma - \frac{h^2}{2} \right) (\Phi^1)^2 - \frac{Z_g^{(0)}}{g^2} \Sigma + C^{(0)} \right]_{\Sigma=\frac{h^2}{2}} \\ &= \frac{1}{2} \int \frac{d^2p}{(2\pi)^2} \log[p^2 + h^2] - \frac{h^2}{2} \int \frac{d^2p}{(2\pi)^2} \frac{1}{p^2 + m_0^2} + C^{(0)}. \end{aligned} \quad (4.56)$$

Note that we did not really need the result for $(\Phi^1)^2$ here because the dependence on this VEV canceled when plugging the value of Σ .

Taking the difference we get the following LO result for the observable⁶

$$\begin{aligned} \mathcal{F}_0(h) &= F_0(h) - F_0(0) = \int \frac{d^2p}{(2\pi)^2} \left\{ \frac{1}{2} \log \left[\frac{p^2 + h^2}{p^2 + m_0^2} \right] - \frac{h^2 - m_0^2}{2} \frac{1}{p^2 + m_0^2} \right\} \\ &= -\frac{h^2}{8\pi} \left[\log \frac{h^2}{m_0^2} - 1 \right] - \frac{m_0^2}{8\pi}. \end{aligned} \quad (4.57)$$

Note that we are slightly abusing notation: the symbols $F_0(h)$ and $F_0(0)$ do not denote the same function evaluated at two different arguments, as is clear from the fact that the difference does not vanish for $h = 0$. This is because we are considering a different stationary point of the effective potential for $h \neq 0$, so we are actually taking the difference between the free energies of two different states, whose energies cross when $h = m_0$ where indeed the observable vanishes (recall that m_0 denotes the physical mass of the bosons at LO). For $h > m_0$ the vacuum with the condensate $\Phi^1 \neq 0$ is energetically favored.

⁶The leading free energy \mathcal{F}_0 was computed in [132], see eq.(2.7), where $\mu_{\text{there}} = h_{\text{here}}$. However, [132] missed the non-perturbative term proportional to m_0^2 , crucial to establish that $\mathcal{F}_0(h = m_0) = 0$.

Next-to-leading order vacuum diagrams

The NLO (next-to-leading order) vacuum energy density for $h = 0$ is given by the following diagrams

$$F_1 = \text{Diagram 1} + \text{Diagram 2} + \text{Diagram 3} + \text{Diagram 4} + \text{Diagram 5} - m_0^2 \frac{\partial F_0}{\partial m_0^2} r . \quad (4.58)$$

It is a general fact that the various diagrams linear in the NLO correction to the VEVs $\delta\Sigma$, $\delta\Phi$ drop from the NLO energy density thanks to the LO tadpole condition, so we avoided drawing such diagrams. We will postpone the NLO tadpole condition for $\hat{\sigma}$ to the subsection 4.3.2 and leave δZ_g as undetermined for the time being. The last contribution comes from the NLO correction to the physical mass-squared

$$m^2 = m_0^2 \left(1 + \frac{r}{N} \right) , \quad (4.59)$$

when F_0 is re-expressed in terms of the physical mass-squared m^2 . Note that in all the NLO diagrams we can just use m^2 as the mass-squared of the bosons.

The first diagram in (4.58) is a closed loop of the $\hat{\sigma}$ field. The propagator coming from the resummation of the $\hat{\phi}$ bubbles is

$$\langle \hat{\sigma}(p) \hat{\sigma}(-p) \rangle = \frac{1}{-2B(m^2, p)} , \quad (4.60)$$

where $B(m^2, p)$ is the ‘‘bubble function’’

$$\begin{aligned} B(m^2, p) &= \int \frac{d^2q}{(2\pi)^2} \frac{1}{(q+p)^2 + m^2} \frac{1}{q^2 + m^2} \\ &= \frac{1}{4\pi m^2} \frac{\log \left(1 + \frac{p^2}{2m^2} + \sqrt{\frac{p^2}{m^2} \left(1 + \frac{p^2}{4m^2} \right)} \right)}{\sqrt{\frac{p^2}{m^2} \left(1 + \frac{p^2}{4m^2} \right)}} . \end{aligned} \quad (4.61)$$

Therefore

$$\text{Diagram 1} = \frac{1}{2} \int \frac{d^2p}{(2\pi)^2} \log[-2B(m^2, p)] . \quad (4.62)$$

Summing up with the other diagrams, we find

$$F_1 = \int \frac{d^2p}{(2\pi)^2} \frac{1}{2} \left\{ \log[-2B(m^2, p)] + \frac{\delta Z_\phi p^2 + \delta m^2}{p^2 + m^2} \right\} - \frac{\delta Z_g}{g^2} \frac{m^2}{2} + \delta C - m_0^2 \frac{\partial F_0}{\partial m_0^2} r. \quad (4.63)$$

The NLO vacuum energy density for $h \neq 0$ is given by the following diagrams

$$F_1(h) = \begin{array}{c} \text{Diagram 1: Double circle} \\ \text{Diagram 2: Dashed circle} \\ \text{Diagram 3: Dashed circle with } \delta m^2 \text{ insertion} \\ \text{Diagram 4: Dashed circle with } \delta Z_\phi \text{ insertion} \\ \text{Diagram 5: Tadpole with } \Sigma \text{ and } \frac{\delta Z_g}{g^2} \\ \text{Diagram 6: Triangle with } \delta m^2 \text{ and } \Phi^1 \\ \text{Diagram 7: Triangle with } h^2 \delta Z_\phi \text{ and } \Phi^1 \\ \text{Diagram 8: Tadpole with } \delta C \end{array} - m_0^2 \frac{\partial F_0(h)}{\partial m_0^2} r. \quad (4.64)$$

We again used the LO tadpole condition to avoid drawing all diagrams with insertions of $\delta \Sigma$ and $\delta \Phi$. Note that due to the quadratic mixing at this order we receive a contribution from the bubble of the $\hat{\sigma}$ - $\hat{\phi}^1$ - $\hat{\phi}^2$ propagator (first diagram) and to avoid overcounting we need to subtract the contribution of $\hat{\phi}^1$ and $\hat{\phi}^2$ to the LO closed loop of the bosons (second diagram).

Using a matrix notation, we can express the quadratic action involving $\hat{\sigma}$, $\hat{\phi}^1$ and $\hat{\phi}^2$ as

$$\int \frac{d^2p}{(2\pi)^2} \frac{1}{2} \begin{pmatrix} \hat{\phi}^1(-p) & \hat{\phi}^2(-p) & \hat{\sigma}(-p) \end{pmatrix} K(p) \begin{pmatrix} \hat{\phi}^1(p) \\ \hat{\phi}^2(p) \\ \hat{\sigma}(p) \end{pmatrix}, \quad (4.65)$$

$$K(p) \equiv \begin{pmatrix} p^2 & -2h p_\tau & 2\Phi^1 \\ 2h p_\tau & p^2 & 0 \\ 2\Phi^1 & 0 & -2B(h^2, p) \end{pmatrix}.$$

Here p_τ is the momentum in the Euclidean time direction. Therefore we have

$$\begin{array}{c} \text{Diagram 1} \\ \text{Diagram 2} \end{array} = \int \frac{d^2p}{(2\pi)^2} \left\{ \frac{1}{2} \log[\det K(p)] - \frac{2}{N} \frac{N}{2} \log[p^2 + h^2] \right\} \quad (4.66)$$

$$= \int \frac{d^2p}{(2\pi)^2} \frac{1}{2} \left\{ \log \left[-2B(h^2, p) - \frac{1}{\pi} \log \frac{h^2}{m^2} \frac{p^2}{p^4 + 4h^2 p_\tau^2} \right] + \log \left[\frac{p^4 + 4h^2 p_\tau^2}{(p^2 + h^2)^2} \right] \right\}.$$

We substituted (4.55) inside the determinant. Summing up with the counterterm diagrams, we

find

$$F_1(h) = \int \frac{d^2p}{(2\pi)^2} \frac{1}{2} \left\{ \log \left[-2B(h^2, p) - \frac{1}{\pi} \log \frac{h^2}{m^2} \frac{p^2}{p^4 + 4h^2 p_\tau^2} \right] + \log \left[\frac{p^4 + 4h^2 p_\tau^2}{(p^2 + h^2)^2} \right] + \frac{\delta Z_\phi p^2 + \delta m_h^2}{p^2 + h^2} \right\} + \frac{\delta m_h^2 - \delta Z_\phi h^2}{8\pi} \log \frac{h^2}{m^2} - \frac{\delta Z_g h^2}{g^2} \frac{1}{2} + \delta C + \delta C_h - m_0^2 \frac{\partial F_0(h)}{\partial m_0^2} r . \quad (4.67)$$

The subscript h in the mass-squared counterterm reminds us that the definition (4.46) of δm^2 contains a factor of the VEV Σ , which depends on whether we are at $h = 0$ or $h \neq 0$.

Taking the difference $F_1(h) - F_1(0)$ we note that all the contributions involving the propagator counterterms cancel and we are left with

$$\mathcal{F}_1(h) = \int \frac{d^2p}{(2\pi)^2} \frac{1}{2} \left\{ \log \left[\frac{B(h^2, p) + \frac{1}{2\pi} \log \frac{h^2}{m^2} \frac{p^2}{p^4 + 4h^2 p_\tau^2}}{B(m^2, p)} \right] + \log \left[\frac{p^4 + 4h^2 p_\tau^2}{(p^2 + h^2)^2} \right] + \frac{\delta Z_\sigma (h^2 - m^2)}{2} \frac{1}{p^2 + m^2} \right\} - \frac{\delta Z_g h^2 - m^2}{g^2} \frac{1}{2} + \delta C_h + \frac{m^2 - h^2}{8\pi} r . \quad (4.68)$$

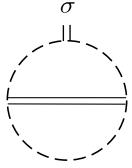
Here we used (4.57) to evaluate the terms involving $m_0^2 \frac{\partial}{\partial m_0^2}$. We still have a UV divergent integral and some counterterms that did not cancel in the difference, so we need to fix those to get the finite result for the observable.

Tadpole condition and propagator correction

The NLO Tadpole condition for $h = 0$ is

$$\begin{aligned} & \text{Diagram 1} + \text{Diagram 2} \\ & + \text{Diagram 3} + \text{Diagram 4} + \text{Diagram 5} + \text{Diagram 6} = 0 . \end{aligned} \quad (4.69)$$

The two-loop diagram gives



$$\begin{aligned}
&= \left(-\frac{2}{\sqrt{N}}\right)^3 \frac{1}{2} N \int \frac{d^2 p}{(2\pi)^2} \int \frac{d^2 q}{(2\pi)^2} \frac{1}{-2B(m^2, p)} \frac{1}{((p+q)^2 + m^2)^2} \frac{1}{q^2 + m^2} \\
&= \frac{2}{\sqrt{N}} \int \frac{d^2 p}{(2\pi)^2} \left\{ \frac{1}{4\pi m^2 (p^2 + 4m^2) B(m^2, p)} + \frac{1}{p^2 + 4m^2} \right\}.
\end{aligned} \tag{4.70}$$

Going to the second line we performed the integral in q , which gives

$$\begin{aligned}
&\int \frac{d^2 q}{(2\pi)^2} \frac{1}{((p+q)^2 + m^2)^2} \frac{1}{q^2 + m^2} \\
&\quad 1 + \frac{\log\left(1 + \frac{p^2}{2m^2} + \sqrt{\frac{p^2}{m^2}\left(1 + \frac{p^2}{4m^2}\right)}\right)}{\sqrt{\frac{p^2}{m^2}\left(1 + \frac{p^2}{4m^2}\right)}} \\
&= \frac{1}{16\pi m^4} \frac{1}{1 + \frac{p^2}{4m^2}} = \frac{1}{4\pi m^2} \frac{1}{p^2 + 4m^2} + \frac{B(m^2, p)}{p^2 + 4m^2}.
\end{aligned} \tag{4.71}$$

Plugging this result and evaluating the one-loop diagrams the NLO tadpole condition can be rewritten as

$$\begin{aligned}
&\frac{\delta Z_g}{g^2} - \frac{\delta Z_\sigma}{2} \int \frac{d^2 p}{(2\pi)^2} \frac{1}{p^2 + m^2} \\
&= -2 \int \frac{d^2 p}{(2\pi)^2} \left\{ \frac{1}{4\pi m^2 (p^2 + 4m^2) B(m^2, p)} + \frac{1}{p^2 + 4m^2} \right\} - \frac{2\delta\Sigma + \delta m^2 - m^2 \delta Z_\phi}{4\pi m^2}.
\end{aligned} \tag{4.72}$$

The left-hand side is precisely the combination that appear in the observable in (4.68) multiplied by $-\frac{h^2 - m^2}{2}$, so substituting this relation we find

$$\begin{aligned}
\mathcal{F}_1(h) &= \int \frac{d^2 p}{(2\pi)^2} \frac{1}{2} \left\{ \log \left[\frac{B(h^2, p) + \frac{1}{2\pi} \log \frac{h^2}{m^2} \frac{p^2}{p^4 + 4h^2 p_\tau^2}}{B(m^2, p)} \right] + \log \left[\frac{p^4 + 4h^2 p_\tau^2}{(p^2 + h^2)^2} \right] \right. \\
&\quad \left. + 2(h^2 - m^2) \left(\frac{1}{4\pi m^2 (p^2 + 4m^2) B(m^2, p)} + \frac{1}{p^2 + 4m^2} \right) \right\} \\
&\quad + (h^2 - m^2) \frac{2\delta\Sigma + \delta m^2 - m^2 \delta Z_\phi}{8\pi m^2} + \delta C_h + \frac{m^2 - h^2}{8\pi} r.
\end{aligned} \tag{4.73}$$

However, we are still left with a UV divergent integral and some combination of counterterms. To fix this remaining combination we need to consider the correction to the physical mass-squared.

4.3.3 The $1/N$ expansion from the Bethe ansatz

As discussed in section 4.2, since the NLSM is integrable, the free energy $\mathcal{F}(h)$ can be calculated exactly by solving the integral equation (4.21). One could think that the $1/N$ expansion of the free energy can be obtained by simply expanding the kernel in a power series in $1/N$. However, this turns out to be subtle, since the kernel is singular in the limit $\Delta \rightarrow 0$, see appendix F. The $1/N$ expansion of the integral equation (4.21) for the NLSM was studied in [132] at the first non-trivial order. The calculation of higher order corrections in similar models introduces additional subtleties, as shown in [133], but in our analysis we will restrict to the next-to-leading order term.

It turns out that the $1/N$ expansion of the kernel requires the introduction of distributions. The expansion of the kernel reads,

$$K(\theta) = \delta(\theta) + \sum_{k \geq 1} \Delta^k K_k(\theta), \quad (4.79)$$

where $\delta(\theta)$ is Dirac's delta function. The first two terms in the expansion read

$$\begin{aligned} K_1(\theta) &= -\frac{d}{d\theta} \mathcal{L}_1(\theta), \\ K_2(\theta) &= -2\pi^2 \delta''(\theta) - \frac{d}{d\theta} \mathcal{L}_2(\theta). \end{aligned} \quad (4.80)$$

In these expressions,

$$\mathcal{L}_1(\theta) = \frac{1}{\theta} + \frac{1}{\sinh(\theta)}, \quad (4.81)$$

and

$$\mathcal{L}_2(\theta) = \frac{i}{4\pi} \left\{ \psi^{(1)}\left(\frac{i\theta + \pi}{2\pi}\right) - \psi^{(1)}\left(\frac{\pi - i\theta}{2\pi}\right) - \psi^{(1)}\left(\frac{i\theta}{2\pi}\right) + \psi^{(1)}\left(-\frac{i\theta}{2\pi}\right) \right\}, \quad (4.82)$$

where $\psi^{(1)}$ is the first derivative of the digamma function. The expansion (4.79) has to be understood in the following sense: when acting on a test function $f(\theta)$ which is differentiable and vanishes at the boundaries, one has

$$\begin{aligned} \int_{-B}^B K(\theta - \theta') f(\theta') d\theta' &= f(\theta) - \Delta \left(\text{P} \int_{-B}^B \mathcal{L}_1(\theta - \theta') f'(\theta') d\theta' \right) \\ &\quad + \Delta^2 \int_{-B}^B K_2(\theta - \theta') f(\theta') d\theta' + \mathcal{O}(\Delta^3). \end{aligned} \quad (4.83)$$

where P means the principal value.

We can now solve the integral equation by using a large N ansatz for the distribution

$$\epsilon(\theta) = \frac{1}{\Delta} \sum_{k \geq 0} \Delta^k \epsilon_k(\theta), \quad (4.84)$$

and for the endpoint

$$B = \sum_{k \geq 0} \Delta^k B_k. \quad (4.85)$$

The leading term in the integral equation (4.21) is then given by

$$\text{P} \int_{-B_0}^{B_0} \mathcal{L}_1(\theta - \theta') \epsilon'_0(\theta') d\theta' = h - m \cosh(\theta). \quad (4.86)$$

By splitting the kernel $\mathcal{L}_1(\theta)$ as

$$\mathcal{L}_1(\theta) = \frac{2}{\theta} + \mathcal{L}_1^r(\theta) \quad (4.87)$$

where

$$\mathcal{L}_1^r(\theta) = \frac{1}{\sinh(\theta)} - \frac{1}{\theta} \quad (4.88)$$

is regular at $\theta = 0$, we can write (4.86) as

$$\text{P} \int_{-B_0}^{B_0} \frac{2\epsilon'_0(\theta')}{\theta - \theta'} d\theta' + \int_{-B_0}^{B_0} \mathcal{L}_1^r(\theta - \theta') \epsilon'_0(\theta') d\theta' = h - m \cosh(\theta). \quad (4.89)$$

After integrating by parts and an integration w.r.t. θ , one can also write (4.86) as

$$\text{P} \int_{-B_0}^{B_0} \mathcal{L}_1(\theta - \theta') \epsilon_0(\theta') d\theta' = h\theta - m \sinh(\theta), \quad (4.90)$$

which is the form used in [132].

We conclude that the large N limit of the distribution appearing in the TBA equation (4.21), $\epsilon_0(\theta)$, can be obtained as a solution of the singular integral equations (4.86) or (4.90). (4.90) is very similar to the integral equation that one would find for the density of states of a large N matrix integral. The singular part of $\mathcal{L}_1(\theta)$ is what one would find for a conventional, Hermitian matrix model. The additional term $\mathcal{L}_1^r(\theta)$ would correspond to a non-conventional eigenvalue interaction. We note that the integral equation (4.90) does not determine by itself the value of B_0 as a function of h . It was argued in [132] that this value is fixed by requiring the following behavior near the edges of the distribution:

$$\epsilon_0(\theta) \sim (B_0^2 - \theta^2)^{3/2}, \quad \theta \rightarrow \pm B_0. \quad (4.91)$$

When $\mathcal{L}_1^r(\theta) = 0$, as it happens in the PCF model studied in the next section, one can show

that the condition (4.91) follows from (4.89), by requiring $\epsilon'_0(\theta)$ to be regular at $\pm B_0$.

The solution to the singular integral equation (4.90) is not known explicitly. However, there is both analytic and numerical evidence that the leading order free energy obtained from this solution,

$$\mathcal{F}_0(h) = -\frac{m}{2\pi} \int_{-B_0}^{B_0} d\theta \cosh(\theta) \epsilon_0(\theta), \quad (4.92)$$

agrees exactly with (4.57). By assuming this analytic value for $\mathcal{F}_0(h)$ one can deduce the value of B_0 [132]:

$$B_0(h) = \sqrt{\log\left(\frac{h}{m}\right) \left(\log\left(\frac{h}{m}\right) + 1\right)} + \sinh^{-1} \left[\sqrt{\log\left(\frac{h}{m}\right)} \right]. \quad (4.93)$$

Let us now write down the equation for the next-to-leading correction $\epsilon_1(\theta)$. By using (4.91), it can be seen that B_0 does not get corrected at that order, and one finds the equation

$$\text{P} \int_{-B_0}^{B_0} \mathcal{L}_1(\theta - \theta') \epsilon_1(\theta') d\theta' = -2\pi^2 \epsilon'_0(\theta) - \int_{-B_0}^{B_0} \mathcal{L}_2(\theta - \theta') \epsilon_0(\theta') d\theta'. \quad (4.94)$$

This equation can be solved numerically to obtain the next-to-leading correction to the free energy, given by

$$\mathcal{F}_1(h) = -\frac{m}{2\pi} \int_{-B_0}^{B_0} d\theta \cosh(\theta) \epsilon_1(\theta). \quad (4.95)$$

We checked, for some values of h , that $\mathcal{F}_1(h)$ computed as above agrees with (4.78). The numerical resolution of the singular integral equation is quite time consuming: with few hours of computation we reached an agreement with a relative error of order 10^{-7} . Proceeding to higher orders in Δ in the expansion of the kernel (4.79) and solving singular integral equations to compute \mathcal{F}_k for $k > 1$ becomes very challenging. We have been able to extract more coefficients of the series in Δ by following an indirect procedure: we first solve numerically with high precision the TBA for fixed h_0 and different values of Δ , and from this sequence of $\mathcal{F}(h_0)$ we compute the value of the asymptotic expansion at each order, using Richardson transforms to accelerate the series. This allowed us to compute, for a given h , the functions $\mathcal{F}_k(h)$ up to $k = 6$. These first coefficients do not present a factorial growth as it would be expected from the properties of the kernel discussed in appendix F. However, they are not enough to allow us to make claims on the nature of the $1/N$ series.

4.3.4 Trans-series expansion and comparison with perturbation theory

We can now compare the exact results for \mathcal{F}_0 and \mathcal{F}_1 found in the previous subsections with perturbation theory. Up to order Δ , (4.28) gives

$$h = e^{\frac{1}{\alpha}} m (1 + \Delta \log \alpha) + \mathcal{O}(\Delta^2). \quad (4.96)$$

Given (4.57) and the definitions (4.30) and (4.34), it is straightforward to get

$$\varphi_0^{(0)}(\alpha) = \frac{1}{\alpha} - \frac{1}{2}, \quad \varphi_0^{(1)}(\alpha) = \frac{1}{2}, \quad \varphi_0^{(\ell)}(\alpha) = 0, \quad \ell \geq 2. \quad (4.97)$$

The perturbative series $\varphi_0^{(0)}$ agrees with (4.40), as it should, but in addition we see a non-perturbative single trans-series term, which cannot be captured in perturbation theory. The mismatch between the exact free energy and its perturbative calculation is due to the h -independent term proportional to m^2 . It is given by the non-perturbative free energy at $h = 0$, evaluated at the non-trivial large N point, which has been calculated in [139] and has the value

$$\Delta\mathcal{F}(0) = \frac{m^2}{8\pi} + \mathcal{O}(\Delta^2). \quad (4.98)$$

This suggests that the difference between perturbation theory and the $1/N$ expansion is only due to the difference between a perturbative and a non-perturbative evaluation at $h = 0$. We will give further evidence of this when we consider the next-to-leading term in the $1/N$ expansion.

A direct expansion in α of the NLO term \mathcal{F}_1 in (4.78) is challenging. Luckily enough, we will verify that it has the same structure of \mathcal{F}_0 , namely its trans-series expansion is composed of only two terms $\varphi_1^{(0)}$ and $\varphi_1^{(1)}$. The coefficient $\varphi_1^{(0)}$ is the perturbative result and its first terms can be read from (4.41). This series is factorially divergent, and its Borel transform has a Borel singularity in the positive real axis (i.e. an IR renormalon), which was analyzed in detail in [134]. We can then use lateral Borel resummations $s_{\pm}(\varphi_1^{(0)})(\alpha)$, i.e. integrating the Borel transform slightly above or below the real axis avoiding in this way the singularities, indicated respectively by s_+ and s_- . They lead to an imaginary piece. Let us denote by $s_{\pm}(\varphi_1^{(0)})$ the function obtained from $\varphi_1^{(0)}$ by using the lateral Borel resummations of the series (4.41). The results of [134] imply that

$$\text{Im} \left(s_{\pm} \left(\varphi_1^{(0)} \right) \right) = \mp \frac{\pi}{2} e^{-\frac{2}{\alpha}}, \quad (4.99)$$

which is the imaginary contribution of the IR renormalon unveiled in [134]. A detailed numerical comparison indicates that the exact $1/N$ result (4.78) agrees precisely with the *real* part of the lateral Borel resummations. Defining $f_1(\alpha) = -h^2/(4\pi)(-\log \alpha + \varphi_1^{(0)}(\alpha))$, we have

$$\mathcal{F}_1(h) = \text{Re} (s_{\pm} (f_1) (\alpha)) , \quad (4.100)$$

where in (4.100) $\alpha = 1/\log(h/m)$. We can use the so-called median resummation, which in this case is simply

$$s_{\text{med}} = \frac{s_+ + s_-}{2} \quad (4.101)$$

to write the above result as

$$\mathcal{F}_1(h) = s_{\text{med}} (f_1) (h) . \quad (4.102)$$

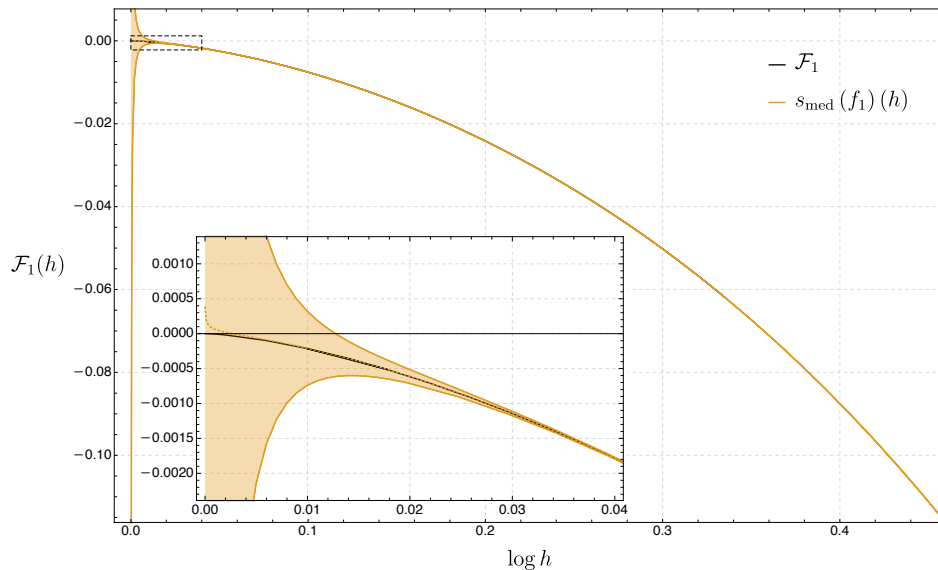


Figure 4.1: Comparison between the median resummation of the perturbative series and the exact result. The orange curve is obtained computing the $+$ and $-$ lateral Padé-Borel resummations of the first 41 terms of the perturbative series and taking their average, while the error is estimated from the convergence of the resummation. The black curve (mostly covered by the orange one) is the numerical evaluation of (4.78). The mass m is set to 1, so $h = 1$ is maximally strong coupling.

| | |
|------------------------------|-----------------------------|
| $\mathcal{F}_1(h = 3)$ | $-1.00252688160157404\dots$ |
| $s_{\text{med}}(f_1)(h = 3)$ | $-1.00252688160157404(4)$ |

Table 4.1: Comparison between the exact result and the median resummation of the perturbative series for $h = 3$ and m set to 1. The error in the Padé-Borel resummations of the first 41 terms of the perturbative series is estimated from the convergence of the resummation.

These results indicate that the trans-series expansion of \mathcal{F}_1 is rather trivial, namely we have

$$\varphi_1^{(1)}(\alpha, C_{\pm}) = C_{\pm} \frac{\pi}{2}, \quad \varphi_1^{(\ell)} = 0, \quad \ell \geq 2, \quad (4.103)$$

where $C_{\pm} = \pm i$. In fig. 4.1 we illustrate the agreement between the median resummation and the numerical evaluation of the exact result. In order to show the high precision of the resummation and the agreement with the exact value, in table 4.1 we report the comparison between the numerical evaluation of \mathcal{F}_1 in (4.78) and the median resummation of f_1 for a fixed value of h , taken to be $h = 3$.

This is similar to the result found in [130, 131] for the PCF model at large N , in which the exact answer is the real part of a Borel-resummed series. One additional insight of the result above is that we have an explicit diagrammatic interpretation of the underlying perturbative

series, in terms of the ring diagrams considered in [134].

4.4 The principal chiral field model

In this section we present our results for the PCF model. In the first subsection we review some general aspects of the model. Then, we present the large N exact solution for $\mathcal{F}_0(h)$. In the final subsection we “decode” this exact solution in terms of an explicit, resurgent trans-series: we find a trans-series extension of the perturbative expansion, and we show that the exact solution can be obtained from this trans-series by Borel resummation.

4.4.1 General aspects

The PCF model is a quantum field theory for maps $\Sigma : \mathbb{R}^2 \rightarrow SU(N)$, with Lagrangian density

$$\mathcal{L} = \frac{1}{g_0^2} \text{Tr} \left(\partial_\mu \Sigma \partial^\mu \Sigma^\dagger \right). \quad (4.104)$$

In our convention (4.24) we have

$$\beta_0 = \frac{1}{16\pi\Delta}, \quad \xi = \frac{1}{2}. \quad (4.105)$$

The PCF has a global symmetry $SU(N)_L \times SU(N)_R$, therefore there are conserved charges that can be used to construct the free energy $F(h)$. We will consider a vectorial symmetry $SU(N)_V \subset SU(N)_L \times SU(N)_R$, and the corresponding charge will be denoted by Q . Its eigenvalues in the fundamental representation will be denoted by $\mathbf{q} = (q_1, \dots, q_N)$. Two choices of charges have been studied in the literature. In [130, 131] one takes

$$q_k = r_k - r_{k-1}, \quad r_k = \frac{\sin(\pi k/N)}{\sin(\pi/N)}. \quad (4.106)$$

This leads to an explicitly solvable large N limit. There is a different setting, considered originally in [116] to determine the mass gap of the theory, in which one chooses the charge

$$\mathbf{q} = \left(\frac{1}{2}, -\frac{1}{2(N-1)}, \dots, -\frac{1}{2(N-1)} \right). \quad (4.107)$$

We will consider in this work the setting (4.107). As we will see, the large N limit is also solvable in this case. In addition, the resulting large N free energy leads to an infinite series of IR renormalon contributions which can be calculated explicitly. The relevant kernel for the choice of charges (4.107) is reported in (F.26). In the PCF model it is convenient to define the

't Hooft coupling

$$\alpha \equiv \alpha\left(\mu = \sqrt{\frac{2\pi}{e}}h\right), \quad (4.108)$$

where $\alpha(\mu)$ is the TBA coupling defined in (4.28).

The free energy $\mathcal{F}(h)$ can be computed in perturbation theory. The one-loop result was presented in [116] for an arbitrary choice of charges, and it is given by

$$\mathcal{F}(h) = -\frac{4h^2}{\bar{g}^2} \sum_{j=1}^N q_j^2 - \frac{h^2}{2\pi} \sum_{1 \leq i < j \leq N} (q_i - q_j)^2 \left[\log |q_i - q_j| - \frac{1}{2} \right] + \mathcal{O}(\bar{g}^2), \quad (4.109)$$

where \bar{g}^2 is the $\overline{\text{MS}}$ coupling defined by

$$\log\left(\frac{\mu}{h}\right) = -\int_g^{\bar{g}} \frac{dx}{\beta^{\overline{\text{MS}}}(x)}. \quad (4.110)$$

It follows from (4.109) that in terms of the 't Hooft coupling α , we have

$$\mathcal{F}_0(h) \sim -\frac{h^2}{8\pi} \left\{ \frac{1}{\alpha} - \frac{1}{2} + \mathcal{O}(\alpha) \right\}, \quad (4.111)$$

where \mathcal{F}_0 is the leading $1/N$ term of \mathcal{F} appearing in (4.31).

The free energy $\mathcal{F}(h)$ can also be computed from the TBA equations (4.21), (4.23). The TBA solution can be used to extract the perturbative expansion of $\mathcal{F}_0(h)$ up to very high orders in the coupling constant and at finite N , by using the methods in [13, 14]. This was done in [123] for the normalized energy density, but the results in that paper can be easily translated into an expansion in α for $\mathcal{F}_0(h)$, and one finds

$$\mathcal{F}_0(h) \sim -\frac{h^2}{8\pi} \left\{ \frac{1}{\alpha} - \frac{1}{2} - \frac{\alpha}{4} - \frac{5\alpha^2}{16} - \frac{53\alpha^3}{96} + \mathcal{O}(\alpha^4) \right\}. \quad (4.112)$$

4.4.2 Exact solution at large N

As in the case of the NLSM, the kernel (4.18) given by (F.26) has a $1/N$ expression which involves distributions:

$$K(\theta) = \delta(\theta) + \sum_{k \geq 1} \bar{\Delta}^k K_k(\theta), \quad (4.113)$$

where the first term is simply

$$K_1(\theta) = -\frac{d}{d\theta} \mathcal{L}_1(\theta), \quad \mathcal{L}_1(\theta) = \frac{2}{\theta}. \quad (4.114)$$

The integral equation at leading order in $1/N$, (4.90), reads in this case

$$\text{P} \int_{-B}^B \frac{2\epsilon_0(\theta')}{\theta - \theta'} d\theta' = h\theta - m \sinh(\theta). \quad (4.115)$$

Here, we have denoted B_0 by B , since we will not consider subleading corrections to the value of the endpoint. Due to the simplicity of the leading kernel, (4.115) is the equation for the density of eigenvalues of a Hermitian matrix model with a potential

$$V(x) = \frac{hx^2}{2} - m \cosh(x). \quad (4.116)$$

Since the support of $\epsilon_0(\theta)$ is the full interval $[-B, B]$, we are considering a so-called one-cut solution. This solution can be obtained by using standard matrix model techniques, see e.g. [138]. The density is given by

$$\epsilon_0(\theta) = \frac{1}{2\pi} \sqrt{B^2 - \theta^2} M(\theta), \quad (4.117)$$

where the function $M(\theta)$ can be written as a contour integral around $z = 0$

$$M(\theta) = \oint_0 \frac{V'(1/z)}{1 - z\theta} \frac{1}{\sqrt{1 - B^2 z^2}} \frac{dz}{2\pi i}. \quad (4.118)$$

To obtain the explicit solution, it turns out to be useful to write $V(x)$ in (4.116) as a power series around $x = 0$,

$$V(x) = \sum_{k \geq 0} g_k x^{2k}, \quad (4.119)$$

where, in our case,

$$g_1 = \frac{h - m}{2}, \quad g_k = -\frac{m}{(2k)!}, \quad k \geq 2. \quad (4.120)$$

Then, by using the expansion

$$\frac{1}{\sqrt{1 - B^2 z^2}} = \sum_{k=0}^{\infty} \binom{2k}{k} \left(\frac{B^2}{4}\right)^k z^{2k}, \quad (4.121)$$

we find the expression

$$\epsilon_0(\theta) = \frac{1}{2\pi} \sqrt{B^2 - \theta^2} \left(h - 2m \sum_{r, k \geq 0} \binom{2k}{k} \frac{r + k + 1}{(2(r + k + 1))!} \left(\frac{B^2}{4}\right)^k \theta^{2r} \right). \quad (4.122)$$

The value of B is determined by the condition (4.91), as in [132], and one finds

$$h - 2m \sum_{r,k \geq 0} \binom{2k}{k} \frac{r+k+1}{(2(r+k+1))!} 4^{-k} B^{2(k+r)} = 0. \quad (4.123)$$

This series defines an entire function of B which can be written down in closed form in terms of the Bessel functions $I_{1,2}(z)$:

$$\frac{2}{B} I_1(B) + I_2(B) = \frac{h}{m}. \quad (4.124)$$

This gives the relation between B and h .

To obtain the large N free energy we just have to calculate the integral

$$\mathcal{F}_0(h) = -\frac{m}{2\pi} \int_{-B}^B \epsilon_0(\theta) \cosh(\theta) d\theta. \quad (4.125)$$

By expanding the cosh, we find

$$\mathcal{F}_0(h) = -\frac{m}{2\pi} \sum_{t \geq 0} \frac{\mathfrak{M}_t}{(2t)!}, \quad (4.126)$$

where

$$\mathfrak{M}_t = \int_{-B}^B \epsilon_0(\theta) \theta^{2t} d\theta \quad (4.127)$$

are the moments of $\epsilon_0(\theta)$. As it is well-known from the matrix model literature, they can be calculated by using the expansion at infinity of the resolvent

$$\omega_0(\theta) = \frac{1}{2} \left(V'(\theta) - \sqrt{\theta^2 - B^2 M(\theta)} \right) = \sum_{t \geq 0} \mathfrak{M}_t \theta^{-2t-1}. \quad (4.128)$$

By doing this, one finds

$$\begin{aligned} \mathcal{F}_0(h) = & -\frac{m^2}{4\pi} \left\{ \frac{h}{m} B I_1(B) \right. \\ & \left. - B^2 \sum_{k,r,t \geq 0} \binom{2k}{k} \frac{(2(r+t))!}{(2(r+k+1))!} \frac{r+k+1}{r+t+1} \frac{1}{((r+t)!)^2 (2t)!} \left(\frac{B^2}{4} \right)^{k+r+t} \right\}. \end{aligned} \quad (4.129)$$

Note that, from the point of view of quantum field theory, this is a strong coupling expansion, since small B corresponds to small h/m . Fortunately, this expression can be summed up in closed form in terms of a generalized hypergeometric function, and we obtain in the end

$$\mathcal{F}_0(h) = -\frac{h^2}{4\pi} \left\{ \frac{B^2 I_1(B)}{2I_1(B) + B I_2(B)} - \frac{1}{2} \frac{B^4}{(2I_1(B) + B I_2(B))^2} {}_1F_2 \left(\frac{1}{2}; 1, 2; B^2 \right) \right\}. \quad (4.130)$$

From these expressions it is also possible to obtain exact formulae for the large N limits of the density of particles and of the energy density, defined by

$$\bar{\Delta}\rho = \rho_0 + \mathcal{O}(\bar{\Delta}), \quad \bar{\Delta}e = e_0 + \mathcal{O}(\bar{\Delta}). \quad (4.131)$$

One finds,

$$\frac{\rho_0}{m} = \frac{B}{4\pi} I_1(B), \quad \frac{e_0}{m^2} = \frac{B^2}{8\pi} {}_1F_2\left(\frac{1}{2}; 1, 2; B^2\right). \quad (4.132)$$

4.4.3 Trans-series expansion

We can now address the question of what is the relation between the exact large N result (4.130), and the trans-series expansion of the free energy, including exponentially small corrections. It turns out that all the special functions appearing in (4.130) and (4.124) have simple trans-series expansions which can be used to obtain a trans-series expansion of $\mathcal{F}_0(h)$. Let us start with (4.124). By using the trans-series asymptotics of the Bessel functions, we have the following equality, valid for $B > 0$:

$$\frac{2}{B} I_1(B) + I_2(B) = \frac{e^B}{\sqrt{2\pi B}} \left(s_{\pm}(\gamma^{(0)})(B) + C_{\pm} e^{-2B} s(\gamma^{(1)})(B) \right). \quad (4.133)$$

Here,

$$\gamma^{(0)}(B) = 1 + \frac{1}{8B} + \frac{9}{128B^2} + \dots, \quad \gamma^{(1)}(B) = \gamma^{(0)}(-B) \quad (4.134)$$

are Gevrey-1 series, s with no subscripts \pm denotes the standard Borel resummation, available when there are no singularities in the positive real axis of the Borel plane, and

$$C_{\pm} = \mp i. \quad (4.135)$$

As usual in Borel-Écalle resummation, the value of C_{\pm} is correlated with the choice of lateral resummation. We also have

$$B I_1(B) \sim \sqrt{\frac{B}{2\pi}} e^B \left(\nu^{(0)}(B) - C_{\pm} e^{-2B} \nu^{(1)}(B) \right), \quad (4.136)$$

where

$$\nu^{(0)}(B) = 1 - \frac{3}{8B} - \frac{15}{128B^2} + \dots, \quad \nu^{(1)}(B) = \nu^{(0)}(-B). \quad (4.137)$$

Finally, we have the following formula for the generalized hypergeometric function,

$$\frac{B^2}{2} {}_1F_2\left(\frac{1}{2}; 1, 2; B_0^2\right) = \frac{e^{2B}}{4\pi} \left(s_{\pm}(f^{(0)})(B) + C_{\pm} e^{-2B} 4B s_{\pm}(f^{(1)})(B) + e^{-4B} s(f^{(2)})(B) \right), \quad (4.138)$$

where

$$f^{(0)}(B) = 1 + \frac{1}{4B} + \dots, \quad f^{(2)}(B) = f^{(0)}(-B), \quad f^{(1)}(B) = 1 - \frac{1}{8B^2} + \dots \quad (4.139)$$

It follows from (4.130) that $\mathcal{F}_0(h)$ has a trans-series expansion in terms of the small parameters $1/B$, e^{-2B} . We are however interested in obtaining the trans-series expansion in terms of the 't Hooft coupling α introduced in (4.28), which makes contact with conventional perturbation theory. To do this, we need the relation between α and B , which is obtained by combining (4.28) and (4.124). This relation can be written as a trans-series equation,

$$B - \frac{1}{2} \log(B) - \frac{1}{2} + \log \gamma^{(0)}(B) + \log \left(1 + C_{\pm} e^{-2B} \frac{\gamma^{(1)}(B)}{\gamma^{(0)}(B)} \right) = \frac{1}{\alpha} + \frac{1}{2} \log(\alpha), \quad (4.140)$$

and it has a trans-series solution of the form

$$B = \frac{1}{\alpha} \mathfrak{B}^{(0)}(\alpha) + \sum_{\ell \geq 1} C_{\pm}^{\ell} e^{-2\ell/\alpha} \mathfrak{B}^{(\ell)}(\alpha). \quad (4.141)$$

The leading term in this trans-series is given by

$$b = \frac{1}{\alpha} \mathfrak{B}^{(0)}(\alpha) = \frac{1}{\alpha} + \frac{1}{2} + \frac{\alpha}{8} - \frac{11\alpha^3}{384} - \frac{35\alpha^4}{768} + \dots \quad (4.142)$$

We can also compute the first exponential corrections. This is better done in terms of b . We find, for the very first terms,

$$\begin{aligned} e^{-2/\alpha} \mathfrak{B}^{(1)}(\alpha) &= -e^{-2b} \left(1 + \frac{1}{4b} + \frac{9}{32b^2} + \dots \right), \\ e^{-4/\alpha} \mathfrak{B}^{(2)}(\alpha) &= -\frac{3}{2} e^{-4b} \left(1 + \frac{2}{3b} + \frac{3}{4b^2} + \dots \right). \end{aligned} \quad (4.143)$$

We obtain in this way the following trans-series structure for $\mathcal{F}_0(h)$:

$$\begin{aligned} \mathcal{F}_0(h) \sim & -\frac{h^2}{8\pi} \left\{ \frac{1}{\alpha} - \frac{1}{2} - \frac{\alpha}{4} - \frac{5\alpha^2}{16} - \frac{53\alpha^3}{96} - \frac{487\alpha^4}{384} - \frac{13789\alpha^5}{3840} - \frac{185143\alpha^6}{15360} + \mathcal{O}(\alpha^7) \right. \\ & - \frac{4C_{\pm}}{e\alpha^2} e^{-2/\alpha} \left(1 + \alpha + \frac{\alpha^2}{4} - \frac{\alpha^3}{16} + \frac{\alpha^4}{96} - \frac{31\alpha^5}{384} - \frac{23\alpha^6}{1280} + \mathcal{O}(\alpha^7) \right) \\ & + \frac{2C_{\pm}^2}{e^2\alpha} e^{-4/\alpha} \left(1 - \frac{\alpha}{4} + \frac{3\alpha^2}{8} - \frac{\alpha^3}{2} + \frac{4\alpha^4}{3} - \frac{181\alpha^5}{64} + \frac{3227\alpha^6}{320} + \mathcal{O}(\alpha^7) \right) \\ & \left. + \mathcal{O}\left(e^{-6/\alpha}\right) \right\}, \end{aligned} \quad (4.144)$$

where $C_{\pm}^2 = -1$. To make this completely explicit, we can write (4.144) with the notations

introduced in (4.34) as a trans-series in α , $e^{-2/\alpha}$. We have

$$\mathcal{F}_0(h) \sim -\frac{h^2}{8\pi} \Phi(\alpha, C_\pm) = -\frac{h^2}{8\pi} \sum_{\ell \geq 0} C_\pm^\ell e^{-2\ell/\alpha} \varphi^{(\ell)}(\alpha), \quad (4.145)$$

where we have factorized C_\pm and dropped the unnecessary subscript 0:

$$\Phi(\alpha, C_\pm) \equiv \Phi_0(\alpha, C_\pm), \quad \varphi_0^{(0)}(\alpha) \equiv \varphi^{(0)}(\alpha), \quad \varphi_0^{(\ell)}(\alpha, C_\pm) \equiv C_\pm^{(\ell)} \varphi^{(\ell)}(\alpha), \quad \ell \geq 1. \quad (4.146)$$

The series $\varphi^{(\ell)}(\alpha)$ can be read from (4.144),

$$\varphi^{(0)}(\alpha) = \frac{1}{\alpha} - \frac{1}{2} + \dots, \quad \varphi^{(1)}(\alpha) = -\frac{4}{e\alpha^2} (1 + \alpha + \dots), \quad \varphi^{(2)}(\alpha) = \frac{2}{e^2\alpha} \left(1 - \frac{\alpha}{4} + \dots\right). \quad (4.147)$$

Then, we have the following equality:

$$\mathcal{F}_0(h) = -\frac{h^2}{8\pi} s_\pm(\Phi)(\alpha; C_\pm) = -\frac{h^2}{8\pi} \sum_{\ell \geq 0} C_\pm^\ell e^{-2\ell/\alpha} s_\pm(\varphi^{(\ell)})(\alpha). \quad (4.148)$$

There are many aspects of the above result which are worth commenting in detail, both at the physical and the mathematical level.

From the physics point of view, let us note that the trans-series (4.145) has an *infinite* number of exponentially small corrections, corresponding to an infinite number of IR renormalon singularities. This is in contrast to the NLO term in the $1/N$ expansion of the NLSM, studied above, and also to the planar solution of the PCF model [130, 131] with the choice of charges (4.106). However, all corrections are built up of a finite number of trans-series in the variable B , appearing in (4.130). A similar phenomenon appears in the trans-series solution of certain Riccati ordinary differential equations [140, 141], in which all the exponential corrections in the trans-series are obtained from a finite number of building blocks.

From a more formal point of view, one can ask whether the exponentially small corrections are determined by the perturbative series. It turns out that, in this case, $\Phi(\alpha; C)$ satisfies the same resurgent equations that the trans-series solution to Painlevé II described in detail in [142]. Namely, we conjecture the following equality of laterally resummed trans-series

$$s_+(\Phi)(\alpha; C) = s_-(\Phi)(\alpha; C + S), \quad (4.149)$$

where

$$S = 2i \quad (4.150)$$

and C is now an *arbitrary* complex parameter. As shown in [142], (4.149) leads to the following

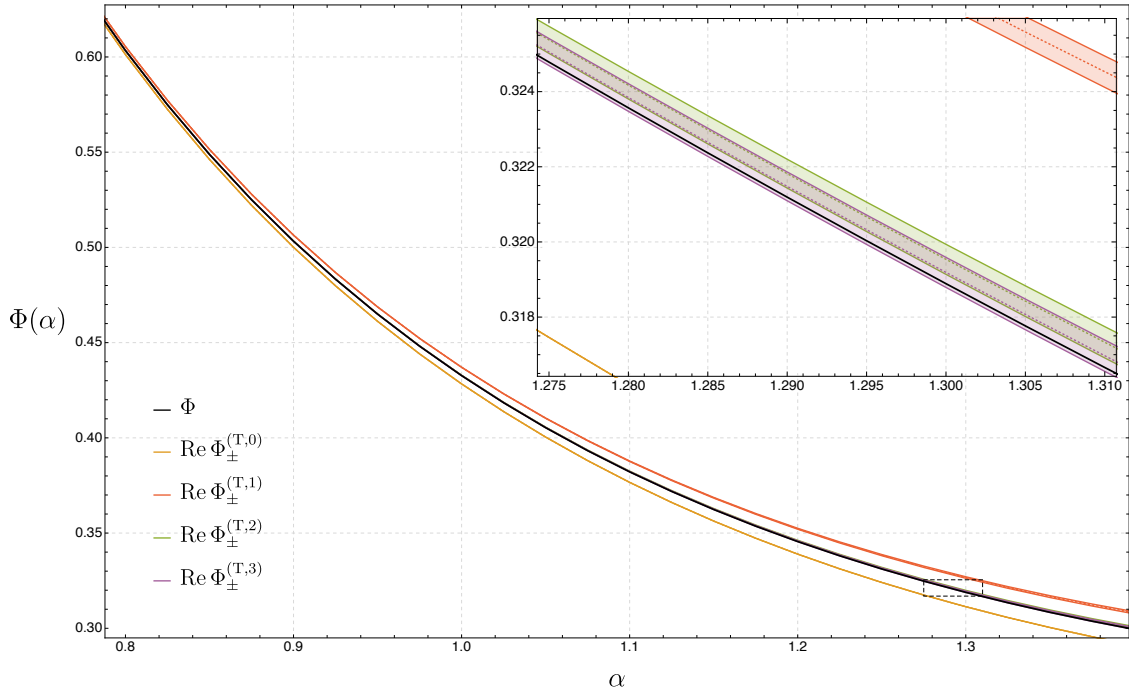


Figure 4.2: Leading rescaled free energy Φ as a function of the coupling α . The black line corresponds to the exact result, the orange, red, green and blue lines to the approximate result given by Borel resumming the first series in the trans-series, as in the legend. The box to the bottom-right is a zoom of the region marked by the dashed black rectangle above. The dashed lines are the central values, while the shaded area corresponds to the error associated to the Borel resummation, as explained in the main text.

relationships

$$s_+(\Phi^{(\ell)})(\alpha) - s_-(\Phi^{(\ell)})(\alpha) = \sum_{k \geq 1} \binom{\ell+k}{\ell} \mathcal{S}^k s_-(\Phi^{(\ell+k)})(\alpha), \quad \ell \geq 0. \quad (4.151)$$

where

$$\Phi^{(\ell)}(\alpha) \equiv e^{-2\ell/\alpha} \varphi^{(\ell)}(\alpha). \quad (4.152)$$

We have explicitly verified some of these equations numerically, by including up to the fourth term in the trans-series. (4.151) gives the so-called Stokes automorphism of $\Phi^{(\ell)}$ across the positive real axis, and it expresses it as an infinite linear combination of the higher order terms in the trans-series, $\Phi^{(\ell+k)}(\alpha)$. The coefficients in the r.h.s. of (4.151) are called Stokes constants and are explicitly known. Equivalently, (4.151) says that the Borel transform of $\Phi^{(\ell)}(\alpha)$, $\mathcal{B}\Phi^{(\ell)}(t)$, has singularities at $t = 2k$, $k \in \mathbb{Z}_{>0}$. By expanding $\mathcal{B}\Phi^{(\ell)}(t)$ around the k -th singularity, one can obtain $\Phi^{(k+\ell)}(\alpha)$. In particular, when applied to $\ell = 0$, (4.151) implies that *all* the higher order terms in the trans-series can be obtained from the perturbative series. It follows from (4.151)

that the Borel resummed trans-series

$$s_+(\Phi)(\alpha; C - S/2) = s_-(\Phi)(\alpha; C + S/2) \quad (4.153)$$

is real for any real C [142]. This is sometimes called a *median resummation* (see also [143]). Since $C_{\pm} = \mp i = \mp S/2$, (4.148) is a median resummation corresponding to $C = 0$.

For illustration we compare in fig. 4.2 the exact value of the leading rescaled free energy $\Phi \equiv s_{\pm}(\Phi)(C_{\pm})$ with the real part of its approximations given by the truncated trans-series

$$\Phi_{\pm}^{(T,n)} \equiv \sum_{\ell=0}^n C_{\pm}^{\ell} s_{\pm}(\Phi^{(\ell)}). \quad (4.154)$$

The term $\Phi_{\pm}^{(T,0)}$ corresponds to the lateral Borel resummation of the perturbative series, $\Phi_{\pm}^{(T,1)}$ to the lateral Borel resummation of the perturbative series plus the first trans-series, and so on. Notice that $\Phi_{+}^{(T,n)}$ and $\Phi_{-}^{(T,n)}$ are complex conjugate. The Borel resummation of the asymptotic series entering $\Phi^{(\ell)}$ with $\ell \leq 2$ has been performed using 89 perturbative coefficients and by reconstructing the Borel function using a diagonal [44/44] Padé approximant, while for $\ell = 3$ we have used 29 coefficients and reconstructed the Borel function with the diagonal [14/14] Padé approximant. The dashed lines represent the central values, with an error band given by the uncertainty in the numerical reconstruction of the Borel function. The dominant source of uncertainty comes from the convergence of the Padé approximation, estimated by taking the difference between the two highest diagonal approximants: $P[44/44] - P[43/43]$. Other subdominant contributions -such as the one obtained by introducing one or more dummy variables (e.g. a Borel-Le Roy parameter) and minimizing with respect to them- have been neglected (see e.g. section 4 in [9] for an overview of possible numerical recipes to estimate the error when using Borel resummation techniques). We see how the exact result is approached when considering more and more terms in the trans-series expansion. In table 4.2 we show more in detail the cancellations happening between the different orders of the trans-series. We report, for fixed $\alpha = \frac{1}{5}$, the difference between the exact value and the real part of the truncated trans-series, and its imaginary part. It is interesting to notice how both values approach zero with a change of magnitude happening every two orders, a consequence of the fact that the $\Phi^{(\ell)}$'s satisfy the relationships (4.151).

In order to better appreciate how the exact result is approached when taking more and more terms in the trans-series, we show in fig. 4.3 the resummation of Φ for a fixed $\alpha = 1$, and as a function of the number of trans-series terms n included in the resummation. In this plot the error interval is given by the left-over ambiguity in the trans-series, namely by the imaginary part of $s_{\pm}(\Phi^{(n)})$ at each order. The numerical error associated to the Borel resummation is sub-leading and has been neglected. Note how quick is the convergence to the exact result and how the choice of the uncertainty gives a reliable estimate of the error.

| | $\Phi(\frac{1}{5}) - \text{Re} \Phi_{\pm}^{(T,n)}(\frac{1}{5})$ | $\text{Im} \Phi_{\pm}^{(T,n)}(\frac{1}{5})$ |
|---------|---|---|
| $n = 0$ | $2.68541385336\dots \cdot 10^{-9}$ | $\pm 0.0020200401313\dots$ |
| $n = 1$ | $-2.685413850(1) \cdot 10^{-9}$ | $\mp 9.162556(5) \cdot 10^{-14}$ |
| $n = 2$ | $-3.9(1) \cdot 10^{-18}$ | $\pm 4.581282(5) \cdot 10^{-14}$ |
| $n = 3$ | $1.4(1) \cdot 10^{-18}$ | $\mp 3(5) \cdot 10^{-20}$ |

Table 4.2: First orders of the truncated trans-series. In the first column the difference between the exact value and its real part and in the second column its imaginary part. The uncertainty correspond to the error associated to the Borel resummation, as explained in the main text.

All the statements above were made for the observable $\mathcal{F}_0(h)$, but a similar trans-series expansion can be made for the normalized energy density using (4.132). In this expansion it is convenient to introduce the coupling a defined by

$$\log\left(\frac{4\sqrt{2}\pi^{3/2}\rho_0}{em}\right) = \frac{1}{a} - \frac{1}{2}\log(a), \quad (4.155)$$

where the numerical factor inside the log has been chosen to match this definition with that in [123]. Note that the coupling a here was denoted by α there. The resulting trans-series is

$$\begin{aligned} \frac{e_0}{2\pi\rho_0^2} &\sim a + \frac{a^2}{2} + \frac{a^3}{4} + \frac{5a^4}{16} + \frac{53a^5}{96} + \dots \\ &+ \frac{4C_{\pm}}{e} e^{-2/a} \left(1 + a + \frac{a^2}{4} - \frac{a^3}{16} + \frac{7a^4}{96} + \dots\right) \\ &+ \frac{2C_{\pm}^2}{e^2} e^{-4/a} \left(a + \frac{a^2}{4} - \frac{7a^3}{8} + a^4 + \dots\right) \\ &+ \mathcal{O}(e^{-6/a}). \end{aligned} \quad (4.156)$$

The first line reproduces the result obtained in [123]. The trans-series appearing here, in terms of a , has the same formal properties of its close cousin (4.144), like for example (4.149).

Our main conclusion is that, in this example, the exact large N free energy of the PCF model can be obtained by a median Borel resummation of a non-trivial resurgent trans-series, and therefore provides a beautiful success for the program of resurgence in an asymptotically free quantum field theory. Mathematically, this works because the building blocks of the exact solution (4.130) are special functions with known trans-series representations. From the physical point of view it is however gratifying to have a non-trivial example of resurgence at work with infinitely many non-trivial IR renormalons, yet analytically tractable.

In a recent *tour de force*, Abbott and collaborators [124, 125] were able to obtain detailed information on the trans-series expansion for the normalized energy density in the $O(4)$ sigma

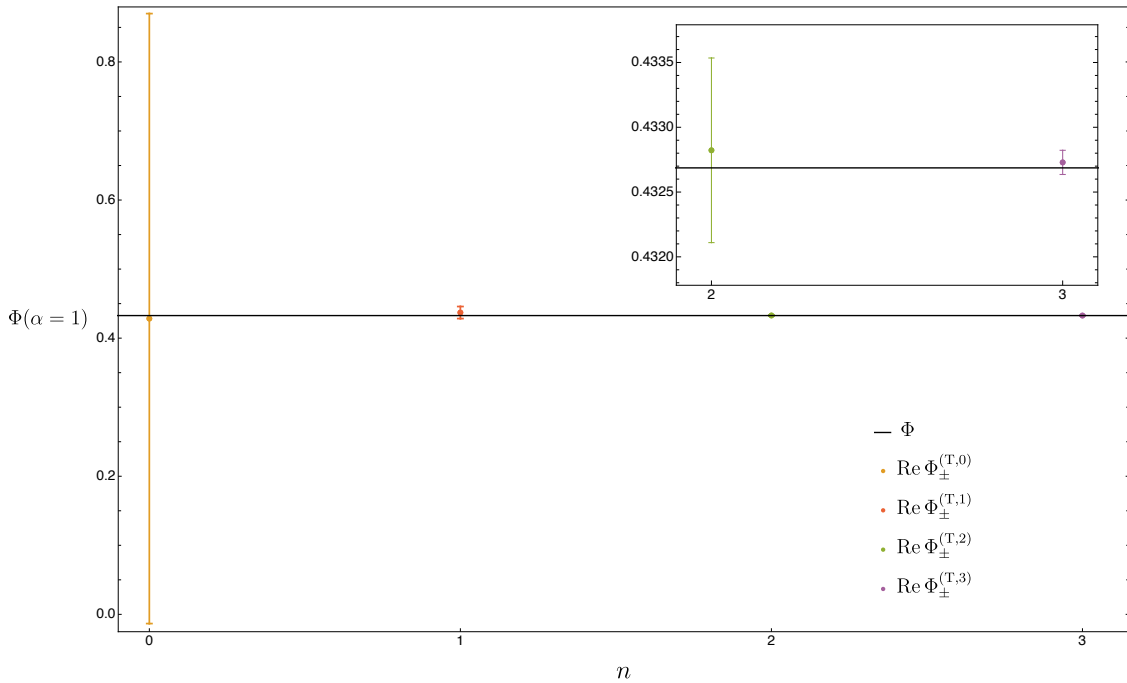


Figure 4.3: The real part of the resummed truncated trans-series $\Phi^{(T,n)}$ defined as in (4.154) as a function of n . The black horizontal line is the exact value. The box to the top-right is a zoom of the last two points and their error bars. The error bars are given by the left-over ambiguity in the truncated trans-series.

model, which is nothing but the PCF model we are studying at $N = 2$. By extrapolating numerical results to analytic results, they obtained an expression very similar to (4.156), and they gave evidence that the exact answer can be recovered by median resummation of the trans-series. Our results are an analytic version, at large N , of their result for $N = 2$.

4.5 The Gross–Neveu model

In this section we present our results for the GN model. In subsection 4.5.1 we review some general aspects of the model. Then, in subsection 4.5.2 we present the trans-series expansion for $\mathcal{F}_0(h)$ and $\mathcal{F}_1(h)$ and show that these trans-series cannot be reconstructed using resurgence. Finally in subsection 4.5.3 we numerically study the $1/N$ series expansion of \mathcal{F} up to high order, we analytically continue the series beyond its radius of convergence, and see how this continuation matches with known dualities between GN models at low N and sine-Gordon theories.

4.5.1 General aspects

The Lagrangian density describing the Gross–Neveu (GN) model [109] is

$$\mathcal{L} = \frac{i}{2} \bar{\chi} \cdot \not{\partial} \chi + \frac{g^2}{8} (\bar{\chi} \cdot \chi)^2, \quad (4.157)$$

where $\chi = (\chi^1, \dots, \chi^N)$ is a set of N Majorana fermions in two dimensions. As is well-known, a non-perturbatively generated mass gap and spontaneous breaking of a \mathbb{Z}_2 chiral symmetry occur in this theory. For $N > 4$ the lightest particle in the spectrum is the fundamental fermion in the Lagrangian (4.157). In our conventions (4.24) we have

$$\beta_0 = \frac{1}{4\pi\Delta}, \quad \xi = -\Delta. \quad (4.158)$$

The GN model has a $O(N)$ global symmetry, under which the N fermions transform as vectors, with conserved currents given by

$$J_\mu^{IJ} = \bar{\chi}^I \gamma^\mu \chi^J. \quad (4.159)$$

We couple the fermions to a chemical potential h associated to the $U(1) \subset O(N)$ charge Q^{12} . In the GN model it is convenient to define the 't Hooft coupling

$$\alpha \equiv \alpha(\mu = 2h), \quad (4.160)$$

where $\alpha(\mu)$ is the TBA coupling defined in (4.28).

The first two terms \mathcal{F}_0 and \mathcal{F}_1 in the $1/N$ expansion (4.32) have been analytically computed in [117, 118] using both QFT and TBA techniques. They read

$$\begin{aligned} \mathcal{F}_0(h) &= -\frac{h^2}{2\pi} \left(\tanh B_0 - \frac{B_0}{\cosh^2 B_0} \right), \\ \mathcal{F}_1(h) &= -\frac{h^2}{2\pi} \frac{2}{\cosh^2 B_0} (\sinh^2 B_0 + B_0^2 - B_0 \text{Shi}(2B_0)), \end{aligned} \quad (4.161)$$

where

$$B_0 = \cosh^{-1} \left(\frac{h}{m} \right), \quad (4.162)$$

and $\text{Shi}(x)$ is the hyperbolic sin integral function

$$\text{Shi}(x) = \int_0^x \frac{\sinh t}{t} dt. \quad (4.163)$$

4.5.2 Trans-series expansion

Let us now work out the explicit form of the first terms of the trans-series $\Phi_k(\alpha)$ defined in (4.32), for $k = 0, 1$, using (4.161) and (4.28) relating α and h . This map depends on Δ through the ξ factor in (4.158). Up to order Δ we get

$$h = e^{\frac{1}{\alpha}} \frac{m}{2} \left(1 - \frac{\Delta}{2} \log(\alpha^2) \right) + \mathcal{O}(\Delta^2). \quad (4.164)$$

For $k = 0$, the first few terms of the series $\varphi_0^{(\ell)}$ defined in (4.34) read

$$\varphi_0^{(0)}(\alpha) = 1, \quad \varphi_0^{(1)}(\alpha) = -2 - \frac{4}{\alpha}, \quad \varphi_0^{(2)}(\alpha) = 2, \quad \varphi_0^{(3)}(\alpha) = 2, \quad \varphi_0^{(4)}(\alpha) = \frac{10}{3}. \quad (4.165)$$

Note that the perturbative expansion $\varphi_0^{(0)}$ is trivial and all trans-series terms $\varphi_0^{(\ell)}$ with $\ell \geq 1$ are truncated, yet non-vanishing. We see that here is no way to reconstruct the non-perturbative terms $\varphi_0^{(\ell)}(\alpha)$ with $\ell \geq 1$ from $\varphi_0^{(0)}$. Since the leading order is somewhat trivial, it is useful to go through the next-to-leading order Φ_1 , where each term $\varphi_1^{(\ell)}(\alpha, C_{\pm})$ has a non-trivial asymptotic expansion in α . After some algebra, the first terms read

$$\begin{aligned} \varphi_1^{(0)}(\alpha) &= -\left(\alpha + \alpha^2 + \frac{3}{2}\alpha^3 + 3\alpha^4 + \frac{15}{2}\alpha^5 + \frac{45}{2}\alpha^6 + \mathcal{O}(\alpha^7) \right), \\ \varphi_1^{(1)}(\alpha, C_{\pm}) &= C_{\pm} \frac{4\pi}{\alpha} + \frac{8}{\alpha^2} - \frac{4}{\alpha} \log(\alpha^2) - 4 + \alpha \left(2 + \alpha + \alpha^2 + \frac{3}{2}\alpha^3 + 3\alpha^4 + \mathcal{O}(\alpha^5) \right), \\ \varphi_1^{(2)}(\alpha, C_{\pm}) &= -C_{\pm} 4\pi - \frac{16}{\alpha} + 4 \log(\alpha^2) + \alpha \left(2 + \frac{1}{2}\alpha + 3\alpha^2 - \frac{3}{4}\alpha^4 + \mathcal{O}(\alpha^5) \right). \end{aligned} \quad (4.166)$$

with $C_{\pm} = \pm i$. The perturbative series $\varphi_1^{(0)}$ turns out to be equal to

$$-2 \sum_{n=1}^{\infty} \Gamma(n+1) \left(\frac{\alpha}{2} \right)^n. \quad (4.167)$$

This series is non-Borel resummable, but can be studied analytically. Its Borel transform is

$$\mathcal{B}\varphi_1^{(0)}(t) = \frac{2t}{t-2}. \quad (4.168)$$

The simple pole at $t = 2$ hinders Borel summability. We can deform the contour to avoid the pole, passing either above (\mathcal{C}_+) or below (\mathcal{C}_-) it. The Borel resummation of this series gives then

$$s_{\pm}(\varphi_1^{(0)})(\alpha) = \frac{2}{\alpha} \int_{\mathcal{C}_{\pm}} dt e^{-\frac{t}{\alpha}} \frac{t}{t-2} = \frac{2}{\alpha} \text{P} \left(\int_0^{\infty} dt e^{-\frac{t}{\alpha}} \frac{t}{t-2} \right) \mp e^{-\frac{2}{\alpha}} \frac{4i\pi}{\alpha}. \quad (4.169)$$

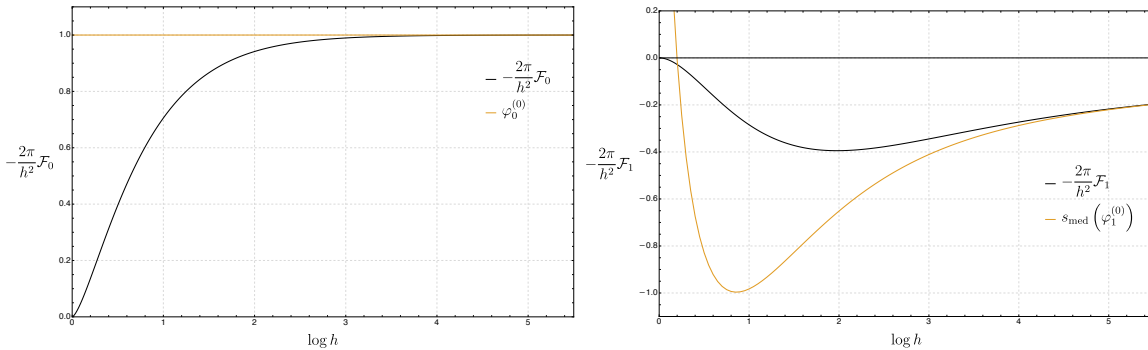


Figure 4.4: Free energy coefficients $\mathcal{F}_{0,1}$ rescaled by $-2\pi/h^2$ as a function of the coupling of the external field h with m set to 1. The orange and black lines correspond to the perturbative and exact results, respectively, for both the leading (left) and next-to-leading (right) orders in Δ .

Nicely enough, the ambiguity in the imaginary part in (4.169) is exactly the same appearing in $\varphi_1^{(1)}(\alpha, C_{\pm})$. The two contributions cancel each other if we choose the contour \mathcal{C}_{\pm} for C_{\pm} , respectively. The terms in parenthesis in the series (4.166) for $\varphi_1^{(1)}(\alpha, C_{\pm})$ form the same asymptotic series (4.167). Their Borel resummation gives

$$s_{\pm}(\varphi_1^{(1)})(\alpha, C_{\pm}) \supset \int_{\mathcal{C}_{\pm}} dt e^{-\frac{t}{\alpha}} \frac{4}{2-t} = \text{P} \left(\int_0^{\infty} dt e^{-\frac{t}{\alpha}} \frac{4}{2-t} \right) \pm e^{-\frac{2}{\alpha}} 4i\pi, \quad (4.170)$$

where for simplicity we have not reported the first four terms of $\varphi_1^{(1)}$ appearing in (4.166) (that's why the \supset sign instead of the equality sign). Again, if we pick up the contour \mathcal{C}_{\pm} , the imaginary part in (4.170) cancels respectively the imaginary terms proportional to $-C_{\pm}$ appearing in the second trans-series $\varphi_1^{(2)}$. In the spirit of resurgence, imaginary parts nicely match between one series and the next, but we see a plethora of real non-perturbative terms which cannot be detected. The asymptotic series $\varphi_1^{(1)}$ and those with $\ell \geq 2$ cannot be reconstructed from the knowledge of $\varphi_1^{(0)}$ only. In order to quantify and illustrate the phenomenon, in fig. 4.4 we compare the exact free energies $\mathcal{F}_{0,1}$, rescaled by h^2 , with the median Borel resummation of their perturbative series expressed in terms of h and m , i.e. $s_{\text{med}}(\varphi_{0,1}^{(0)})(1/\log(2h/m))$.⁷ We restrict to the perturbative series because higher trans-series terms can not be obtained from a resurgence analysis. As expected, for both $k = 0, 1$, the perturbative and full results are in good agreement at large h , i.e. weak coupling, but they significantly differ at strong coupling, when the terms with $\ell \geq 1$ are no longer negligible.

All the above analysis could be repeated for the energy density $e(\rho)$, Legendre transform of

⁷Since $\varphi_0^{(0)}(\alpha) = 1$, there is no need of resummation at LO and this order does not contribute at the next one, differently to what happens in the NLSM.

$\mathcal{F}(h)$, expanded in Δ and written as a trans-series as

$$e(\rho) \sim \frac{\pi}{2} \rho^2 \sum_{k \geq 0} \tilde{\Phi}_k(a, C_{\pm}) \Delta^k, \quad (4.171)$$

where

$$\tilde{\Phi}_k(a, C_{\pm}) = \sum_{\ell=0}^{\infty} e^{-\frac{2\ell}{a}} \tilde{\varphi}_k^{(\ell)}(a, C_{\pm}). \quad (4.172)$$

The asymptotic expansion in this case is more conveniently written in terms of the coupling

$$a \equiv \alpha(\mu = 2\pi\rho). \quad (4.173)$$

For $\tilde{\varphi}_0$ we get

$$\tilde{\varphi}_0^{(0)}(a) = 1, \quad \tilde{\varphi}_0^{(1)}(a) = 2 + \frac{4}{a}, \quad \tilde{\varphi}_0^{(2)}(a) = 2, \quad \tilde{\varphi}_0^{(3)}(a) = -2, \quad \tilde{\varphi}_0^{(4)}(a) = \frac{10}{3}, \quad (4.174)$$

while for $\tilde{\varphi}_1$ we have

$$\begin{aligned} \tilde{\varphi}_1^{(0)}(a) &= a + a^2 + \frac{3}{2}a^3 + 3a^4 + \frac{15}{2}a^5 + \frac{45}{2}a^6 + \mathcal{O}(a^7), \\ \tilde{\varphi}_1^{(1)}(a) &= -C_{\pm} \frac{4\pi}{a} - \frac{8}{a^2} + \frac{4}{a} \log(a^2) + 4 + a \left(2 + a + a^2 + \frac{3}{2}a^3 + 3a^4 + \mathcal{O}(a^5) \right), \\ \tilde{\varphi}_1^{(2)}(a) &= -C_{\pm} 4\pi - \frac{16}{a} + 4 \log(a^2) - a \left(2 + \frac{1}{2}a + 3a^2 - \frac{3}{4}a^4 + \mathcal{O}(a^5) \right). \end{aligned} \quad (4.175)$$

We see that the expansions of $\tilde{\Phi}_0$ and $\tilde{\Phi}_1$ in terms of a are very similar to those of Φ_0 and Φ_1 in terms of α . The perturbative series $\tilde{\varphi}_1^{(0)}$ in (4.175) agrees with the perturbative expansion found in eq.(A.12) of [123] using the techniques of [13, 14], while $\tilde{\varphi}_1^{(\ell)}$, with $\ell > 0$, are non-perturbative terms that could not be captured in that analysis. All the considerations made above about imaginary part cancellations and impossibility of recovering the non-perturbative terms from the perturbative series of $\mathcal{F}(h)$ apply also for $e(\rho)$ and will not be repeated.

4.5.3 Higher orders in the $1/N$ expansion

In contrast to the NLSM and PCF models, the kernel in the GN model is analytic at $N = \infty$. This implies that the TBA solution can easily be expanded in powers of $1/N$, with each term a regular function of θ , making it possible to solve the integral equations (4.21) in a systematic $1/N$ expansion:

$$K(\theta) = \sum_{k \geq 1} K_k(\theta) \Delta^k, \quad \epsilon(\theta) = \sum_{k \geq 0} \epsilon_k(\theta) \Delta^k, \quad B = \sum_{k \geq 0} B_k \Delta^k. \quad (4.176)$$

The kernel coefficients $K_k(\theta)$ are trivially derived from the GN kernel reported in (F.32). The B_k with $k \geq 1$ can be expressed in terms of the values of the $\epsilon_m(B_0)$ with $m \leq k$ and their derivatives by solving recursively the condition (4.22) at each order in Δ . For instance, for the first few orders we have

$$\epsilon_0(B_0) + \Delta \left(\epsilon_1(B_0) + \partial_\theta \epsilon_0|_{B_0} B_1 \right) + \Delta^2 \left(\epsilon_2(B_0) + \partial_\theta \epsilon_1|_{B_0} B_1 + \partial_\theta^2 \epsilon_0|_{B_0} \frac{B_1^2}{2} + \partial_\theta \epsilon_0|_{B_0} B_2 \right) + \dots = 0. \quad (4.177)$$

Plugging (4.176) in (4.21) we have

$$\begin{aligned} \epsilon(\theta) = & h - m \cosh \theta + \sum_{k \geq 1} \Delta^k \int_{-B_0}^{B_0} d\theta' \left(\sum_{n=0}^{k-1} K_{k-n}(\theta - \theta') \epsilon_n(\theta') \right) \\ & + \sum_{p \geq 1} \frac{1}{p!} \left(\sum_{q \geq 1} B_q \Delta^q \right)^p \partial_{\theta'}^{p-1} \left(\sum_{k \geq 1} \Delta^k \sum_{n=0}^{k-1} (K_{k-n}(\theta - \theta') + K_{k-n}(\theta + \theta')) \epsilon_n(\theta') \right) \Big|_{B_0}, \end{aligned} \quad (4.178)$$

where we used the fact that $K_n(\theta)$ and $\epsilon_n(\theta)$ are even functions. Solving the equation at each order in Δ , we can compute iteratively all the $\epsilon_k(\theta)$ knowing the values of $\epsilon_m(\theta)$ for $m < k$ and the B_q with $q < k - 1$. Finally, in order to compute $\mathcal{F}_k(h)$ it is enough to expand (4.23) in Δ :

$$\begin{aligned} \mathcal{F}(h) = & -\frac{m}{2\pi} \int_{-B}^B d\theta \cosh \theta \left(\sum_{k \geq 0} \epsilon_k(\theta) \Delta^k \right) \\ = & -\frac{m}{2\pi} \left(\sum_{k \geq 0} \Delta^k \int_{-B_0}^{B_0} d\theta \cosh \theta \epsilon_k(\theta) + 2 \sum_{p \geq 1} \frac{1}{p!} \left(\sum_{q \geq 1} B_q \Delta^q \right)^p \sum_{n \geq 0} \Delta^n \partial_\theta^{p-1} \left(\cosh \theta \epsilon_n(\theta) \right) \Big|_{B_0} \right), \end{aligned} \quad (4.179)$$

where we used once again the fact that $\epsilon_n(\theta)$ is an even function.

In order to make more explicit the procedure and show how the iterative process starts, let's rederive $\mathcal{F}_0(h)$ and $\mathcal{F}_1(h)$ given in (4.161). At order Δ^0 we simply have

$$K_0 = 0, \quad \epsilon_0(\theta, h) = h - m \cosh(\theta), \quad B_0 = \cosh^{-1} \left(\frac{h}{m} \right). \quad (4.180)$$

The leading order free energy reads

$$\mathcal{F}_0(h(B_0)) = -\frac{m}{2\pi} \int_{-B_0}^{B_0} d\theta \cosh(\theta) \epsilon_0(\theta, h(B_0)) = -\frac{h^2}{2\pi} \left(\tanh(B_0) - \frac{B_0}{\cosh^2(B_0)} \right), \quad (4.181)$$

as already reported in the first equation of (4.161).

At order $k = 1$ we have

$$K_1(\theta) = \frac{1}{\theta^2} - \frac{\cosh(\theta)}{\sinh^2(\theta)}, \quad (4.182)$$

and

$$\epsilon_1(\theta, h) = \int_{-B_0}^{B_0} K^{(1)}(\theta - \theta') \epsilon_0(\theta', h) d\theta'. \quad (4.183)$$

Performing the integral we get

$$\begin{aligned} \epsilon_1(\theta, h(B_0)) &= m \sinh(\theta) (\text{Chi}(B_0 + \theta) - \text{Chi}(B_0 - \theta) - \log(\sinh(B_0 + \theta) \text{csch}(B_0 - \theta))) \\ &\quad + m \cosh(\theta) (2B_0 - \text{Shi}(B_0 - \theta) - \text{Shi}(B_0 + \theta)), \end{aligned} \quad (4.184)$$

and from it

$$B_1(B_0) = - \frac{\epsilon_1(B_0, h(B_0))}{\partial_\theta \epsilon_0(\theta, h(B_0)) \Big|_{B_0}} = \text{Chi}(2B_0) + (2B_0 - \text{Shi}(2B_0)) \coth(B_0) - \log(\sinh(2B_0)) - \gamma_E, \quad (4.185)$$

where $\text{Chi}(x)$ is the hyperbolic cos integral function

$$\text{Chi}(x) = \gamma_E + \log(x) + \int_0^x \frac{\cosh t - 1}{t} dt. \quad (4.186)$$

Given that $\epsilon_0(B_0) = 0$, the next-to-leading term of the the free energy reads

$$\mathcal{F}_1(h(B_0)) = - \frac{m}{2\pi} \int_{-B_0}^{B_0} d\theta \cosh(\theta) \epsilon_1(\theta, h(B_0)). \quad (4.187)$$

Plugging (4.184) in (4.187) and computing the integral gives the second equation of (4.161).

At higher order in Δ the computation becomes analytically prohibitive. On the other hand, it is straightforward to proceed numerically and, for a given B_0 , automatize the iteration procedure to compute higher order terms in Δ . We have been able to compute with high precision, for different values of h , \mathcal{F}_k up to $k = 28$. This allowed us to study the large order behavior of the series. We get⁸

$$\mathcal{F}_k \propto \rho^{-k} \sin(k \vartheta), \quad (4.188)$$

where ρ and ϑ are two parameters that we can numerically evaluate. For example, for $h = 3$ we get

$$\rho = 0.50 \pm 0.02 \quad \text{and} \quad \vartheta = 0.35 \pm 0.07. \quad (4.189)$$

This result confirms that the $1/N$ series of $\mathcal{F}(h)$ is convergent in the GN model, in agreement with what found in appendix F. The radius of convergence ρ should equal $1/2$ independently of h , while we did not investigate the possible dependence on h of ϑ . The value $\Delta = 1/2$ corresponds to $N = 4$, so we see that for any integer value $N > 4$, where the fundamental fermions are stable and the TBA equations (4.17) and (4.21) apply, the free energy can be recovered from its $1/N$

⁸The presence of a period of oscillation in the $1/N$ coefficients makes less straightforward the determination of the large order behavior. We have made use of a program written by Jie Gu and based on the work [144].

expansion.

It is now natural to ask if the analytic continuation of the series in Δ beyond $|\Delta| \geq 1/2$ contains any physical information. This analytic continuation can be obtained by considering Padé approximants $\text{P}\mathcal{F}_{[m/n]}(\Delta, h)$ of the series of \mathcal{F}_k we computed. It is known that for convergent series, parametrically diagonal Padé approximants converge (in capacity) to the exact function and the location of their poles and zeros define an appropriate locus of branch-cuts connecting branch-point singularities [30] (see e.g. app. D of [31] for a brief overview and [32] for a comprehensive introduction). Moreover, as we will see below, $\mathcal{F}(\Delta, h)$, at fixed h , is analytic at $\Delta = \infty$ and non-vanishing, hence diagonal approximants are the optimal choice to reconstruct the function.

We calculated $\text{P}\mathcal{F}_{[14/14]}(\Delta, h)$ for a given set of values of h , and compared the result with $\mathcal{F}(\Delta, h)$ computed by directly solving (numerically) (4.21) at given h and Δ . We find full agreement for all values of h sampled and for $0 < \Delta < \frac{1}{2}$, and consider it a sanity check of the correctness of the coefficients \mathcal{F}_k . The location of the poles and zeros of $\text{P}\mathcal{F}_{[14/14]}(\Delta, h)$ shows that the point $\Delta = 1/2$ is a branch-point of $\mathcal{F}(\Delta)$. On the other hand, no singularities appear for $\Delta < 0$ (as expected from the form of the GN kernel) and hence we can reliably continue $\mathcal{F}(\Delta)$ for $\Delta < 0$ using its approximant $\text{P}\mathcal{F}_{[14/14]}(\Delta, h)$. The two interesting points to discuss are $\Delta = 1/2$ ($N = 4$) and $\Delta = -\infty$ ($N = 2$).

For $N = 4$ the stable particles in the model are the kinks and their mass equals

$$m_k = \frac{m}{2}. \quad (4.190)$$

Since the fermions are exactly at threshold and are marginally unstable, we can use (4.21) to compute the free energy by choosing either kinks or fermions as particles populating the vacuum, but some care is needed. It is useful to briefly review how the analysis goes [117].

Kinks are in the $(\pm 1/2, \pm 1/2)$ spinorial representation of $O(4)$, so their charges are half those of the fermions. When $h/2 > m/2$ (or $h > m$) the vacuum is populated by kinks with $O(4)$ components $(1/2, 1/2)$ and $(1/2, -1/2)$, which do not interact with each other. The S -matrix is identical for the two chiralities and the associated kernel is

$$K_k(\theta) = \frac{1}{\pi^2} \sum_{n=1}^{\infty} (-1)^{n+1} \frac{n}{n^2 + (\theta/\pi)^2}. \quad (4.191)$$

If we consider kinks, the associated TBA equation is

$$\epsilon_k(\theta) - \int_{-B}^B K_k(\theta - \theta') \epsilon_k(\theta') d\theta' = \frac{1}{2}(h - m \cosh \theta), \quad (4.192)$$

where ϵ_k describes the excitation of the kink holes. Given $\epsilon_k(\theta)$, the free energy is computed as

$$\mathcal{F}(h) = -2\frac{m_k}{2\pi} \int_{-B}^B d\theta \epsilon_k(\theta) \cosh \theta = -\frac{m}{2\pi} \int_{-B}^B d\theta \epsilon_k(\theta) \cosh \theta, \quad (4.193)$$

where the factor 2 counts the two-fold degeneracy of the kink and exactly compensates for the 1/2 factor in the mass. The kink kernel (4.191) is naively 1/2 of the fermion kernel in (F.33) for $\Delta = 1/2$. If we take the limit carefully, however, we also get a δ function because

$$\lim_{y \rightarrow 0} \frac{1}{\pi} \frac{y}{y^2 + x^2} = \delta(x). \quad (4.194)$$

Hence

$$\lim_{\Delta \rightarrow 1/2} K_f(\theta) = -\delta(\theta) + 2K_k(\theta), \quad (4.195)$$

where we denote by K_f the fermion kernel. So, for $\Delta \rightarrow 1/2$, the TBA equation (4.21) for the fermion excitation holes ϵ_f becomes

$$\epsilon_f(\theta) - \int_{-B}^B \left(-\delta(\theta) + 2K_k(\theta) \right) \epsilon_f(\theta') d\theta' = 2\epsilon_f(\theta) - 2 \int_{-B}^B K_k(\theta) \epsilon_f(\theta') d\theta' = h - m \cosh \theta, \quad (4.196)$$

which is identical to (4.192) with

$$\epsilon_k(\theta) = \epsilon_f(\theta). \quad (4.197)$$

Note that we would *not* get the correct result by setting $N = 4$ directly in the fermion case, because in this way we would not detect the $\delta(\theta)$ term in (4.195). On the other hand, the analytic continuation of $\text{PF}_{[14/14]}(\Delta, h)$, computed using fermion states for $\Delta < 1/2$, gives the correct result at $\Delta = 1/2$.

The $N = 4$ model is also equivalent to a pair of decoupled sine-Gordon models:

$$\mathcal{L} = \sum_{j=1,2} \left(\frac{1}{2} \frac{8\pi}{b^2} (\partial\phi_j)^2 + \frac{\pi}{4} \left(\frac{8\pi}{b^2} - 1 \right) \cos \sqrt{8\pi} \phi_j \right), \quad (4.198)$$

where b is the inverse radius of the compact scalars. For $b^2 > 4\pi$ the only asymptotic states in the sine-Gordon models are given by kinks and anti-kinks. In presence of a chemical potential h , the vacuum gets populated by kinks (and no anti-kinks) with a kernel whose Fourier transform is given by [145]

$$\tilde{K}_{\text{SG}}(\omega, p) = \frac{\sinh \frac{\pi(p+1)\omega}{2}}{2 \cosh \frac{\pi\omega}{2} \sinh \frac{\pi p\omega}{2}}, \quad (4.199)$$

where the parameter p is defined in terms of b as follows:

$$\frac{8\pi}{b^2} \equiv \frac{p+1}{p}. \quad (4.200)$$

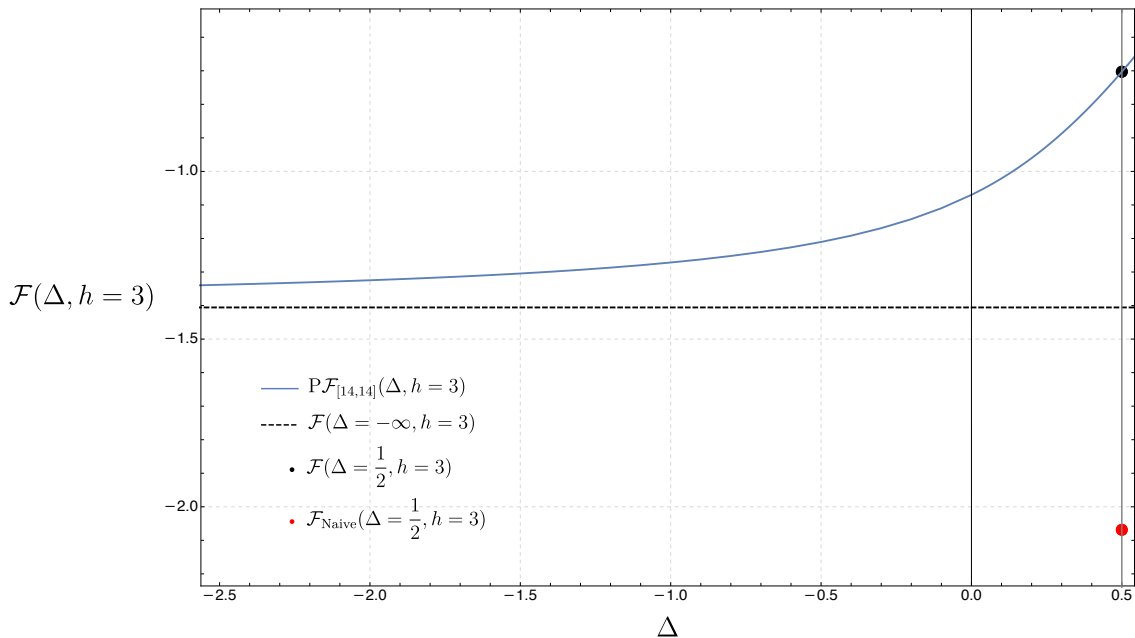


Figure 4.5: Free energy as a function of Δ at fixed $h = 3$. The red dot corresponds to the (wrong) free energy one would get by setting $\Delta = 1/2$ in the kernel appearing in (4.21). The black dot is the correct value found using (4.193).

On the other hand, the Fourier transform of the kink kernel (4.191) reads

$$\tilde{K}_k(\omega) \equiv \int_{-\infty}^{\infty} e^{i\omega\theta} K_k(\theta) d\theta = \frac{1}{1 + e^{\pi|\omega|}}. \quad (4.201)$$

Interestingly enough,

$$\lim_{p \rightarrow \infty} \tilde{K}_{\text{SG}}(\omega, p) = \tilde{K}_k(\omega), \quad (4.202)$$

so there is an equivalence of the free energy $F(h)$ in the two models provided

$$b^2 = 8\pi \quad (4.203)$$

in the two sine-Gordon models. Note that when $b^2 \rightarrow 8\pi$, the coupling of the sine-Gordon interaction at the same time becomes marginal and vanishes. From (4.198) it might seem that we get in this limit a pair of decoupled free field scalars, but in fact this is an artefact. The only asymptotic states are kinks and these are still interacting, as evident from the non-triviality of the kernel (4.202).⁹ In the correspondence the kink mass of the GN model is mapped to the mass of the sine-Gordon kink: $m_k = m_{\text{SG}}^{N=4}$.

For $N = 2$, i.e. $|\Delta| = \infty$, the TBA equations (4.21) are physically meaningless, since funda-

⁹See e.g. [146] for a detailed analysis of the sine-Gordon model when $b^2 \sim 8\pi^2$.

mental particles are no longer asymptotic states. Yet, we can wonder if its analytic continuation is of physical interest and is related in some way to the actual $N = 2$ Gross-Neveu model. The latter is nothing else than the Thirring model, famously dual to the sine-Gordon theory [147]. If we approach the infinite limit from negative values of Δ , we see from direct inspection of either (F.32) or (F.33) that the GN kernel is analytic at infinity (recall that the digamma function $\psi(z)$ is meromorphic with simple poles at $z = -n$, with integer $n \geq 0$). By direct inspection we can also check that this kernel is a contraction:

$$\int_{-B}^B K(\theta - \theta') d\theta' < 1. \quad (4.204)$$

All iterated kernels are hence bounded and the solution of the TBA equation is analytic in Δ . By taking the analytic continuation of (F.34) for $\Delta < 0$ and then the limit $\Delta \rightarrow -\infty$ we immediately see that the Fourier transform of the kernel equals the kernel for the kink in the sine-Gordon theory as $p \rightarrow \infty$ (and the kernel for kinks in the $N = 4$ GN model). Quite interestingly, the in principle meaningless $|\Delta| = \infty$ point of the GN TBA equation (4.21) is related to the free energy $\mathcal{F}(h)$ of a sine-Gordon model at $b^2 = 8\pi$! In the correspondence the fermion mass appearing in (4.21) is identified with the mass of the sine-Gordon kink: $m_f = m_{\text{SG}}^{N=2}$.

We can match the values of h in the $N = 2$ and $N = 4$ theories, since h multiplies a conserved quantity and does not renormalize. In particular, we can compute the ratio $h^{N=2}/h^{N=4}$. Recall that h is the chemical potential for a single $U(1)$ current of the form $\bar{\chi}^1 \gamma^\mu \chi^2$. Bosonizing we have

$$\bar{\chi}^1 \gamma^\mu \chi^2 = \frac{i}{\sqrt{\pi}} \epsilon^{\mu\nu} \partial_\nu \phi. \quad (4.205)$$

When $N = 2$ the scalar is free and its Lagrangian reads

$$\frac{1}{2} \frac{4\pi}{b^2} (\partial\phi)^2 + \frac{h}{\sqrt{\pi}} \partial_x \phi \xrightarrow{b^2=8\pi} \frac{1}{4} (\partial\phi)^2 + \frac{h}{\sqrt{\pi}} \partial_x \phi, \quad (4.206)$$

while for $N = 4$ the Lagrangian of the two scalars at $b^2 = 8\pi$ reads¹⁰

$$\sum_{j=1,2} \left(\frac{1}{2} (\partial\phi_j)^2 + \frac{h}{\sqrt{2\pi}} \partial_x \phi_j \right). \quad (4.208)$$

¹⁰Note that the relation between the inverse radius of the sine-Gordon and the GN coupling is different in the two cases, namely

$$b_{N=4}^2 = \frac{8\pi}{1 + \frac{g^2}{2\pi}}, \quad b_{N=2}^2 = \frac{4\pi}{1 + \frac{g^2}{2\pi}}. \quad (4.207)$$

Both for $N = 2$ and for $N = 4$ the kernel on the GN side (for fermions and for kinks, respectively) coincides with the kernel of the sine-Gordon kink, when their corresponding b^2 parameters are set to 8π . Curiously, this corresponds to $g^2 = 0$ for $N = 4$ and $g^2 = -\pi^2$ for $N = 2$.

| | $\Delta = 1/2$ | $\Delta = -\infty$ |
|--|----------------|--------------------|
| $\mathcal{F}_{\text{TBA}}(\Delta, h_0 = 3)$ | -0.7028... | -1.4056352... |
| $\text{P}\mathcal{F}_{[14/14]}(\Delta, h_0 = 3)$ | -0.7029(2) | -1.4056353(10) |

Table 4.3: Comparison between the numerical values of the free energy at $h_0 = 3$ obtained by a direct numerical evaluation of the TBA equation and by using the analytic continuation given by $\text{P}\mathcal{F}_{[14/14]}(\Delta, h_0)$ for $\Delta = 1/2$ and $\Delta = -\infty$.

Rescaling the fields to have a canonically normalized kinetic term in (4.205) we get

$$h^{N=2} = 2h^{N=4}. \quad (4.209)$$

When $h < m$ the vacuum is empty and $\mathcal{F}(h = m) = 0$ for both $N = 2$ and $N = 4$. This implies that the kink mass ratio is the same as in (4.209), $m_{\text{SG}}^{N=2} = 2m_{\text{SG}}^{N=4}$ and hence that the free energies of the two models are related, namely

$$\mathcal{F}(\Delta = -\infty, h) = 2\mathcal{F}(\Delta = 1/2, h). \quad (4.210)$$

In figure 4.5 we plot $\text{P}\mathcal{F}_{[14/14]}(\Delta, h_0)$ as a function of Δ at fixed h_0 . At $\Delta = 1/2$ the black dot corresponds to the (correct) free energy numerically computed using (4.193), while the red dot is the (wrong) value one would get by naively setting $\Delta = 1/2$ in the fermion kernel appearing in (4.21). We see that the analytic continuation given by $\text{P}\mathcal{F}_{[14/14]}(\Delta, h_0)$ gives the correct value. The dashed black line corresponds to the asymptotic value for $\Delta = -\infty$ which should equal to $2\mathcal{F}(\Delta = 1/2, h)$, according to (4.210). In table 4.3 we compare the numerical values of $\mathcal{F}(h_0)$ obtained by a direct numerical evaluation of the TBA equation and by using the analytic continuation given by $\text{P}\mathcal{F}_{[14/14]}(\Delta, h_0)$ for $\Delta = 1/2$ and $\Delta = -\infty$. The two results are in total agreement.

Chapter 5

Conclusions

In this thesis we investigated low-dimensional QFTs with perturbation theory by means of Borel resummation and resurgence. We decided to organize the conclusions and the outlook of our work following its two main directions, namely the study of theories where perturbative series are Borel summable and where they are not.

Chapter 3

In chapter 3 we investigated $O(N)$ ϕ^4 vector models in $d = 2$ and $d = 3$ using perturbation theory around the Gaussian fixed point. In particular, we have pointed out the importance of the RS in the proof of their Borel summability. We have shown that the proofs in refs. [7, 8] and ref. [9] are both based on the minimal RSs, which we denoted by \mathcal{S} . Despite the absence of a non-trivial β -function, the RS \mathcal{S} can be used to determine the strong coupling behavior of the theory and its critical regime. Physical observables such as critical exponents can be extracted from correlation functions or from the behavior of the mass gap as the critical coupling is approached. On the other hand, most of the results in the literature that make use of the resummation of the fixed dimension expansion (not ϵ -expansion) are based on other RSs, such as the one we denoted by $\tilde{\mathcal{S}}$ (momentum subtraction) where a non-trivial β -function occurs. We have shown that in the RS $\tilde{\mathcal{S}}$ the proof given in ref. [9] no longer holds, and we are not aware of papers in constructive quantum field theory generalising the proofs in refs. [7, 8] to other RSs such as $\tilde{\mathcal{S}}$. Focusing on minimal RSs, we studied the scheme dependence in an one-parameter family of RSs (parametrized by κ) and have been able to find exact finite changes of scheme, given in (3.51) and (3.59), for $d = 2$ and $d = 3$ respectively. This allowed us to write down the exact analytic renormalization dependence of the critical couplings. In $d = 2$, we verified it Borel resumming the perturbative series for the mass gap for different values of κ , see fig. 3.6. In $d = 3$, where the structure of the classically unbroken phase is richer, we have reassessed the strong-weak Magruder duality. Starting from the weak branch in perturbation theory, for certain schemes we encounter a critical coupling where the theory is gapless and a second-order phase transition

takes place. On the other hand, for other choices of schemes, if one restricts to real values of the coupling the theory always turns out gapped and a pair of complex conjugate critical couplings appears. In this case the weak and strong branches are no longer separated by a phase transition (for real parameters in the Lagrangian) and we can access the strong branch from the Gaussian fixed point. We have, once again, numerically verified these considerations by Borel resumming the perturbative series of the 3d $O(N)$ models for the vacuum energy and for the mass gap, see figs. 3.10 and 3.11.

The merging of critical points is reminiscent of the fixed point annihilation advocated in [148] as a mechanism for loss of conformality in QFT, see also [149–151]. The fixed point annihilation described in those papers occurs when parameters (such as the number of fields) in a family of critical theories are varied and so differs from the merging found in this paper, which is within a given theory when the renormalization scheme is varied.¹ The two CFTs, that we would have at the two complex conjugate complex values $x_c^{(w)}(\kappa)$ and $x_c^{(s)}(\kappa)$ for $\kappa < \kappa_*$, should eventually correspond to the usual $O(N)$ symmetric CFTs, because they merely arise from a coupling constant redefinition. It would be interesting however to better establish the correspondence because it is not obvious if (and how) the CFT data of the two complex CFTs are in fact identical to those of the ordinary unitary $O(N)$ symmetric CFTs. The appearance and disappearance of fixed points makes also clear that a phase diagram of a theory is not universally determined, but it depends on the renormalization scheme. For example, we see that according to fig. 3.2 in the $N = 1$ case the number of critical points that occur in the entire range of the real squared mass parameter is either three or one, depending on the renormalization scheme. The universal presence of a second-order phase transition could be argued from the fact that this number modulo two is always one.²

Computing the perturbative series for the 0, 2 and 4-point functions at zero momentum up to order eight, we extended to the next order with respect to the literature the series for the β -function and the critical exponents η and ν for the $d = 3$ $O(N)$ models in the RS $\tilde{\mathcal{S}}$, see appendix D.2. Borel resumming them, we computed the value of the critical coupling and of these critical exponents for several values of N obtaining very accurate results, see table 3.4. While for $d = 2$ the accuracy of Borel resummations in the RS \mathcal{S} , found in [9], is greater than the one found in $\tilde{\mathcal{S}}$, the opposite is true in $d = 3$. We suspect that this might be related to the different analytic structure for observables in $d = 2$ and $d = 3$ in the RS \mathcal{S} : in three dimensions the presence of the self-duality in the classically unbroken phase gives rise to two fixed points and makes observables more difficult to reconstruct numerically. In the spirit of our study, it would be very interesting to understand more in detail the reasons behind such differing outcomes. Especially taking in account all our considerations made on the RS $\tilde{\mathcal{S}}$.

¹Note however that a renormalization scheme dependence on the position of the critical points always occurs. It would be interesting to study more carefully the interplay between the position of fixed points determined by the parameters of the theory and by the renormalization scheme dependence of its couplings.

²It would be nice to understand if this is associated to an index, in the spirit of [152].

Chang and Magruder dualities are crucially based on the super-renormalizability properties of ϕ^4 theories in $d = 2$ and $d = 3$. One can then try to derive similar dualities from more general super-renormalizable theories. The dualities so obtained would be in general only valid to all orders in perturbation theory, but not non-perturbatively. In order to hope to have exact dualities, one should argue for the absence or decoupling of non-perturbative effects, like in the 2d $N = 1$ and 3d $O(N)$ ϕ^4 models in infinite volume studied in this work.

Extending our methods to other QFTs would be exciting, namely starting from perturbation theory at fixed dimension to study strongly coupled regions via Borel resummation procedure. In this direction, the recent results in [153] provide a first positive answer for a study in 3d abelian gauge theories at finite N . However, for these theories there are no proof about the Borel summability of the perturbative series. At the same time, neither instantons nor renormalon singularities are expected to obstruct the Borel resummation. Thus attempting to investigate the critical behavior in sQED₃ and QED₃ for different values of N is appealing. Moreover, in these theories and more in general in fermionic QFTs we still do not have a clear prediction for the large-order behavior of the perturbative series, see [154] for an old review in this regard.

Chapter 4

In chapter 4 we have discussed the interplay between resurgence and the $1/N$ expansion in three integrable theories with a continuous global symmetry: the non-linear sigma model, the principal chiral field and the Gross-Neveu models. All these theories have marginal interactions, they are UV free and are affected by IR renormalon singularities. A notable observable is the relative free energy $\mathcal{F}(h)$ defined in (4.16). Its special role comes from the fact that it is possible to compute it exactly using TBA techniques [113] and has a non-trivial structure (unlike, e.g., S -matrix elements in integrable theories). Standard large N QFT and/or TBA techniques also allow to analytically determine the first $1/N$ coefficients $\mathcal{F}_k(h)$ defined in (4.30)-(4.32).

We have computed \mathcal{F}_0 and \mathcal{F}_1 in the NLSM, given respectively in (4.57) and (4.78), and determined \mathcal{F}_0 analytically in the PCF model (for the choice of charges in [116]), given in (4.130). Crucial for the latter computation has been the observation that the NLSM and the PCF kernels can be expanded in $1/N$ if the non-analytic term is treated separately. In this way we have also been able to check \mathcal{F}_1 in the NLSM by using TBA techniques. These expressions, as well as the previously known coefficients $\mathcal{F}_{0,1}$ in the GN model [117, 118], have then been compared to the asymptotic series expansion, one gets in terms of the coupling constant defined in (4.28). While the perturbative asymptotic expansion agrees with the ones previously determined [123], we get a plethora of non-perturbative trans-series terms which are associated to the non-Borel summability of the series due to the presence of IR renormalons.

The final results turned out to be different in the three models. In the NLSM \mathcal{F}_0 contains a non-perturbative term which cannot be captured from the (trivial) perturbative expansion. On the other hand, the median Borel resummation of the perturbative series reconstructs the

full next-to-leading coefficient \mathcal{F}_1 , see fig.4.1. The series for \mathcal{F}_1 is non-Borel resummable because of the presence of an IR renormalon, yet somehow unexpectedly no non-perturbative terms are missed. In the PCF model the expansion of \mathcal{F}_0 gives rise to the non-trivial trans-series (4.144), with a perturbative series affected by an infinite number of IR renormalon singularities. In this case, resurgence techniques work nicely and allow us to reconstruct the full answer from the perturbative series. In the GN model the expansion of both \mathcal{F}_0 and \mathcal{F}_1 give rise to trans-series (4.165) and (4.166) which can *not* be reconstructed from the perturbative series only, using resurgence.

We also studied the behavior of the $1/N$ series for $\mathcal{F}(h)$. The non-analyticity of the kernel at $N = \infty$ for the NLSM and the PCF models suggest that the $1/N$ expansion of $\epsilon(\theta)$ and $\chi(\theta)$ should be divergent asymptotic. This points towards a divergent $1/N$ expansion of $\mathcal{F}(h)$, as well as of its Legendre transform $e(\rho)$. In contrast, the $1/N$ expansion of $\mathcal{F}(h)$ (and $e(\rho)$) in the GN model is expected to be convergent. We have numerically computed higher values of \mathcal{F}_k in each model (for some values of h) in order to verify these expectations. Our results for the NLSM and PCF models are inconclusive. The number of coefficients \mathcal{F}_k we computed does not allow us to establish whether the series are convergent or divergent asymptotic. The first possibility is not in contradiction with the $1/N$ non-analyticities of the kernel, because $\mathcal{F}(h)$ is obtained by integrating $\epsilon(\theta)$ over rapidities and we cannot exclude that these non-analyticities are smoothed out by the integration procedure. It would be nice to settle this issue in future studies. In the Gross-Neveu model the expected convergence of the $1/N$ series is numerically confirmed. We analytically continued the series beyond its radius of convergence (see fig.4.5), where the TBA equations (4.21) and (4.17) no longer make sense, and showed how this continuation gives values of $\mathcal{F}(h)$ in complete agreement with those obtained for the sine-Gordon theories dual to the GN models with $N = 2$ and $N = 4$.

There are several directions worth exploring in future studies. From the point of view of the general theory of resurgence, our most important finding is its breakdown in certain models, when combined with the $1/N$ expansion. By a breakdown of resurgence we mean that the structure of non-perturbative corrections at each order in the $1/N$ expansion can not be predicted from the study of the perturbative series only. A better understanding of this breakdown is perhaps the most important problem open by our investigation. There are two possibilities here. One possibility is that this is a feature of the $1/N$ expansion and does not apply at finite N . It might happen that, when fixing the order in the $1/N$ expansion, the resulting perturbative series in the coupling constant is not sufficiently generic and cannot be used to predict non-perturbative corrections. This would be somewhat similar to the ‘‘Cheshire cat resurgence’’ in supersymmetric theories [155]. The other possibility is that the phenomenon we have found is generic in theories with renormalons. The detailed study performed for the $O(4)$ sigma model in [124, 125, 156] validates standard resurgence expectations and seems to favor the first possibility. Clearly, additional studies are necessary in order to clarify this fundamental

issue. A detailed resurgent analysis of the free energy of the GN model at finite N , along the lines of [124,125,156], would be very useful. It would be interesting to clarify if the failure of resurgence in the GN model is related to the different analyticity properties in $1/N$ of its kernels. More generally, it would be important to study observables other than $\mathcal{F}(h)$ which can be computed exactly in the $1/N$ expansion and can be analytically decoded in terms of trans-series.

Let us propose a distinction between three different levels of validity of the theory of resurgence, in order to understand what is at stake. The first, more general level of validity is the statement that observables in quantum theory are given by ambiguity-free Borel–Écalle resummations of trans-series. This statement is probably true and it is implicit in many of the early studies of renormalons, like e.g. [110,111]. All of our results, including the example of the GN model, vindicate this first level of validity. The second level of validity is the stronger statement that the trans-series is *fully* determined by its perturbative part, up to the numerical values of the trans-series parameters. It is this second level of validity that breaks down in some of the examples that we have studied, when restricting to a fixed order in the $1/N$ expansion. Finally, a third and largely independent issue is whether renormalon singularities and the associated trans-series have a semi-classical interpretation, in terms of expansions around saddle-points of a classical action. It has been argued that, after a twisted compactification, the renormalon sectors of the PCF model and the NLSM can be interpreted semiclassically [157,158]. Note however that the successful examples of resurgence that we have considered (like e.g. the PCF model at large N) are independent of such a semiclassical interpretation. It is perfectly conceivable (and, in our opinion, quite likely) that, for theories with renormalons at infinite volume, one does not have a semiclassical interpretation of the trans-series, but some version of resurgence will be still valid. In that scenario, a crucial open question will be to find a generalization of perturbation theory which makes it possible to calculate the trans-series from first principles, and without relying on resurgence properties or integrability. The use of the OPE, as in QCD sum rules, goes along this direction, but it is clear that a more general procedure has to be devised in order to compute general observables for which OPE techniques are in principle not applicable, as it is the case of the free energy studied in this paper.

The results that we have obtained apply to the TBA renormalization scheme defined in (4.28) and might not be valid in others. It would be useful to better understand if and to what extent resurgence methods depend on the renormalization scheme, given also the impact that the choice of scheme can have when resumming perturbative series even in absence of renormalons, as we have seen in details in chapter 3. It would be nice to investigate how resurgence methods apply, for example, in the $\overline{\text{MS}}$ scheme.³

Finally, it would be very interesting to extend these considerations to non-integrable theories. One possibility would be to compute $\mathcal{F}(h)$ in the quartic linear $O(N)$ model when $m^2 < 0$ at some order in $1/N$ and check if the result can be reconstructed from a perturbative expansion

³see e.g. [159] for a recent study addressing related questions.

around the naive vacuum, where IR renormalons have been shown to appear [83].

There has been recently much progress in investigating trans-series in integrable field theories starting from the TBA equations and Volin's method [13, 14]. The results have been very interesting and quite unexpected. New unconventional IR renormalons have been uncovered in [160]. Their location at finite N on the Borel plane goes against the common lore. Instead, they become indistinguishable from the conventional ones at large N and give rise to the those studied in this work for the PCF and the GN model. At the same time, the $O(3)$ NLSM seems to present another counter-example to the strong version of resurgence [160, 161] and, even more surprisingly, seems to come from an instanton contribution, while the renormalon ones seem to satisfy the resurgence relations [162, 163].

This thesis and the recent progresses, we have just mentioned, show and confirm how, if we are able to compute (possibly long) perturbative series, they can play a central role in understanding many aspects of QFT. This is valid whether the perturbative series are Borel summable or not. Note, at the same time, that in this effort to compute perturbative series, we are helped by the growing computational power at our disposal.

Appendix A

The Lambert W Function

Many results of chapter 3 of this work feature the Lambert function, so it is useful to review here some of its properties. We refer the reader to [164] for more details. The Lambert function is the function $W(x)$ that is obtained by inverting the relation

$$we^w = x. \tag{A.1}$$

For large values of w it behaves like the log function, but it deviates from it for small values. For $x > 0$, $W(x)$ is monotonic, while for $x < 0$ it is double-valued, see fig. A.1. Over the reals, $W(x)$ has non-trivial support for $x \in [-1/e, \infty)$. As analytic complex function, $W(z)$ has an infinite number of branches, parametrized by an integer k . Only two branches, denoted by W_0 and W_{-1} , have real sections over x , see fig. A.1. In all other branches $W_k(z)$, with $k \neq -1, 0$, take complex values. The function $W_0(z)$ is analytic at $z = 0$ and it admits there the series expansion

$$W_0(z) = \sum_{n=1}^{\infty} \frac{(-n)^{n-1}}{n!} z^n. \tag{A.2}$$

The series above has a convergence radius equal to $1/e$. At $z = -1/e$ W_0 has a branch-cut singularity, where it branches into W_1 and W_{-1} . Aside from W_0 , all W_k have a branch-cut at the origin and a logarithmic singularity at infinity. In particular, for any branch, we have

$$\lim_{z \rightarrow \infty} W_k(z) \approx \log z + 2i\pi k + \mathcal{O}(\log \log z), \tag{A.3}$$

and in particular for real x

$$\lim_{x \rightarrow \infty} W_0(x) \approx \log x - \log \log x + \mathcal{O}\left(\frac{\log \log x}{\log x}\right). \tag{A.4}$$

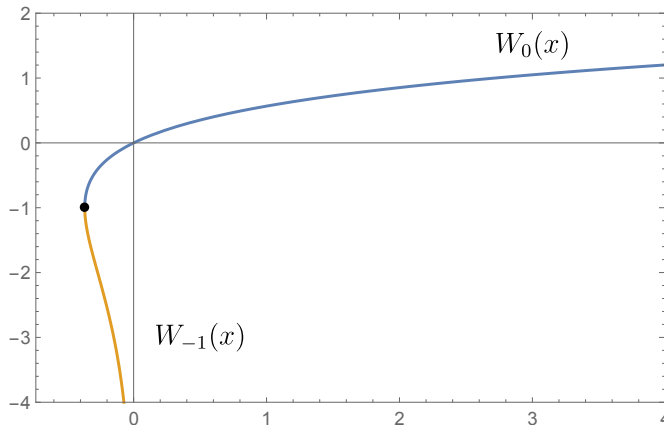


Figure A.1: The two branches of the Lambert function that take real values over x . The black dot corresponds to the branching point $x = -1/e$.

We will be mostly considering the branches $k = -1$ and $k = 0$. A useful formula is

$$\lim_{x \rightarrow 0^-} W_{-1}(x) = \log(-x) + \mathcal{O}(\log(-\log(-x))). \quad (\text{A.5})$$

Another useful formula for W is the following:

$$\frac{d^n W(x)}{dx^n} = \frac{e^{-nW(x)} p_n(W)}{(1 + W(x))^{2n-1}}, \quad n \geq 1, \quad (\text{A.6})$$

where p_n are polynomials of degree $n - 1$ in W , defined by the recursion relation

$$p_{n+1}(x) = -(nx + 3n - 1)p_n(x) + (1 + x)p'_n(x), \quad p_1(x) = 1. \quad (\text{A.7})$$

It is worth recalling a few QFT works where the Lambert W -function has appeared: in [165] it has been shown that the two-loop QCD beta-function can exactly be solved in terms of W and studied the analyticity properties of the solution. In [166] it has been shown that an infinite subset of diagrams in the 4d SUSY massless Wess-Zumino model can be resummed and leads to a beta-function and field anomalous dimension in terms of W . A solution for the 2-point function for a non-commutative version of the 2d ϕ^4 theory in terms of W was found in [167]. More recently [168] found that a subset of diagrams for the field anomalous dimensions in 4d massless Yukawa theory can be computed to all orders using a truncation of the Schwinger-Dyson equations. The ansatz for the trans-series associated with the known perturbative coefficients can be expressed in terms of W .

Appendix B

Large N for $O(N)$ Models in $d < 4$

Large N techniques are typically used in $O(N)$ models by taking $m^2 = 0$ and by going directly at the critical point, avoiding the problem of IR divergences. In this way one can extract physical quantities such as scaling dimensions of the CFT operators, see e.g. section 2 of [169] for a clear and concise review. In contrast, in this appendix we consider large N of the massive $O(N)$ models, in line with the analysis in the main text. In particular, we compute the vacuum energy $\Lambda = \Gamma^{(0)}$ and the mass gap $M^2 = \Gamma^{(2)}(p = 0)$ at the first non-trivial leading order in large N and to all orders in the coupling λ . Although the diagrams surviving in the large N limit are a small subset of the total and are not the hardest to determine, a comparison with large N has been useful as a sanity check of the accuracy of the numerical evaluation of Feynman diagrams. We report here once again the euclidean action of the theory

$$S = \int d^d x \left[\frac{1}{2} (\partial_\mu \phi_i)^2 + \frac{1}{2} m_B^2 \phi_i^2 + \lambda (\phi_i^2)^2 + \rho_B \right], \quad i = 1, \dots, N, \quad (\text{B.1})$$

and we consider the large N -limit

$$N \rightarrow \infty, \quad \lambda \rightarrow 0, \quad \text{with} \quad \check{\lambda} \equiv N\lambda = \text{fixed}. \quad (\text{B.2})$$

We define the renormalized parameters

$$m_B^2 = m^2 + \delta m^2, \quad \rho_B = \rho + \delta \rho, \quad (\text{B.3})$$

where

$$\delta m^2 = \delta m_{(0)}^2 + \frac{1}{N} \delta m_{(1)}^2 + o(N^{-2}), \quad \delta \rho = N \delta \rho_{(-1)} + \delta \rho_{(0)} + o(N^{-1}), \quad (\text{B.4})$$

and we choose a renormalization scheme where the vacuum energy counterterm $\delta \rho$ and the mass counterterm δm^2 exactly cancel the contributions in Λ and M^2 up to order $\lambda^{d/(4-d)}$ and $\lambda^{2/(4-d)}$,

respectively.¹ Introducing a Hubbard-Stratonovich auxiliary field $\sigma(x)$, we can rewrite S as

$$\hat{S} = \int d^d x \left[\frac{1}{2} (\partial_\mu \phi_i)^2 + \frac{1}{2} (m^2 + \check{\delta} m^2) \phi_i^2 - \frac{1}{2} \sigma^2 + \frac{1}{2} \check{\nu} \sigma \phi_i^2 + \sigma \delta_T + \rho + \check{\delta} \rho \right]. \quad (\text{B.5})$$

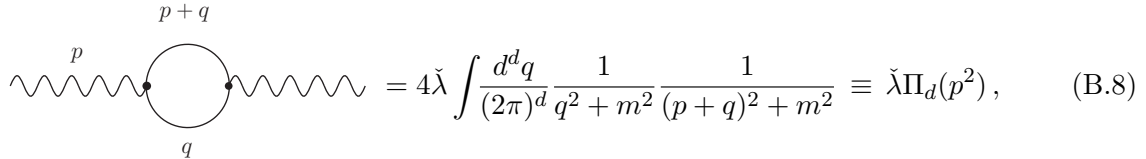
If we integrate out σ we recover the action (B.1) provided we identify²

$$\check{\nu} = 2\sqrt{2\check{\lambda}}, \quad \check{\delta} \rho = \delta \rho - \frac{\delta_T^2}{2}, \quad \check{\nu} \delta_T + \check{\delta} m^2 = \delta m^2. \quad (\text{B.6})$$

There is an arbitrariness in splitting the mass counterterm δm^2 in terms of δ_T and $\check{\delta} m^2$. We choose

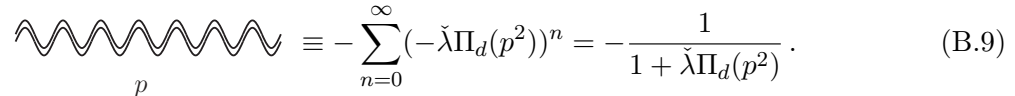
$$\check{\nu} \delta_T = \delta m_{(0)}^2, \quad \check{\delta} m^2 = \frac{1}{N} \delta m_{(1)}^2, \quad (\text{B.7})$$

so that the tadpole counterterm δ_T for σ completely cancels the radiatively induced tadpole at $o(N^0)$. Let us first consider the 2-point function $\langle \phi_i(-p) \phi_j(p) \rangle = \Gamma_{ij}^{(2)}(p^2) \equiv \delta_{ij} \Gamma^{(2)}(p^2)$. Since $\Gamma_{ij}^{(2)}$ is 1PI with respect to the ϕ_i , but not with respect to σ , Feynman diagrams reducible when cutting a σ -propagator should be considered. At $o(N^0)$ and $o(\check{\lambda})$ only one diagram contributes. In the chosen renormalization scheme its contribution is canceled by δ_T . The cancellation of tadpole-like graphs at $o(N^0)$ persists to all orders in $\check{\lambda}$, so no contribution whatsoever arises at $o(N^0)$ in $\Gamma^{(2)}(p^2)$. We now compute the $\langle \sigma \sigma \rangle$ propagator at $o(N^0)$. The relevant 1PI diagram is



$$\text{Diagram} = 4\check{\lambda} \int \frac{d^d q}{(2\pi)^d} \frac{1}{q^2 + m^2} \frac{1}{(p+q)^2 + m^2} \equiv \check{\lambda} \Pi_d(p^2), \quad (\text{B.8})$$

where we used wavy lines for the field σ along with the usual solid lines for the vector field ϕ_i . For $d < 4$ the loop integral converges. The resummation of the bubbles leads to the exact $o(N^0)$ propagator, which will be denoted by a double wavy line:



$$\text{Diagram} \equiv - \sum_{n=0}^{\infty} (-\check{\lambda} \Pi_d(p^2))^n = - \frac{1}{1 + \check{\lambda} \Pi_d(p^2)}. \quad (\text{B.9})$$

We are now ready to study $\Gamma^{(2)}$ at $o(N^{-1})$. At this order 3 diagrams and the $\delta m_{(1)}^2$ counterterm contribute, see fig. B.1. Note that we also have $o(N^{-1})$ corrections to the σ propagator, but these can enter in $\Gamma^{(2)}$ at this order only through tadpole graphs, and hence they vanish. The divergences in graph (a) arising from $n = 0$ ($d < 3$) or $n = 1$ ($3 \leq d < 4$) insertions of Π_d in the

¹This is the generalization for any $d < 4$ of what we denoted intermediate scheme in section 3.8.1 of the main text. We have omitted in this appendix the subscript I to avoid clutter.

²The Gaussian integral in σ is computed by analytic continuation from pure imaginary values, where the path integral converges.

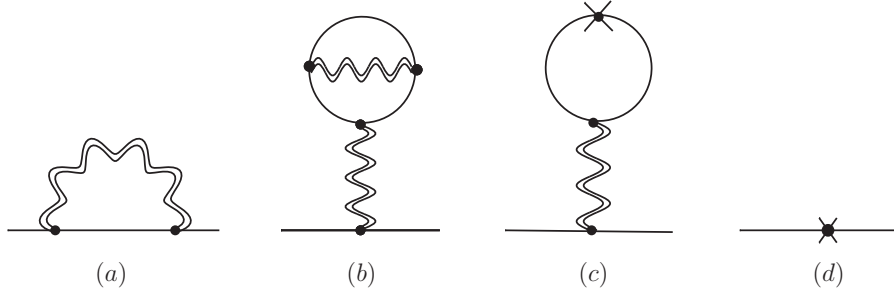


Figure B.1: Contributions of $o(N^{-1})$ to the two-point function $\langle \phi_i(-p)\phi_j(p) \rangle$. The counterterm depicted in (c) and (d) corresponds to δm^2 .

expansion of the resummed propagator are cancelled by the mass counterterm, so (a) + (d) is finite. Similar considerations apply for the graphs (b) + (c). We do not report the expressions for these graphs, that can be derived by standard manipulations. Let us now consider the vacuum energy. In the chosen renormalization scheme, the $o(N)$ contributions to the vacuum energy are exactly canceled.³ So the leading finite contribution arises at $o(N^0)$ and is given by a one-loop vacuum diagram of the exact $o(N^0)$ σ -propagator. Collecting the results above, we finally get

$$\Lambda = \frac{1}{2} \int \frac{d^d q}{(2\pi)^d} \log \left(1 + \check{\lambda} \Pi_d(q^2) \right) + \delta, \quad (\text{B.10})$$

$$M^2 = m^2 + \frac{8\check{\lambda}}{N} \int \frac{d^d q}{(2\pi)^d} \sum_{n=2}^{\infty} \check{\lambda}^n \frac{(-\Pi_d(q^2))^n}{q^2 + m^2} + (b) + (c) + o(N^{-2}), \quad (\text{B.11})$$

$$\Gamma^{(4)}(p=0) = -\frac{24\check{\lambda}}{N} \frac{1}{1 + \check{\lambda} \Pi_d(0)} + o(N^{-2}). \quad (\text{B.12})$$

We have also reported the leading order expression of the 4-point 1PI function $\Gamma^{(4)}$, which is $o(N^{-1})$, and is trivially given by tree level diagrams only. There is no need to keep track of the form of the counterterm δ appearing in (B.10), because in our scheme it is equal and opposite to the first divergent terms arising from the loop integral when expanded in powers of $\check{\lambda}$. The form of $\Pi_d(q^2)$ and more explicit expressions for M^2 will be given below for the specific $d=2$ and $d=3$ cases. In what follows it will be useful to use dimensionless quantities and rewrite

$$\check{\lambda} \Pi_d(q^2) \equiv \check{g} U_d(y), \quad \check{g} \equiv \frac{\check{\lambda}}{m^{4-d}}, \quad y \equiv \frac{q^2}{4m^2}. \quad (\text{B.13})$$

³It is easy to see that the $o(N)$ counterterm $\delta\rho_{(-1)}$ in (B.4) precisely cancels the term $\delta_T^2/2$ in (B.6), which is also of order $o(N)$, so that the counterterm $\check{\delta}\rho$ is $o(N^0)$.

$d = 2$

We specialize here to the $d = 2$ case. Working out the contributions from graphs (b) + (c) in fig. B.1, we obtain the following expression for M^2 :

$$\frac{M^2}{m^2} = 1 - \frac{8\check{g}}{\pi N} \int_0^\infty dy \sum_{n=1}^\infty (-\check{g} U_2(y))^n \left(\frac{1}{1+4y} - \frac{\check{g}}{1+\frac{\check{g}}{\pi}} V_2(y) \right) + o(N^{-2}), \quad (\text{B.14})$$

where

$$U_2(y) = \frac{1}{\pi} \frac{\log(\sqrt{y} + \sqrt{1+y})}{\sqrt{y(1+y)}}, \quad V_2(y) \equiv \frac{1}{4\pi} \frac{\sqrt{y(y+1)} + \operatorname{arctanh}\left(\sqrt{\frac{y}{1+y}}\right)}{\sqrt{y}(1+y)^{3/2}}. \quad (\text{B.15})$$

We report below the numerical values for the first coefficients in an expansion in \check{g} of Λ and M^2 :

$$\begin{aligned} \Lambda &= -0.016961\check{g}^2 + 0.0015425\check{g}^3 - 0.00023173\check{g}^4 + o(\check{g}^5) + o(N^{-1}), \\ \frac{M^2}{m^2} &= 1 + \frac{1}{N} \left(\check{g}(-0.47497\check{g}^2 + 0.23046\check{g}^3 - 0.090670\check{g}^4 + o(\check{g}^5)) \right) + o(N^{-2}), \\ \frac{\Gamma^{(4)}(0)}{m^2} &= -\frac{24\check{g}}{N} \frac{1}{1+\frac{\check{g}}{\pi}} + o(N^{-2}). \end{aligned} \quad (\text{B.16})$$

It is known that generally the large-order behavior of the large N coupling expansion, at given order in N , is convergent. The above results are in agreement with this expectation. From a numerical exploration we find that the series in \check{g} for Λ at $o(N^0)$ and $\Gamma^{(2)}$ at $o(N^{-1})$ are convergent, with a radius of convergence equal to π . This is in agreement with the radius of convergence of $\Gamma^{(4)}$ that is manifest from its analytic form at $o(N^{-1})$.

$d = 3$

Proceeding as above for the $d = 3$ case, we get the following expression for M^2 :

$$\frac{M^2}{m^2} = 1 - \frac{\check{g}^3 \log\left(\frac{4}{3}\right)}{N\pi^3\left(1+\frac{\check{g}}{2\pi}\right)} + \frac{2\check{g}}{N\pi^2} \int_0^\infty dy \sqrt{y} \sum_{n=2}^\infty (-\check{g} U_3(y))^n \left(\frac{8}{4y+1} - \frac{\check{g}}{\pi\left(1+\frac{\check{g}}{2\pi}\right)} \frac{1}{y+1} \right) + o(N^{-2}),$$

where the function $U_3(y)$ is given by

$$U_3(y) = \frac{1}{4\pi} \frac{\operatorname{arccot}\left(\frac{1}{2y}\right)}{y}. \quad (\text{B.17})$$

The numerical values for the first coefficients in an expansion in \check{g} read

$$\Lambda = -0.000073108\check{g}^4 + 3.4816 \times 10^{-6}\check{g}^5 + o(\check{g}^6) + o(N^{-1}),$$

$$\begin{aligned}\frac{M^2}{m^2} &= 1 + \frac{1}{N} \left(0.023840\check{g}^3 - 0.0053959\check{g}^4 + o(\check{g}^5) \right) + o(N^{-2}), \\ \frac{\Gamma^{(4)}(0)}{m} &= -\frac{24\check{g}}{N} \frac{1}{1 + \frac{\check{g}}{2\pi}} + o(N^{-2}).\end{aligned}\tag{B.18}$$

Like in the $d = 2$ case, the series in \check{g} for Λ at $o(N^0)$ and $\Gamma^{(2)}$ at $o(N^{-1})$ are convergent, with a radius of convergence equal to 2π . This is in agreement with the radius of convergence of $\Gamma^{(4)}$ that is manifest from its analytic form at $o(N^{-1})$.

Appendix C

Vacuum Energy Renormalization in $d = 3$ $O(N)$ Models

In the following we derive the counterterm, in the 3d $O(N)$ models, for the vacuum energy in the $\overline{\text{MS}}$ scheme needed to establish the duality of the theory.

First, we recall the determination of the mass counterterm δm^2 . Within dimensional regularization only the *sunset* diagram has a pole in $\epsilon = d - 3$ and contributes to the mass counterterm δm^2 . Below we give the explicit expressions for the three diagrams in fig. C.1:

$$\begin{aligned}\Sigma_1 &= -\lambda m \frac{N+2}{\pi}, \\ \Sigma_{2a}(k) &= -\lambda^2 \frac{N+2}{\pi^2} \left[\frac{1}{\epsilon} + 3 + \log \frac{\mu^2}{9m^2} - \log \left(1 + \frac{k^2}{9m^2} \right) - \frac{6m}{|k|} \arctan \left(\frac{|k|}{3m} \right) \right], \\ \Sigma_{2b} &= \lambda^2 \frac{(N+2)^2}{2\pi^2}.\end{aligned}$$

Hence we find

$$\delta m^2 = \frac{\lambda^2}{\epsilon} \frac{N+2}{\pi^2}. \quad (\text{C.1})$$

Secondly, we turn to the determination of the vacuum energy counterterm $\delta\rho$. Since the divergences in the vacuum energy can be found up to four loops we have explicitly computed the diagrams in fig. C.2 within dimensional regularization and we report their values below. The contributions at order zero and one are finite within dimensional regularization and give

$$\Upsilon_0 = -m^3 \frac{N}{12\pi}, \quad \Upsilon_1 = \lambda m^2 \frac{N(N+2)}{16\pi^2}.$$

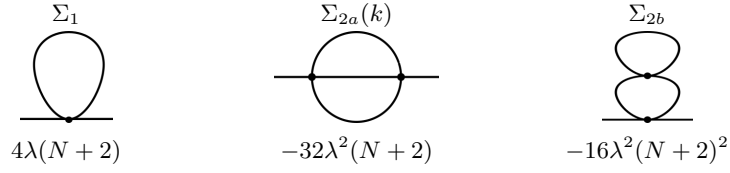
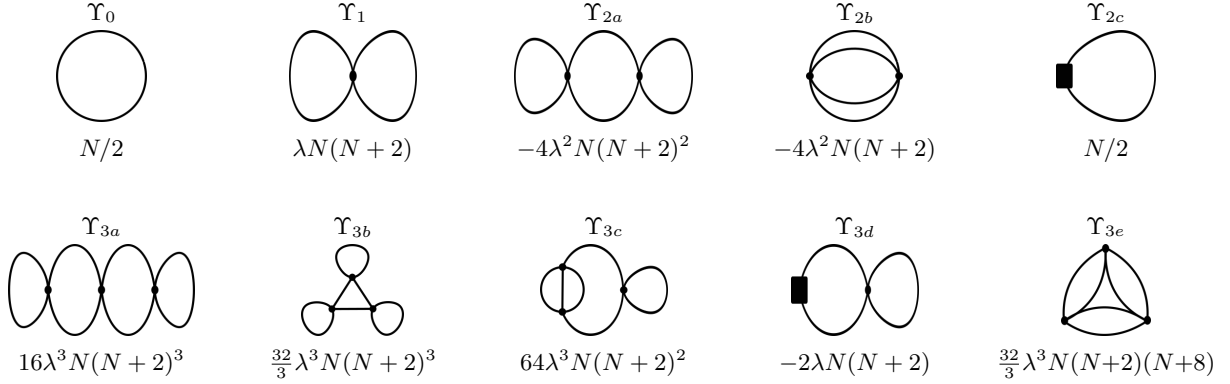


Figure C.1: The two-point diagrams up to 2 loops together with the multiplicity factors.


 Figure C.2: The zero-point diagrams up to 4 loops together with the multiplicity factors. The filled black squares represent factors of δm^2 .

At order two we find two diagrams giving $1/\epsilon$ poles that cancel out:

$$\begin{aligned}\Upsilon_{2a} &= -\lambda^2 m \frac{N(N+2)^2}{32\pi^3}, \\ \Upsilon_{2b} &= \lambda^2 m \frac{N(N+2)}{8\pi^3} \left[\frac{1}{\epsilon} - \frac{3}{2} \log \frac{m^2}{\mu^2} + 4 - 5 \log 2 \right], \\ \Upsilon_{2c} &= -\lambda^2 m \frac{N(N+2)}{8\pi^3} \left[\frac{1}{\epsilon} - \frac{1}{2} \log \frac{m^2}{\mu^2} + 1 - \log 2 \right].\end{aligned}$$

At order three the poles given by the diagrams Υ_{3c} and Υ_{3d} cancel out, leaving one divergent contribution from Υ_{3e} only:

$$\begin{aligned}\Upsilon_{3a} &= \lambda^3 \frac{N(N+2)^3}{64\pi^4}, \\ \Upsilon_{3b} &= -\lambda^3 \frac{N(N+2)^3}{192\pi^4}, \\ \Upsilon_{3c} &= -\lambda^3 \frac{N(N+2)^2}{16\pi^4} \left(\frac{1}{\epsilon} - 2 \log \frac{m^2}{\mu^2} + 2 - 6 \log 2 \right), \\ \Upsilon_{3d} &= \lambda^3 \frac{N(N+2)^2}{16\pi^4} \left[\frac{1}{\epsilon} - \log \frac{m^2}{\mu^2} + 1 - 2 \log 2 \right],\end{aligned}$$

$$\Upsilon_{3e} = \lambda^3 \frac{N(N+2)(N+8)}{384\pi^2} \left(\frac{1}{\epsilon} - 2 \log \frac{m^2}{\mu^2} + 1 - 2 \log 2 - \frac{42\zeta(3)}{\pi^2} \right).$$

Therefore the counterterm $\delta\rho$ is determined as

$$\delta\rho = -\frac{\lambda^3 N(N+2)(N+8)}{\epsilon 384\pi^2}, \quad (\text{C.2})$$

which implies

$$\beta_\rho = -4\lambda^3 \frac{N(N+2)(N+8)}{384\pi^2}, \quad \rho(\mu) = \rho(m) + \lambda^3 \frac{N(N+2)(N+8)}{384\pi^2} 2 \log \frac{m^2}{\mu^2}. \quad (\text{C.3})$$

The self-duality is then obtained by mapping the parameters between the theory at the scale m and the theory at the scale m' . In other words we find the scale $\mu = m'$ such that $m^2(m') = m'^2$. From (C.3) we find the constant contribution to the vacuum energy $\rho(m')$ that one has to take into account in order to completely match the two theories.

Appendix D

Series Coefficients in $d = 3$ $O(N)$ Models

In this appendix, we report the coefficients for some series expansions in the three-dimensional $O(N)$ models.

D.1 Series Coefficients in the RS \mathcal{S}

In this section, we report the coefficients for the series expansion of the vacuum energy Λ and of the mass gap M^2 in the $\overline{\text{MS}}$ scheme (i.e. at $\mu = m$ or equivalently $\kappa = 0$) obtained as explained in section 3.8.1. The numerical coefficients appearing without error have been computed to a higher accuracy and have been truncated here to nine relevant digits.

$$\begin{aligned}
\frac{\Lambda - \rho}{m^3} = & -\frac{N}{12\pi} + g \frac{N(N+2)}{16\pi^2} - g^2 \frac{N(N+2)}{8\pi^3} \left(\frac{N+2}{4} - 3 + 4 \log 2 \right) \\
& - g^3 \frac{N(N+2)}{384\pi^4} \left[(N+8) (42\zeta(3) - \pi^2 + 2\pi^2 \log 2) - 24(N+2)(4 \log 2 - 1) - 4(N+2)^2 \right] \\
& - g^4 \left[0.0103030380(14)N + 0.0073758023(10)N^2 + 0.00138423945(16)N^3 \right. \\
& \quad \left. + 0.000148813598N^4 + \frac{N^5}{512\pi^5} \right] \\
& + g^5 \left[0.00174385(8)N - 7.97(9) \times 10^{-6}N^2 - 0.000543315(31)N^3 \right. \\
& \quad \left. - 0.0000463208(26)N^4 + 2.68116618 \times 10^{-6}N^5 \right] \\
& - g^6 \left[0.00348107(8)N + 0.00204121(9)N^2 + 0.00002997(4)N^3 - 0.000060341(10)N^4 \right. \\
& \quad \left. - 6.346(8) \times 10^{-7}N^5 - 3.31589818 \times 10^{-7}N^6 - \frac{N^7}{12288\pi^7} \right] \\
& + g^7 \left[0.00463840(9)N + 0.00311902(11)N^2 + 0.00029512(6)N^3 - 0.000043397(17)N^4 \right. \\
& \quad \left. + 5.8275(22) \times 10^{-6}N^5 + 5.9986(13) \times 10^{-7}N^6 - 3.20181996 \times 10^{-8}N^7 \right] \\
& - g^8 \left[0.007050(7)N + 0.004976(9)N^2 + 0.000506(4)N^3 - 0.0001247(10)N^4 - 4.67(11) \times 10^{-6}N^5 \right. \\
& \quad \left. + 1.314(7) \times 10^{-6}N^6 - 2.519(11) \times 10^{-8}N^7 + 1.84663100(33) \times 10^{-9}N^8 + \frac{N^9}{131072\pi^9} \right].
\end{aligned} \tag{D.1}$$

$$\begin{aligned}
\frac{M^2}{m^2} = & 1 - g \frac{N+2}{\pi} + g^2 \frac{(N+2)(N+4 \log 3)}{2\pi^2} + g^3 \left[0.254293918 + 0.0394597748N \right. \\
& \quad \left. - 0.0519064757N^2 - \frac{N^3}{8\pi^3} \right] \\
& - g^4 \left[0.30782412(5) + 0.170601023(33)N + 0.001281784(5)N^2 - 0.00353134874N^3 \right] \\
& + g^5 \left[0.38362587(23) + 0.24910600(22)N + 0.02194130(8)N^2 \right. \\
& \quad \left. - 0.002994545(9)N^3 + 0.000230093158N^4 + \frac{N^5}{128\pi^5} \right] \\
& - g^6 \left[0.5571505(8) + 0.3825440(10)N + 0.0381541(5)N^2 - 0.00760405(12)N^3 \right. \\
& \quad \left. - 0.000234300(11)N^4 + 0.0000550745909N^5 \right] \\
& + g^7 \left[0.976392(5) + 0.732438(7)N + 0.1065630(35)N^2 - 0.00120274(10)N^4 \right. \\
& \quad \left. - 0.0105821(8)N^3 + 0.000096815(7)N^5 - 1.9329992326(35) \times 10^{-6}N^6 - \frac{N^7}{1024\pi^7} \right] \\
& - g^8 \left[1.923506(21) + 1.546272(32)N + 0.281617(19)N^2 - 0.012955(6)N^3 - 0.0033825(9)N^4 \right. \\
& \quad \left. + 0.00023996(7)N^5 + 9.1854(28) \times 10^{-6}N^6 - 1.0854670647(15) \times 10^{-6}N^7 \right].
\end{aligned} \tag{D.2}$$

Recall that we have normalized the vacuum energy by taking $\rho = \rho(m) = 0$.

D.2 Series Coefficients in the RS $\tilde{\mathcal{S}}$

In this section, we report the coefficients for the series expansion of the β -function, of the critical exponents η and ν in the physical scheme of [10] for generic N . They are obtained as explained in section 3.9.2. We use the normalization used by Nickel in [98] $\tilde{g} = \tilde{g}(N + 8)/(48\pi)$. The numerical coefficients appearing without error have been computed to a higher accuracy and have been truncated at 10^{-15} .

$$\begin{aligned}
\tilde{\beta}(\tilde{g}) = & -\tilde{g} + \tilde{g}^2 - \frac{\tilde{g}^3}{(N+8)^2} \frac{4(41N+190)}{27} + \frac{\tilde{g}^4}{(N+8)^3} \left[1.348942760866478 N^2 \right. \\
& \left. + 54.940377049302200 N + 199.640417221105907 \right] \\
& - \frac{\tilde{g}^5}{(N+8)^4} \left[-0.155645907585201 N^3 + 35.82020347182(7)N^2 + 602.5212285602(6)N \right. \\
& \left. + 1832.2067281779(14) \right] \\
& + \frac{\tilde{g}^6}{(N+8)^5} \left[0.051236212811530 N^4 + 3.237874(11)N^3 + 668.55456(24)N^2 \right. \\
& \left. + 7819.5673(20)N + 20770.183(5) \right] \\
& - \frac{\tilde{g}^7}{(N+8)^6} \left[-0.023424226049759 N^5 - 1.07182(8)N^4 + 265.8411(20)N^3 \right. \\
& \left. + 12669.295(24)N^2 + 114181.79(13)N + 271300.61(28) \right] \\
& + \frac{\tilde{g}^8}{(N+8)^7} \left[0.012640642324067 N^6 + 0.5433(5)N^5 - 14.386(16)N^4 + 8828.74(25)N^3 \right. \\
& \left. + (246972.5 \pm 2.0)N^2 + (1840997 \pm 8)N + (3981620 \pm 14) \right].
\end{aligned} \tag{D.3}$$

$$\begin{aligned}
\tilde{\eta}(\tilde{g}) = & \frac{\tilde{g}^2}{(N+8)^2} \frac{8(N+2)}{27} + \frac{\tilde{g}^3}{(N+8)^3} \left[0.0246840009259343 (N^2 + 10N + 16) \right] \\
& + \frac{\tilde{g}^4}{(N+8)^4} \left[-0.004298563333341 N^3 + 0.667985910868(20)N^2 + 4.60922100685(3)N \right. \\
& \quad \left. + 6.51210986356(18) \right] \\
& - \frac{\tilde{g}^5}{(N+8)^5} \left[0.006550923035200 N^4 - 0.13245107140(8)N^3 + 1.891116(10)N^2 \right. \\
& \quad \left. + 15.18794(6)N + 21.64700(9) \right] \\
& + \frac{\tilde{g}^6}{(N+8)^6} \left[-0.005548920737435 N^5 - 0.02039935040(31)N^4 + 3.05407(7)N^3 \right. \\
& \quad \left. + 64.0777(8)N^2 + 300.7218(34)N + 369.714(4) \right] \\
& - \frac{\tilde{g}^7}{(N+8)^7} \left[0.004390810855773 N^6 + 0.0612032025(13)N^5 - 1.2705(4)N^4 + 35.311(7)N^3 \right. \\
& \quad \left. + 751.79(5)N^2 + 3345.53(18)N + 3988.40(21) \right] \\
& + \frac{\tilde{g}^8}{(N+8)^8} \left[-0.003473417276666 N^7 - 0.070431737(5)N^6 + 0.151(3)N^5 + 11.6(1)N^4 \right. \\
& \quad \left. + (1111 \pm 1.5)N^3 + (13674 \pm 9)N^2 + (52140 \pm 27)N + (58297 \pm 30) \right].
\end{aligned} \tag{D.4}$$

$$\begin{aligned}
\tilde{\nu}(\tilde{g}) = & \frac{1}{2} + \frac{\tilde{g}}{(N+8)} \frac{(N+2)}{4} + \frac{\tilde{g}^2}{(N+8)^2} \frac{(27N^2 + 16N - 76)}{216} + \frac{\tilde{g}^3}{(N+8)^3} \left[\frac{N^3}{16} + 0.357987483753229 N^2 \right. \\
& \quad \left. + 2.20259658610878 N + 3.473243237204659 \right] \\
& - \frac{\tilde{g}^4}{(N+8)^4} \left[-\frac{N^4}{32} - 0.399474877149036 N^3 + 0.609039560891(5)N^2 + 14.977065564467(32)N \right. \\
& \quad \left. + 24.82217386818(4) \right] \\
& + \frac{\tilde{g}^5}{(N+8)^5} \left[\frac{N^5}{64} + 0.333425900294786 N^4 + 0.7393030(9)N^3 + 27.122009(18)N^2 \right. \\
& \quad \left. + 184.70641(11)N + 262.00439(15) \right] \\
& - \frac{\tilde{g}^6}{(N+8)^6} \left[-\frac{N^6}{128} - 0.245952216148592 N^5 - 1.875537(5)N^4 + 0.87861(19)N^3 \right. \\
& \quad \left. + 417.7907(19)N^2 + 2385.941(7)N + 3130.387(8) \right] \\
& + \frac{\tilde{g}^7}{(N+8)^7} \left[\frac{N^7}{256} + 0.170195139781328 N^6 + 2.298000(25)N^5 + 0.1341(20)N^4 + 328.511(29)N^3 \right. \\
& \quad \left. + 7521.91(19)N^2 + 35180.6(6)N + 42962.6(6) \right] \\
& - \frac{\tilde{g}^8}{(N+8)^8} \left[-\frac{N^8}{512} - 0.11381144429731 N^7 - 2.23349(12)N^6 - 9.232(14)N^5 - 116.02(24)N^4 \right. \\
& \quad \left. + (9073.7 \pm 2.2)N^3 + (139051 \pm 11)N^2 + (567393 \pm 30)N + (652860 \pm 29) \right].
\end{aligned} \tag{D.5}$$

Appendix E

$d = 0$ reduction of quartic vector models

In this appendix we present the details necessary to reproduce the $1/N$ large order behavior (4.4) of the coefficients in the $0d$ reduction of quartic vector models and provide some further technical comments. To make contact with QFT models, it is useful to introduce an Hubbard-Stratonovich like parameter σ to rewrite the quartic term $(\mathbf{x} \cdot \mathbf{x})^2$ as

$$e^{-\frac{g}{N}(\mathbf{x} \cdot \mathbf{x})^2} = \frac{1}{\sqrt{2\pi}} \int_{-\infty}^{\infty} d\sigma e^{-\frac{\sigma^2}{2} + i\sqrt{\frac{2g}{N}}\sigma \mathbf{x} \cdot \mathbf{x}}. \quad (\text{E.1})$$

Inserting in (4.1) and integrating over \mathbf{x} gives

$$I(m, g) = \sqrt{\frac{N}{2\pi}} 2^{-\frac{N}{2}} \int_{-\infty}^{\infty} d\sigma e^{-NK(\sigma)}, \quad (\text{E.2})$$

where

$$K(z) = \frac{z^2}{2} + \frac{1}{2} \log \left(\frac{m}{2} - i\sqrt{2gz} \right), \quad (\text{E.3})$$

and we rescaled $\sigma \rightarrow \sqrt{N}\sigma$. The function K is complex and the original contour of integration is not a downward flow, so that we have to decompose it in terms of Lefschetz thimbles. We get two critical points

$$z_c^{(\pm)} = \frac{i}{4\sqrt{2g}} \left(-m \pm \sqrt{m^2 + 16g} \right). \quad (\text{E.4})$$

The function K has a branch-cut singularity at $z_{bc} = -im/\sqrt{8g}$. The point $z_c^{(-)}$ sits on top of the branch-cut and $K(z)$ has two saddles for each of the infinite Riemann sheets associated to the log function. The deformed contour passing through $z_c^{(+)} \equiv z_c$ is a regular Lefschetz thimble. As shown in [17], this is a sufficient condition for Borel summability to the exact result of the

asymptotic saddle point series expansion around z_c . The large-order behavior of the coefficients c_p around a saddle z_c is given by the lowest-order coefficients of the series associated to the so-called adjacent saddles \hat{z}_c [19]. In our case, we have one adjacent saddle $\hat{z}_c = z_c^{(-)}$ which contributes twice according to the two different analytic continuations of the log function in $K(z)$:

$$K^\eta(\hat{z}_c) = \text{Re } K(\hat{z}_c) + \frac{i\pi\eta}{2}, \quad \eta = \pm. \quad (\text{E.5})$$

The large order behavior is given by eq.(20) of [19] as follows:

$$c_p = \frac{\hat{I}_c}{2\pi i} \sum_{\eta=\pm} \eta \frac{\Gamma(p)}{(K^\eta(\hat{z}_c) - K(z_c))^p} \left(1 + \mathcal{O}\left(\frac{1}{p}\right)\right), \quad (\text{E.6})$$

where

$$\hat{I}_c = \sqrt{\frac{K''(z_c)}{K''(\hat{z}_c)}} = \frac{\sqrt{m^2 + 16g} - m}{4\sqrt{g}}, \quad (\text{E.7})$$

$$K^\eta(z_c^{(-)}) - K(z_c^{(+)}) = \rho e^{i\eta\theta}, \quad \rho = \sqrt{Z^2 + \frac{\pi^2}{4}}, \quad \theta = \arccos\left(\frac{Z}{\rho}\right), \quad (\text{E.8})$$

and

$$Z = -\frac{m\sqrt{m^2 + 16g}}{16g} - \frac{1}{2} \log \frac{\sqrt{m^2 + 16g} + m}{\sqrt{m^2 + 16g} - m}. \quad (\text{E.9})$$

For $p \gg 1$ we then get (4.4), which agrees with the earlier result (2.16) of [170] for $m = 1$. Note that the large order behavior for $m = 1$ and $m = -1$ are related, since $\theta \rightarrow \pi - \theta$ and $\hat{I}_c \rightarrow 1/\hat{I}_c$ when $m \rightarrow -m$. We see that the large order coefficients oscillate with a period given by θ .

When $\theta = \pi/2$, $c_p = 0$ for even p and one has to look at the sub-leading $\mathcal{O}(1/N)$ corrections. This situation is realized when $m = 0$. In this case, the integral (4.1) simply equals to

$$I(0, g) = \left(\frac{N}{16g}\right)^{\frac{N}{4}} \frac{\sqrt{\pi}}{\Gamma(\frac{N+2}{4})}, \quad (\text{E.10})$$

and (4.4) simplifies to

$$c_p(m = 0) = \frac{\Gamma(p)}{\pi} \left(\frac{2}{\pi}\right)^p \sin \frac{\pi p}{2} \left(1 + \mathcal{O}\left(\frac{1}{p}\right)\right). \quad (\text{E.11})$$

The sub-leading contributions are captured by the full resurgent (asymptotic) formula [19]

$$c_p \approx \frac{\hat{I}_c}{2\pi i} \sum_{\eta=\pm} \eta \sum_{q=0}^{\infty} \frac{\Gamma(p-q)\hat{c}_q^\eta}{(K^\eta(\hat{z}_c) - K(z_c))^{p-q}}, \quad (\text{E.12})$$

where \hat{c}_q^η are the first terms of the expansion around the adjacent saddle \hat{z}_c , normalized so that $\hat{c}_0^\eta = 1$. Interestingly, $c_q^\eta = c_q$, because these saddles are all equivalent for $m = 0$. We easily get

$$c_p = \frac{\Gamma(p)}{\pi} \left(\frac{2}{\pi}\right)^p \left(\sin \frac{\pi p}{2} \left(1 - \left(\frac{\pi}{2}\right)^2 \frac{1}{72(p-1)(p-2)}\right) - \cos \frac{\pi p}{2} \left(\frac{\pi}{2} \frac{1}{6(p-1)}\right) + \mathcal{O}\left(\frac{1}{p^3}\right) \right). \quad (\text{E.13})$$

This series alternates every two terms and has odd terms parametrically larger than the even ones by a factor of p , for large p .

Appendix F

Existence, uniqueness and analyticity in $1/N$ of the TBA equations

Both TBA equations (4.17) and (4.21) are instances of a class of equations of the form

$$f(\theta) - \int_{-B}^B K(\theta - \theta') f(\theta') d\theta' = L(\theta), \quad (\text{F.1})$$

where $L(\theta)$ is a given continuous function, $K(\theta)$ is an integral kernel, and $f(\theta)$ is the function to be determined. Equations of this kind are known as non-homogeneous Fredholm linear integral equations. In this appendix we would like to show the existence and uniqueness of the solutions of (4.17) and (4.21) in the three models considered in chapter 4 of this work, as well as some analyticity properties in $1/N$ of the kernel $K(\theta)$.

Let us start by briefly reviewing basic mathematical facts. The above equation (F.1) can be compactly written as a fixed point equation $Tf = f$, where

$$Tf(\theta) = L(\theta) + \int_{-B}^B K(\theta - \theta') f(\theta') d\theta'. \quad (\text{F.2})$$

Importantly, the operator T is a contraction if

$$\sup_{-B \leq \theta \leq B} \left| \int_{-B}^B K(\theta - \theta') d\theta' \right| \equiv k < 1. \quad (\text{F.3})$$

Indeed, for arbitrary functions f_1 and f_2 we have

$$|Tf_1 - Tf_2| = |Kf_1 - Kf_2| \leq k|f_1 - f_2| < |f_1 - f_2|. \quad (\text{F.4})$$

If T is a contraction, by the contraction theorem (also known as Banach fixed point) the solution

$Tf = f$ exists and is unique, and it can be written schematically as

$$f = \sum_{p=0}^{\infty} K^p L. \quad (\text{F.5})$$

The key quantity to study is the kernel K , which will be discussed separately for each model in the next subsections. Our goal will be two-fold: we will first show that K is a contraction, hence proving the existence and uniqueness of the solution, in each case. Secondly, we will study the analyticity in $1/N$ of the solution. Thanks to (F.5), the analyticity of the solution in a certain region can be established by proving that all the iterated kernels K^p are analytic in that region (in particular it is not enough to establish this property for K alone). We will see that there is analyticity in a disk close to the origin of the $1/N$ plane, but not including it, for the NLSM and PCF, while in the case of GN the solution is analytic in the origin within a certain radius. The analysis will be quite detailed for the NLSM and more sketchy for the PCF and GN models.

F.1 Non-Linear sigma model

For the non-linear sigma model the kernel reads

$$K(\theta) = \frac{1}{4\pi^2} \left(\psi\left(1 + \frac{i\theta}{2\pi}\right) - \psi\left(\frac{1}{2} + \frac{i\theta}{2\pi}\right) + \psi\left(\frac{1}{2} + \Delta + \frac{i\theta}{2\pi}\right) - \psi\left(\Delta + \frac{i\theta}{2\pi}\right) \right) + c.c., \quad (\text{F.6})$$

where ψ is the digamma function and $\Delta = 1/(N-2)$. The Fourier transform $\tilde{K}(\omega)$ of $K(\theta)$ admits a simple analytic expression [115], which is straightforwardly obtained by expanding the digamma functions. For $\Delta > 0$ it reads

$$\tilde{K}(\omega) \equiv \int_{-\infty}^{\infty} e^{i\omega\theta} K(\theta) d\theta = \frac{1 + e^{\pi|\omega|(1-2\Delta)}}{1 + e^{\pi|\omega|}}. \quad (\text{F.7})$$

The kernel (F.6) is point-wise positive definite, i.e. $K(\theta) \geq 0$ for any $\theta \in \mathbb{R}$.¹ This allows us to immediately prove that the kernel is a contraction and there exists a unique solution to (F.1) for any finite positive N . Indeed,

$$\sup_{-B \leq \theta \leq B} \int_{-B}^B |K(\theta - \theta')| d\theta' < \int_{-\infty}^{\infty} K(\theta - \theta') d\theta' = \tilde{K}(0) = 1. \quad (\text{F.9})$$

¹It is also positive definite in the sense that

$$\int_{-\infty}^{\infty} d\theta d\theta' K(\theta - \theta') f(\theta) f(\theta') \geq 0 \quad (\text{F.8})$$

for any square integrable function $f(\theta)$.

Following the appendix B of [171], we can also prove some analyticity properties in θ of $f(\theta)$, by showing that the kernel K and all its derivatives are bounded, and so are the iterated kernels K^n . We omit this analysis and instead focus on analyticity in Δ for small values of Δ , which is the limit relevant for large N . Let then $\Delta = z/2$ be complex and focus on a small disc D around the point $0 \leq \lambda \ll 1$, defined as $z = \lambda + \alpha + i\beta$ and $\alpha^2 + \beta^2 \leq \delta^2$, where $0 \leq \delta \leq \lambda/\sqrt{2}$. The kernel (F.6) can be conveniently written as

$$\pi^2 K(\theta, z) = \frac{z}{z^2 + (\theta/\pi)^2} + F(\theta, z), \quad (\text{F.10})$$

where

$$F(\theta, z) \equiv \sum_{n=1}^{\infty} (-1)^n \left(\frac{z+n}{(z+n)^2 + (\theta/\pi)^2} - \frac{n}{n^2 + (\theta/\pi)^2} \right). \quad (\text{F.11})$$

Note that the first term in (F.10) coincides with the integral kernel appearing in the Bethe ansatz solution of the Lieb–Liniger model [171], while the second term is an analytic function of z for small z . For sufficiently small z , we have

$$|F(\theta, z)| = |zF'(\theta) + \mathcal{O}(z^2)| \leq (\lambda + \delta)|F'(\theta)|, \quad (\text{F.12})$$

where

$$F'(\theta) = -\frac{\pi^2}{2\theta^2} + \frac{\pi^2}{8} \left(\text{sech}^2(\theta/2) + \text{csch}^2(\theta/2) \right). \quad (\text{F.13})$$

We also have [171]

$$\left| \frac{z}{z^2 + (\theta/\pi)^2} \right| \leq \frac{\lambda + \delta}{(\lambda - \delta)^2 + (\theta/\pi)^2} \leq \frac{\lambda + \delta}{(\lambda - \delta)^2}. \quad (\text{F.14})$$

For sufficiently small λ , we then get

$$|K(\theta, z)| \leq \frac{1}{\pi^2} \left(\frac{\lambda + \delta}{(\lambda - \delta)^2} + (\lambda + \delta)|F'(\theta)| \right). \quad (\text{F.15})$$

Let us now define the iterated kernel (z dependence omitted for simplicity)

$$K^{(p+1)}(\theta - \theta') \equiv \int_{-B}^B K^{(p)}(\theta - \theta'') K(\theta'' - \theta') d\theta'', \quad K^{(1)}(\theta) \equiv K(\theta), \quad p \geq 1, \quad (\text{F.16})$$

and suppose that for a certain $p \geq 1$ and for any $-B \leq \theta \leq B$

$$|K^{(p)}(\theta)| \leq \frac{C^{p-1}}{\pi^2} \frac{\lambda + \delta}{(\lambda - \delta)^2}. \quad (\text{F.17})$$

Then

$$\begin{aligned} |K^{(p+1)}(\theta - \theta')| &= \left| \int_{-B}^B K^{(p)}(\theta - \theta'') K(\theta'' - \theta') d\theta'' \right| \leq \frac{C^{p-1}}{\pi^2} \frac{\lambda + \delta}{(\lambda - \delta)^2} \left| \int_{-B}^B K(\theta'' - \theta') d\theta'' \right| \\ &\leq \frac{C^{p-1}}{\pi^2} \frac{\lambda + \delta}{(\lambda - \delta)^2} \left(\frac{1}{\pi^2} \int_{-B}^B \frac{\lambda + \delta}{(\lambda - \delta)^2 + \delta \theta^2} d\theta'' + \frac{\lambda + \delta}{\pi^2} \int_{-B}^B |F'(\delta \theta)| d\theta'' \right), \end{aligned} \quad (\text{F.18})$$

where $\delta \theta \equiv (\theta'' - \theta')/\pi$. Let us first set $F = 0$, in which case we recover the same kernel as in [171]. Performing the integral, we have, for $\delta \ll \lambda$,

$$|K^{(p+1)}(\theta - \theta')| \leq \frac{C^{p-1}}{\pi^2} \frac{\lambda + \delta}{(\lambda - \delta)^2} \left[1 - \frac{1}{\pi} \left(\arctan \left(\frac{\pi \lambda}{B - \theta} \right) + \arctan \left(\frac{\pi \lambda}{B + \theta} \right) \right) \right]. \quad (\text{F.19})$$

For any positive B , $\theta \leq B$ and (small) λ strictly greater than 0, the square bracket is bounded by $(1 - \epsilon)$, with $0 < \epsilon < 1$. Then, if we choose

$$C = 1 - \epsilon, \quad (\text{F.20})$$

the relation (F.17), if valid for p , is also valid for $p + 1$. Since it applies for $p = 1$, it follows that it is valid for any $p \geq 1$. It then follows that the resolvent kernel

$$\kappa(\theta, z) \equiv \sum_{p=0}^{\infty} K^{(p+1)}(\theta, z), \quad (\text{F.21})$$

and the solution of (F.1)

$$f(\theta) = L(\theta) + \int_{-B}^B \kappa(\theta - \theta') L(\theta') d\theta' \quad (\text{F.22})$$

exists and is analytic for $\Delta > 0$. The point $\Delta = 0$ is excluded, because for $\lambda = 0$ we have $C = 1$ and the resolvent series does not converge. This reproduces the analysis in appendix B of [171].

Let us now come back to the situation of interest with $F' \neq 0$. The second integral in (F.18) is easily bounded by a finite constant M . For instance, we have

$$|F'(\theta)| < \frac{\pi^2}{12} \frac{1}{1 + \theta^2/8} \quad (\text{F.23})$$

and

$$\frac{1}{\pi^2} \int_{-B}^B |F'(\theta'' - \theta')| d\theta'' < \frac{1}{\pi^2} \int_{-\infty}^{\infty} \frac{\pi^2}{12} \frac{d\theta}{1 + \theta^2/8} = \frac{\pi}{3\sqrt{2}}. \quad (\text{F.24})$$

We then get

$$|K^{(p+1)}(\theta - \theta')| \leq \frac{C^{p-1}}{\pi^2} (1 - \epsilon + \lambda M). \quad (\text{F.25})$$

For any finite M there exists a sufficiently small λ (and $\delta \ll \lambda$) such that the bracket in (F.25) equals $(1 - \epsilon')$, with $\epsilon' > 0$. By choosing $C = 1 - \epsilon'$ we see that the resolvent kernel and the solution are analytic for small $\Delta > 0$ but not at $\Delta = 0$. The analyticity region is given by $0 < |\Delta| < 1/2$, with $\Delta = -1/2$ a non-analytic point, as can be inferred from (F.11).

F.2 Principal Chiral Field

In the PCF model the kernel equals

$$K(\theta) = \frac{1}{4\pi^2} \left(2\psi\left(1 + \frac{i\theta}{2\pi}\right) - \psi\left(1 - \bar{\Delta} + \frac{i\theta}{2\pi}\right) - \psi\left(\bar{\Delta} + \frac{i\theta}{2\pi}\right) \right) + c.c. , \quad (\text{F.26})$$

where $\bar{\Delta} = 1/N$. It can also be rewritten as

$$\pi^2 K(\theta, 2\bar{\Delta}) = \frac{2\bar{\Delta}}{(2\bar{\Delta})^2 + (\theta/\pi)^2} + F(\theta, 2\bar{\Delta}), \quad (\text{F.27})$$

where

$$F(\theta, z) \equiv \sum_{n=1}^{\infty} \left(\frac{2n + z}{(z + 2n)^2 + (\theta/\pi)^2} + \frac{2n - z}{(z - 2n)^2 + (\theta/\pi)^2} - \frac{4n}{(2n)^2 + (\theta/\pi)^2} \right). \quad (\text{F.28})$$

For $0 < \bar{\Delta} < 1$ its Fourier transform reads

$$\tilde{K}(\omega) \equiv \int_{-\infty}^{\infty} e^{i\omega\theta} K(\theta) d\theta = \frac{e^{-2\pi|\omega|(1-\bar{\Delta})} + e^{-2\pi|\omega|\bar{\Delta}} - 2e^{-2\pi|\omega|}}{1 - e^{-2\pi|\omega|}}. \quad (\text{F.29})$$

Like in the NLSM, the kernel is point-wise positive definite and is a contraction:

$$\sup_{-B \leq \theta \leq B} \int_{-B}^B |K(\theta - \theta')| d\theta' < \int_{-\infty}^{\infty} K(\theta - \theta') d\theta' = \tilde{K}(0) = 1. \quad (\text{F.30})$$

We can similarly study the analyticity in $1/N = \bar{\Delta}$ of K . We will be very brief since the analysis is similar to the one performed in the NLSM. Let $\bar{\Delta} = z/2$ be complex and focus on a small disc D around the origin, defined as in the NLSM case. The function $F(\theta, z)$ is analytic around $z = 0$ and can be expanded for small z as

$$|F(\theta, z)| = |z^2 F''(\theta) + \mathcal{O}(z^3)| < (\lambda + \delta)^2 |F''(\theta)|. \quad (\text{F.31})$$

For sufficiently small z , the analyticity properties of the PCF kernel coincide with those of both the NLSM model and the Lieb–Liniger model. The iterated kernels $K^{(p+1)}$ are bounded as in (F.18), with the replacement $(\lambda + \delta) |F'(\delta\theta)| \rightarrow (\lambda + \delta)^2 |F''(\delta\theta)|$ in the last term of the second row

of (F.18). The integral involving $|F''(\delta\theta)|$ is easily bounded by a finite constant, so we conclude that the kernel in the PCF model is analytic for $0 < |\bar{\Delta}| < 1$, but not at $\bar{\Delta} = 0$ and at $\bar{\Delta} = \pm 1$, as evident from (F.28).

F.3 Gross-Neveu model

In the Gross-Neveu model the kernel equals

$$K(\theta) = \frac{1}{4\pi^2} \left(\psi\left(\frac{i\theta}{2\pi}\right) - \psi\left(\frac{1}{2} + \frac{i\theta}{2\pi}\right) + \psi\left(\frac{1}{2} - \Delta + \frac{i\theta}{2\pi}\right) - \psi\left(1 - \Delta + \frac{i\theta}{2\pi}\right) \right) + c.c. , \quad (\text{F.32})$$

where $\Delta = 1/(N - 2)$, which can also be written as

$$\pi^2 K(\theta) = \sum_{n=1}^{\infty} (-1)^n \left(\frac{n - 2\Delta}{(2\Delta - n)^2 + (\theta/\pi)^2} - \frac{n}{n^2 + (\theta/\pi)^2} \right) . \quad (\text{F.33})$$

Its Fourier transform for $\Delta < 1/2$ reads

$$\tilde{K}(\omega) \equiv \int_{-\infty}^{\infty} e^{i\omega\theta} K(\theta) d\theta = e^{-\pi|\omega|} \frac{e^{-2\pi|\Delta||\omega|} - 1}{1 + e^{-\pi|\omega|}} . \quad (\text{F.34})$$

The kernel (F.32) is not point-wise positive, as in the NLSM and PCF models, but it is still a contraction. For small Δ this can be established by noticing that the kernel vanishes for $\Delta = 0$. For any B and $-B \leq \theta \leq B$, for small Δ , we have

$$\int_{-B}^B |K(\theta - \theta')| d\theta' \approx \Delta \int_{-B}^B |K'(\theta - \theta', \Delta = 0)| d\theta' < 2\Delta M , \quad (\text{F.35})$$

where M is finite. So, for sufficiently small Δ , K is a contraction. Numerically we see that K is a contraction for arbitrary Δ , not necessarily small. So the unique solution (F.5) is guaranteed to exist. The analyticity in Δ is trivial in the GN model (see also Appendix A of [117]). Let again be $\Delta = z/2$ and $z = \lambda + \alpha + i\beta$, where α and β span a disc of radius δ around the point λ , with $\lambda > 0$. Suppose that for a certain $p \geq 1$

$$|K^{(p)}(\theta)| \leq \sigma^p , \quad \sigma \equiv (\lambda + \delta)M . \quad (\text{F.36})$$

Then

$$|K^{(p+1)}(\theta - \theta')| = \left| \int_{-B}^B K^{(p)}(\theta - \theta'') K(\theta'' - \theta') d\theta'' \right| \leq \sigma^p \int_{-B}^B |K(\theta'' - \theta')| d\theta'' \leq \sigma^{p+1} . \quad (\text{F.37})$$

The relation (F.36), if valid for p , is then also valid for $p+1$. Since it applies for $p=1$, it follows that it is valid for any $p \geq 1$. We see that K and the associated solution $f(\theta)$ are analytic for small $\Delta > 0$, *including* $\Delta = 0$. By looking at (F.33) we can determine the radius of convergence of the small Δ expansion. The above expression is analytic up to the point $2\Delta = z < 1$. Replacing $z = 1 + w$ in (F.33) gives

$$\pi^2 K(\theta) = \frac{w}{w^2 + (\theta/\pi)^2} - F(\theta, w). \quad (\text{F.38})$$

with the function F as in (F.11). We see that around $z = 1$ the kernel is locally identically to the one of the NLSM close to the origin. Hence the point $z = 1$ is non-analytic. We conclude that the large N expansion should be convergent with a radius of convergence around $\Delta = 0$

$$\rho = \frac{1}{2}. \quad (\text{F.39})$$

Bibliography

- [1] G. Sberveglieri, M. Serone, and G. Spada, *Renormalization scheme dependence, RG flow, and Borel summability in ϕ^4 Theories in $d < 4$* , *Phys. Rev. D* **100** (2019), no. 4 045008, [[arXiv:1905.02122](#)]. 5
- [2] G. Sberveglieri, M. Serone, and G. Spada, *Self-Dualities and Renormalization Dependence of the Phase Diagram in 3d $O(N)$ Vector Models*, *JHEP* **02** (2021) 098, [[arXiv:2010.09737](#)]. 5
- [3] L. Di Pietro, M. Mariño, G. Sberveglieri, and M. Serone, *Resurgence and $1/N$ Expansion in Integrable Field Theories*, *JHEP* **10** (2021) 166, [[arXiv:2108.02647](#)]. 5
- [4] G. Sberveglieri and G. Spada, *in preparation*, . 5, 12, 66, 69, 74, 75, 76
- [5] F. J. Dyson, *Divergence of perturbation theory in quantum electrodynamics*, *Phys. Rev.* **85** (Feb, 1952) 631–632. 9, 15
- [6] J. Écalle, *Les fonctions réurgentes*, *Publ. math. d'Orsay/Univ. de Paris, Dep. de math.* (1981). 10, 22
- [7] J.-P. Eckmann, J. Magnen, and R. Sénéor, *Decay properties and borel summability for the schwinger functions in $p(\phi)_2$ theories*, *Comm. Math. Phys.* **39** (1974), no. 4 251–271. 10, 11, 18, 30, 38, 39, 41, 123
- [8] J. Magnen and R. Seneor, *Phase Space Cell Expansion and Borel Summability for the Euclidean ϕ^4 in Three-Dimensions Theory*, *Commun. Math. Phys.* **56** (1977) 237. 10, 11, 18, 30, 38, 39, 41, 123
- [9] M. Serone, G. Spada, and G. Villadoro, *$\lambda\phi^4$ Theory I: The Symmetric Phase Beyond NNNNNNNLO*, *JHEP* **08** (2018) 148, [[arXiv:1805.05882](#)]. 10, 11, 18, 22, 26, 30, 35, 37, 38, 40, 41, 47, 54, 55, 56, 58, 59, 60, 64, 75, 109, 123, 124
- [10] G. Parisi, *Field theoretic approach to second order phase transitions in two-dimensional and three-dimensional systems*, *J. Stat. Phys.* **23** (1980) 49–82. 11, 29, 30, 31, 33, 60, 65, 143

- [11] S.-J. Chang, *The Existence of a Second Order Phase Transition in the Two-Dimensional ϕ^4 Field Theory*, *Phys. Rev. D* **13** (1976) 2778. [Erratum: *Phys.Rev.D* 16, 1979 (1977)]. 11, 30, 48
- [12] S. F. Magruder, *The Existence of Phase Transition in the (ϕ^4) in Three-Dimensions Quantum Field Theory*, *Phys. Rev. D* **14** (1976) 1602. 11, 30, 48
- [13] D. Volin, *From the mass gap in $O(N)$ to the non-Borel-summability in $O(3)$ and $O(4)$ sigma-models*, *Phys. Rev.* **D81** (2010) 105008, [[arXiv:0904.2744](https://arxiv.org/abs/0904.2744)]. 12, 78, 102, 115, 128
- [14] D. Volin, *Quantum integrability and functional equations: Applications to the spectral problem of AdS/CFT and two-dimensional sigma models*, *J. Phys.* **A44** (2011) 124003, [[arXiv:1003.4725](https://arxiv.org/abs/1003.4725)]. 12, 78, 102, 115, 128
- [15] G. H. Hardy, *Divergent Series*. Oxford University Press, 1949. 18, 39
- [16] A. D. Sokal, *An improvement of Watson's theorem on Borel summability*, *J. Math. Phys.* **21** (1980) 261–263. 18, 39, 40, 41, 63
- [17] M. Serone, G. Spada, and G. Villadoro, *The Power of Perturbation Theory*, *JHEP* **05** (2017) 056, [[arXiv:1702.04148](https://arxiv.org/abs/1702.04148)]. 18, 38, 41, 147
- [18] E. Witten, *Analytic Continuation Of Chern-Simons Theory*, *AMS/IP Stud. Adv. Math.* **50** (2011) 347–446, [[arXiv:1001.2933](https://arxiv.org/abs/1001.2933)]. 21
- [19] M. Berry and C. Howls, *Hyperasymptotics for integrals with saddles*, *Proceedings of the Royal Society A: Mathematical and Physical Sciences* **A434** (1991) 657 – 675. 21, 148
- [20] C. M. Bender and T. T. Wu, *Anharmonic oscillator. 2: A Study of perturbation theory in large order*, *Phys. Rev. D* **7** (1973) 1620–1636. 21
- [21] L. N. Lipatov, *Divergence of the Perturbation Theory Series and the Quasiclassical Theory*, *Sov. Phys. JETP* **45** (1977) 216–223. 21
- [22] E. Brezin, J. C. Le Guillou, and J. Zinn-Justin, *Perturbation Theory at Large Order. 1. The φ^{2N} Interaction*, *Phys. Rev.* **D15** (1977) 1544–1557. 21, 30
- [23] E. Brezin, J. C. Le Guillou, and J. Zinn-Justin, *Perturbation Theory at Large Order. 2. Role of the Vacuum Instability*, *Phys. Rev. D* **15** (1977) 1558–1564. 21, 41
- [24] E. Brezin, G. Parisi, and J. Zinn-Justin, *Perturbation Theory at Large Orders for Potential with Degenerate Minima*, *Phys.Rev.* **D16** (1977) 408–412. 21
- [25] G. 't Hooft, *A Two-Dimensional Model for Mesons*, *Nucl. Phys. B* **75** (1974) 461–470. 22

- [26] G. Parisi, *Singularities of the Borel Transform in Renormalizable Theories*, *Phys. Lett.* **76B** (1978) 65–66. 22
- [27] I. Aniceto, G. Basar, and R. Schiappa, *A Primer on Resurgent Transseries and Their Asymptotics*, *Phys. Rept.* **809** (2019) 1–135, [[arXiv:1802.10441](#)]. 22, 25
- [28] M. Mariño, *Lectures on non-perturbative effects in large N gauge theories, matrix models and strings*, *Fortsch. Phys.* **62** (2014) 455–540, [[arXiv:1206.6272](#)]. 22
- [29] D. Dorigoni, *An Introduction to Resurgence, Trans-Series and Alien Calculus*, *Annals Phys.* **409** (2019) 167914, [[arXiv:1411.3585](#)]. 22
- [30] H. Stahl, *The convergence of Padé approximants to functions with branch points*, *Journal of Approximation Theory* **91** (1997), no. 2 139 – 204. 27, 118
- [31] L. Di Pietro and M. Serone, *Looking through the QCD Conformal Window with Perturbation Theory*, *JHEP* **07** (2020) 049, [[arXiv:2003.01742](#)]. 27, 118
- [32] G. A. Baker Jr. and P. Peter Graves-Morris, *Padé Approximants*. Encyclopedia of Mathematics and its Applications. Cambridge University Press, 1996. 27, 118
- [33] J. C. Le Guillou and J. Zinn-Justin, *Critical Exponents from Field Theory*, *Phys. Rev. B* **21** (1980) 3976–3998. 27, 35
- [34] A. Pelissetto and E. Vicari, *Critical phenomena and renormalization-group theory*, *Physics Reports* **368** (2002), no. 6 549–727. 29
- [35] K. G. Wilson and M. E. Fisher, *Critical exponents in 3.99 dimensions*, *Phys. Rev. Lett.* **28** (1972) 240–243. 29
- [36] M. V. Kompaniets and E. Panzer, *Minimally subtracted six loop renormalization of $O(n)$ -symmetric ϕ^4 theory and critical exponents*, *Phys. Rev.* **D96** (2017), no. 3 036016, [[arXiv:1705.06483](#)]. 30
- [37] J. P. Eckmann and H. Epstein, *Borel summability of the mass and the s matrix in ϕ^{**4} models*, *Commun. Math. Phys.* **68** (1979) 245–258. 30
- [38] M. Serone, G. Spada, and G. Villadoro, *$\lambda\phi_2^4$ theory — Part II. the broken phase beyond $NNNN(NNNN)LO$* , *JHEP* **05** (2019) 047, [[arXiv:1901.05023](#)]. 30, 41
- [39] A. Milsted, J. Haegeman, and T. J. Osborne, *Matrix product states and variational methods applied to critical quantum field theory*, *Phys. Rev. D* **88** (Oct, 2013) 085030. 30, 38

- [40] P. Bosetti, B. De Palma, and M. Guagnelli, *Monte Carlo determination of the critical coupling in ϕ_2^4 theory*, *Phys. Rev. D* **92** (2015), no. 3 034509, [[arXiv:1506.08587](#)]. 30, 38
- [41] S. Bronzin, B. De Palma, and M. Guagnelli, *New Monte Carlo determination of the critical coupling in ϕ_2^4 theory*, *Phys. Rev. D* **99** (2019), no. 3 034508, [[arXiv:1807.03381](#)]. 30, 38
- [42] D. Kadoh, Y. Kuramashi, Y. Nakamura, R. Sakai, S. Takeda, and Y. Yoshimura, *Tensor network analysis of critical coupling in two dimensional ϕ^4 theory*, *JHEP* **05** (2019) 184, [[arXiv:1811.12376](#)]. 30, 38
- [43] S. Rychkov and L. G. Vitale, *Hamiltonian truncation study of the ϕ^4 theory in two dimensions*, *Phys. Rev. D* **91** (2015) 085011, [[arXiv:1412.3460](#)]. 30, 38
- [44] J. Elias-Miro, S. Rychkov, and L. G. Vitale, *High-Precision Calculations in Strongly Coupled Quantum Field Theory with Next-to-Leading-Order Renormalized Hamiltonian Truncation*, *JHEP* **10** (2017) 213, [[arXiv:1706.06121](#)]. 30, 38
- [45] J. Elias-Miro, S. Rychkov, and L. G. Vitale, *NLO Renormalization in the Hamiltonian Truncation*, *Phys. Rev. D* **96** (2017), no. 6 065024, [[arXiv:1706.09929](#)]. 30, 38
- [46] M. Burkardt, S. S. Chabysheva, and J. R. Hiller, *Two-dimensional light-front ϕ^4 theory in a symmetric polynomial basis*, *Phys. Rev. D* **94** (2016), no. 6 065006, [[arXiv:1607.00026](#)]. 30
- [47] N. Anand, V. X. Genest, E. Katz, Z. U. Khandker, and M. T. Walters, *RG flow from ϕ^4 theory to the 2D Ising model*, *JHEP* **08** (2017) 056, [[arXiv:1704.04500](#)]. 30
- [48] A. L. Fitzpatrick, J. Kaplan, E. Katz, L. G. Vitale, and M. T. Walters, *Lightcone effective Hamiltonians and RG flows*, *JHEP* **08** (2018) 120, [[arXiv:1803.10793](#)]. 30
- [49] A. L. Fitzpatrick, E. Katz, and M. T. Walters, *Nonperturbative Matching Between Equal-Time and Lightcone Quantization*, *JHEP* **10** (2020) 092, [[arXiv:1812.08177](#)]. 30
- [50] M. Gell-Mann and F. E. Low, *Quantum electrodynamics at small distances*, *Phys. Rev.* **95** (Sep, 1954) 1300–1312. 31
- [51] C. G. Callan, Jr., *Broken scale invariance in scalar field theory*, *Phys. Rev. D* **2** (1970) 1541–1547. 33
- [52] K. Symanzik, *Small distance behavior in field theory and power counting*, *Commun. Math. Phys.* **18** (1970) 227–246. 33

- [53] S. Meneses, J. Penedones, S. Rychkov, J. M. Viana Parente Lopes, and P. Yvernay, *A structural test for the conformal invariance of the critical 3d Ising model*, *JHEP* **04** (2019) 115, [[arXiv:1802.02319](#)]. 34
- [54] G. A. Baker, Jr., B. G. Nickel, and D. I. Meiron, *Critical Indices from Perturbation Analysis of the Callan-Symanzik Equation*, *Phys. Rev. B* **17** (1978) 1365–1374. 35, 69, 75
- [55] E. Orlov and A. Sokolov, *Critical thermodynamics of the two-dimensional systems in five-loop renormalization-group approximation*, *Physics of the Solid State* **42** (04, 2000) [[hep-th/0003140](#)]. 35
- [56] A. Sokolov, *Pseudo-epsilon expansion and the two-dimensional ising model*, *Physics of the Solid State* **47** (10, 2005) [[cond-mat/0510088](#)]. 35
- [57] R. Guida and J. Zinn-Justin, *Critical exponents of the N vector model*, *J. Phys. A* **31** (1998) 8103–8121, [[cond-mat/9803240](#)]. 35, 65, 75, 76
- [58] R. Schloms and V. Dohm, *Minimal renormalization without ϵ -expansion: Critical behavior in three dimensions*, *Nuclear Physics* **328** (1989) 639–663. 35
- [59] R. Schloms and V. Dohm, *Minimal renormalization without ϵ expansion: Critical behavior above and below t_c* , *Phys. Rev. B* **42** (Oct, 1990) 6142–6152. [Erratum: *Phys. Rev. B* **46**, 5883 (1992)]. 35
- [60] R. Guida and P. Ribeca, *Towards a fully automated computation of RG-functions for the 3-d $O(N)$ vector model: Parametrizing amplitudes*, *J. Stat. Mech.* **0602** (2006) P02007, [[cond-mat/0512222](#)]. 36, 59, 67
- [61] A. Pelissetto and E. Vicari, *Four-point renormalized coupling constant and callan-symanzik β -function in $o(n)$ models*, *Nuclear Physics B* **519** (1998), no. 3 626–660, [[cond-mat/9711078](#)]. 38
- [62] P. Calabrese, M. Caselle, A. Celi, A. Pelissetto, and E. Vicari, *Non-analyticity of the callan-symanzik β -function of two-dimensional $o(n)$ models*, *Journal of Physics A: Mathematical and General* **33** (nov, 2000) 8155–8170, [[hep-th/0005254](#)]. 38
- [63] A. Pelissetto and E. Vicari, *Critical mass renormalization in renormalized ϕ^4 theories in two and three dimensions*, *Phys. Lett. B* **751** (2015) 532–534, [[arXiv:1508.00989](#)]. 38
- [64] A. Jaffe, *Constructive quantum field theory*, *Mathematical Physics 2000* (05, 2000) 111–127. 39
- [65] V. Rivasseau, *From Perturbative to Constructive Renormalization*. Princeton University Press, 1991. 39

- [66] G. H. Derrick, *Comments on nonlinear wave equations as models for elementary particles*, *Journal of Mathematical Physics* **5** (1964), no. 9 1252–1254, [<https://doi.org/10.1063/1.1704233>]. 41
- [67] H. Erbin, V. Lahoche, and M. Tamaazousti, *Constructive expansion for vector field theories i. quartic models in low dimensions*, *Journal of Mathematical Physics* **62** (2021), no. 4 043501. 41
- [68] K. Iwaki and T. Nakanishi, *Exact wkb analysis and cluster algebras*, *Journal of Physics A: Mathematical and Theoretical* **47** (01, 2014). 43
- [69] O. Costin, *Asymptotics and Borel summability*, vol. 141. Chapman and Hall, 2008. 43
- [70] G. Auberson and G. Mennessier, *Some properties of borel summable functions*, *Journal of Mathematical Physics* **22** (1981), no. 11 2472–2481, [<https://doi.org/10.1063/1.524806>]. 43
- [71] G. Auberson and G. Mennessier, *The reciprocal of a Borel summable function is Borel summable*, *Communications in Mathematical Physics* **100** (1985), no. 3 439 – 446. 43
- [72] V. Berezinsky, *Destruction of long range order in one-dimensional and two-dimensional systems having a continuous symmetry group. I. Classical systems*, *Sov. Phys. JETP* **32** (1971) 493–500. 45
- [73] V. Berezinsky, *Destruction of Long-range Order in One-dimensional and Two-dimensional Systems Possessing a Continuous Symmetry Group. II. Quantum Systems.*, *Sov. Phys. JETP* **34** (1972), no. 3 610. 45
- [74] J. Kosterlitz and D. Thouless, *Ordering, metastability and phase transitions in two-dimensional systems*, *J. Phys. C* **6** (1973) 1181–1203. 45
- [75] V. Gorbenko and B. Zan, *Two-dimensional $O(n)$ models and logarithmic CFTs*, *JHEP* **10** (2020) 099, [[arXiv:2005.07708](https://arxiv.org/abs/2005.07708)]. 45
- [76] S. R. Coleman, *There are no Goldstone bosons in two-dimensions*, *Commun. Math. Phys.* **31** (1973) 259–264. 47
- [77] N. Mermin and H. Wagner, *Absence of ferromagnetism or antiferromagnetism in one-dimensional or two-dimensional isotropic Heisenberg models*, *Phys. Rev. Lett.* **17** (1966) 1133–1136. 47
- [78] P. Cea and L. Tedesco, *Perturbation theory with a variational basis: The Generalized Gaussian effective potential*, *Phys. Rev. D* **55** (1997) 4967–4989, [[hep-th/9607156](https://arxiv.org/abs/hep-th/9607156)]. 51

- [79] I. Stancu, *The Post Gaussian effective potential in scalar and scalar - fermion theories*, *Phys. Rev. D* **43** (1991) 1283–1299. 51
- [80] M. Windolowski, *A Nonperturbative study of three-dimensional ϕ^4 theory*, [hep-th/0002243](#). 51
- [81] S. R. Coleman, R. Jackiw, and H. Politzer, *Spontaneous Symmetry Breaking in the $O(N)$ Model for Large N^** , *Phys. Rev. D* **10** (1974) 2491. 52
- [82] M. Yamazaki and K. Yonekura, *Confinement as analytic continuation beyond infinite coupling*, *Phys. Rev. Res.* **2** (2020), no. 1 013383, [[arXiv:1911.06327](#)]. 53
- [83] M. Mariño and T. Reis, *A new renormalon in two dimensions*, *JHEP* **07** (2020) 216, [[arXiv:1912.06228](#)]. 53, 128
- [84] E. Brezin and G. Parisi, *Critical exponents and large order behavior of perturbation theory*, *J. Stat. Phys.* **19** (1978) 269–292. 55, 59
- [85] G. Baker, B. Nickel, M. Green, and D. Meiron, *Ising Model Critical Indices in Three-Dimensions from the Callan-Symanzik Equation*, *Phys. Rev. Lett.* **36** (1976) 1351–1354. 59, 60, 69
- [86] B. Nickel, *Evaluation of Simple Feynman Graphs*, *J. Math. Phys.* **19** (1978) 542–548. 59, 60, 67
- [87] W. Zimmermann, *Convergence of Bogolyubov’s method of renormalization in momentum space*, *Commun. Math. Phys.* **15** (1969) 208–234. 59
- [88] G. Lepage, *A New Algorithm for Adaptive Multidimensional Integration*, *J. Comput. Phys.* **27** (1978) 192. 60, 75
- [89] S. Antonenko and A. Sokolov, *Critical exponents for 3-D $O(n)$ - symmetric model with $n > 3$* , *Phys. Rev. E* **51** (1995) 1894–1898, [[hep-th/9803264](#)]. 60
- [90] R. Jackiw and S. Templeton, *How Superrenormalizable Interactions Cure their Infrared Divergences*, *Phys. Rev. D* **23** (1981) 2291. 63
- [91] X.-p. Sun, *Monte Carlo studies of three-dimensional $O(1)$ and $O(4)$ ϕ^4 theory related to BEC phase transition temperatures*, *Phys. Rev. E* **67** (2003) 066702, [[hep-lat/0209144](#)]. 66
- [92] P. B. Arnold and G. D. Moore, *Monte Carlo simulation of $O(2)$ ϕ^4 field theory in three-dimensions*, *Phys. Rev. E* **64** (2001) 066113, [[cond-mat/0103227](#)]. [Erratum: *Phys.Rev.E* 68, 049902 (2003)]. 66

- [93] P. B. Arnold and G. D. Moore, *Transition temperature of a dilute homogeneous imperfect Bose gas*, *Phys. Rev. Lett.* **87** (2001) 120401, [[cond-mat/0103228](#)]. 66
- [94] J. Elias-Miró and E. Hardy, *Exploring Hamiltonian Truncation in $\mathbf{d} = \mathbf{2} + \mathbf{1}$* , *Phys. Rev. D* **102** (2020), no. 6 065001, [[arXiv:2003.08405](#)]. 66
- [95] N. Anand, E. Katz, Z. U. Khandker, and M. T. Walters, *Nonperturbative dynamics of $(2+1)d$ ϕ^4 -theory from Hamiltonian truncation*, *JHEP* **05** (2021) 190, [[arXiv:2010.09730](#)]. 66
- [96] M. Borinsky, *Feynman graph generation and calculations in the Hopf algebra of Feynman graphs*, *Comput. Phys. Commun.* **185** (2014) 3317–3330. 67
- [97] J. F. Nagle, *On ordering and identifying undirected linear graphs*, *Journal of Mathematical Physics* **7** (1966), no. 9 1588–1592. 68
- [98] B. Nickel, D. Meiron, and G. Baker Jr, *Compilation of 2-pt and 4-pt graphs for continuous spin model*, *University of Guelph report* (1977). 68, 75, 143
- [99] D. Melrose, *Reduction of feynman diagrams*, *Il Nuovo Cimento A (1965-1970)* **40** (1965), no. 1 181–213. 69
- [100] J. M. Carmona, A. Pelissetto, and E. Vicari, *The N component Ginzburg-Landau Hamiltonian with cubic anisotropy: A Six loop study*, *Phys. Rev. B* **61** (2000) 15136–15151, [[cond-mat/9912115](#)]. 76
- [101] A. Pelissetto and E. Vicari, *Renormalised four-point coupling constant in the three-dimensional $O(N)$ model with $N \rightarrow 0$* , *J. Phys. A* **40** (2007) F539, [[cond-mat/0703114](#)]. 76
- [102] H.-P. Hsu, W. Nadler, and P. Grassberger, *Scaling of star polymers with 1-80 arms*, *Macromolecules* **37** (2004), no. 12 4658–4663, [<https://doi.org/10.1021/ma0355958>]. 76
- [103] H. E. Stanley, *Spherical model as the limit of infinite spin dimensionality*, *Phys. Rev.* **176** (1968) 718–722. 77
- [104] G. 't Hooft, *A Planar Diagram Theory for Strong Interactions*, *Nucl. Phys. B* **72** (1974) 461. 77
- [105] J. Koplik, A. Neveu, and S. Nussinov, *Some Aspects of the Planar Perturbation Series*, *Nucl. Phys. B* **123** (1977) 109–131. 77

- [106] E. Brezin, C. Itzykson, G. Parisi, and J. B. Zuber, *Planar Diagrams*, *Commun. Math. Phys.* **59** (1978) 35, 77
- [107] D. J. Broadhurst, *Large N expansion of QED: Asymptotic photon propagator and contributions to the muon anomaly, for any number of loops*, *Z. Phys.* **C58** (1993) 339–346. 77
- [108] M. Beneke, *Renormalons*, *Phys. Rept.* **317** (1999) 1–142, [[hep-ph/9807443](#)]. 77
- [109] D. J. Gross and A. Neveu, *Dynamical Symmetry Breaking in Asymptotically Free Field Theories*, *Phys. Rev.* **D10** (1974) 3235. 78, 112
- [110] F. David, *Nonperturbative Effects and Infrared Renormalons Within the $1/N$ Expansion of the $O(N)$ Nonlinear σ Model*, *Nucl. Phys. B* **209** (1982) 433–460. 78, 127
- [111] F. David, *On the Ambiguity of Composite Operators, IR Renormalons and the Status of the Operator Product Expansion*, *Nucl. Phys. B* **234** (1984) 237–251. 78, 127
- [112] V. A. Novikov, M. A. Shifman, A. I. Vainshtein, and V. I. Zakharov, *Two-Dimensional Sigma Models: Modeling Nonperturbative Effects of Quantum Chromodynamics*, *Phys. Rept.* **116** (1984) 103. 78
- [113] A. M. Polyakov and P. Wiegmann, *Theory of Nonabelian Goldstone Bosons*, *Phys. Lett. B* **131** (1983) 121–126. 78, 83, 125
- [114] P. Hasenfratz, M. Maggiore, and F. Niedermayer, *The Exact mass gap of the $O(3)$ and $O(4)$ nonlinear sigma models in $d = 2$* , *Phys. Lett.* **B245** (1990) 522–528. 78, 86
- [115] P. Hasenfratz and F. Niedermayer, *The Exact mass gap of the $O(N)$ sigma model for arbitrary $N \geq 3$ in $d = 2$* , *Phys. Lett.* **B245** (1990) 529–532. 78, 86, 152
- [116] J. Balog, S. Naik, F. Niedermayer, and P. Weisz, *Exact mass gap of the chiral $SU(n) \times SU(n)$ model*, *Phys. Rev. Lett.* **69** (1992) 873–876. 78, 79, 101, 102, 125
- [117] P. Forgacs, F. Niedermayer, and P. Weisz, *The Exact mass gap of the Gross-Neveu model. 1. The Thermodynamic Bethe ansatz*, *Nucl. Phys.* **B367** (1991) 123–143. 78, 112, 118, 125, 156
- [118] P. Forgacs, F. Niedermayer, and P. Weisz, *The Exact mass gap of the Gross-Neveu model. 2. The $1/N$ expansion*, *Nucl. Phys.* **B367** (1991) 144–157. 78, 112, 125
- [119] T. J. Hollowood, *The Exact mass gaps of the principal chiral models*, *Phys. Lett.* **B329** (1994) 450–456, [[hep-th/9402084](#)]. 78

- [120] J. M. Evans and T. J. Hollowood, *The Exact mass gap of the supersymmetric $O(N)$ sigma model*, *Phys. Lett.* **B343** (1995) 189–197, [[hep-th/9409141](#)]. 78
- [121] J. M. Evans and T. J. Hollowood, *The Exact mass gap of the supersymmetric \mathbb{CP}^{N-1} sigma model*, *Phys. Lett.* **B343** (1995) 198–206, [[hep-th/9409142](#)]. 78
- [122] J. M. Evans and T. J. Hollowood, *Exact results for integrable asymptotically - free field theories*, *Nucl. Phys. Proc. Suppl.* **45A** (1996), no. 1 130–139, [[hep-th/9508141](#)]. 78
- [123] M. Mariño and T. Reis, *Renormalons in integrable field theories*, *JHEP* **04** (2020) 160, [[arXiv:1909.12134](#)]. 78, 102, 110, 115, 125
- [124] M. C. Abbott, Z. Bajnok, J. Balog, and A. Hegedús, *From perturbative to non-perturbative in the $O(4)$ sigma model*, *Phys. Lett. B* **818** (2021) 136369, [[arXiv:2011.09897](#)]. 78, 79, 110, 126, 127
- [125] M. C. Abbott, Z. Bajnok, J. Balog, A. Hegedús, and S. Sadeghian, *Resurgence in the $O(4)$ sigma model*, *JHEP* **05** (2021) 253, [[arXiv:2011.12254](#)]. 78, 79, 110, 126, 127
- [126] M. Mariño and T. Reis, *Exact perturbative results for the Lieb-Liniger and Gaudin-Yang models*, *Journal of Statistical Physics* **177** (2019) 1148–1156, [[arXiv:1905.09575](#)]. 78
- [127] M. Mariño and T. Reis, *Resurgence for superconductors*, *Journal of Statistical Mechanics: Theory and Experiment* **2019** (2019), no. 12 123102, [[arXiv:1905.09569](#)]. 78
- [128] M. Mariño and T. Reis, *Resurgence and renormalons in the one-dimensional Hubbard model*, [[arXiv:2006.05131](#)]. 78
- [129] M. Mariño and T. Reis, *Three roads to the energy gap*, [[arXiv:2010.16174](#)]. 78
- [130] V. A. Fateev, P. B. Wiegmann, and V. A. Kazakov, *Large N chiral field in two-dimensions*, *Phys. Rev. Lett.* **73** (1994) 1750–1753. 78, 79, 100, 101, 107
- [131] V. A. Fateev, V. A. Kazakov, and P. B. Wiegmann, *Principal chiral field at large N* , *Nucl. Phys.* **B424** (1994) 505–520, [[hep-th/9403099](#)]. 78, 79, 100, 101, 107
- [132] K. Zarembo, *Quantum Giant Magnons*, *JHEP* **05** (2008) 047, [[arXiv:0802.3681](#)]. 78, 90, 96, 97, 98, 104
- [133] V. Kazakov, E. Sobko, and K. Zarembo, *Double-Scaling Limit in the Principal Chiral Model: A New Noncritical String?*, *Phys. Rev. Lett.* **124** (2020), no. 19 191602, [[arXiv:1911.12860](#)]. 78, 96
- [134] M. Mariño, R. Miravitllas Mas, and T. Reis, *Testing the Bethe ansatz with large N renormalons*, [[arXiv:2102.03078](#)]. 78, 79, 86, 87, 99, 101

- [135] “*NIST Digital Library of Mathematical Functions.*” <http://dlmf.nist.gov/>, Release 1.1.1 of 2021-03-15. F. W. J. Olver, A. B. Olde Daalhuis, D. W. Lozier, B. I. Schneider, R. F. Boisvert, C. W. Clark, B. R. Miller, B. V. Saunders, H. S. Cohl, and M. A. McClain, eds. 81
- [136] Z. Bajnok, J. Balog, B. Basso, G. P. Korchemsky, and L. Palla, *Scaling function in AdS/CFT from the $O(6)$ sigma model*, *Nucl. Phys.* **B811** (2009) 438–462, [[arXiv:0809.4952](https://arxiv.org/abs/0809.4952)]. 84, 86
- [137] E. Brezin and J. Zinn-Justin, *Spontaneous Breakdown of Continuous Symmetries Near Two-Dimensions*, *Phys. Rev.* **B14** (1976) 3110. 87
- [138] M. Mariño, *Instantons and large N . An introduction to non-perturbative methods in quantum field theory*. Cambridge University Press, 2015. 87, 103
- [139] P. Biscari, M. Campostrini, and P. Rossi, *Quantitative Picture of the Scaling Behavior of Lattice Nonlinear σ Models From the $1/N$ Expansion*, *Phys. Lett. B* **242** (1990) 225–233. 99
- [140] C. Bonet, D. Sauzin, T. Seara, and M. València, *Adiabatic invariant of the harmonic oscillator, complex matching and resurgence*, *SIAM J. Math. Anal.* **29** (1998), no. 6 1335–1360. 107
- [141] T. M. Seara and D. Sauzin, *Resumació de Borel i teoria de la ressurgència*, *Butl. Soc. Catalana Mat.* **18** (2003) 131–153. 107
- [142] M. Mariño, *Nonperturbative effects and nonperturbative definitions in matrix models and topological strings*, *JHEP* **0812** (2008) 114, [[arXiv:0805.3033](https://arxiv.org/abs/0805.3033)]. 107, 109
- [143] I. Aniceto and R. Schiappa, *Nonperturbative ambiguities and the reality of resurgent transseries*, *Commun. Math. Phys.* **335** (2015), no. 1 183–245, [[arXiv:1308.1115](https://arxiv.org/abs/1308.1115)]. 109
- [144] C. Hunter and B. Guerrieri, *Deducing the properties of singularities of functions from their Taylor series coefficients*, *SIAM Journal on Applied Mathematics* **39** (1980), no. 2 248–263, [<https://doi.org/10.1137/0139022>]. 117
- [145] A. B. Zamolodchikov, *Mass scale in the sine-Gordon model and its reductions*, *Int. J. Mod. Phys. A* **10** (1995) 1125–1150. 119
- [146] D. J. Amit, Y. Y. Goldschmidt, and G. Grinstein, *Renormalization Group Analysis of the Phase Transition in the 2D Coulomb Gas, Sine-Gordon Theory and xy Model*, *J. Phys. A* **13** (1980) 585. 120

- [147] S. R. Coleman, *The Quantum Sine-Gordon Equation as the Massive Thirring Model*, *Phys. Rev. D* **11** (1975) 2088. 121
- [148] D. B. Kaplan, J.-W. Lee, D. T. Son, and M. A. Stephanov, *Conformality Lost*, *Phys. Rev.* **D80** (2009) 125005, [[arXiv:0905.4752](#)]. 124
- [149] V. Gorbenko, S. Rychkov, and B. Zan, *Walking, Weak first-order transitions, and Complex CFTs*, *JHEP* **10** (2018) 108, [[arXiv:1807.11512](#)]. 124
- [150] V. Gorbenko, S. Rychkov, and B. Zan, *Walking, Weak first-order transitions, and Complex CFTs II. Two-dimensional Potts model at $Q > 4$* , *SciPost Phys.* **5** (2018), no. 5 050, [[arXiv:1808.04380](#)]. 124
- [151] F. Benini, C. Iossa, and M. Serone, *Conformality Loss, Walking, and 4D Complex Conformal Field Theories at Weak Coupling*, *Phys. Rev. Lett.* **124** (2020), no. 5 051602, [[arXiv:1908.04325](#)]. 124
- [152] S. Gukov, *RG Flows and Bifurcations*, *Nucl. Phys. B* **919** (2017) 583–638, [[arXiv:1608.06638](#)]. 124
- [153] G. Galati and M. Serone, *Cancellation of IR divergences in 3d Abelian gauge theories*, *JHEP* **02** (2022) 123, [[arXiv:2111.02124](#)]. 125
- [154] J. C. Le Guillou and J. Zinn-Justin, eds., *Large order behavior of perturbation theory*. 1990. 125
- [155] C. Kozçaz, T. Sulejmanpasic, Y. Tanizaki, and M. Ünsal, *Cheshire Cat resurgence, Self-resurgence and Quasi-Exact Solvable Systems*, *Commun. Math. Phys.* **364** (2018), no. 3 835–878, [[arXiv:1609.06198](#)]. 126
- [156] Z. Bajnok, J. Balog, and I. Vona, *Analytic resurgence in the $O(4)$ model*, *JHEP* **04** (2022) 043, [[arXiv:2111.15390](#)]. 126, 127
- [157] G. V. Dunne and M. Unsal, *Resurgence and Dynamics of $O(N)$ and Grassmannian Sigma Models*, *JHEP* **09** (2015) 199, [[arXiv:1505.07803](#)]. 127
- [158] A. Cherman, D. Dorigoni, G. V. Dunne, and M. Unsal, *Resurgence in Quantum Field Theory: Nonperturbative Effects in the Principal Chiral Model*, *Phys. Rev. Lett.* **112** (2014) 021601, [[arXiv:1308.0127](#)]. 127
- [159] G. V. Dunne and M. Meynig, *Instantons or renormalons? Remarks on ϕ^4 theory in the MS scheme*, *Phys. Rev. D* **105** (2022), no. 2 025019, [[arXiv:2111.15554](#)]. 127

- [160] M. Mariño, R. Miravitllas, and T. Reis, *New renormalons from analytic trans-series*, [arXiv:2111.11951](#). 128
- [161] Z. Bajnok, J. Balog, A. Hegedus, and I. Vona, *Instanton effects vs resurgence in the $O(3)$ sigma model*, *Phys. Lett. B* **829** (2022) 137073, [[arXiv:2112.11741](#)]. 128
- [162] M. Mariño, R. Miravitllas, and T. Reis, *Instantons, renormalons and the theta angle in integrable sigma models*, [arXiv:2205.04495](#). 128
- [163] Z. Bajnok, J. Balog, A. Hegedus, and I. Vona, *Running coupling and non-perturbative corrections for $O(N)$ free energy and for disk capacitor*, [arXiv:2204.13365](#). 128
- [164] R. M. Corless, G. H. Gonnet, D. E. G. Hare, D. J. Jeffrey, and D. E. Knuth, *On the Lambert W function*, *Adv. Comput. Math* **5** (1996) 329. 129
- [165] E. Gardi, G. Grunberg, and M. Karliner, *Can the QCD running coupling have a causal analyticity structure?*, *JHEP* **07** (1998) 007, [[hep-ph/9806462](#)]. 130
- [166] M. P. Bellon and P. J. Clavier, *Alien calculus and a Schwinger–Dyson equation: two-point function with a nonperturbative mass scale*, *Lett. Math. Phys.* **108** (2018), no. 2 391–412, [[arXiv:1612.07813](#)]. 130
- [167] E. Panzer and R. Wulkenhaar, *Lambert-W Solves the Noncommutative Φ^4 -Model*, *Commun. Math. Phys.* **374** (2019), no. 3 1935–1961, [[arXiv:1807.02945](#)]. 130
- [168] M. Borinsky and G. V. Dunne, *Non-Perturbative Completion of Hopf-Algebraic Dyson-Schwinger Equations*, *Nucl. Phys. B* **957** (2020) 115096, [[arXiv:2005.04265](#)]. 130
- [169] L. Fei, S. Giombi, and I. R. Klebanov, *Critical $O(N)$ models in $6 - \epsilon$ dimensions*, *Phys. Rev. D* **90** (2014), no. 2 025018, [[arXiv:1404.1094](#)]. 131
- [170] S. Hikami and E. Brezin, *Large Order Behavior of the $1/N$ Expansion in Zero-dimensions and One-dimensions*, *J. Phys. A* **12** (1979) 759–770. 148
- [171] E. H. Lieb and W. Liniger, *Exact analysis of an interacting Bose gas. 1. The General solution and the ground state*, *Phys. Rev.* **130** (1963) 1605–1616. 153, 154